ATTACHMENT E
Slope Stability Plan & Critical Section

INSTALL 20' WIDE DOUBLE CHAIN LINK GATE. SEE INSTALLATION DETAIL ON DWG. D-2.

20'x50' TRAKING PAD

N
W
E
S

NJ State '83

5' MIN.

LAYDOWN AREA

BRUSH

REPLACE CHAIN LINK FENCE TO MATCH EXISTING. SEE INSTALLATION DETAIL ON DWG. D-2.

BRUSH

CLEAR AND GRUB WITHIN THIS BOUNDARY

4"-6" RIPRAP APRON (15" THICK) (d_{50}=5") FLUSH WITH GROUND SURFACE

INV. IN=95.5'

15'

ALL HAYBALE BACKED SILT ALONG CHAIN LINK FENCE

INV. OUT=95.0'

STORMWATER DETENTION/RECHARGE AREA

BRUSH

REPLACE CHAIN LINK FENCE TO MATCH EXISTING. SEE INSTALLATION DETAIL ON DWG. D-2.

CLEAR AND GRUB WITHIN THIS BOUNDARY

DENSE VEGETATION

CLEAR AND GRUB WITHIN THIS BOUNDARY

DENSE VEGETATION

DEBRIS

IN-SITU SOIL MOISTURE MONITORING STATION (TYP. 8 LOCATIONS). SEE DETAIL ON DRAWING D-3.

GB-2

MATCH POINT FOR WEST SIDE AND EAST SIDE CHANNELS

INSTALL HAYBALE BACKED SILT FENCE ALONG INSIDE OF CHAIN LINK FENCE

X 109.0

GB-3

GB-5

LIMIT OF CLAY BARRIER LAYER

STORMWATER DETENTION/RECHARGE AREA

INSTALL HAYBALE BACKED SILT FENCE

REPLACE CHAIN LINK FENCE TO MATCH EXISTING. SEE INSTALLATION DETAIL ON DWG. D-2.

CLEAR AND GRUB WITHIN THIS BOUNDARY

LEGEND

PROPOSED	EXISTING	DESCRIPTION
		PROPERTY LINE
		DIRT ROAD
		PAVED ROAD
105	105	5 FOOT CONTOUR
		1 FOOT CONTOUR
X 103.0		SPOT ELEVATION
		FENCE LINE
		RAILROAD TRACK
		EDGE OF WATER
		LIMIT OF BRUSH
		LIMIT OF VEGETATION
		BUILDING
		TREE
		CATCH BASIN

SOURCE:
PHOTOMETRIC SURVEY BY PROMAPS DATED JANUARY 18, 2005.

NOTE:
HORIZONTAL DATUM IS NEW JERSEY STATE PLANE COORDINATES NAD '83.

VERTICAL DATUM IS NAVD 88.

0 80' 160'

GRAPHIC SCALE

J:\CAD\105106\000100\CAP Design 7-09\
C1-C8.dwg Layout:S-1 11x17 August 14, 2009-8:52AM Khollenbeck

TRC
21 Griffin Road North
Windsor, CT 06095
(860) 298-9692

SHIELDALLOY METALLURGICAL CORPORATION
NEWFIELD, NEW JERSEY
DECOMMISSIONING PLAN FOR THE NEWFIELD FACILITY
REV. 1B INTERM

STORAGE YARD ENGINEERED BARRIER SLOPE STABILITY MODEL SECTION LOCATION PLAN

Date: 8/13/09 | Project No. 105106.000100.000000

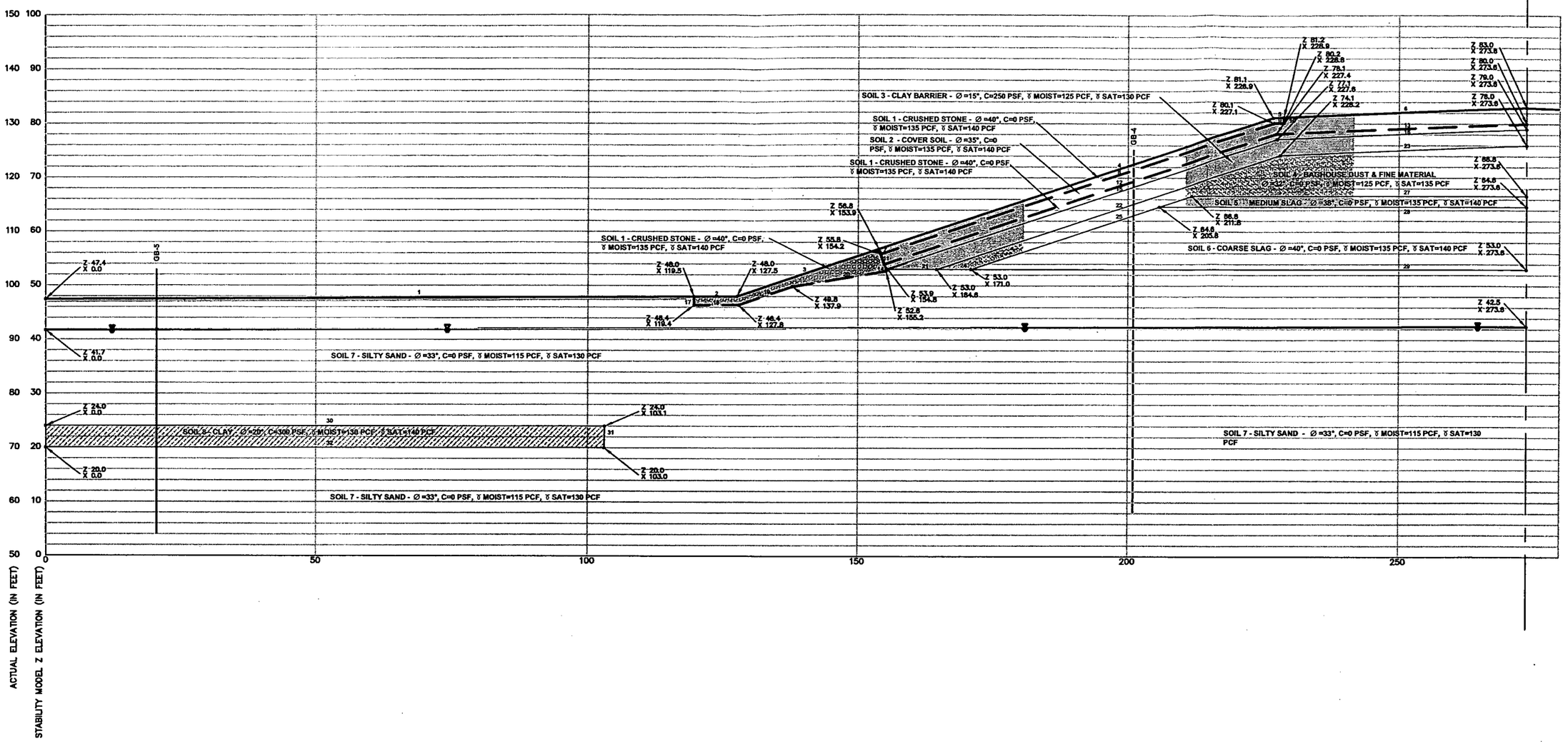

40'
20'
0
VERTICAL GRAPHIC SCALE

NOTE:
SEE DRAWING S-1 FOR SECTION LOCATION.

0 20' 40'
HORIZONTAL GRAPHIC SCALE

J:\CAD\105106\000100\CAP Design 7-09\
S-2.dwg Layout:S-2 11x17 August 14, 2009-8:34AM Khollenbeck

TRC
21 Griffin Road North
Windsor, CT 06095
(860) 298-9692

SHIELDALLOY METALLURGICAL CORPORATION
NEWFIELD, NEW JERSEY
DECOMMISSIONING PLAN FOR THE NEWFIELD FACILITY
REV. 1B INTERM

STORAGE YARD
ENGINEERED BARRIER
SLOPE STABILITY
MODEL SECTION

Date: 8/13/09 | Project No. 105106.000100.000000

ATTACHMENT F
Settlement Analysis Parameters

Shieldalloy Metallurgical Corporation - Newfield, New Jersey Facility - Decommissioning

Settlement Analysis Parameters

Location: Boring GB-1

ELEVATION (ft.)	DEPTH (ft.)	Vertical Stress (TSF)	Eff. Vertical Stress (TSF)	BLOWS/ft $(N_1)_{60}$	Relative Density (D_r)
110					
108					
106					
104					
102	0	0.00	0.00		
100	2	0.12	0.12	20	100
98	4	0.24	0.24	13	80
96	6	0.36	0.36	4	45
94	8	0.48	0.48	10	65
92	10	0.60	0.60	12	70
90	12	0.72	0.72	10	60
88	14	0.84	0.78	8	55
86	16	0.96	0.84	16	75
84	18	1.08	0.89	24	90
82	20	1.20	0.95	21	85
80	22	1.32	1.01	17	75
78	24	1.44	1.07	30	95
76	26	1.56	1.12	20	80
74	28	1.68	1.18	5	40
72	30	1.80	1.24	5	40
70	32	1.92	1.30	4	30
68	34	2.04	1.35	13	60

AVERAGE D_r	67
AVERAGE Submerged D_r	66

Shieldalloy Metallurgical Corporation - Newfield, New Jersey Facility - Decommissioning

Settlement Analysis Parameters

Location: Boring GB-2

ELEVATION (ft.)	DEPTH (ft.)	Vertical Stress (TSF)	Eff. Vertical Stress (TSF)	BLOWS/ft $(N_1)_{60}$	Relative Density (D_r)
110					
108					
106	0	0.00	0.00		
104	2	0.12	0.12	27	100
102	4	0.24	0.24	9	70
100	6	0.36	0.36	8	65
98	8	0.48	0.48	9	65
96	10	0.60	0.60	9	65
94	12	0.72	0.72	2	15
92	14	0.84	0.78	43	100
90	16	0.96	0.84	16	80
88	18	1.08	0.89	19	85
86	20	1.20	0.95	10	60
84	22	1.32	1.01	8	50
82	24	1.44	1.07	14	70
80	26	1.56	1.12	13	65
78	28	1.68	1.18	9	55
76	30	1.80	1.24	21	80
74	32	1.92	1.30	8	50
72	34	2.04	1.35	10	55
70	36	2.16	1.41		
68	38	2.28	1.47		

AVERAGE D_r 66

AVERAGE Submerged D_r 68

Shieldalloy Metallurgical Corporation - Newfield, New Jersey Facility - Decommissioning

Settlement Analysis Parameters

Location: Boring GB-3

ELEVATION (ft.)	DEPTH (ft.)	Vertical Stress (TSF)	Eff. Vertical Stress (TSF)	BLOWS/ft $(N_1)_{60}$	Relative Density (D_r)
110	0				
108	2	0.00	0.00	18	95
106	4	0.12	0.12	21	100
104	6	0.24	0.24	24	100
102	8	0.36	0.36	30	100
100	10	0.48	0.48	24	95
98	12	0.60	0.60	13	70
96	14	0.72	0.72	22	90
94	16	0.84	0.84	18	80
92	18	0.96	0.90	13	65
90	20	1.08	0.96	15	70
88	22	1.20	1.01	10	60
86	24	1.32	1.07	19	80
84	26	1.44	1.13	14	65
82	28	1.56	1.19	18	75
80	30	1.68	1.24	18	75
78	32	1.80	1.30	14	65
76	34	1.92	1.36	13	65
74	36	2.04	1.42	24	85
72	38	2.16	1.47	17	70
70	40	2.28	1.53		
68	42	2.40	1.59		

AVERAGE D_r	79
AVERAGE Submerged D_r	70

Shieldalloy Metallurgical Corporation - Newfield, New Jersey Facility - Decommissioning

Settlement Analysis Parameters

Location: Boring GB-4

ELEVATION (ft.)	DEPTH (ft.)	Vertical Stress (TSF)	Eff. Vertical Stress (TSF)	BLOWS/ft $(N_1)_{60}$	Relative Density (D_r)
110					
108	0	0.00	0.00		
106	2	0.12	0.12	Refusal	100
104	4	0.24	0.24	Refusal	100
102	6	0.36	0.36	10	70
100	8	0.48	0.48	5	45
98	10	0.60	0.60	6	50
96	12	0.72	0.66	3	15
94	14	0.84	0.72	13	70
92	16	0.96	0.77	10	60
90	18	1.08	0.83	13	70
88	20	1.20	0.89	10	60
86	22	1.32	0.95	8	55
84	24	1.44	1.00	8	55
82	26	1.56	1.06	11	60
80	28	1.68	1.12	13	65
78	30	1.80	1.18	8	50
76	32	1.92	1.23	9	55
74	34	2.04	1.29	20	80
72	36	2.16	1.35	4	30
70	38	2.28	1.41		
68	40	2.40	1.46		

AVERAGE D_r 61

AVERAGE Submerged D_r 56

Shieldalloy Metallurgical Corporation - Newfield, New Jersey Facility - Decommissioning

Settlement Analysis Parameters

Location: Boring GB-5

ELEVATION (ft.)	DEPTH (ft.)	Vertical Stress (TSF)	Eff. Vertical Stress (TSF)	BLOWS/ft $(N_1)_{60}$	Relative Density (D_r)
110					
108					
106					
104					
102	0	0.00	0.00		
100	2	0.12	0.12	Refusal	100
98	4	0.24	0.24	Refusal	100
96	6	0.36	0.36	Refusal	100
94	8	0.48	0.48	4	45
92	10	0.60	0.54	18	85
90	12	0.72	0.60	11	65
88	14	0.84	0.65	10	65
86	16	0.96	0.71	9	60
84	18	1.08	0.77	13	70
82	20	1.20	0.83	12	65
80	22	1.32	0.88	12	65
78	24	1.44	0.94	16	75
76	26	1.56	1.00	12	65
74	28	1.68	1.06	18	80
72	30	1.80	1.11	13	65
70	32	1.92	1.17	11	
68	34	2.04	1.23		

AVERAGE D_r 74

AVERAGE Submerged D_r 69

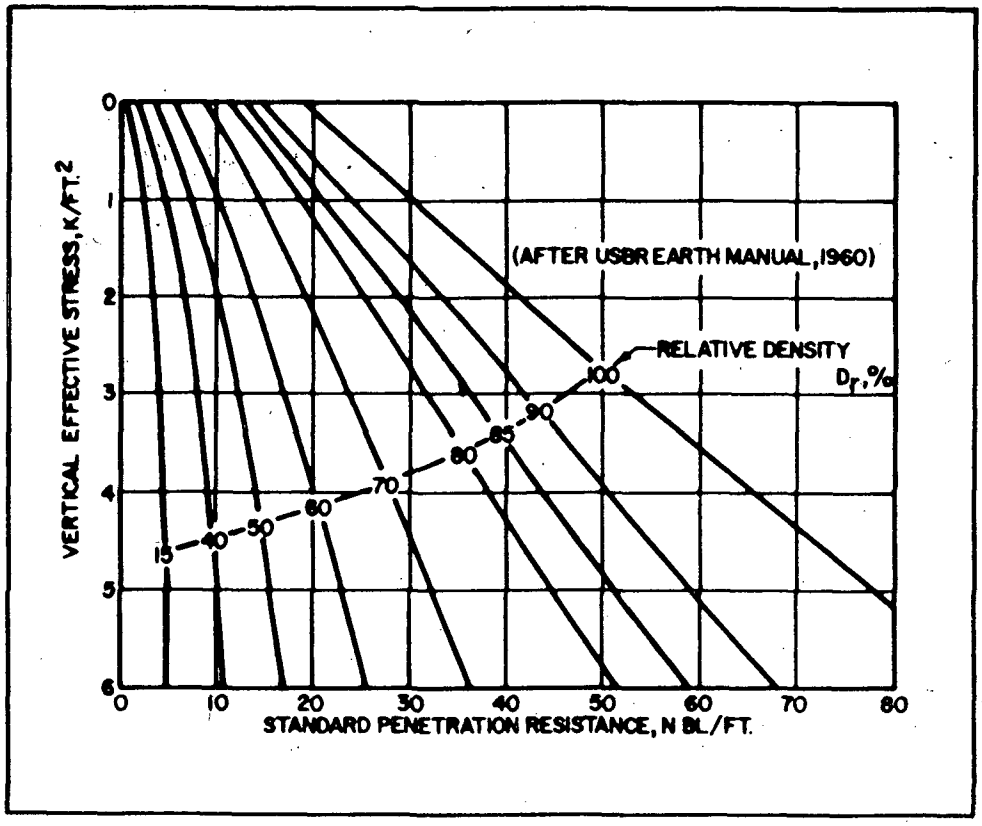

FIGURE 3
Correlations Between Relative Density and Standard Penetration Resistance in Accordance with Gibbs and Holtz

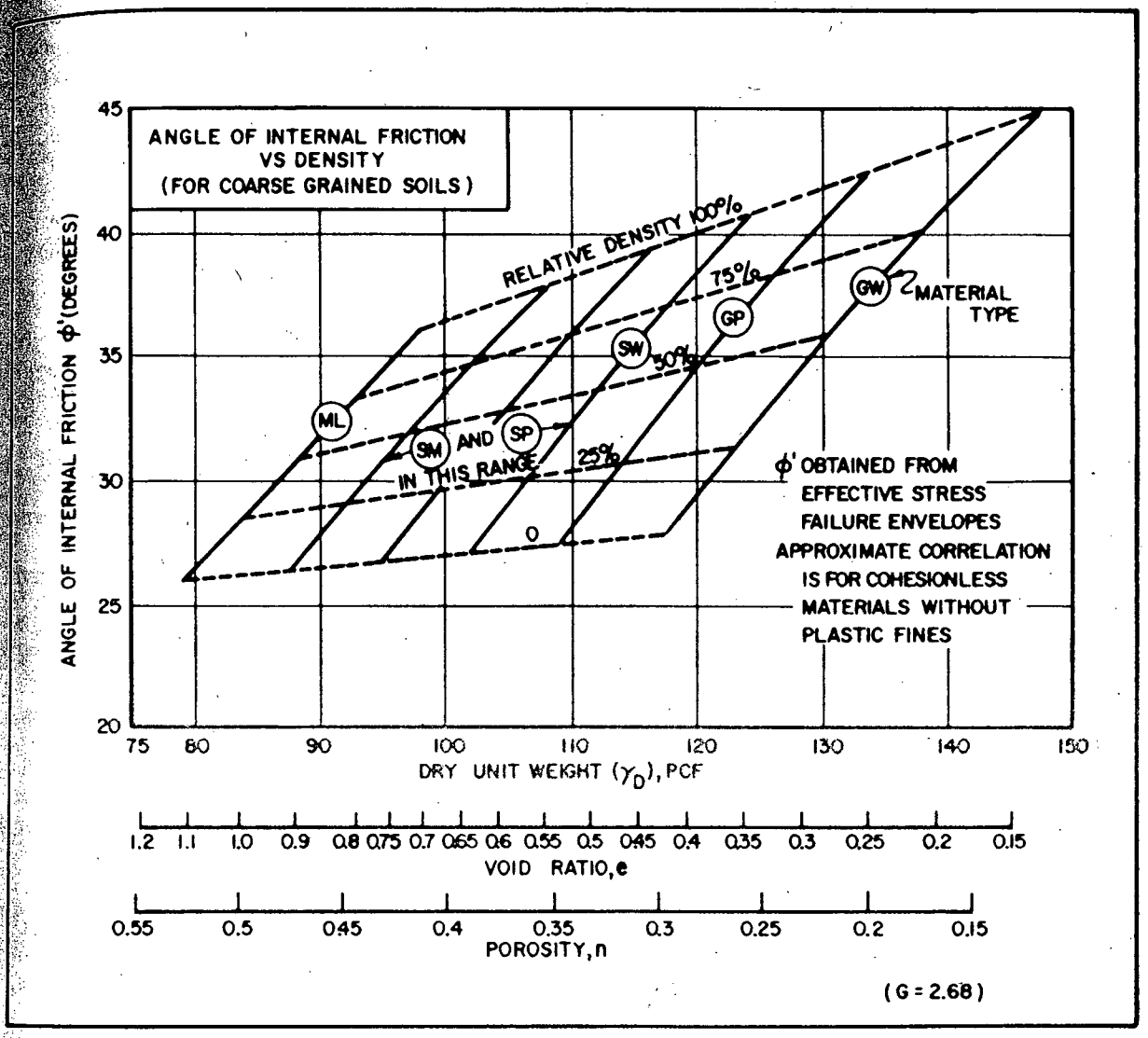

FIGURE 7
Correlations of Strength Characteristics for Granular Soils

ATTACHMENT G
Stabl Computer Program Methods

STABL FOR WINDOWS 2.0
MANUAL

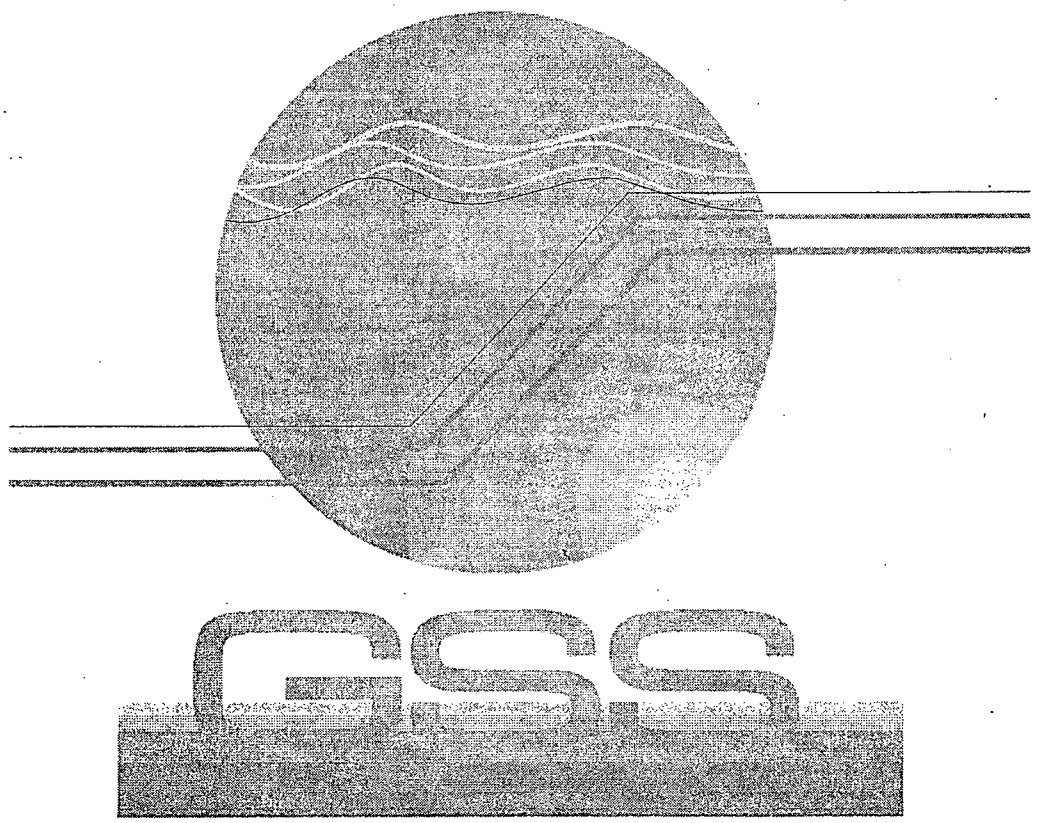

GEOTECHNICAL SOFTWARE
SOLUTIONS
2003

STABL FOR WINDOWS
VERSION 2.0
USER'S MANUAL

BISHOP'S SIMPLIFIED METHOD

The Bishop Simplified Method was initially developed for circular slip surfaces, but it can be applied for non-circular slip surfaces by adopting a fictional center of rotation. This method neglects the vertical components of the interslice forces and satisfies moment equilibrium only. Figure A1 shows the forces acting on a slice including tieback and reinforcement loads. The total normal force ΔN' is assumed to act at the center of the base of each slice, and it is determine by imposing equilibrium of vertical forces on each slice (Figure A1) as follows:

$$\Delta U_{\beta}\cos\beta + \Delta Q\cos\delta + \Delta W(1-k_v) + (\Delta T_{NORM} - \Delta N' - \Delta U_{\alpha})\cos\alpha - (\Delta T_{TAN}) + \Delta S_r)\sin\alpha = 0 \quad \text{(E1)}$$

in which: ΔN' and ΔS_r = effective normal force and mobilized resisting shear force, respectively, on the base of each slice; ΔU_{α} and ΔU_{β} = water force acting on base and top of the slice; ΔW = weight of the slice soil mass; k_v = vertical earthquake coefficient; ΔQ = resultant of uniform surcharge acting on the slice top; ΔT_{NORM} and ΔT_{TAN} = normal and tangential forces acting on the midpoint of the base of the slice produced by all rows of tiebacks or/and by soil reinforcement, whatever applies; α = inclination of shear surface with respect to the horizontal; β = slope inclination angle; δ = inclination of the uniform surcharge acting on the slice top, measured positive counterclockwise from the vertical.

Based on the Mohr-Coulomb's criterion, ΔS_r can be written as:

$$\Delta S_r = \frac{C' + \Delta N' \tan\phi'}{FS} \quad \text{(E2)}$$

$$C' = \frac{c' DX}{\cos\alpha} \quad \text{(E3)}$$

in which C' = cohesion force at the slice base; FS = factor of safety; c' and ϕ' = effective soil strength parameters; DX = slice width.

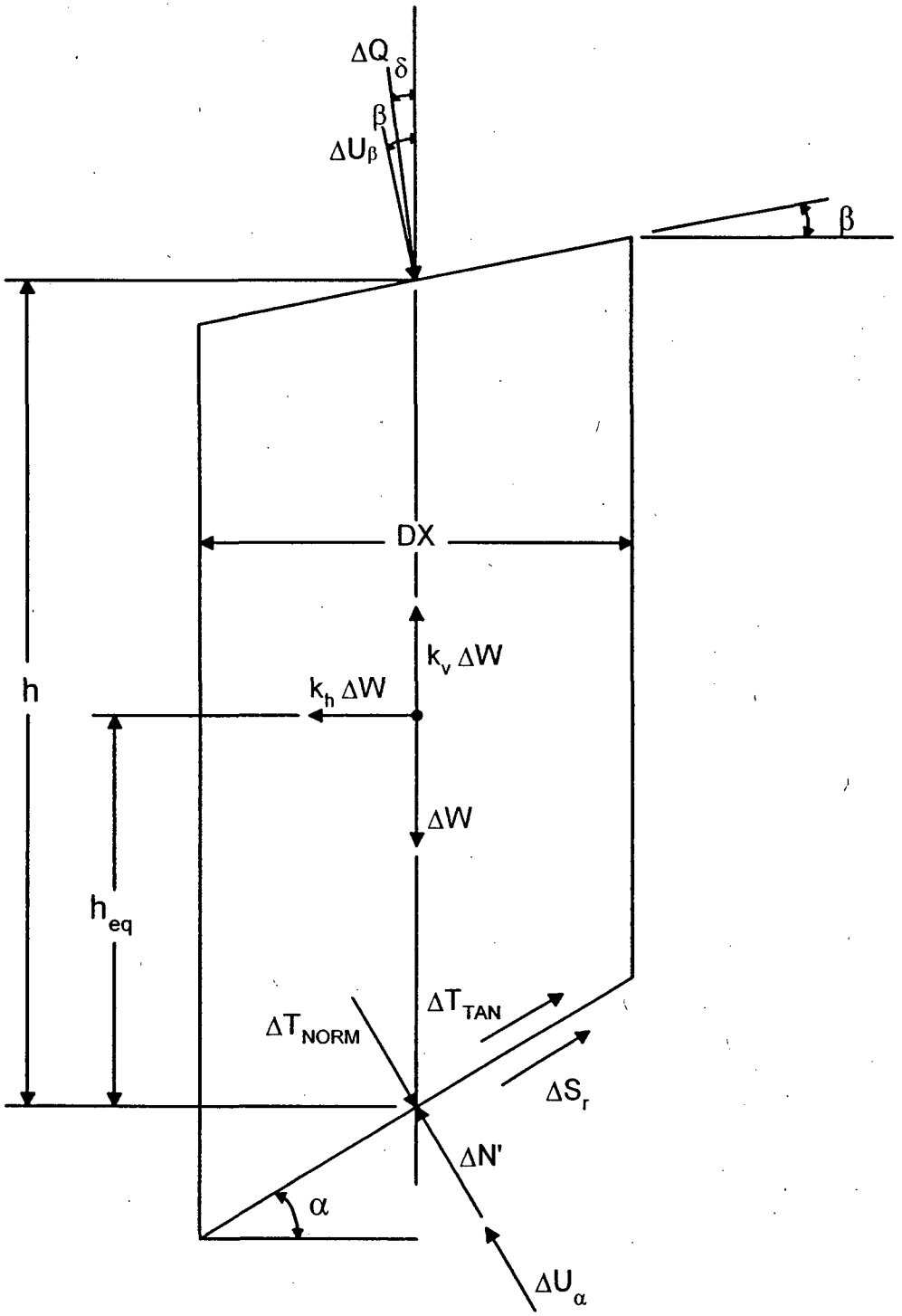

Figure A1. Slice forces considered by the Bishop and Janbu methods

Substituting (E2) and (E3) into (E1), and solving for ΔN':

$$\Delta N' = \frac{\Delta U_\beta \cos\beta + \Delta Q \cos\delta + \Delta W(1-k_v) + (\Delta T_{NORM} - \Delta U_\alpha)\cos\alpha - \Delta T_{TAN} \sin\alpha - \frac{C' \sin\alpha}{FS}}{\cos\alpha + \frac{\tan\phi' \sin\alpha}{FS}} \quad \text{(E4)}$$

Overall moment equilibrium of forces acting on the sliding circular slip surface is given by the expression:

$$\sum_{i=1}^{n} \{\{[\Delta W(1-k_v) + \Delta U_\beta \cos\beta + \Delta Q \cos\delta](R \sin\alpha)\} - [(\Delta S_r + \Delta T_{TAN})R] - [(\Delta U_\beta \sin\beta + \Delta Q \sin\delta)(R\cos\alpha - h)] + [\Delta W k_h (R\cos\alpha - h_{eq})]\} = 0 \quad \text{(E5)}$$

where: R = distance from center of rotation about which moments are summed to the center of each slice; k_h = horizontal earthquake coefficient; h = height of the slice at midpoint; h_{eq} = vertical distance from point of application of k_h to the slice base; n = number of slices.

The Bishop Simplified Method assumes that FS is the same for each slice. Substituting (E2) and (E4) into (E5), and solving for FS, it is obtained the expression for FS:

$$FS = \frac{\sum_{i=1}^{n} \left| \frac{A_1}{1 + \frac{A_2}{FS}} \right|}{\sum_{i=1}^{n} (A_3 - A_4 + A_5 - A_6)} \quad \text{(E6)}$$

in which:

$$A_1 = C' + \tan\phi' \sec\alpha \left[\Delta W(1-k_v) + (\Delta T_{NORM} - \Delta U_\alpha)\cos\alpha + \Delta U_\beta \cos\beta + \Delta Q \cos\delta - \Delta T_{TAN} \sin\alpha\right] \quad \text{(E7)}$$

$$A_2 = \tan\alpha \tan\phi' \quad \text{(E8)}$$

$$A_3 = \left[\Delta W(1-k_v) + \Delta U_\beta \cos\beta + \Delta Q \cos\delta\right] \sin\alpha \quad \text{(E9)}$$

$$A_4 = \left(\Delta U_\beta + \Delta Q \sin\delta\right)\left(\cos\alpha - \frac{h}{R}\right) \tag{E10}$$

$$A_5 = \Delta W\, k_h \left(\cos\alpha - \frac{h_{eq}}{R}\right) \tag{E11}$$

$$A_6 = \Delta T_{TAN} \tag{E12}$$

JANBU SIMPLIFIED METHOD

The Janbu Simplified Method assumes that the failure occurs by sliding of a block of soil on a non-circular slip surface. Also, in this method the interslice shear forces are assumed to be zero. Thus, the expression for the effective normal force ΔN' on the base of each slice is the same as that obtained for the Bishop Simplified Method (Eq. 11).

Overall equilibrium of horizontal forces (Figure A1) is given by the expression:

$$\sum_{i=1}^{n} \{\Delta S_r \cos a - \Delta N' \sin a + \Delta Q \sin\delta + \Delta U_\beta \sin\beta - k_h \Delta W + \Delta T_{TAN} \cos a + \Delta T_{NORM} \sin a - \Delta U_a \sin a\} = 0 \tag{E13}$$

The Janbu Simplified Method assumes that FS is the same for each slice. Substituting (E2) into (E4), and solving (E13) for FS, it is obtained the expression for the factor of safety:

$$FS = \frac{\sum_{i=1}^{n} \left| \frac{B_1}{1 + \frac{B_2}{FS}} \right|}{\sum_{i=1}^{n} B_3} \tag{E14}$$

in which:

$$B_1 = \frac{C' + \tan\phi' \sec\alpha \left[\Delta W\,(1 - k_v) - \Delta T_{TAN}\ \sin\alpha + (\Delta T_{NORM} - \Delta U_\alpha)\cos\alpha + \Delta U_\beta\ \cos\beta + \Delta Q\ \cos\delta\right]}{\cos\alpha} \tag{E15}$$

$$B_2 = \tan\alpha\ \tan\phi' \tag{E16}$$

$$B_3 = \left[\Delta W(\tan\alpha + k_h - k_v\ \tan\alpha) + \Delta U_\beta\ (\cos\beta\ \tan\alpha - \sin\beta) + \Delta Q\ (\cos\delta \tan\alpha - \sin\delta) - \frac{\Delta T_{TAN}}{\cos\alpha}\right] \tag{E17}$$

Since the Bishop Simplified and the Janbu Simplified Methods assume that the factor of safety on each slice is the same, results from (E6) and (E14) are average FS for all the slices. This assumption implies that each slice must fail simultaneously.

Boutrup (1977) found that STABL with the Janbu Simplified Method may give non conservative and erroneous results for slip surfaces that intersect the top of the slope at steep angles, and where the strength of the soil is defined mainly in terms of strength intercept c'. Since this problem arose mainly for deep circular failure surfaces, it was solved by including in the STABL program the Bishop Simplified solution, applicable to circular slip surfaces. It is recommended that the Simplified Bishop Method be used for circular slip surfaces (use CIRCL2 instead of CIRCLE). Precautions should be taken if a similar situation occurs for irregularly shaped slip surfaces. In any case, it is advisable to make a preliminary estimate of the factor of safety by means of simple slope stability charts for homogeneous slopes (averaging soil parameters, etc.).

SPENCER'S METHOD

Spencer's Method of slices has been incorporated into STABL to enhance the versatility of the program. Spencer's Method is a limiting equilibrium method which satisfies both force and moment equilibrium of a sliding mass of soil, whereas the Janbu Simplified and the Bishop Simplified Methods satisfy only force or moment equilibrium, respectively.

Description of Spencer's Method

Spencer's Method was first developed for circular slip surfaces, assuming parallel interslice side forces inclined at a constant angle, θ, on each slice (Figure A2). This method was later extended to general or irregular failure surfaces. The factor of safety,

FS, on each slice is assumed to be the same such that all slices of the sliding mass will fail simultaneously. The interslice forces acting at both sides of each slide can be replaced with a single statically equivalent resultant interslice force, QF, acting through the midpoint of the base of the slice and inclined at an angle, θ. The method also assumes a constant inclination of the resultant force, QF, throughout the slope.

The equilibrium equations for the forces normal and tangent to the base of each slice are (Figure A2), respectively (Carpenter 1985):

$$\Delta N' + \Delta U_{\alpha} + QF \sin(\alpha - \theta) + \Delta W[k_h \sin\alpha - (1 - k_v)\cos\alpha]$$

$$- \Delta U_{\beta} \cos(\alpha - \beta) - \Delta Q \cos(\alpha - \delta) - \Delta T_{NORM} = 0$$

(E18)

$$\Delta S_r - QF \cos(\alpha - \theta) - \Delta W[(1 - k_v)\sin\alpha - k_h \cos\alpha]$$

$$+ \Delta U_{\beta} \sin(\alpha - \beta) + \Delta Q \sin(\alpha - \delta) + \Delta T_{TAN} = 0$$

(E19)

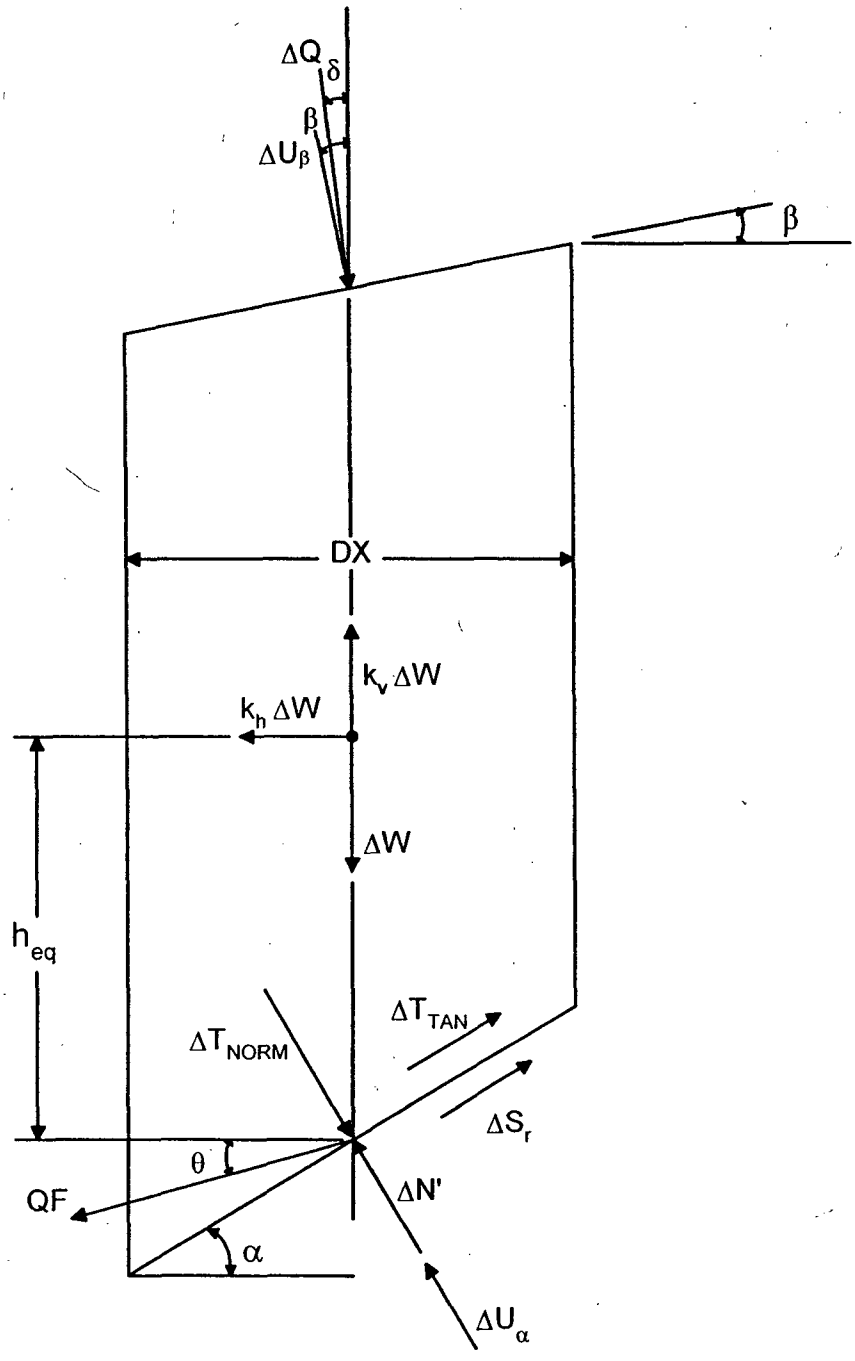

Figure A2. Slice forces considered by Spencer's method

From (E18) the effective normal force ΔN' acting on the base of each slice is found to be equal to:

$$\Delta N' = \Delta W[(1 - k_v)\cos\alpha - k_h \sin\alpha)] - \Delta U_\alpha + \Delta U_\beta \cos(\alpha - \beta) + \Delta Q\cos(\alpha - \delta) - QF \sin(\alpha - \theta) + \Delta T_{NORM} \quad \text{(E20)}$$

Combining (E2) and (E20) into (E19), and solving for QF, it is obtained the following expression:

$$QF = \frac{\frac{S_1}{FS} + S_2}{\cos(\alpha - \theta)\left(1 + \frac{S_3}{FS}\right)} \quad \text{(E21)}$$

where:

$$S_1 = C' + \tan\phi' \{\Delta W[(1 - k_v)\cos\alpha - k_h \sin\alpha] - \Delta U_\alpha + \Delta U_\beta \cos(\alpha - \beta) + \Delta Q\cos(\alpha - \delta) + \Delta T_{NORM})\} \quad \text{(E22)}$$

$$S_2 = \Delta U_\beta \sin(\alpha - \beta) - \Delta W[(1 - k_v)\sin\alpha + k_h \cos\alpha] + \Delta Q\sin(\alpha - \delta) + \Delta T_{TAN}) \quad \text{(E23)}$$

$$S_3 = \tan\phi' \tan(\alpha - \theta) \quad \text{(E24)}$$

Overall moment and force equilibrium are satisfied by the conditions:

$$\sum_{i=1}^{n} QF = 0 \quad \text{(E25)}$$

$$\sum_{i=1}^{N} M_{external\ forces} = 0$$

Thus

$$\begin{aligned} &\sum_{i=1}^{n}[(\Delta N' + \Delta U_a - T_{NORM})(\cos a \cdot (x_{pol} - x_b) + \sin a(y_{pol} - y_b)) + \\ &+ (\Delta S_r + \Delta T_{TAN})(\sin a \cdot (x_{pol} - x_b) - \cos a(y_{pol} - y_b)) - \Delta W(1 - k_v)(x_{pol} - x_b) + \\ &+ k_h \Delta W(y_{pol} - y_b - h_{eq}) - \Delta U_\beta(\cos\beta \cdot (x_{pol} - x_b) + \sin\beta(y_{pol} - y_b - h)) - \\ &- \Delta Q(\cos\delta \cdot (x_{pol} - x_b) + \sin\delta(y_{pol} - y_b - h))] = 0 \end{aligned} \quad \text{(E26)}$$

where h it is the height of the individual slice, (x_b, y_b) are the coordinates of the midpoint of the slice base, and (x_{pol}, y_{pol}) are the coordinates of an arbitrary pole.

The moments of the external forces are taken with respect to the arbitrary pole. To facilitate the convergence of the algorithm that calculates the F.S., the pole is chosen to be the center of the circle passing through 3 points: the 2 endpoints and the midpoint of the trial slip surface. For the case of circular trial slip surfaces, the pole coincides with the center of the circular slip surface.

Two FS values are obtained when (E25) and (E26) are solved for each assumed value of θ. The solution is reached by iteration when a unique value of FS, and its corresponding θ, that satisfies both force and moment equilibrium is found. More detailed information concerning the derivation and method of solution of Spencer's method of slices implemented in STABL5M, PCSTABL5M, PCSTABL5M2, and PCSTABL6 may be found in Carpenter (1985, 1986). Given that PCSTABL6 assumes parallel interslice forces, the F.S. calculations may not converge for certain trial slip surfaces, especially in cases of very irregular slip surfaces and/or high seismic coefficients. For randomly generated slip surfaces, STABL reports the number of convergent and non-convergent trials in the output file.

SPENCR Option

Analyses using Spencer's method use an optional scheme that generates irregular trial slip surfaces with no reverse curvature at any point of the surfaces. Unless the user judges that slip surfaces with reverse curvature are essential for the analysis of a specific problem, the command RANSP2 should be used, since it facilitates the convergence of Spencer's method and makes the search for the critical F.S. more efficient.

Significantly more computation time is required for analysis of potential slip surfaces using Spencer's method of slices than either the Bishop Simplified or the Janbu Simplified methods. The use most efficient use of the **STABL for Windows** capabilities will be realized if the user first investigates a number of potential slip surfaces using one of STABL's random slip surface generation techniques, which determine the factor of safety using either the Janbu Simplified or the Bishop Simplified Methods of slices. Once the critical region of the slope has been identified, the search can be narrowed using the SPENCR option to obtain a factor of safety (FS) satisfying both force and moment equilibrium equations, *i.e.*, complete equilibrium. It is important to remember that the critical slip surface found using Janbu or Bishop's methods, does not correspond to the critical slip surface found using Spencer. Thus the user should not simply re-analyze the

critical slip surface found using one of the simplified methods with a more accurate method, but instead re-run the search.

Analysis and design of veneer cover soils

R. M. Koerner[1] and T.-Y. Soong[2]

[1]*Emeritus Proffesor, Drexel University and Director, Geosynthetic Research Institute, 475 Kedron Avenue, Folsom, PA 19033-1208, USA, Telephone: +1 610 522 8440, Telefax: +1 610 522 8441, E-mail: robert.koerner@coe.drexel.edu*
[2]*CTI and Associates, 12842 Emerson Drive, Brighton, MI 48116, USA; Telephone: +1 248 846 5100, Telefax: +1 248 846 5101, E-mail: tsoong@cti-assoc.com*

Received 10 July 2003, accepted 10 July 2003

ABSTRACT: Cover soil sliding on slopes underlain by geosynthetics is obviously an unacceptable situation and, if the number of occurrences becomes excessive, can eventually reflect poorly on the entire technology. Steeply sloped leachate collection layers and final covers of landfills are situations where incidents of such sliding have occurred. Paradoxically, the analytic formulation of the situation is quite straightforward. This paper presents an analysis of the common problem of a veneer of cover soil (0.3 to 1.0 m thick) on a geosynthetic material at a given slope angle and length. The paper then presents different scenarios that create lower FS (factor of safety) -values than the gravitational stresses of the above situation, e.g. equipment loads, seepage forces and seismic loads. As a counterpoint, different scenarios that create higher FS-values also are presented, e.g. toe berms, tapered thicknesses and veneer reinforcement. In this latter category, a subdivision is made into intentional reinforcement (using geogrids or high-strength geotextiles) and non-intentional reinforcement (cases where geosynthetics overlay a weak interface within a multilined slope). A standard numeric example is used in each of the above situations to illustrate the various influences on the resulting FS-value. In many cases, design curves are also formulated. Suggested minimum FS-values are presented for final closures of landfills, waste piles, leach pads, etc., which are the situations where veneer slides of this type are the most serious. Hopefully, the paper will serve as a vehicle to bring a greater awareness to this situation so as to avert such slides from occurring in the future. Note: This paper was initially published as the Giroud Lecture in the *Proceedings of the Sixth International Geosynthetics Conference* held in Atlanta, USA, in 1998.

KEYWORDS: Geosynthetics, Analysis, Design, Limit equilibrium methods, Steep slopes, Veneer stability

REFERENCE: Koerner, R. M. & Soong, T-Y. (2005). Analysis and design of veneer cover soils. *Geosynthetics International*, Special Issue on the Giroud Lectures, **12**, No. 1, 28–49

1. INTRODUCTION

There have been numerous cover soil stability problems in the past, resulting in slides that range from being relatively small (which can be easily repaired), to very large (involving litigation and financial judgments against the parties involved). Furthermore, the number of occurrences appears to have increased over the past few years. Soong and Koerner (1996) report on eight cover soil failures resulting from seepage-induced stresses alone. While such slides can occur in transportation and geotechnical applications, it is in the environmental applications area where they are most frequent. Specifically, the sliding of relatively thin cover soil layers (called 'veneer') above both geosynthetic and natural soil liners, i.e. geomembranes (GM), geosynthetic clay liners (GCL) and compacted clay liners (CCL), are the particular materials of concern. These situations represent a major challenge due (in part) to the following reasons:

- The underlying barrier materials generally represent a low interface shear strength boundary with respect to the soil placed above them.
- The liner system is oriented precisely in the direction of potential sliding.
- The potential shear planes are usually linear and are essentially uninterrupted along the slope.
- Liquid (water or leachate) cannot continue to percolate downward through the cross-section owing to the presence of the barrier material.

When such slopes are relatively steep and uninterrupted in

their length (which is the design goal for landfills, waste piles and surface impoundments so as to maximize containment space and minimize land area), the situation is exacerbated.

There are two specific applications in which cover soil stability has been difficult to achieve in light of this discussion;

- leachate collection soil placed above a GM, GCL and/or CCL along the sides of a landfill before waste is placed and stability achieved accordingly;
- final cover soil placed above a GM, GCL and/or CCL in the cap or closure of a landfill or waste pile after the waste has been placed to its permitted height.

For the leachate collection soil situation the time frame is generally short (from months to a few years), and the implications of a slide may be minor in that repairs can sometimes be done by on-site personnel. For the final cover soil situation the time frame is invariably long (from decades to centuries), and the implications of a slide can be serious in that repairs often call for a forensic analysis, engineering redesign, separately engaged contractors and quite high remediation costs. These latter cases sometime involve litigation, insurance carriers, and invariably technical experts, thus becoming quite contentious.

Since both situations (leachate collection and final covers) present the same technical issues, the paper will address them simultaneously. It should be realized, however, that the final cover situation is of significantly greater concern.

In the sections to follow, geotechnical engineering considerations will be presented leading to the goal of establishing a suitable factor of safety against slope instability. A number of common situations will then be analyzed, all of which have the tendency to decrease stability. A number of design options will follow, all of which have the objective of increasing stability. A summary and conclusions section will counterpoint the various situations which tend to either create slope instability or aid in slope stability. It is hoped that an increased awareness of the analysis and design details offered herein, and elsewhere, will lead to a significant decrease in the number of veneer cover soil slides that have occurred.

2. GEOTECHNICAL ENGINEERING CONSIDERATIONS

As just mentioned, the potential failure surface for veneer cover soils is usually linear with cover soil sliding with respect to the lowest interface friction layer in the underlying cross-section. The potential failure plane being linear allows for a straightforward stability calculation without the need for trial center locations and different radii, as with soil stability problems analyzed by rotational failure surfaces. Furthermore, full static equilibrium can be achieved without solving simultaneous equations or making simplified design assumptions.

2.1. Limit equilibrium concepts

The free body diagram of an infinitely long slope with uniformly thick cohesionless cover soil on an incipient planar shear surface, like the upper surface of a geomembrane, is shown in Figure 1. The situation can be treated quite simply. By taking force summation parallel to the slope and comparing the resisting force with the driving or mobilizing force, a global factor of safety (FS) results:

$$\mathrm{FS} = \frac{\sum \text{Resisting forces}}{\sum \text{Driving forces}} \tag{1a}$$

$$= \frac{N \tan\delta}{W \sin\beta} = \frac{W \cos\beta \tan\delta}{W \sin\beta}$$

Hence:

$$\mathrm{FS} = \frac{\tan\delta}{\tan\beta} \tag{1b}$$

Here it is seen that the FS-value is the ratio of tangents of the interface friction angle of the cover soil against the upper surface of the geomembrane (δ), and the slope angle of the soil beneath the geomembrane (β). As simple as this analysis is, its teachings are very significant. For example:

- To obtain an accurate FS-value, an accurately determined laboratory δ-value is absolutely critical. The accuracy of the final analysis is only as good as the accuracy of the laboratory-obtained δ-value.
- For low δ-values, the resulting soil slope angle will be proportionately low. For example, for a δ-value of 20°, and a required FS-value of 1.5, the maximum slope angle is 14°. This is equivalent to a 4(H) on 1(V) slope, which is relatively low. Furthermore, many geomembranes have even lower δ-values than 20°.
- This simple formula has driven geosynthetic manufacturers to develop products with high δ-values, e.g. textured geomembranes, thermally bonded drainage geocomposites, internally reinforced GCLs, etc.

Unfortunately, the above analysis is too simplistic to use in most realistic situations. For example, the following situations cannot be accommodated:

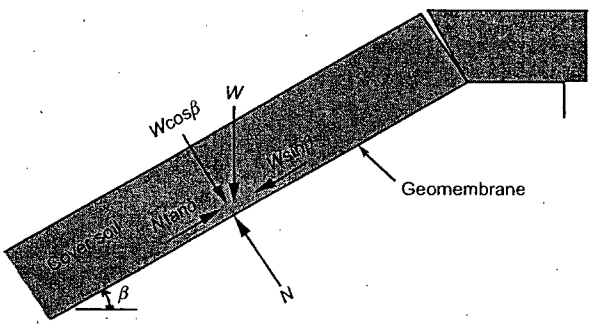

Figure 1. Limit equilibrium forces involved in an infinite slope analysis for a uniformly thick cohesionless cover soil

- a finite-length slope with the incorporation of a passive soil wedge at the toe of the slope;
- the incorporation of equipment loads on the slope;
- consideration of seepage forces within the cover soil;
- consideration of seismic forces acting on the cover soil;
- the use of soil masses acting as toe berms;
- the use of tapered covered soil thicknesses;
- reinforcement of the cover soil using geogrids or high-strength geotextiles.

These specific situations will be treated in subsequent sections. For each situation, the essence of the theory will be presented, followed by the necessary design equations. This will be followed, in each case, with a design graph and a numeric example. First, however, the important issue of interface shear testing will be discussed.

2.2. Interface shear testing

The interface shear strength of a cover soil with respect to the underlying material (often a geomembrane) is critical to properly analyze the stability of the cover soil. This value of interface shear strength is obtained by laboratory testing of the project-specific materials at the site-specific conditions. By project-specific materials, we mean sampling of the candidate geosynthetics to be used at the site, as well as the cover soil at its targeted density and moisture conditions. By site-specific conditions we mean normal stresses, strain rates, peak or residual shear strengths and temperature extremes (high and/or low). Note that it is completely inappropriate to use values of interface shear strengths from the literature for final cover soil design.

While the above list of items is formidable, at least the type of test is established. It is the direct shear test which has been utilized in geotechnical engineering testing for many years. The test has been adapted to evaluate geosynthetics and is designated as ASTM D5321 or ISO 12957.

In conducting a direct shear test on a specific interface, one typically performs three replicate tests, with the only variable being different values of normal stress. The middle value is usually targeted to the site-specific condition, with a lower and higher value of normal stress covering the range of possible values. These three tests result in a set of shear displacement against shear stress curves: see Figure 2a. From each curve, a peak shear strength (τ_p) and a residual shear strength (τ_r) is obtained. As a next step, these shear strength values, together with their respective normal stress values, are plotted in Mohr–Coulomb stress space to obtain the shear strength parameters of friction and adhesion: see Figure 2b.

The points are then connected (usually with a straight line), and the two fundamental shear strength parameters are obtained. These shear strength parameters are: δ, the angle of shearing resistance, peak and/or residual, of the two opposing surfaces (often called the interface friction angle); and c_a, the adhesion of the two opposing surfaces, peak and/or residual (synonymous with cohesion when testing fine-grained soils).

Each set of parameters constitutes the equation of a straight line, which is the Mohr–Coulomb failure criterion common to geotechnical engineering. The concept is readily adaptable to geosynthetic materials in the following form:

$$\tau_p = c_{ap} + \sigma_n \tan \delta_p \quad (2a)$$

$$\tau_r = c_{ar} + \sigma_n \tan \delta_r \quad (2b)$$

The upper limit of δ when soil is involved as one of the interfaces is ϕ, the angle of shearing resistance of the soil component. The upper limit of the c_a value is c, the cohesion of the soil component. In the slope stability analyses to follow, the c_a term will be included for the sake of completeness, but then it will be neglected (as being a conservative assumption) in the design graphs and numeric examples. To utilize an adhesion value, there must be a clear physical justification for the use of such values when geosynthetics are involved. Only unique situations such as textured geomembranes with physical interlocking of soils having cohesion, or the bentonite component of a GCL, are valid reasons for including such a term.

Note that residual strengths are equal to, or lower, than peak strengths. The amount of difference is very dependent on the material, and no general guidelines can be given. Clearly, material-specific and site-specific direct shear tests must be performed to determine the appropriate values. Further, each direct shear test must be conducted to a relatively large displacement to determine the residual behavior (Stark and Poeppel 1994). The decision as to the use of peak or residual strengths in the subsequent analy-

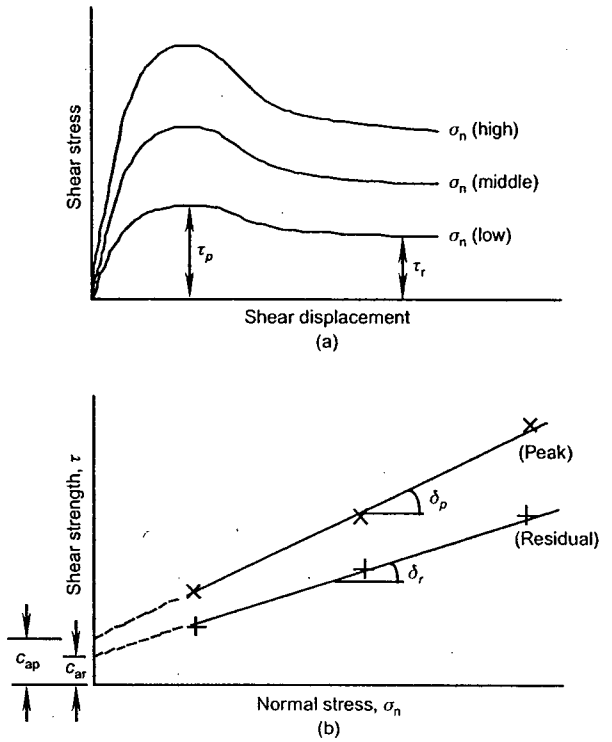

Figure 2. Direct shear test results and method of analysis to obtain shear strength parameters: (a) direct shear test data; (b) Mohr–Coulomb stress space

sis is a very subjective one. It is both a materials-specific and site-specific issue, which is left up to the designer and/or regulator. Even further, the use of peak values at the crest of a slope and residual values at the toe may be justified. As such, the analyses to follow will use an interface δ-value with no subscript, thereby concentrating on the computational procedures rather than this particular detail. However, the importance of an appropriate and accurate δ-value should not be minimized.

Owing to the physical structure of many geosynthetics, the size of the recommended shear box is quite large. It must be at least 300 mm by 300 mm, unless it can be shown that data generated by a smaller device contain no scale or edge effects, i.e. that no bias exists with a smaller shear box. The implications of such a large shear box should not be taken lightly. Some issues which should receive particular attention are the following:

- Unless it can be justified otherwise, the interface will usually be tested in a saturated state. Thus complete and uniform saturation over the entire specimen area must be achieved. This is particularly necessary for CCLs and GCLs (Daniel *et al.* 1993). Hydration takes relatively long in comparison with soils in conventional (smaller) testing shear boxes.
- Consolidation of soils (including CCLs and GCLs) in larger shear boxes is similarly affected.
- Uniformity of normal stress over the entire area must be maintained during consolidation and shearing so as to avoid stress concentrations from occurring.
- The application of relatively low normal stresses, e.g. 10 to 30 kPa simulating typical cover soil thicknesses, challenges the accuracy of some commercially available shear box setups and monitoring systems, particularly the accuracy of pressure gages.
- Shear rates necessary to attain drained conditions (if this is the desired situation) are extremely slow, requiring long testing times.
- Deformations necessary to attain residual strengths require large relative movement of the two respective halves of the shear box. So as not to travel over the edges of the opposing shear box sections, devices should have the lower shear box significantly longer than 300 mm. However, with a lower shear box longer than the upper traveling section, new surface is constantly being added to the shearing plane. This influence is not clear in the material's response or in the subsequent behavior.
- The attainment of a true residual strength is difficult to achieve. ASTM D5321 states that one should 'run the test until the applied shear force remains constant with increasing displacement'. Many commercially available shear boxes have insufficient travel to reach this condition.
- The ring torsion shearing apparatus is an alternative device to determine true residual strength values, but is not without its own problems. See Stark and Poeppel (1994) for information and data using this alternative test method.

2.3. Various types of loading

There are a large variety of slope stability problems that may be encountered in analyzing and/or designing final covers of engineered landfills, abandoned dumps and remediation sites as well as leachate collection soils covering geomembranes beneath the waste. Perhaps the most common situation is a uniformly thick cover soil on a geomembrane placed over the subgrade at a given and constant slope angle. This 'standard' problem will be analyzed in the next section. A variation of this problem will include equipment loads used during placement of cover soil on the geomembrane. This problem will be solved with equipment moving up the slope and then moving down the slope.

Unfortunately, cover soil slides have occurred, and it is felt that the majority of the slides have been associated with seepage forces. Indeed, drainage above a geomembrane (or other barrier material) in the cover soil cross-section must be accommodated to avoid the possibility of seepage forces. A section will be devoted to this class of slope stability problems.

Lastly, the possibility of seismic forces exists in earthquake-prone locations. If an earthquake occurs in the vicinity of an engineered landfill, abandoned dump or remediation site, the seismic wave travels through the solid waste mass, reaching the upper surface of the cover. It then decouples from the cover soil materials, producing a horizontal force, which must be appropriately analyzed. A section will be devoted to the seismic aspects of cover soil slope analysis as well.

All of the above actions are destabilizing forces tending to cause slope instability. Fortunately, there are a number of actions that can be taken to increase the stability of slopes.

Other than geometrically redesigning the slope with a flatter slope angle or shorter slope length, a designer can always use geogrids or high-strength geotextiles within the cover soil acting as reinforcement materials. This technique is usually referred to as 'veneer reinforcement'. Additionally, the designer can add soil mass at the toe of the slope, thereby enhancing stability. Both toe berms and tapered soil slopes are available options and will be analyzed accordingly.

Thus it is seen that a number of strategies influence slope stability. Each will be described in the sections to follow. First, the basic gravitational problem will be presented, followed by those additional loading situations which tend to decrease slope stability. Second, various actions that can be taken by the designer to increase slope stability will be presented. The summary will contrast the FS-values obtained in the similarly crafted numeric examples.

3. SITUATIONS CAUSING DESTABILIZATION OF SLOPES

This section treats the standard slope stability problem and then superimposes upon it a number of situations, all of which tend to destabilize slopes. Included are gravita-

tional, construction equipment, seepage and seismic forces. Each will be illustrated by a design graph and a numeric example.

3.1. Cover soil (gravitational) forces

Figure 3 illustrates the common situation of a finite length, uniformly thick cover soil placed over a liner material at a slope angle β. It includes a passive wedge at the toe and has a tension crack of the crest. The analysis that follows is after Koerner and Hwu (1991), but comparable analyses are available from Giroud and Beech (1989), McKelvey and Deutsch (1991) and others.

The symbols used in Figure 3 are defined as: W_A = total weight of the active wedge; W_P = total weight of the passive wedge; N_A = effective force normal to the failure plane of the active wedge; N_P = effective force normal to the failure plane of the passive wedge; γ = unit weight of the cover soil; h = thickness of the cover soil; L = length of slope measured along the geomembrane; β = soil slope angle beneath the geomembrane; ϕ = friction angle of the cover soil; δ = interface friction angle between cover soil and geomembrane; C_a = adhesive force between cover soil of the active wedge and the geomembrane; c_a = adhesion between cover soil of the active wedge and the geomembrane; C = cohesive force along the failure plane of the passive wedge; c = cohesion of the cover soil; E_A = interwedge force acting on the active wedge from the passive wedge; E_p = interwedge force acting on the passive wedge from the active wedge; and FS = factor of safety against cover soil sliding on the geomembrane.

The expression for determining the factor of safety can be derived as follows. Considering the active wedge:

$$W_A = \gamma h^2 \left(\frac{L}{h} - \frac{1}{\sin\beta} - \frac{\tan\beta}{2} \right) \tag{3}$$

$$N_A = W_A \cos\beta \tag{4}$$

$$C_a = c_a \left(L - \frac{h}{\sin\beta} \right) \tag{5}$$

By balancing the forces in the vertical direction, the following formulation results:

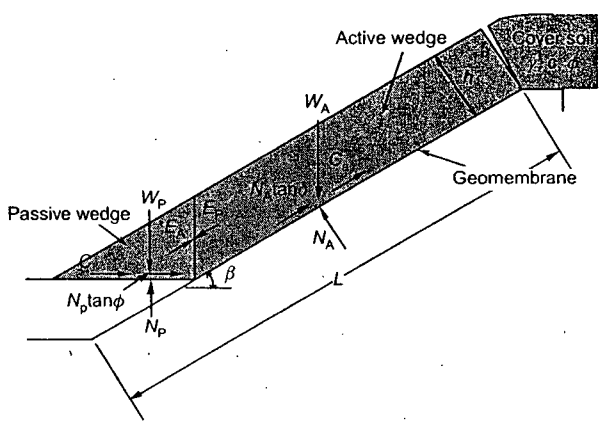

Figure 3. Limit equilibrium forces involved in a finite length slope analysis for a uniformly thick cover soil

$$E_A \sin\beta = W_A - N_A \cos\beta - \frac{N_A \tan\delta + C_a}{FS} \sin\beta \tag{6}$$

Hence the interwedge force acting on the active wedge is

$$E_A = \frac{(FS)(W_A - N_A \cos\beta) - (N_A \tan\delta + C_a)\sin\beta}{\sin\beta (FS)} \tag{7}$$

The passive wedge can be considered in a similar manner:

$$W_P = \frac{\gamma h^2}{\sin 2\beta} \tag{8}$$

$$N_p = W_P + E_P \sin\beta \tag{9}$$

$$C = \frac{ch}{\sin\beta} \tag{10}$$

By balancing the forces in the horizontal direction, the following formulation results:

$$E_P \cos\beta = \frac{C + N_P \tan\phi}{FS} \tag{11}$$

Hence the interwedge force acting on the passive wedge is

$$E_P = \frac{C + W_P \tan\phi}{\cos\beta (FS) - \sin\beta \tan\phi} \tag{12}$$

By setting $E_A = E_P$, the resulting equation can be arranged in the form of the quadratic equation $ax^2 + bx + c = 0$, which in our case, using FS-values, is

$$a(FS)^2 + b(FS) + c = 0 \tag{13}$$

where

$$\begin{aligned} a &= (W_A - N_A \cos\beta)\cos\beta \\ b &= -[(W_A - N_A \cos\beta)\sin\beta \tan\phi \\ &\quad + (N_A \tan\delta + C_a)\sin\beta\cos\beta \\ &\quad + \sin\beta (C + W_P \tan\phi)] \\ c &= (N_A \tan\delta + C_a)\sin^2\beta \tan\phi \end{aligned} \tag{14}$$

The resulting FS-value is then obtained from the solution of the quadratic equation:

$$FS = \frac{-b + \sqrt{b^2 - 4ac}}{2a} \tag{15}$$

When the calculated FS-value falls below 1.0, sliding of the cover soil on the geomembrane is to be anticipated. Thus a value of greater than 1.0 must be targeted as being the minimum factor of safety. How much greater than 1.0 the FS-value should be, is a design and/or regulatory issue. The issue of minimum allowable FS-values under different conditions will be assessed at the end of the paper. In order to better illustrate the implications of Equations 13, 14 and 15, typical design curves for various FS-values as a function of slope angle and interface friction angle are given in Figure 4. Note that the curves

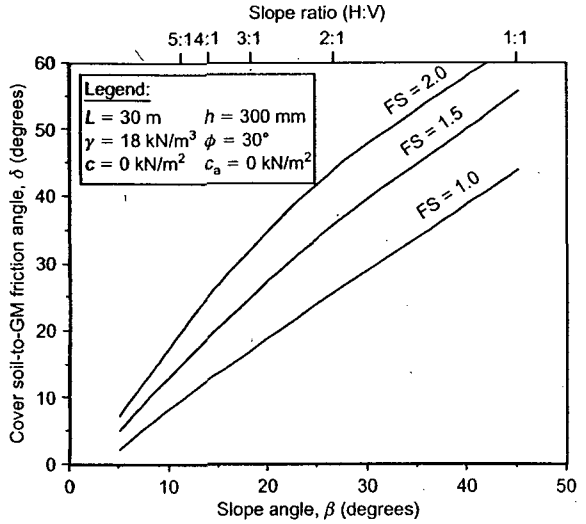

Figure 4. Design curves for stability of uniform-thickness cohesionless cover soils on linear failure planes for various global factors of safety

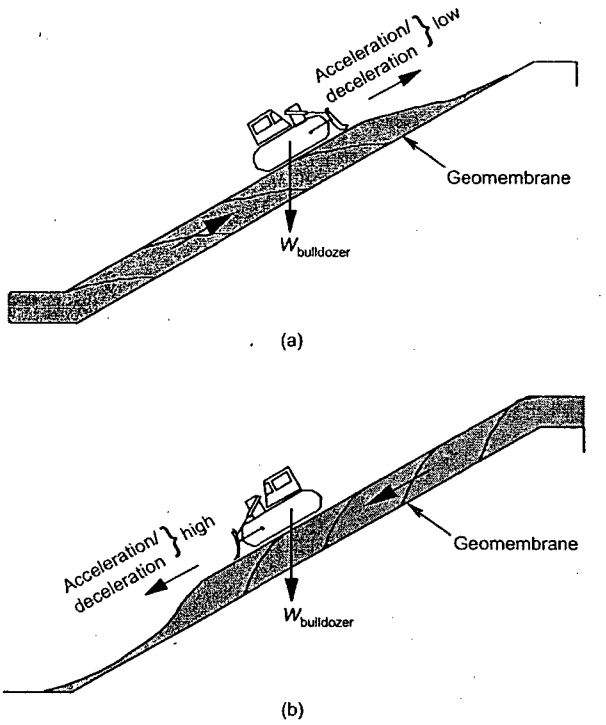

Figure 5. Construction equipment placing cover soil on slopes containing geosynthetics: (a) equipment backfilling up slope (the recommended method); (b) equipment backfilling down slope (method not recommended)

are developed specifically for the variables stated in the legend of the figure. Example 1 illustrates the use of the curves in what will be the standard example to which other examples will be compared.

Example 1

Given a 30 m long slope with a uniformly thick 300 mm cover soil at a unit weight of 18 kN/m^3. The soil has a friction angle of 30° and zero cohesion, i.e. it is a sand. The cover soil is placed directly on a geomembrane as shown in Figure 3. Direct shear testing has resulted in an interface friction angle between the cover soil and geomembrane of 22° with zero adhesion. What is the FS-value at a slope angle of 3(H)-to-1(V), i.e. 18.4°?

Substituting Equation 14 into Equation 15 and solving for the FS-value results in the following, which is seen to be in agreement with the curves of Figure 4:

$$\left.\begin{array}{l} a = 14.7\,\text{kN/m} \\ b = -21.3\,\text{kN/m} \\ c = 3.5\,\text{kN/m} \end{array}\right\} \text{FS} = 1.25$$

In general, this is too low a value for a final cover soil factor of safety, and a redesign is necessary. While there are many possible options for changing the geometry of the situation, the example will be revisited later in this section using toe berms, tapered cover soil thickness and veneer reinforcement. Furthermore, this general problem will be used throughout the main body of this paper for comparison purposes to other cover soil slope stability situations.

3.2. Construction equipment forces

The placement of cover soil on a slope with a relatively low shear strength inclusion (like a geomembrane) should always be from the toe upward to the crest. Figure 5a shows the recommended method. In so doing, the gravitational forces of the cover soil and live load of the construction equipment are compacting previously placed soil and working with an ever-present passive wedge and stable lower portion beneath the active wedge. While it is necessary to specify low ground pressure equipment to place the soil, the reduction of the FS-value for this situation of equipment working up the slope will be seen to be relatively small.

For soil placement down the slope, however, a stability analysis cannot rely on toe buttressing, and a dynamic stress should also be included in the calculation. These conditions decrease the FS-value, in some cases to a great extent. Figure 5b shows this procedure. Unless absolutely necessary, it is not recommended to place cover soil on a slope in this manner. If it is necessary, the design must consider the unsupported soil mass and the dynamic force of the specific type of construction equipment and its manner of operation.

For the first case of a bulldozer pushing cover soil up from the toe of the slope to the crest, the analysis uses the free body diagram of Figure 6a. The analysis uses a specific piece of construction equipment (like a bulldozer characterized by its ground contact pressure) and dissipates this force or stress through the cover soil thickness to the surface of the geomembrane. A Boussinesq analysis is used (Poulos and Davis 1974). This results in an equipment force per unit width as follows:

$$W_e = qwI \tag{16}$$

where W_e = equivalent equipment force per unit width at the geomembrane interface; $q = W_b/(2 \times w \times b)$; W_b = actual weight of equipment (e.g. a bulldozer); w = length of equipment track; b = width of equipment track; and

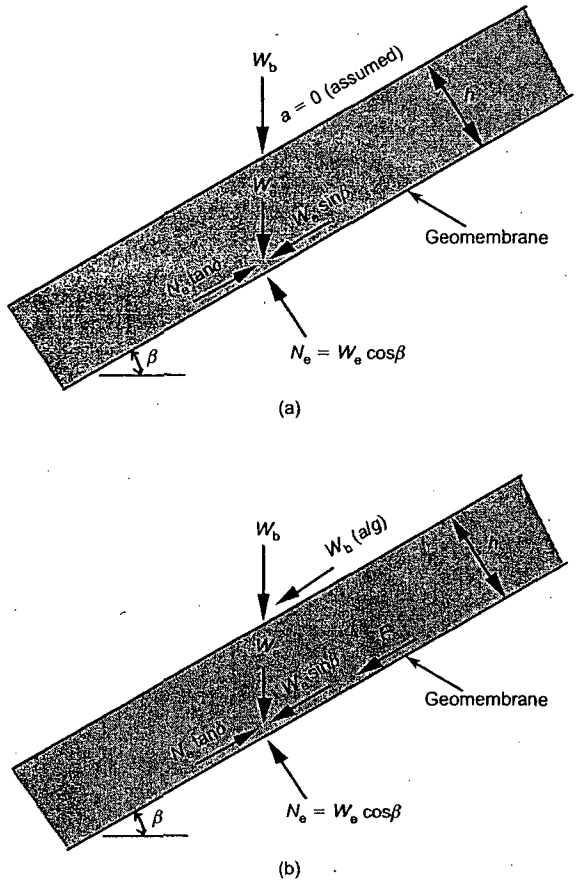

Figure 6. Additional (to gravitational forces) limit equilibrium forces due to construction equipment moving on cover soil (see Figure 3 for the gravitational soil force to which the above forces are added): (a) equipment moving up slope (load with no acceleration); (b) equipment moving down slope (load plus acceleration)

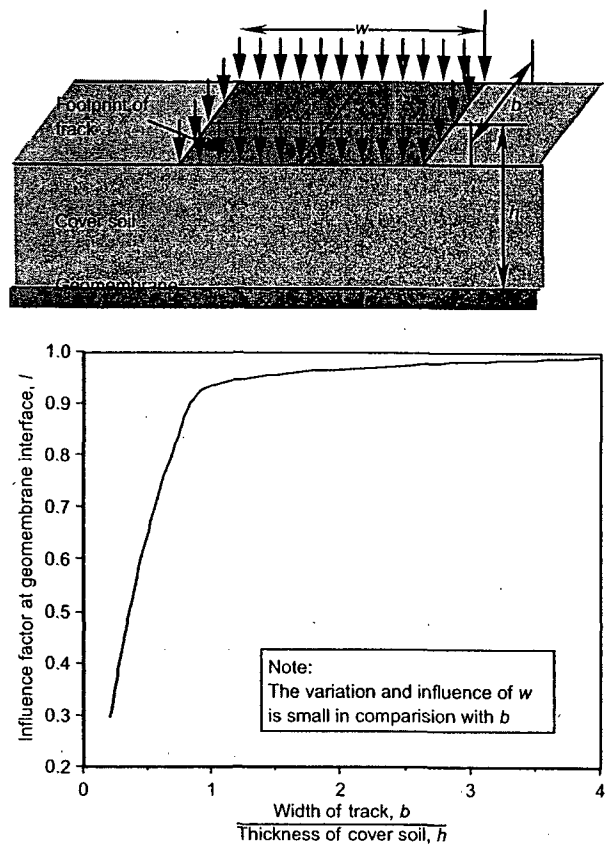

Figure 7. Values of influence factor I for use in Equation 16 to dissipate surface force through cover soil to geomembrane interface (after Poulos and Davis 1974)

I = influence factor at the geomembrane interface (see Figure 7).

Upon determining the additional equipment force at the interface between cover soil and geomembrane, the analysis proceeds as described in Section 3.1 for gravitational forces only. In essence, the equipment moving up the slope adds an additional term, W_e, to the W_A-force in Equation 3. Note, however, that this involves the generation of a resisting force as well. Thus the net effect of increasing the driving force as well as the resisting force is somewhat neutralized insofar as the resulting FS-value is concerned. It should also be noted that no acceleration/deceleration forces are included in this analysis, which is somewhat optimistic. Using these concepts (the same equations as used in Section 3.1 are used here), typical design curves for various FS-values as a function of equivalent ground contact equipment pressures and cover soil thicknesses are given in Figure 8. Note that the curves are developed specifically for the variables stated in the legend. Example 2a illustrates the use of the formulation.

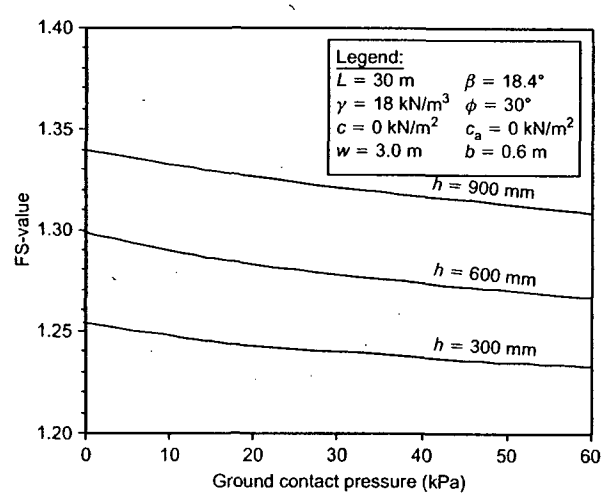

Figure 8. Design curves for stability of different thickness of cover soil for various construction equipment ground contact pressures

Example 2a

Given a 30 m long slope with uniform cover soil of 300 mm thickness at a unit weight of 18 kN/m^3. The soil has a friction angle of 30° and zero cohesion, i.e. it is a sand. It is placed on the slope using a bulldozer moving from the toe of the slope up to the crest. The bulldozer has a ground pressure of 30 kN/m^2 and tracks that are 3.0 m long and 0.6 m wide. The cover soil to geomembrane friction angle is 22° with zero adhesion. What is the FS-value at a slope angle 3(H)-to-1(V), i.e. 18.4°?

This problem follows Example 1 exactly except for the addition of the bulldozer moving up the slope. Using the additional equipment load, Equation 16 substituted into Equations 14 and 15 results in the following:

$$\left.\begin{aligned} a &= 73.1\,\text{kN/m} \\ b &= -104.3\,\text{kN/m} \\ c &= 17.0\,\text{kN/m} \end{aligned}\right\} \text{FS} = 1.24$$

While the resulting FS-value is low, the result is best assessed by comparing it with Example 1, i.e. the same problem but without the bulldozer. It is seen that the FS-value has only decreased from 1.25 to 1.24. Thus, in general, a low ground contact pressure bulldozer placing cover soil up the slope with negligible acceleration/deceleration forces does not significantly decrease the factor of safety.

For the second case of a bulldozer pushing cover soil down from the crest of the slope to the toe, as shown in Figure 5b, the analysis uses the force diagram of Figure 6b. While the weight of the equipment is treated as just described, the lack of a passive wedge along with an additional force due to acceleration (or deceleration) of the equipment significantly modifies the resulting FS-values. This analysis again uses a specific piece of construction equipment operated in a specific manner. It produces a force parallel to the slope equivalent to W_b (a/g), where W_b = the weight of the bulldozer, a = the acceleration of the bulldozer, and g = the acceleration due to gravity. Its magnitude is equipment operator dependent and related to both the equipment speed and the time to reach such a speed; see Figure 9.

The acceleration of the bulldozer, coupled with an influence factor I from Figure 7, results in the dynamic force per unit width at the interface between cover soil and geomembrane, F_e. The relationship is as follows:

$$F_e = W_e\left(\frac{a}{g}\right) \tag{17}$$

where F_e = dynamic force per unit width parallel to the slope at the geomembrane interface; W_e = equivalent equipment (bulldozer) force per unit width at geomembrane interface (recall Equation 16); β = soil slope angle beneath geomembrane; a = acceleration of the bulldozer; and g = acceleration due to gravity.

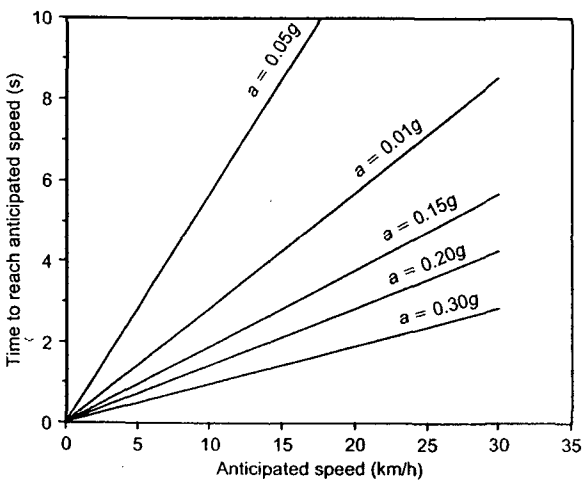

Figure 9. Graphic relationship of construction equipment speed and rise time to obtain equipment acceleration

Using these concepts, the new force parallel to the cover soil surface is dissipated through the thickness of the cover soil to the interface of the geomembrane. Again, a Boussinesq analysis is used (Poulos and Davis 1974). The expression for determining the FS-value can now be derived as follows.

Considering the active wedge, and balancing the forces in the direction parallel to the slope, the following formulation results:

$$E_A + \frac{(N_e + N_A)\tan\delta + C_a}{\text{FS}} = (W_A + W_e)\sin\beta + F_e \tag{18}$$

where N_e = effective equipment force normal to the failure plane of the active wedge according to

$$N_e = W_e\cos\beta \tag{19}$$

Note that all the other symbols have been previously defined.

The interwedge force acting on the active wedge can now be expressed as

$$E_A = (W_A + W_e)\sin\beta + F_e - \frac{(N_e + N_A)\tan\delta + C_a}{\text{FS}} \tag{20}$$

The passive wedge can be treated in a similar manner. The following formulation of the interwedge force acting on the passive wedge results:

$$E_P = \frac{C + W_P\tan\phi}{\cos\beta(\text{FS}) - \sin\beta\tan\phi} \tag{21}$$

By setting $E_A = E_P$, the following terms can be arranged in the form of Equation 13, in which the a, b and c terms are defined as follows:

$$\begin{aligned} a &= [(W_A + W_e)\sin\beta + F_e]\cos\beta \\ b &= -\{[(N_e + N_A)\tan\delta + C_a]\cos\beta \\ &\quad + [(W_A + W_e)\sin\beta + F_e]\sin\beta\tan\phi \\ &\quad + (C + W_P\tan\phi)\} \\ c &= [(N_e + N_A)\tan\delta + C_a]\sin\beta\tan\phi \end{aligned} \tag{22}$$

Finally, the resulting FS-value can be obtained using Equation 15. Using these concepts, typical design curves for various FS-values as a function of equipment ground contact pressure and equipment acceleration can be developed; see Figure 10. Note that the curves are developed specifically for the variables stated in the legend. Example 2b illustrates the use of the formulation.

Example 2b

Given a 30 m long slope with uniform cover soil of 300 mm thickness at a unit weight of 18 kN/m^3. The soil has a friction angle of 30° and zero cohesion, i.e. it is a

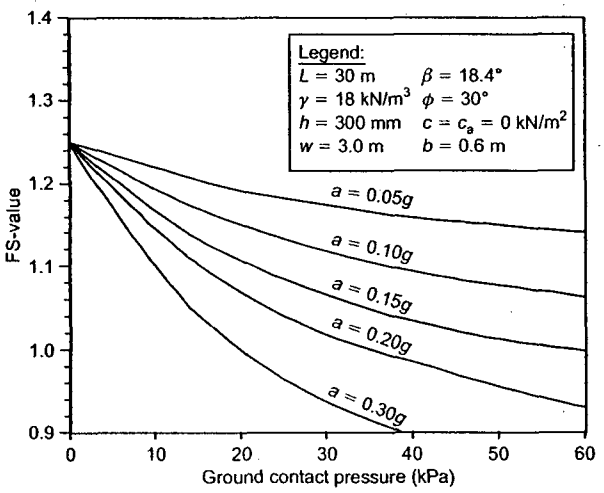

Figure 10. Design curves for stability of different construction equipment ground contact pressure for various equipment accelerations

sand. It is placed on the slope using a bulldozer moving from the crest of the slope down to the toe. The bulldozer has a ground contact pressure of 30 kN/m^2 and tracks that are 3.0 m long and 0.6 m wide. The estimated equipment speed is 20 km/h and the time to reach this speed is 3.0 s. The cover soil to geomembrane friction angle is 22° with zero adhesion. What is the FS-value at a slope angle of 3(H)-1(V), i.e. 18.4°?

First, using the design curves of Figure 10 along with Equations 22 substituted into Equation 15 the solution can be obtained:

- From Figure 9 at 20 km/h and 3.0 s the bulldozer's acceleration is 0.19g.
- From Equations 22 substituted into Equation 15 we obtain

$$\left.\begin{aligned} a &= 88.8\,\text{kN/m} \\ b &= -107.3\,\text{kN/m} \\ c &= 17.0\,\text{kN/m} \end{aligned}\right\} \text{FS} = 1.03$$

This problem solution can now be compared with the previous two examples:

Example 1: cover soil with no bulldozer loading FS = 1.25
Example 2a: cover soil plus bulldozer moving up slope FS = 1.24
Example 2b: cover soil plus bulldozer moving down slope FS = 1.03

The inherent danger of a bulldozer moving down the slope is readily apparent. Note that the same result comes about by the bulldozer decelerating instead of accelerating. The sharp braking action of the bulldozer is arguably the more severe condition owing to the extremely short times involved when stopping forward motion. Clearly, only in unavoidable situations should the cover soil placement equipment be allowed to work down the slope. If it is unavoidable, an analysis should be made of the specific stability situation, and the construction specifications should reflect the exact conditions made in the design. The maximum weight and ground contact pressure of the equipment should be stated, along with suggested operator movement of the cover soil placement operations. Truck traffic on the slopes can also give as high, or even higher, stresses, and should be avoided in all circumstances.

3.3. Consideration of seepage forces

The previous sections presented the general problem of slope stability analysis of cover soils placed on slopes under different conditions. The tacit assumption throughout was that either permeable soil or a drainage layer was placed above the barrier layer with adequate flow capacity to efficiently remove permeating water safely away from the cross-section. The amount of water to be removed is obviously a site-specific situation. Note that in extremely arid areas, or with very low-permeability cover soils, drainage may not be required, although this is generally the exception.

Unfortunately, adequate drainage of final covers has sometimes not been available, and seepage-induced slope stability problems have occurred. The following situations have resulted in seepage-induced slides:

- drainage soils with hydraulic conductivity (permeability) too low for site-specific conditions;
- inadequate drainage capacity at the toe of long slopes where seepage quantities accumulate and are at their maximum;
- fines from quarried drainage stone either clogging the drainage layer or accumulating at the toe of the slope, thereby decreasing the as-constructed permeability over time;
- fine, cohesionless, cover soil particles migrating through the filter (if one is present) either clogging the drainage layer or accumulating at the toe of the slope, thereby decreasing the as-constructed outlet permeability over time;
- freezing of the drainage layer at the toe of the slope, while the top of the slope thaws, thereby mobilizing seepage forces against the ice wedge at the toe.

If seepage forces of the types described occur, a variation in slope stability design methodology is required. Such an analysis is the focus of this subsection. Additional discussion is given by Thiel and Stewart (1993) and Soong and Koerner (1996).

Consider a cover soil of uniform thickness placed directly above a geomembrane at a slope angle β as shown in Figure 11. Different from the previous examples, however, is that within the cover soil there exists a saturated soil zone for part or all of the thickness. The saturated boundary is shown as two possibly different phreatic surface orientations. This is because seepage can be built up in the cover soil in two different ways: a horizontal build-up from the toe upward, or a parallel-to-slope build-up outward. These two hypotheses are defined and

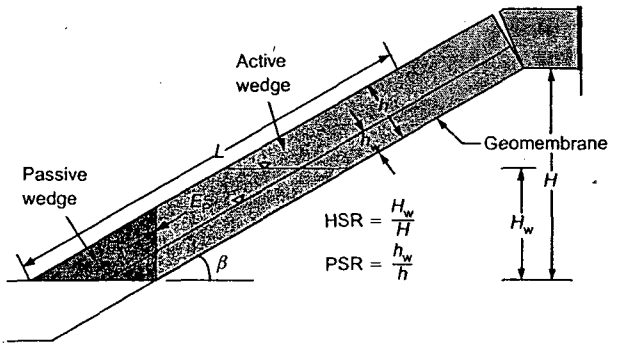

Figure 11. Cross-section of uniform thickness cover soil on geomembrane illustrating different submergence assumptions and related definitions (Soong and Koerner 1996)

quantified as a horizontal submergence ratio (HSR) and a parallel submergence ratio (PSR). The dimensional definitions of both ratios are given in Figure 11.

When analyzing the stability of slopes using the limit equilibrium method, free body diagrams of the passive and active wedges are taken with the appropriate forces (now including porewater pressures) being applied. Note that the two interwedge forces, E_A and E_P, are also shown in Figure 11. The formulation for the resulting factor of safety, for horizontal seepage build-up and then for parallel-to-slope seepage build-up, follows.

3.3.1. *Horizontal seepage build-up*

Figure 12 shows the free body diagram of both the active and passive wedge assuming horizontal seepage building. All symbols used in Figure 12 were previously defined except the following: $\gamma_{sat'd}$ = saturated unit weight of the cover soil; γ_{dry} = dry unit weight of the cover soil; γ_w = unit weight of water; H = vertical height of the slope measured from the toe; H_w = vertical height of the free water surface measured from the toe; U_h = resultant of the pore pressures acting on the interwedge surfaces; U_n = resultant of the pore pressures acting perpendicular to the slope; and U_v = resultant of the vertical pore pressures acting on the passive wedge.

The expression for finding the factor of safety can be derived as follows. Considering the active wedge:

$$W_A = \frac{\gamma_{sat'd}(h)(2H_w\cos\beta - h)}{\sin 2\beta} + \frac{\gamma_{dry}(h)(H - H_w)}{\sin\beta} \tag{23}$$

$$U_n = \frac{\gamma_w(h)(\cos\beta)(2H_w\cos\beta - h)}{\sin 2\beta} \tag{24}$$

$$U_h = \frac{\gamma_w h^2}{2} \tag{25}$$

$$N_A = W_A\cos\beta + U_h\sin\beta - U_n \tag{26}$$

The interwedge force acting on the active wedge can then be expressed as

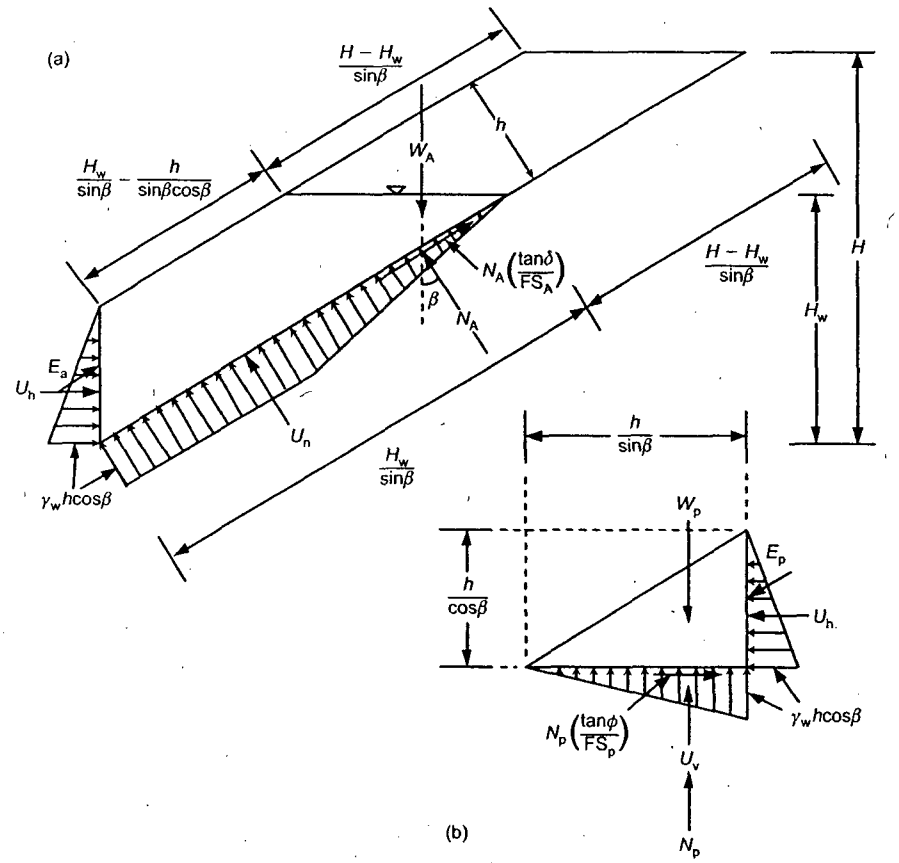

Figure 12. Limit equilibrium forces involved in finite-length slope of uniform cover soil with horizontal seepage build-up: (a) active wedge; (b) passive wedge

$$E_A = W_A \sin\beta - U_h \cos\beta - \frac{N_A \tan\delta}{FS} \quad (27)$$

The passive wedge can be considered in a similar manner, and the following expressions result:

$$W_P = \frac{\gamma_{sat'd} h^2}{\sin 2\beta} \quad (28)$$

$$U_V = U_h \cot\beta \quad (29)$$

The interwedge force acting on the passive wedge can then be expressed as

$$E_P = \frac{U_h(FS) - (W_P - U_V)\tan\phi}{\sin\beta\tan\phi - \cos\beta(FS)} \quad (30)$$

By setting $E_A = E_P$, the following terms can be arranged in the form $ax^2 + bx + c = 0$, which in this case is given by Equation 13, where:

$$\left.\begin{aligned} a &= W_A \sin\beta\cos\beta - U_h\cos^2\beta + U_h \\ b &= -W_A \sin^2\beta\tan\phi + U_h \sin\beta\cos\beta\tan\phi \\ &\quad - N_A\cos\beta\tan\delta - (W_P - U_V)\tan\phi \\ c &= N_A \sin\beta\tan\delta\tan\phi \end{aligned}\right\} \quad (31)$$

As with the previous solution, the resulting FS-value is obtained using Equation 15.

3.3.2. *Parallel-to-slope seepage build-up*

Figure 13 shows the free body diagrams of both the active and passive wedges with seepage build-up in the direction parallel to the slope. Identical symbols as defined in the previous cases are used here, with an additional definition of h_w equal to the height of free water surface measured in the direction perpendicular to the slope.

Note that the general expression of factor of safety shown in Equation 15 is still valid. However, the a, b and c terms shown in Equation 31 have different definitions in this case owing to the new definitions of the following terms:

$$W_A = \frac{\gamma_{dry}(h - h_w)[2H\cos\beta - (h + h_w)]}{\sin 2\beta} + \frac{\gamma_{sat'd} h_w (2H\cos\beta - h_w)}{\sin 2\beta} \quad (32)$$

$$U_n = \frac{\gamma_w h_w \cos\beta(2H\cos\beta - h_w)}{\sin 2\beta} \quad (33)$$

$$U_h = \frac{\gamma_w h_w^2}{2} \quad (34)$$

$$W_P = \frac{\gamma_{dry}(h^2 - h_w^2) + \gamma_{sat'd} h_w^2}{\sin 2\beta} \quad (35)$$

In order to illustrate the behavior of these equations, the design curves of Figure 14 have been developed. They show the decrease in FS-value with increasing submer-

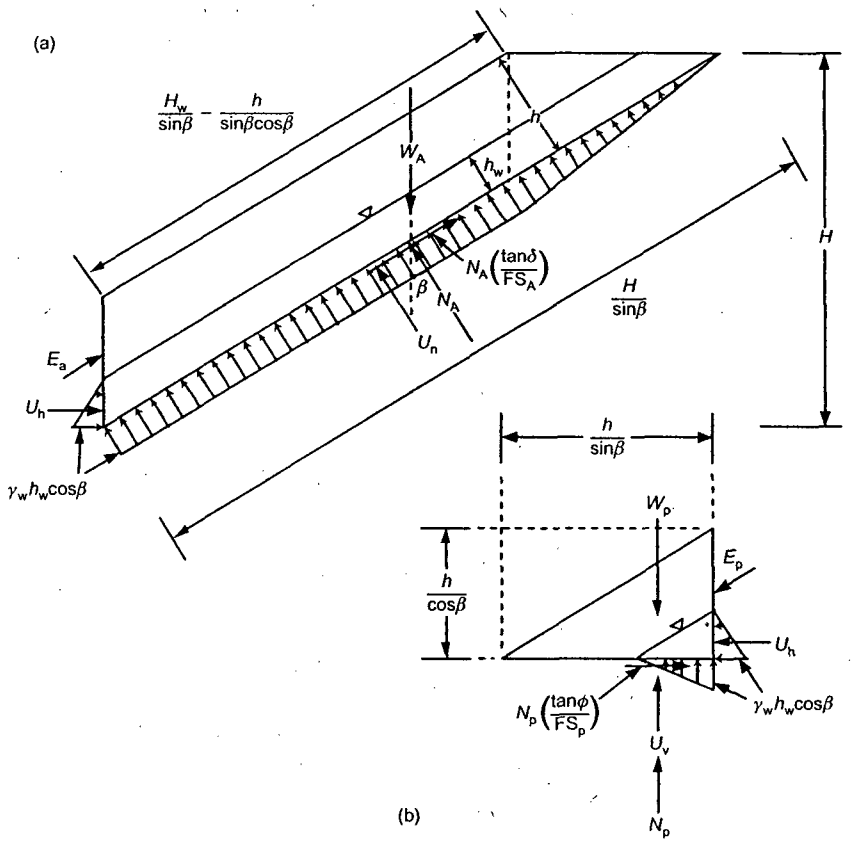

Figure 13. Limit equilibrium forces involved in finite-length slope of uniform cover soil with parallel-to-slope seepage build-up: (a) active wedge; (b) passive wedge

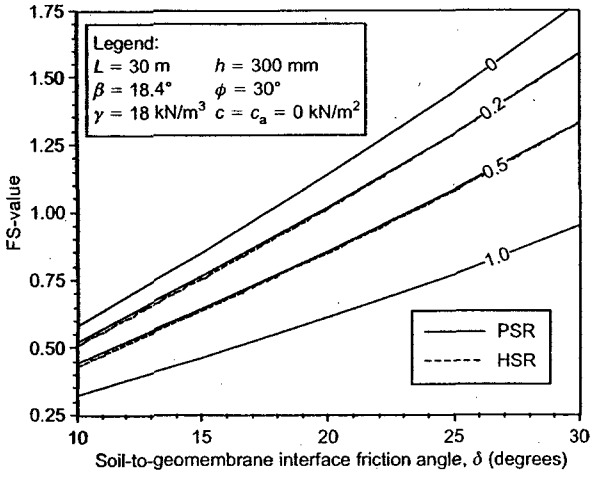

Figure 14. Design curves for stability of cohesionless, uniform thickness cover soils for different submergence ratios

gence ratio for all values of interface friction. Furthermore, the differences in response curves for the parallel and horizontal submergence ratio assumptions are seen to be very small. Note that the curves are developed specifically for variables stated in the legend. Example 3 illustrates the use of the design curves.

Example 3

Given a 30 m long slope with a uniform thickness cover soil of 300 mm at a dry unit weight of 18 kN/m^3. The soil has a friction angle of 30° and zero cohesion, i.e. it is a sand. The soil becomes saturated through 50% of its thickness, i.e. it is a parallel seepage problem with PSR = 0.5, and its saturated unit weight increases to 21 kN/m^3. Direct shear testing has resulted in an interface friction angle of 22° with zero adhesion. What is the factor of safety at a slope of 3(H)-to-1(V), i.e. 18.4°?

Solving Equations 31 with the values of Equations 32 to 35 for the a, b and c terms and substituting them into Equation 15 results in the following:

$$\left.\begin{aligned} a &= 51.7\,\text{kN/m} \\ b &= -57.8\,\text{kN/m} \\ c &= 9.0\,\text{kN/m} \end{aligned}\right\} \text{FS} = 0.93$$

The seriousness of seepage forces in a slope of this type is immediately obvious. Had the saturation been 100% of the drainage layer thickness, the FS-value would have been even lower. Furthermore, the result using a horizontal assumption of saturated cover soil with the same saturation ratio will give identically low FS-values. Clearly, the teaching of this example problem is that adequate *long-term* drainage above the barrier layer in cover soil slopes must be provided to avoid seepage forces from occurring.

3.4. Consideration of seismic forces

In areas of anticipated earthquake activity, the slope stability analysis of a final cover soil over an engineered landfill, abandoned dump or remediated site must consider seismic forces. In the United States, the Environmental Protection Agency (EPA) regulations require such an analysis for sites that have a probability of $\geq 10\%$ of experiencing a 0.10g peak horizontal acceleration within 250 years. For the continental USA this includes not only the western states, but major sections of the midwest and northeast states, as well. If practiced worldwide, such a criterion would have huge implications.

The seismic analysis of cover soils of the type under consideration in this report is a two-part process:

- An FS-value is calculated using a pseudo-static analysis via the addition of a horizontal force acting at the centroid of the cover soil cross-section.
- If the FS-value in the above calculation is less than 1.0, a permanent deformation analysis is required. The calculated deformation is then assessed in light of the potential damage to the cover soil section, and either it is accepted, or the slope requires an appropriate redesign. The redesign is then analyzed until the situation becomes acceptable.

The first part of the analysis is a pseudo-static approach which follows the previous examples except for the addition of a horizontal force at the centroid of the cover soil in proportion to the anticipated seismic activity. It is first necessary to obtain an average seismic coefficient (C_S) from a seismic zone map (e.g. Algermissen 1969). Such maps are available on a worldwide basis. The value of C_S is non-dimensional and is a ratio of the bedrock acceleration to gravitational acceleration. This value of C_S is modified using available computer codes such as SHAKE (Schnabel *et al.* 1972), for propagation to the site and then to the landfill cover as shown in Figure 15. The computational process within such programs is quite intricate. For detailed discussion see Seed and Idriss (1982) and Idriss (1990). The analysis is then similar to those previously presented.

Using Figure 15, the additional seismic force is $C_S W_A$ acting horizontally on the active wedge. All additional symbols used in Figure 15 have been previously defined, and the expression for finding the FS-value can be derived as follows.

Considering the active wedge, by balancing the forces

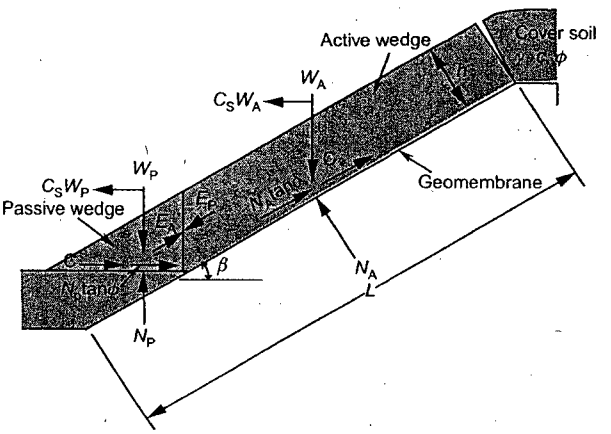

Figure 15. Limit equilibrium forces involved in pseudo-static analysis using average seismic coefficient

in the horizontal direction, the following formulation results:

$$E_A \cos\beta + \frac{(N_A \tan\delta + C_a)\cos\beta}{FS} = C_S W_A + N_A \sin\beta \tag{36}$$

Hence the interwedge force acting on the active wedge results:

$$E_A = \frac{(FS)(C_S W_A + N_A \sin\beta)}{(FS)\cos\beta} - \frac{(N_A \tan\delta + C_a)\cos\beta}{(FS)\cos\beta} \tag{37}$$

The passive wedge can be considered in a similar manner, and the following formulation results:

$$E_P \cos\beta + C_S W_P = \frac{C + N_P \tan\phi}{FS} \tag{38}$$

Hence the interwedge force acting on the passive wedge is

$$E_P = \frac{C + W_P \tan\phi - C_S W_P (FS)}{(FS)\cos\beta - \sin\beta \tan\phi} \tag{39}$$

Again, by setting $E_A = E_P$, the following equation can be arranged in the form $ax^2 + bx + c = 0$, which in this case is given by Equation 13 where:

$$\begin{aligned} a &= (C_S W_A + N_A \sin\beta)\cos\beta + C_S W_P \beta \\ b &= -[(C_S W_A + N_A \sin\beta)\sin\beta \tan\phi \\ &\quad + (N_A \tan\delta + C_a)\cos^2\beta + (C + W_P \tan\phi)\cos\beta] \\ c &= (N_A \tan\delta + C_a)\cos\beta \sin\beta \tan\phi \end{aligned} \tag{40}$$

The resulting FS-value is then obtained from Equation 15.

Using these concepts, a design curve for the general problem under consideration as a function of seismic coefficient can be developed; see Figure 16. Note that the curve is developed specifically for the variables stated in the legend. Example 4a illustrates the use of the curve.

Example 4a

Given a 30 m long slope with uniform thickness cover soil of 300 mm at a unit weight of 18 kN/m^3. The soil has a friction angle of 30° and zero cohesion, i.e. it is a sand. The cover soil is on a geomembrane, as shown in Figure 15. Direct shear testing has resulted in an interface friction angle of 22° with zero adhesion. The slope angle is 3(H)-to-1(V), i.e. 18.4°. A design earthquake appropriately transferred to the site's cover soil results in an average seismic coefficient of 0.10. What is the FS-value?

Solving Equations 40 for the values given in the example and substituting into Equation 15 results in the following FS-value:

$$\left.\begin{aligned} a &= 59.6\,\text{kN/m} \\ b &= -66.9\,\text{kN/m} \\ c &= 10.4\,\text{kN/m} \end{aligned}\right\} \text{FS} = 0.94$$

Note that the value of FS = 0.94 agrees with the design curve of Figure 16 at a seismic coefficient of 0.10.

Had the above FS-value been greater than 1.0, the analysis would be complete, the assumption being that cover soil stability can withstand the short-term excitation of an earthquake and still not slide. However, since the value in this example is less than 1.0, a second part of the analysis is required.

The second part of the analysis is directed toward calculating the estimated deformation of the lowest shear strength interface in the cross-section under consideration. The deformation is then assessed in light of the potential damage that may be imposed on the system.

To begin the permanent deformation analysis, a yield acceleration, C_{sy}, is obtained from a pseudo-static analysis under an assumed FS = 1.0. Figure 16 illustrates this procedure for the assumptions stated in the legend. It results in a value of C_{sy} = 0.075. Coupling this value with the time history response obtained for the actual site location and cross-section results in a comparison as shown in Figure 17a. If the earthquake time history response never exceeds the value of C_{sy}, there is no anticipated permanent deformation. However, whenever any part of the time history exceeds the value of C_{sy}, permanent deformation is expected. By double integration of the acceleration time history curve, to velocity (Figure 17b) and then to displacement (Figure 17c), the anticipated value of deformation can be obtained. It is usually based on residual stresses of the interface involved, but this may be excessively conservative (Matasovic *et al.* 1997). This value is considered to be permanent deformation and is then assessed based on the site-specific implications of damage to the final cover system. Example

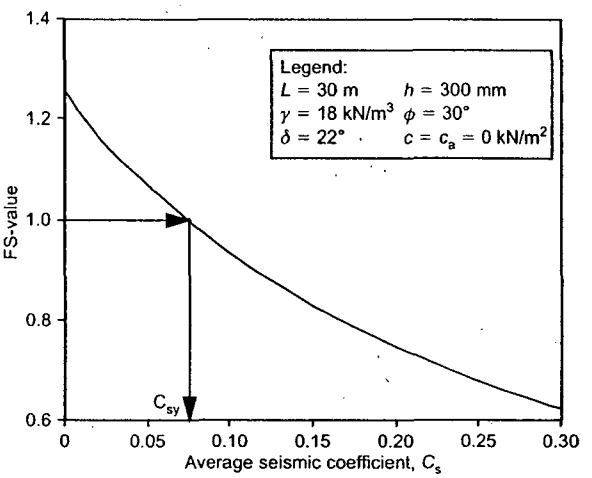

Figure 16. Design curve for a uniformly thick cover soil pseudo-static seismic analysis with varying average seismic coefficients

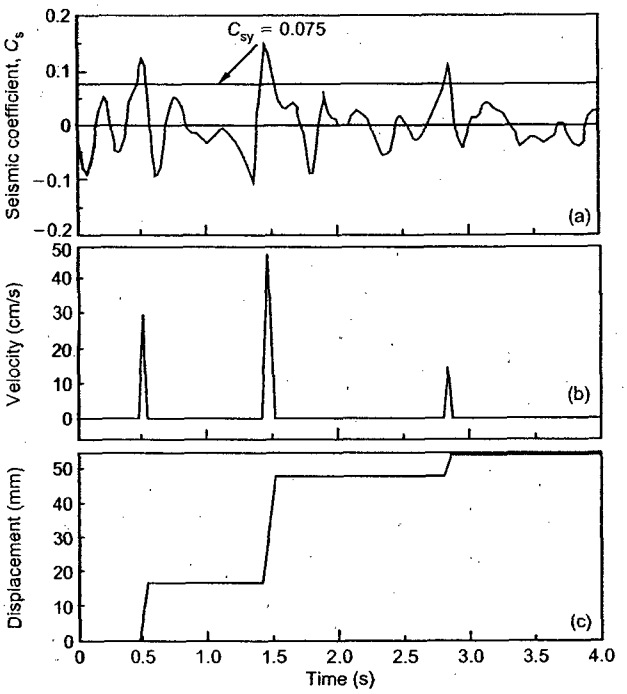

Figure 17. Design curves to obtain permanent deformation utilizing (a) acceleration, (b) velocity and (c) displacement curves

4b continues the previous pseudo-static analysis into the deformation calculation.

Example 4b

Continue Example 4a and determine the anticipated permanent deformation of the weakest interface in the cover soil system. The site-specific seismic time-history diagram is given in Figure 17a.

The interface of concern is that between the cover soil and geomembrane for this particular example. With a yield acceleration of 0.075 from Figure 16 and the site-specific design time history shown in Figure 17a, integration produces Figure 17b and then Figure 17c. The three peaks exceeding the yield acceleration value of 0.075 produce a cumulative deformation of approximately 54 mm. This value is now viewed in light of the deformation capability of the cover soil above the particular interface used at the site.

An assessment of the implications of deformation (in this example it is 54 mm) is very subjective. For example, this problem could easily have been framed to produce much higher permanent deformation. Such deformation can readily be envisioned in highly seismic-prone areas. In addition to an assessment of cover soil stability, the concerns for appurtenances and ancillary piping must also be addressed.

4. SITUATIONS CAUSING THE ENHANCED STABILIZATION OF SLOPES

This section represents a counterpoint to the previous section on slope destabilization situations, in that all situations presented here tend to stabilize slopes. Thus they represent methods to increase the cover soil FS-value. Included are toe berms, tapered cover soils and veneer reinforcement (both intentional and non-intentional). Not included, but very practical in site-specific situations, is simply to decrease the slope angle and/or decrease the slope length. These solutions, however, do not incorporate new design techniques and are therefore not illustrated. They are, however, very viable alternatives for the design engineer.

4.1. Toe (buttress) berm

A common method of stabilizing highway slopes and earth dams is to place a soil mass, i.e. a berm, at the toe of the slope. In so doing one provides a soil buttress, acting in a passive state providing a stabilizing force. Figure 18 illustrates the two geometric cases necessary to provide the requisite equations. While the force equilibrium is performed as previously described, i.e. equilibrium along the slope with abutting interwedge forces aligned with the slope angle or horizontal, the equations are extremely long. Owing to space limitations (and the resulting trends in FS-value improvement) they are not presented.

Example 5

Given a 30 m long slope with a uniform cover soil thickness of 300 mm and a unit weight of 18 kN/m^3. The soil has a friction angle of 30° and zero cohesion, i.e. it is a sand. The cover soil is on a geomembrane, as shown in Figure 18. Direct shear testing has resulted in an interface

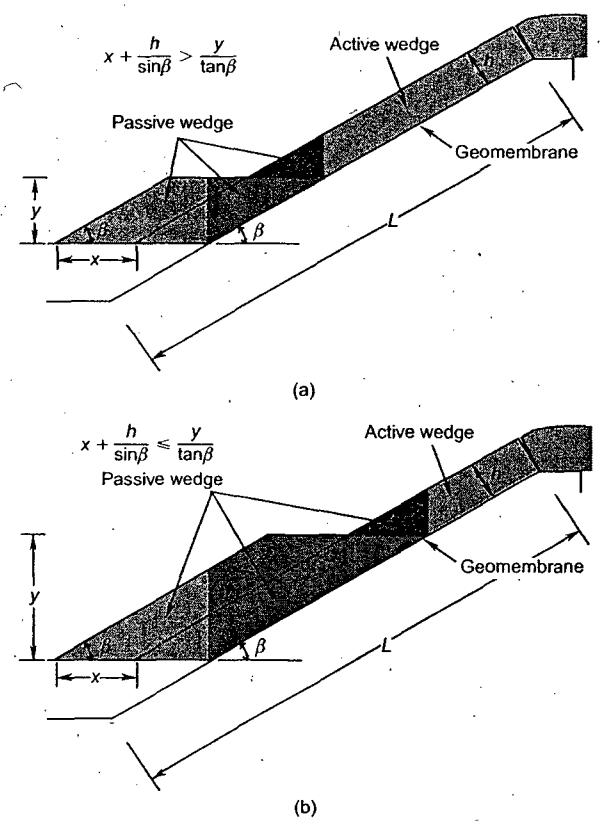

Figure 18. Dimensions of toe (buttress) berms acting as passive wedges to enhance stability

friction angle between the cover soil and geomembrane of 22° and zero adhesion. The FS-value at a slope angle of 3(H)-to-1(V), i.e. 18.4°, was shown in Section 3.1 to be 1.25. What is the increase in FS-value using different-sized toe berms with values of x = 1, 2 and 3 m, and gradually increasing y-values?

The FS-value response to this type of toe berm stabilization is given in two parts; see Figure 19. Using thickness values of x = 1, 2 and 3 m, the lower berm section by itself is seen to have high FS-values initially, which decrease rapidly as the height of the toe berm increases. This is a predictable response for this passive wedge zone. Unfortunately, the upper layer of soil above the toe berm (the active zone) is only nominally increasing in its FS-value. Note that, at the crossover points of the upper and lower FS-values (which is the optimum solution for each set of conditions), the following occurs:

- For x = 1 m: y = 6.0 m (63% of the slope height) and FS = 1.35 (only an 8% improvement in stability).
- For x = 2 m: y = 6.8 m (72% of the slope height) and FS = 1.37 (only a 12% improvement in stability).
- For x = 3 m: y = 7.3 m (77% of the slope height) and FS = 1.40 (only a 16% improvement in stability).

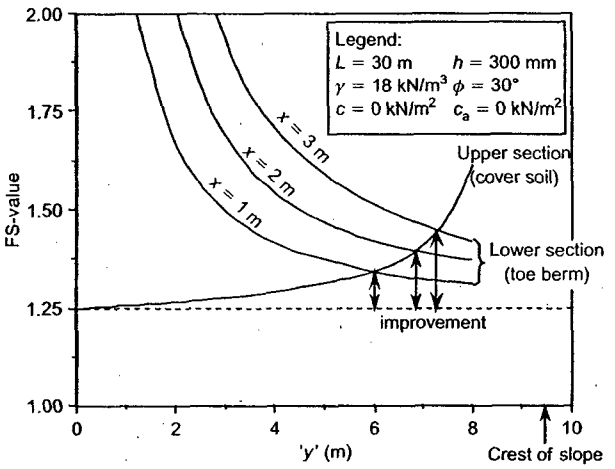

Figure 19. Design curves for FS-values using toe (buttress) berms of different dimensions

Readily seen is that construction of a toe berm is *not* a viable strategy to stabilize relatively thin layers of sloped cover soil of the type under investigation. Essentially what is happening is that the remaining upper section of the cover soil (the active wedge) is sliding off the top of the toe berm. While the upper slope length is becoming shorter (as evidenced by the slight improvement in FS-values), it is doing so only with the addition of a tremendous amount of soil fill. Thus this toe berm concept is a poor strategy for the stabilization of forces oriented in the slope's direction. Conversely, it is an excellent strategy for embankments and dams, where the necessary resisting force for the toe berm is horizontal, thereby counteracting a horizontal thrust by the potentially unstable soil and/or water mass.

4.2. Slopes with tapered thickness cover soil

An alternative method available to the designer to increase the FS-value of a given slope is to uniformly taper the cover soil thickness from thick at the toe to thin at the crest; see Figure 20. The FS-value will increase in approximate proportion to the thickness of soil at the toe. The analysis for tapered cover soils includes the design assumptions of a tension crack at the top of the slope, the upper surface of the cover soil tapered at a constant angle ω, and the earth pressure forces on the respective wedges oriented at the average of the surface and slope angles, i.e. the E-forces are at an angle of $(\omega + \beta)/2$. The procedure follows that of the uniform cover soil thickness analysis. Again, the resulting equation is not an explicit solution for the FS, and must be solved indirectly. All symbols used in Figure 20 were previously defined (see Section 3.1) except the following: D = thickness of cover soil at bottom of the landfill, measured perpendicular to the base liner; h_c = thickness of cover soil at crest of the slope, measured perpendicular to the slope; y (Figure 20), where:

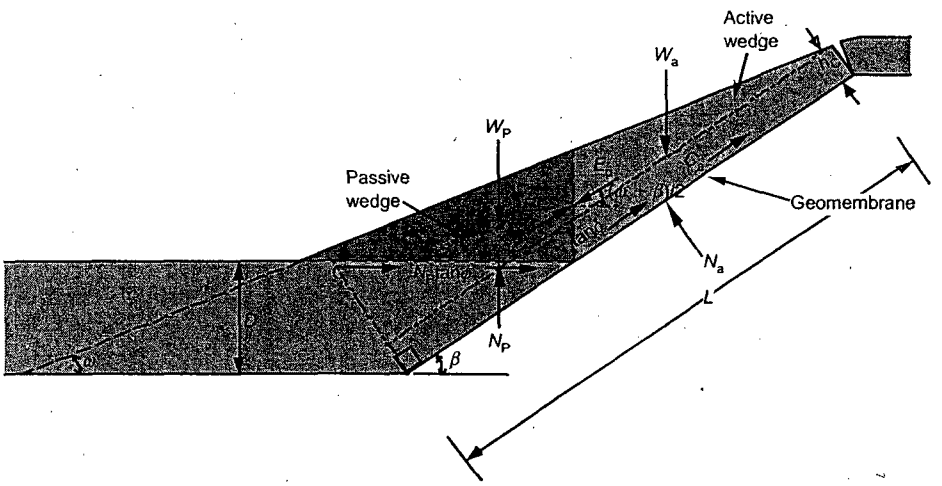

Figure 20. Limit equilibrium forces involved in finite length slope analysis with tapered thickness cover soil from toe to crest

$$y = \left(L - \frac{D}{\sin\beta} - h_c \tan\beta\right)(\sin\beta - \cos\beta\tan\omega) \quad (41)$$

and ω = finished slope angle of cover soil. Note that $\omega < \beta$.

The expression for determining the FS-value can be derived as follows. Considering the active wedge:

$$W_A = \gamma\left[\left(L - \frac{D}{\sin\beta} - h_c\tan\beta\right)\left(\frac{y\cos\beta}{2} + h_c\right) + \frac{h_c^2\tan\beta}{2}\right] \quad (42)$$

$$N_A = W_A\cos\beta \quad (43)$$

$$C_a = c_a\left(L - \frac{D}{\sin\beta}\right) \quad (44)$$

By balancing the forces in the vertical direction, the following formulation results:

$$E_A\sin\left(\frac{\omega+\beta}{2}\right) = W_A - N_A\cos\beta - \frac{N_A\tan\delta + C_a}{FS}\sin\beta \quad (45)$$

Hence the interwedge force acting on the active wedge is

$$E_A = \frac{(FS)(W_A - N_A\cos\beta) - (N_A\tan\delta + C_a)\sin\beta}{\sin\left(\frac{\omega+\beta}{2}\right)(FS)} \quad (46)$$

The passive wedge can be considered in a similar manner:

$$W_P = \frac{\gamma}{2\tan\omega}\left[\left(L - \frac{D}{\sin\beta} - h_c\tan\beta\right)(\sin\beta - \cos\beta\tan\omega) + \frac{h_c}{\cos\beta}\right]^2 \quad (47)$$

$$N_P = W_P + E_P\sin\left(\frac{\omega+\beta}{2}\right) \quad (48)$$

$$C = \frac{\gamma}{\tan\omega}\left[\left(L - \frac{D}{\sin\beta} - h_c\tan\beta\right)(\sin\beta - \cos\beta\tan\omega) + \frac{h_c}{\cos\beta}\right] \quad (49)$$

By balancing the forces in the horizontal direction, the following formulation results:

$$E_P\cos\left(\frac{\omega+\beta}{2}\right) = \frac{C + N_P\tan\phi}{FS} \quad (50)$$

Hence the interwedge force acting on the passive wedge is

$$E_P = \frac{C + W_P\tan\phi}{\cos\left(\frac{\omega+\beta}{2}\right)(FS) - \sin\left(\frac{\omega+\beta}{2}\right)\tan\phi} \quad (51)$$

Again, by setting $E_A = E_P$, the following terms can be arranged in the form $ax^2 + bx + c = 0$, which in our case is Equation 13 where:

$$a = (W_A - N_A\cos\beta)\cos\left(\frac{\omega+\beta}{2}\right)$$

$$b = -\left[(W_A - N_A\cos\beta)\sin\left(\frac{\omega+\beta}{2}\right)\tan\phi + (N_A\tan\delta + C_a)\sin\beta\cos\left(\frac{\omega+\beta}{2}\right) + \sin\left(\frac{\omega+\beta}{2}\right)(C + W_P\tan\phi)\right] \quad (52)$$

$$c = (N_A\tan\delta + C_a)\sin\beta\sin\left(\frac{\omega+\beta}{2}\right)\tan\phi$$

Again, the resulting FS-value can then be obtained using Equation 15. To illustrate the use of the above-developed equations, the design curves of Figure 21 are offered. They show that the FS-value increases in proportion to greater cover soil thicknesses at the toe of the slope with respect to the thickness at the crest. This is evidenced by a shallower finished slope angle than that of the slope of the geomembrane and the soil beneath, i.e. the value of ω being less than β. Note that the curves are developed specifically for the variables stated in the legend. Example 6 illustrates the use of the curves.

Example 6

Given a 30 m long slope with a tapered thickness cover soil of 150 mm at the crest extending at an angle ω of 16° to the intersection of the cover soil at the toe. The unit weight of the cover soil is 18 kN/m^3. The soil has a friction angle of 30° and zero cohesion, i.e. it is a sand. The interface friction angle with the underlying geomembrane is 22° with zero adhesion. What is the FS-value at an underlying soil slope angle β of 3(H)-to-1(V), i.e. 18.4°?

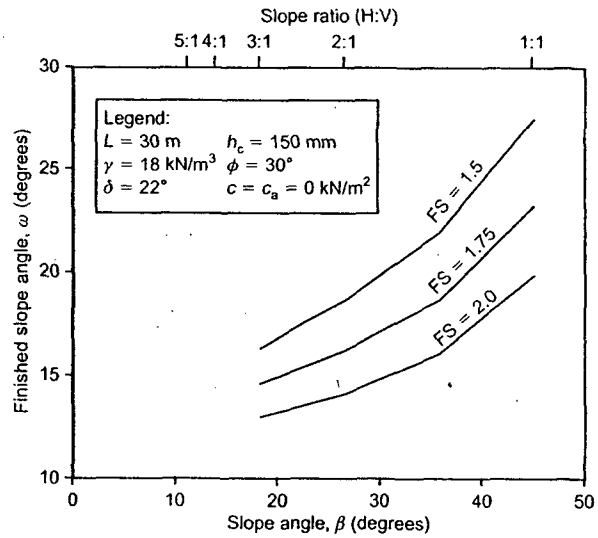

Figure 21. Design curves for FS-values of tapered cover soil thickness

Using Equations 52 and substituting into Equation 15 yields the following:

$$\left.\begin{aligned} a &= 37.0\,\text{kN/m} \\ b &= -63.6\,\text{kN/m} \\ c &= 8.6\,\text{kN/m} \end{aligned}\right\} \text{FS} = 1.57$$

The result of this problem (with tapered thickness cover soil) is FS = 1.57, compared with Example 1 (with a uniform thickness cover soil), which was FS = 1.25. Thus the increase in FS-value is 24%. Note, however, that at $\omega = 16°$ the thickness of the cover soil normal to the slope at the toe is approximately 1.4 m. Thus the increase in cover soil volume used over Example 1 is from 8.9 to 24.1 m^3/m ($\approx$ 170%), and the increase in necessary toe space distance is from 1.0 to 4.8 m ($\approx$ 380%). The trade-offs between these issues should be considered when using the strategy of tapered cover soil thickness to increase the FS-value of a particular cover soil slope.

4.3. Veneer reinforcement: intentional

A fundamentally different way of increasing a given slope's factor of safety is to reinforce it with a geosynthetic material. Such reinforcement can be either intentional or non-intentional. By *intentional*, we mean to include a geogrid or high-strength geotextile within the cover soil to purposely reinforce the system against instability; see Figure 22. Depending on the type and amount of reinforcement, the majority, or even all, of the driving, or mobilizing, stresses can be supported, resulting in a major increase in FS-value. By *non-intentional*, we refer to multi-component liner systems where a low shear strength interface is located beneath an overlying geosynthetic(s). In this case, the overlying geosynthetic(s) is inadvertently acting as veneer reinforcement to the composite system. In some cases, the designer may not realize that such geosynthetic(s) are being stressed in an identical manner as a geogrid or high-strength geotextile, but they are. The situation where a relatively low strength protection geotextile is placed over a geomembrane and beneath the cover soil is a case in point. Intentional, or non-intentional, the stability analysis is identical. The difference is that the geogrids and/or high-strength geotextiles give a major increase in the FS-value, while a protection geotextile (or other lower strength geosynthetics) only nominally increases the FS-value.

Seen in Figure 22 is that the analysis follows Section 3.1, but a force from the reinforcement, T, acting parallel to the slope, provides additional stability. This force T acts only within the active wedge. By taking free body force diagrams of the active and passive wedges, the following formulation for the factor of safety results. All symbols used in Figure 22 were previously defined (see Section 3.1), except the following: $T = T_{\text{allow}}$, the allowable (long-term) strength of the geosynthetic reinforcement inclusion.

Considering the active wedge, by balancing the forces in the vertical direction, the following formulation results:

$$E_A \sin\beta = W_A - N_A \cos\beta - \left(\frac{N_A \tan\delta + C_a}{\text{FS}} + T\right)\sin\beta \tag{53}$$

Hence the interwedge force acting on the active wedge is

$$E_A = \frac{(W_A - N_A\cos\beta - T\sin\beta)}{\sin\beta} - \frac{(N_A\tan\delta + C_a)\sin\beta}{\sin\beta(\text{FS})} \tag{54}$$

Again, by setting $E_A = E_P$ (see Equation 12 for the expression of E_P), the following terms can be arranged in the usual form, in which the a, b and c terms are defined as follows:

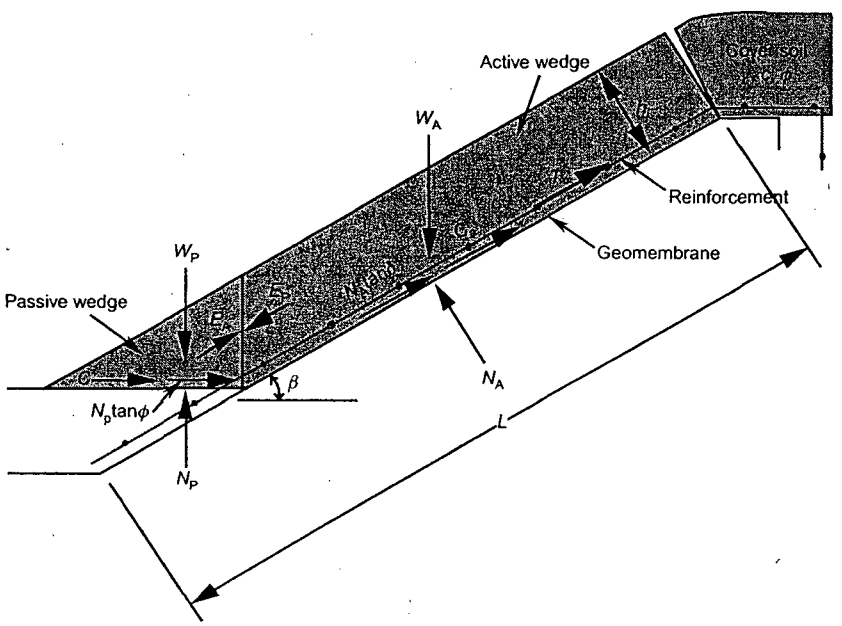

Figure 22. Limit equilibrium forces involved in finite length slope analysis for uniformly thick cover soil including use of veneer reinforcement

$$a = (W_A - N_A \cos\beta - T \sin\beta)\cos\beta$$

$$b = -[(W_A - N_A \cos\beta - T \sin\beta)\sin\beta \tan\phi + (N_A \tan\delta + C_A)\sin\beta\cos\beta + \sin\beta(C + W_P \tan\phi)]$$

$$c = (N_A \tan\delta + C_A)\sin^2\beta \tan\phi \quad (55)$$

Again, the resulting FS-value can be obtained using Equation 15.

As noted, the value of T in the design formulation is T_{allow}, which is invariably less than the as-manufactured strength of the geosynthetic reinforcement material. Considering the as-manufactured strength as being T_{ult}, the value should be reduced by such factors as installation damage, creep and long-term degradation. Note that if seams are involved in the reinforcement, a reduction factor should be added accordingly. See Koerner, 2005 (among others) for recommended numeric values.

$$T_{allow} = T_{ult}\left(\frac{1}{RF_{ID} \times RF_{CR} \times RF_{CBD}}\right) \quad (56)$$

where T_{allow} = allowable value of reinforcement strength; T_{ult} = ultimate (as-manufactured) value of reinforcement strength; RF_{ID} = reduction factor for installation damage; RF_{CR} = reduction factor for creep; and RF_{CBD} = reduction factor for chemical/biological degradation.

To illustrate the use of the above-developed equations, the design curves of Figure 23 have been developed. The reinforcement strength can come either from geogrids or from high-strength geotextiles. If geogrids are used, the friction angle is the cover soil to the underlying geomembrane, under the assumption that the apertures are large enough to allow for soil strike-through. If geotextiles are used this is not the case, and the friction angle is the geotextile to the geomembrane. Also note that this value under discussion is the required reinforcement strength, which is essentially T_{allow} in Equation 56. The curves clearly show the improvement of FS-values with increasing strength of the reinforcement. Note that the curves are developed specifically for the variables stated in the legend. Example 7 illustrates the use of the design curves.

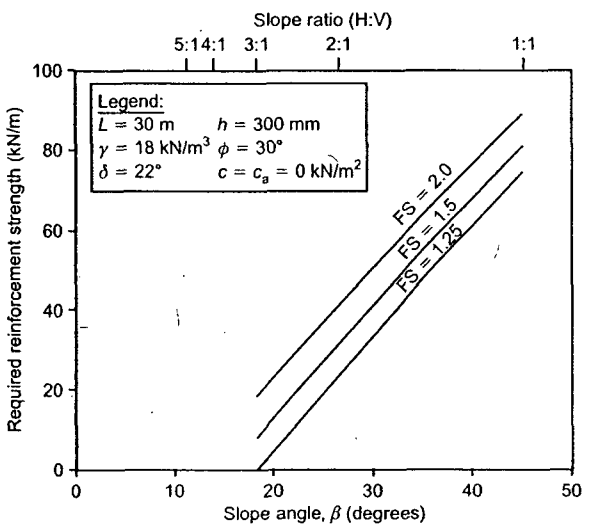

Figure 23. Design curves for FS-values for different slope angles and veneer reinforcement strengths of uniform thickness cohesionless cover soils

Example 7

Given a 30 m long slope with a uniform thickness cover soil of 300 mm and a unit weight of 18 kN/m^3. The soil has a friction angle of 30° and zero cohesion, i.e. it is a sand. The proposed reinforcement is a geogrid with an allowable wide width tensile strength of 10 kN/m. Thus reduction factors in Equation 56 have already been included. The geogrid apertures are large enough that the cover soil will strike through and provide an interface friction angle with the underlying geomembrane of 22° with zero adhesion. What is the FS-value at a side slope angle of 3(H)-to-1(V), i.e. 18.4°?

Solving Equations 55 and substituting into Equation 15 produces the following:

$$\left.\begin{aligned} a &= 11.8\,\text{kN/m} \\ b &= -20.7\,\text{kN/m} \\ c &= 3.5\,\text{kN/m} \end{aligned}\right\} \text{FS} = 1.57$$

Note that the use of T_{allow} = 10 kN/m in the analysis will require a significantly higher T_{ult} value of the geogrid per Equation 56. For example, if the summation of the reduction factors in Equation 55 were 4.0, the ultimate (as-manufactured) strength of the geogrid would have to be 40 kN/m. Also, note that this same type of analysis could also be used for high-strength geotextile reinforcement. The analysis follows along the same general lines as presented here.

4.4 Veneer reinforcement: non-intentional

It should be emphasized that the preceding analysis is focused on intentionally improving the FS-value by the inclusion of geosynthetic reinforcement. This is provided by geogrids or high-strength geotextiles being placed above the upper surface of the low-strength interface material. The reinforcement is usually placed directly above the geomembrane or other geosynthetic material.

Interestingly, some amount of veneer reinforcement is often non-intentionally provided by a geosynthetic(s) material placed over an interface with a lower shear strength. Several situations are possible in this regard;

- geotextile protection layer placed over a geomembrane;
- geomembrane placed over an underlying geotextile protection layer;
- geotextile/geomembrane placed over a compacted clay liner or geosynthetic clay liner;
- multilayered geosynthetics placed over a compacted clay liner or a geosynthetic clay liner.

Each of these four situations is illustrated in Figure 24. They represent precisely the formulation of Section 4.3, which is based on Figure 22. On the condition that the geosynthetics above the weakest interface are held in their respective anchor trends, the overlying geosynthetics

ATTACHMENT H
FHWA Publication No. HI-99-012
Geotechnical Earthquake Engineering

TRAINING COURSE IN GEOTECHNICAL AND FOUNDATION ENGINEERING

NHI COURSE NO. 13239 - MODULE 9

PUBLICATION NO. FHWA HI-99-012
DECEMBER 1998

GEOTECHNICAL EARTHQUAKE ENGINEERING

REFERENCE MANUAL

U.S. Department
of Transportation
Federal Highway Administration

National Highway Institute

Technical Report Documentation Page

1. Report No.	2. Government Accession No.	3. Recipient's Catalog No.
FHWA-HI-99-012		

4. Title and Subtitle	5. Report Date
GEOTECHNICAL EARTHQUAKE ENGINEERING REFERENCE MANUAL	December 1998
	6. Performing Organization Code

7. Author(s)	8. Performing Organization Report No.
Principal Investigator: George Munfakh[★] Authors: Edward Kavazanjian, Jr.[▲], Neven Matasović[▲], Tarik Hadj-Hamou[▲], and Jaw-Nan (Joe) Wang[★]	

9. Performing Organization Name and Address	10. Work Unit No. (TRAIS)
[★] Parsons Brinckerhoff Quade & Douglas, Inc. One Penn Plaza, New York, NY 10119 In association with: [▲] GeoSyntec Consultants 2100 Main St., Suite 150, Huntington Beach, CA 92648	11. Contract or Grant No. DTFH61-94-C-00104

12. Sponsoring Agency Name and Address	13. Type of Report and Period Covered
Federal Highway Administration National Highway Institute 901 North Stuart Street, Suite 300 Arlington, Virginia 22203	14. Sponsoring Agency Code

15. Supplementary Notes

FHWA Technical Consultants - J.A. DiMaggio, A. Munoz and P. Osborn
FHWA Contracting Officer - J. Mowery III; COTR - L. Jones, National Highway Institute

16. Abstract

This manual has been written to provide training on how to apply principles of geotechnical earthquake engineering to planning, design, and retrofit of highway facilities. Geotechnical earthquake engineering topics discussed in Part I of this manual include:

- deterministic and probabilistic seismic hazard assessment;
- evaluation of design ground motions;
- seismic site response analyses;
- evaluation of liquefaction potential and seismic settlements;
- seismic slope stability and deformation analyses; and
- seismic design of foundations and retaining structures.

The manual provides detailed information on basic principles and analyses, with reference to where detailed information on these analyses can be obtained. Design examples illustrating these principles and analyses are provided in Part II of this manual.

17. Key Words	18. Distribution Statement
Geotechnical earthquake engineering, soil dynamics, engineering seismology, engineering geology, liquefaction, slopes, foundations, retaining walls	No restrictions.

19. Security Classif. (of this report)	20. Security Classif. (of this page)	21. No. of Pages	22. Price
UNCLASSIFIED	UNCLASSIFIED	392	

Form DOT F 1700.7(8-72) Reproduction of completed page authorized

MODULE 9

TABLE OF CONTENTS

PART I- DESIGN PRINCIPLES

PART II- DESIGN EXAMPLES

Page

CHAPTER 4.0
GROUND MOTION CHARACTERIZATION

4.1 BASIC GROUND MOTION CHARACTERISTICS

Results of the seismic hazard analysis will establish the peak horizontal ground acceleration (PHGA) for use in design analysis. However, PHGA is only one of the characteristics of the earthquake ground motion at a site that influence the potential for damage. The damage potential of seismically-induced ground motions may also depend upon the duration of strong shaking, the frequency content of the motion, the energy content of the motion, peak vertical ground acceleration (PVGA), peak ground velocity and displacement, and the intensity of the motion at times other than when the peak acceleration occurs, as elaborated below.

The acceleration response spectrum is one commonly used index of the character of earthquake ground motions. An acceleration response spectrum provides quantitative information on both the intensity and frequency content of the acceleration time history. However, while widely used in structural engineering, response spectra are of limited use in geotechnical analysis. The primary application of response spectra to geotechnical practice is as an aid in selection of time histories for input to site response and deformation analyses, for comparison of accelerograms, and for illustration and evaluation of the influence of local soil conditions on ground motions.

Other parameters used less frequently than PHGA and the acceleration response spectrum to describe the character of earthquake ground motions include various measures of the duration and energy content of the acceleration time history. Duration is sometimes expressed directly as the length of time from the initiation of strong shaking to its cessation. Alternatively, indirect measures of duration, including the number of equivalent cycles and the number of positive zero crossings of the acceleration time history, are sometimes employed in earthquake engineering practice.

The energy content of the strong ground motion may be expressed in terms of the *root-mean-square* (RMS) and duration of the acceleration time history or in terms of the Arias intensity. The RMS, discussed in detail in Section 4.4, represents an "average" or representative value for the acceleration over the defined duration of the strong ground motion. The Arias intensity is the square of the acceleration integrated over the duration of the motion. The time history of the normalized Arias intensity, referred to as a Husid plot, is sometimes used to define the duration of strong shaking.

These various indices of the character of strong ground motions (*ground motion parameters*) commonly used in engineering practice are defined and described in this chapter. Following their definition and description, procedures for using these indices for selection of representative time histories to characterize earthquake ground motions at a site are presented.

4.2 PEAK VALUES

4.2.1 Evaluation of Peak Parameters

Peak horizontal ground acceleration (PHGA) is the most common index of the intensity of strong ground motion at a site. The PHGA is directly related to the peak inertial force imparted by strong shaking to a structure founded on the ground surface and to the peak shear stress induced within the ground itself. Peak vertical ground acceleration (PVGA), peak horizontal ground velocity (PHGV), and peak horizontal

ground displacement (PHGD) are also used in some engineering analyses to characterize the damage potential of ground motions. For instance, PHGV is a common index of structural damage and PHGD may be used in analyses of retaining walls, tunnels, and underground pipelines. PVGA is an important parameter in the design of base-isolated structures.

Peak values for design analyses are evaluated on the basis of the seismic hazard analysis. For major projects, a site or project specific seismic hazard analysis may be performed. Alternatively, results from published regional seismic hazard analyses or from seismic hazard analyses performed for previous projects in the same vicinity may be used. Most published seismic hazard maps tend to be probabilistic in nature. Both deterministic and probabilistic project-specific analyses are used in practice.

4.2.2 Attenuation of Peak Values

A key step in both deterministic and probabilistic seismic hazard analyses is calculation of the ground motion parameter of interest at a given site from an earthquake of a given magnitude and site-to-source distance. These ground motion parameter values are typically evaluated using an *attenuation relationship*, an equation that relates the parameter value to the key variables on which the ground motion parameter depends (e.g., earthquake magnitude, site-to-source distance, style of faulting). Attenuation relationships may be developed either from statistical analyses of values observed in previous earthquakes or from theoretical models of the propagation of strong ground motions. These observations and analyses indicate that the most important factors influencing peak values of earthquake strong ground motions at a site are the magnitude of the earthquake, the distance between the site and the earthquake source, the style of faulting, and local ground conditions (e.g., rock or soil site conditions).

There are many different attenuation relationships that have been proposed. Campbell (1985), Joyner and Boore (1988), and Atkinson and Boore (1990) provide excellent summaries of many of the available attenuation relationships.

A large number of attenuation relationships are available for the western United States. These attenuation relationships are based primarily on statistical analysis of recorded data. For the eastern and central United States, where little to no recorded strong motion data are available for statistical analysis, relatively few attenuation relationships are available. The few attenuation relationships that do exist for the eastern and central United States are based primarily upon theoretical models of ground motion propagation due to the lack of observational data.

Even when restricted to a relatively narrow geographic locale like the northwestern United States, there may still be a need to use different attenuation relationships for different tectonic conditions. For example, Youngs, *et al.* (1988) found differences in attenuation of ground motions between earthquakes occurring along the interface between the subducting Juan de Fuca tectonic plate and the North American plate (interplate events) and earthquakes occurring within the subducting Juan de Fuca plate (intraplate events) in the Pacific northwest (see Figure 2-1).

PHGA attenuation relationships for shallow earthquakes that occur at the interface between the Pacific and American tectonic plates in the western United States have been developed by many investigators, including Campbell and Duke (1974), Campbell (1993), Campbell and Bozorgnia (1994), Boore, *et al.*, (1993), Boore and Joyner (1994), Sadigh, *et al.*, (1993), Geomatrix (1995), Silva and Abrahamson (1993), Abrahamson and Silva (1996), and Idriss (1995). Table 4-1 presents a summary of commonly used PHGA attenuation relationships in the western United States. These relationships consider earthquake magnitude, site-to-source distance, and local ground conditions (soil or rock). These relationships may also

TABLE 4-1
ATTENUATION RELATIONSHIPS FOR THE WESTERN UNITED STATES
(For Shallow Crustal Earthquakes)

Reference[1]	Magnitude Measure[2]	Distance Measure[3]	Limitation[4]
Schnabel and Seed (1973)	M[5]	Closest Horizontal Distance to the Zone of Energy Release, R_E	Available only in the form of charts. $3 \le R_E \le 1{,}000$ km
Campbell and Duke (1974)	M_S	Hypocentral Distance, R_H	Attenuation of I_A only. $15 \le R_H \le 110$ km
Kavazanjian, *et al.* (1985a)	M_w	Closest Distance to the Rupture Zone, R_R	Attenuation of RMSA only. $0 < R_R < 100$ km
Idriss (1993; 1995)	M_L if $M < 6$ M_S if $M > 6$	Closest Distance to the Rupture Zone, R_R	$1 \le R_R \le 60$ km
Joyner and Boore (1988); Boore, *et al.* (1993)	M_w	Closest *Horizontal* Distance to the Vertical Projection of the Rupture Zone, R_{JB}	$0 < R_{JB} \le 80$ km
Geomatrix (1991, 1995); Sadigh, *et al.* (1993); Silva and Abrahamson (1993); Abrahamson and Silva (1996)	M_w	Closest Distance to the Rupture Zone, R_R	$0 < R_R \le 100$ km
Campbell (1990; 1993); Campbell and Bozorgnia (1994)	M_L if $M < 6$ M_S if $M > 6$	Seismogenic Distance, R_S	$0 < R_S \le 60$ km

Notes:
(1) Table lists main references and their latest updates. The following references also include coefficients for spectral values: Joyner and Boore (1988); Geomatrix (1991, 1995); Campbell (1990, 1993); and Idriss (1993). Relationship by Schnabel and Seed (1973) is shown by dashed lines in Figure 4-2. Relationship by Kavazanjian, *et al.* (1985) is shown in Figure 4-7. See Equation 4-4 for Campbell and Duke (1974) relationship.
(2) M_w = Moment Magnitude, M_L = Local (Richter) Magnitude, M_S = Surface Wave Magnitude. Note that for $M < 6$, $M_L \approx M_W$ and for $M > 6$, $M_s \approx M_w$.
(3) Refer to the original references for detailed definition of distance measures. Note that <u>for design</u>, it is commonly assumed that the rupture zone equals to the area of the fault plane.
(4) I_A = Arias Intensity, as defined in Chapter 4.5; RMSA = Root Mean Square Acceleration as defined in Chapter 4.4.
(5) Magnitude measure was not specified by Schnabel and Seed (1973).

discriminate on the basis of style of faulting, as statistical analysis shows that reverse (thrust) fault events generate peak ground accelerations approximately 20 to 30 percent greater than strike-slip events of the same magnitude at the same distance. Figure 4-1 compares mean value PHGA attenuation curves for magnitude 6.5 and 8.0 events on a strike-slip fault calculated by three commonly used attenuation relationships for western United States earthquakes.

Different attenuation relationships than those used for shallow crustal earthquakes are used for the subduction zone earthquakes that occur along the Pacific Coast in Alaska, Washington, Oregon, and the northwest corner of California. For subduction zone earthquakes, PHGA attenuation relationships by Cohee, *et al.*, (1991) and Youngs, *et al.*, (1988) are often used in earthquake engineering practice. Table 4-2 presents the relationships for attenuation of PHGA in subduction zone earthquakes developed by Cohee, *et al.* (1991) and Youngs, *et al.* (1988).

With respect to differences in ground motion attenuation between the western United States and the eastern and central United States, it is generally agreed that ground motions east of the Rocky Mountains attenuate more slowly than ground motions in the west. However, due to the much lower rates of seismicity and the absence of large magnitude earthquakes since the deployment of strong motion accelerographs in the eastern and central United States, there is insufficient data to characterize the attenuation of strong ground motions east of the Rocky Mountains using statistical methods. Therefore, attenuation relationships used for earthquakes occurring in eastern and central United States are based upon theoretical modeling of ground motion attenuation. Attenuation relationships for the eastern and central United States commonly used in engineering practice include relationships developed by Nuttli and Herrmann (1984), Boore and Atkinson (1987), McGuire, *et al.* (1988), Boore and Joyner (1991), and Atkinson and Boore (1995).

Table 4-2 includes the PHGA attenuation relationships developed by Toro, et. al (1997) for the Mid-Continent and Gulf Coast regions that were used in developing the 1996 USGS seismic hazard maps. Figure 4-2 compares typical PHGA attenuation relationship for the eastern and central United States to that used in the western United States (dashed lines).

Factors other than distance, magnitude, and style of faulting may influence the attenuation of strong ground motions. These factors include depth of earthquake hypocenter, the strike and dip of the fault plane (see Figure 2-6), location of the site relative to the hanging and foot walls of a thrust fault (see Figure 2-7), rupture directivity effects, topographic effects, depth to crystalline bedrock, velocity contrasts, asperities on the rupture surface, wave reflection, wave refraction, and wave scattering. Figure 4-3 presents a recent attenuation relationship developed by Abrahamson and Silva (1996) for reverse (thrust) faults showing the influence of the location of the site with respect to the hanging wall and the foot wall of the fault. Most other factors (e.g., directivity, rupture effects) are not explicitly considered in attenuation relationships and can only be accounted for by detailed seismologic modeling.

4.2.3 Selection of Attenuation Relationships

The engineer choosing an attenuation relationship for use in practice should keep in mind that new attenuation relationships are regularly being developed. Many of the investigators who have developed attenuation relationships for the western United States revise their relationships after almost ever major earthquake to include newly recorded motions. Therefore, when selecting an attenuation relationship, it is prudent to review the current literature and select the most appropriate relationship or relationships for the project site. When evaluating whether or not a certain attenuation relationship is appropriate, the engineer should thoroughly review the published information regarding its development, especially the tectonic regime for which it was developed, the ranges of magnitude and distance to which it is restricted,

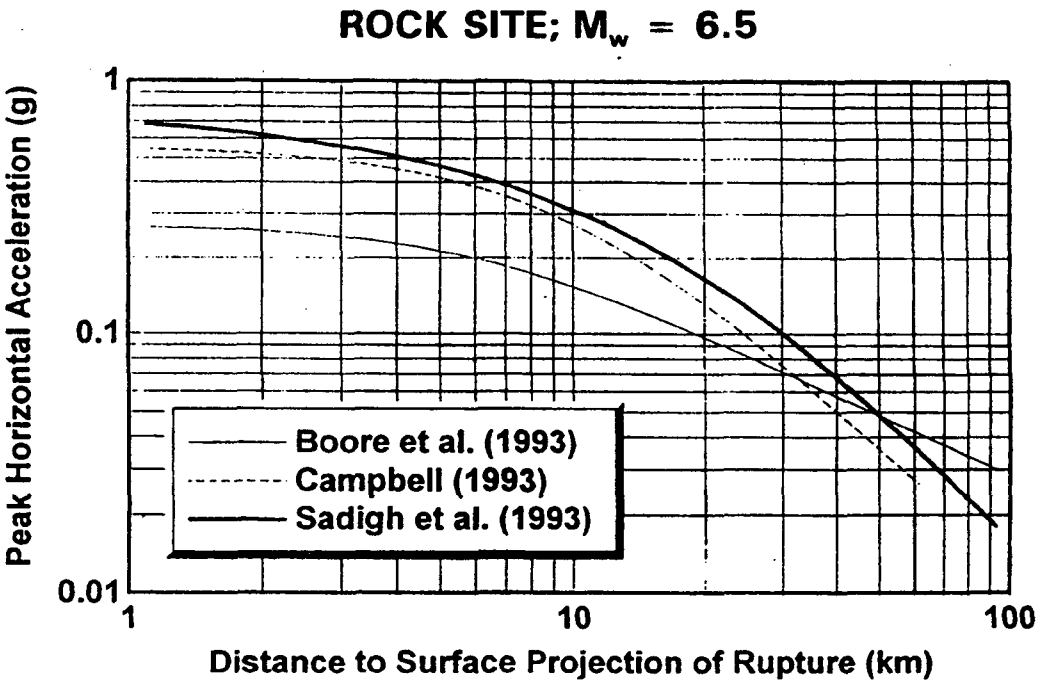

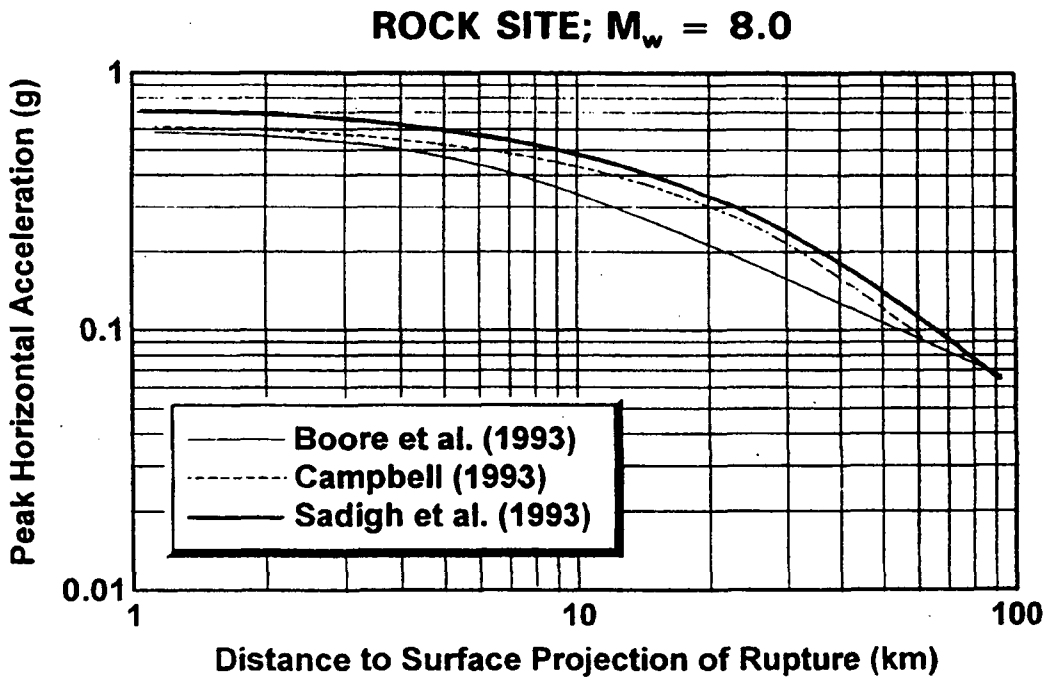

Figure 4-1: Comparison of Attenuation Relationships by Various Investigators. (For Strike-Slip Faults)

TABLE 4-2
ATTENUATION RELATIONSHIP FOR SUBDUCTION ZONE AND CENTRAL AND EASTERN UNITED STATES EARTHQUAKES

Reference	Attenuation Relationship	Limitation[1]
Subduction Zone Youngs, *et al.* (1988)	$\ln(PGA) = 19.16 + 1.045M_w - 4.738 \ln[R_H + 205.5 \exp(0.0968M_w)] + 0.54Z_t$	$20 < R_H \leq 40$ km $M_w \leq 8$
Subduction Zone Youngs, *et al.* (1988)	$\ln(PGA) = 19.16 + 1.045M_w - 4.738 \ln[R_H + 154.7 \exp(0.1323M_w)]$	$20 < R_H \leq 40$ km $M_w > 8$
Subduction Zone Cohee, *et al.* (1991)	$\ln(PGA) = 1.5 - 3.33 \ln(R_S + 128) + 0.79s$	$25 < R_S < 175$ km $M_w \leq 8$
Subduction Zone Cohee, *et al.* (1991)	$\ln(PGA) = 2.8 - 1.26 \ln(R_R) + 0.79s$	$30 < R_R < 100$ km $M_w > 8$
Mid-Continent Toro, *et al.* (1997)	$\ln(PGA) = 2.20 + 0.81 (M_W - 6) - 1.27 \ln(R_m) - 0.11 \text{ Max}[\ln (R_m/100), 0] - 0.0021 R_m$	
Gulf Coast Toro, *et al.* (1997)	$\ln(PGA) = 2.80 + 1.31 (M_W - 6) - 1.49 \ln(R_m) - 0.09 \text{ Max}[\ln (R_m/100), 0] - 0.0017 R_m$	

Notes:
M_w = Moment magnitude.
R_H = Hypocentral distance.
R_R = Closest distance to the rupture zone (fault plane).
R_S = Seismogenic distance (closest distance from the fault asperity).
R_m = $\sqrt{R_{JB}^2 + C_J^2}$
C_J = 9.3 for Mid-Continent, 10.9 for Gulf Coast
R_{JB} = Closest Horizontal Distance to Vertical Projection of Fault Plane (see Figure 2-7)
Z_t = The tectonics term in Youngs, *et al.* (1988). Equal to 0 for interplate events, and 1 for intraplate events.
s = The site term in Cohee, *et al.* (1991) relationship. Equal to 0 for rock sites and 1 for soil sites.
[1] = Refer to the original references for detailed description of distance measures and limitations.

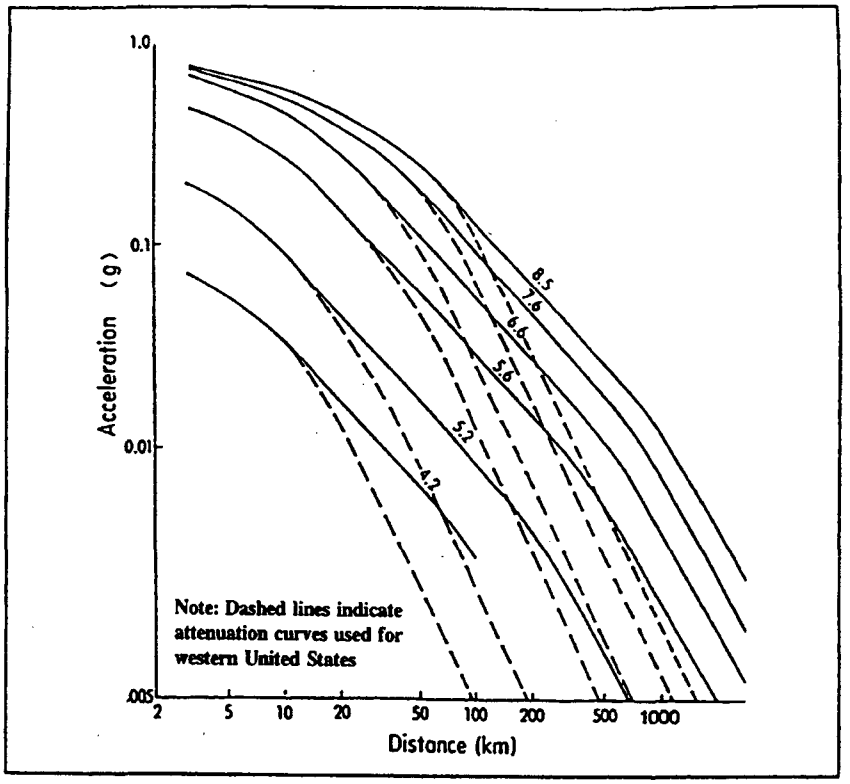

Figure 4-2: Comparison of Attenuation Relationship for Eastern and Central United States to Attenuation Relationship for Western United States.

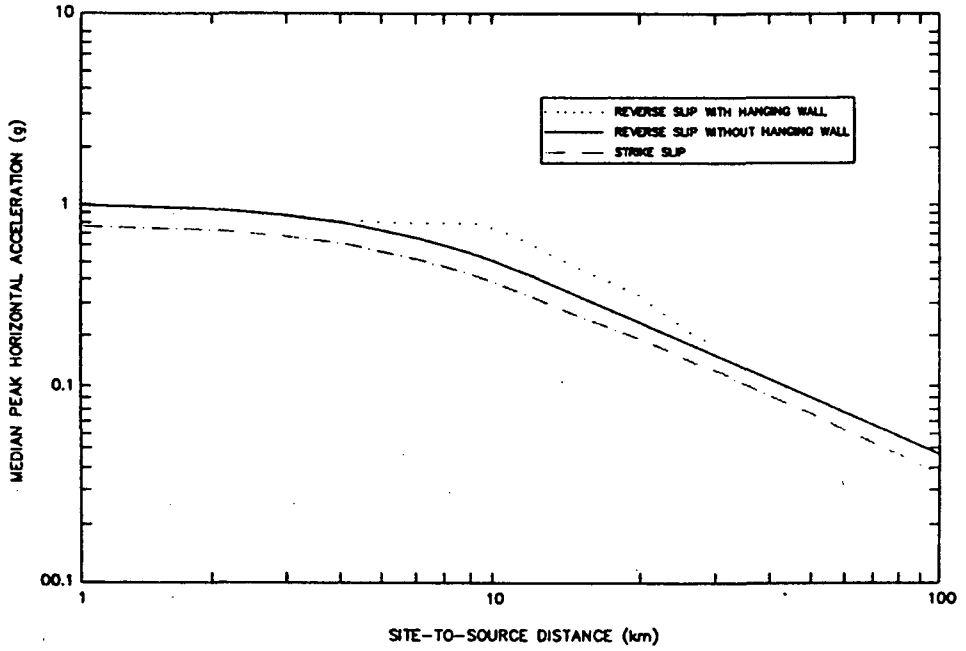

Figure 4-3: Abrahamson and Silva (1997) Attenuation Relationship

and the local ground conditions to which it applies. Frequently, several different attenuation relationships may be found to be equally appropriate. In such a case, the geometric mean (i.e., $\ln X_{mean} = (\Sigma \ln X_i)/n$) of the values calculated using all of the appropriate attenuation relationships is commonly employed in practice. By using the geometric mean of the values calculated by multiple relationships, bias inherent to individual relationships is minimized. However, when this approach is used, the multiple attenuation relationships *should not* include two generations of an attenuation relationship from the same investigator (e.g., Campbell, 1989 and Campbell and Bozorgnia, 1994).

Usually, attenuation relationships for both rock and soil sites will be available for use. Except for soil sites with less than 10 m of soil overlying bedrock and for soft soil sites where the average shear wave velocity over the top 30 m is less than 120 m/s, soil-site attenuation relationships may be used directly to characterize ground motions at a soil site. However, due to the variability in conditions at soil sites and the resulting uncertainty in soil site response, engineers often prefer to use a rock site attenuation relationship to characterize the design earthquake motions at a *hypothetical bedrock outcrop* at the geometric center of the project site and then conduct a site response analysis to evaluate the influence of local soil conditions on the earthquake motions at the site. The hypothetical bedrock outcrop concept is congruent with both the *free-field* (i.e., not affected by structure and/or topography) criterion used to develop the attenuation relationships and with the concepts used to specify motions for input to computer programs for seismic site response analyses (rock outcrop and transmitting boundary models, see Sections 6.4 and 6.5).

4.2.4 Selection of Attenuation Relationship Input Parameters

When using an attenuation relationship, it is important to use the magnitude scale consistent with the scale used to develop the attenuation relationship. In the eastern and central United States, the magnitude measure generally used in practice is body wave magnitude, m_b. In California, moment magnitude, M_w, local (Richter) magnitude, M_L, or surface wave magnitude, M_S, are used. The differences in these scales are due to the type of earthquake waves being measured, the type of instrument used to measure them, and local scaling factors. The relationship between these magnitude scales is shown on Figure 2-5.

Consistency with the site-to-source distance measure used in developing the attenuation relationship is also important, especially for near-field earthquakes. In the early days of development of attenuation relationships, the epicentral distance was often used because it was generally the most reliable distance measure (seismographs were too sparsely located to adequately constrain the focal depth). As seismographs became more numerous and portable arrays were deployed to measure aftershock patterns that roughly delineate the rupture zone, the focal depth and extent of the rupture surface were able to be better located. Statistical analyses indicate that measures of distance from the recording site to the rupture surface provide a more robust measure of seismic wave attenuation than epicentral distance. Therefore, most current attenuation relationships for the western United States use some measure of the distance to the rupture zone. In the eastern and central United States, hypocentral and epicentral distance measures are still commonly used due to the sparsity of strong-motion recordings from significant earthquakes.

4.2.5 Distribution of Output Ground Motion Parameter Values

All of the attenuation relationships commonly used in practice assume that the output ground motion parameter values are log-normally distributed (i.e., the logarithm of the parameter value is normally distributed). Most of the traditional attenuation relationships used in practice characterize the distribution of the output parameter values with a single, constant value for the log normal standard deviation, independent of earthquake magnitude. In these traditional relationships, the mean plus one standard

deviation peak acceleration values are typically about 1.5 times the corresponding mean values. Recently, Sadigh, *et al.* (1993), Idriss (1993), and Campbell and Bozorgnia (1994) have developed magnitude dependent values for the standard deviation, with smaller standard deviations for larger magnitudes.

4.3 FREQUENCY CONTENT

The importance of the frequency content of the earthquake ground motions with respect to the damage potential of the motions has been demonstrated repeatedly by damage surveys following earthquakes. Such damage surveys show strong correlations between damage to engineered structures, the natural period of the damaged structure, and the predominant frequency of the ground motion to which the structure was subjected. The frequency content of earthquake ground motions is generally characterized by the shape of the acceleration response spectrum. Velocity and displacement response spectra are also used in practice to characterize the frequency content of ground motions.

The same statistical analyses used to develop peak ground motion attenuation equations for the western United States have been used to develop attenuation relationships for spectral values. Joyner and Boore (1988), Geomatrix (1991), Campbell (1993), and Idriss (1993) present the coefficients for spectral acceleration attenuation for spectral periods of up to 7.5 seconds. These coefficients can be used to generate smoothed response spectra that illustrate the influence of magnitude and distance on the frequency content of strong ground motions.

Figure 4-4 compares smoothed acceleration response spectra for a rock site from Campbell (1993) for magnitude 5.5, 6.5, and 7.5 events at a distance of 15 km. For comparison purposes, these spectra are all normalized to a zero period (peak ground) acceleration value of 1.0. This figure clearly illustrates the increased damage potential of larger magnitude earthquakes. The larger magnitude events have larger peak spectral accelerations and larger spectral accelerations in the long period range where ground motions are often most damaging, even though all three spectra are scaled to the same peak acceleration value.

Figure 4-5 compares smoothed acceleration response spectra from three different investigators (Campbell, 1993; Sadigh, *et al.*, 1993; and Boore, *et al.*, 1993) for a rock site for a magnitude 6.5 event at a distance of 15 km. This figure illustrates the differences among attenuation relationships developed by different investigators using essentially the same data base. These differences are primarily due to the weighting scheme used in statistical analysis and the screening criteria used by each investigator in culling records from the common data base of world-wide strong motion records available for the analysis and theoretical assumptions on the shape of the attenuationship in the near field (whether or not it "saturates" (plateaus) at low distances) and the rate of decay of ground motion in the far field. The decision on which attenuation to use is a subjective one that is generally based on a comparison between the data base and assumptions used to develop the attenuation relationship and the problem at hand. Alternatively, the arithmetic average or geometric mean of multiple attenuation relationships may be used.

The smoothed acceleration response spectra illustrated in Figures 4-4 and 4-5 are important tools for selection of appropriate time histories for geotechnical analysis. When selecting or synthesizing ground motion time histories for use in engineering analysis, the smoothed spectra are used as a guide to the appropriateness of the time history frequency content. As illustrated in Figure 4-6, a suite of time histories for use in engineering analysis is selected such that the suite as a group conforms to the smoothed spectra, though no single time history is expected to conform to the spectra.

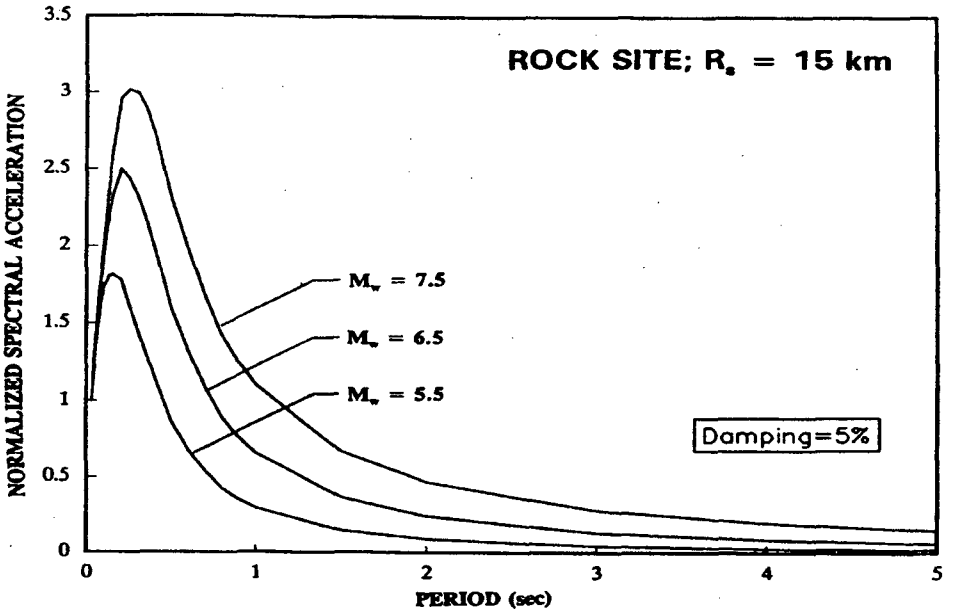

Figure 4-4: Comparison of Smoothed Acceleration Response Spectra for Various Earthquake Magnitudes. (Campbell, 1993 Attenuation Relationship)

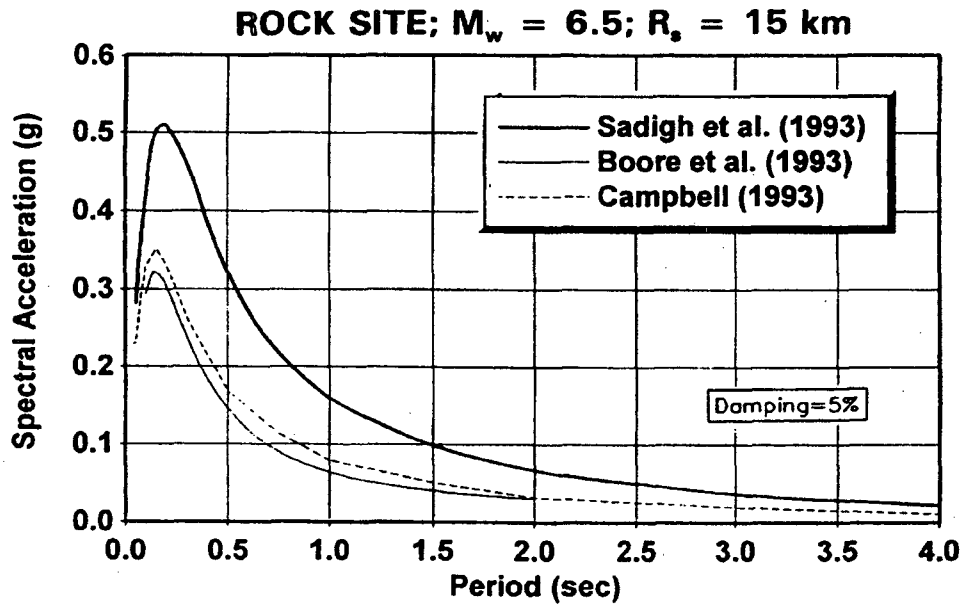

Figure 4-5: Comparison of Smoothed Acceleration Response Spectra by Various Investigators.

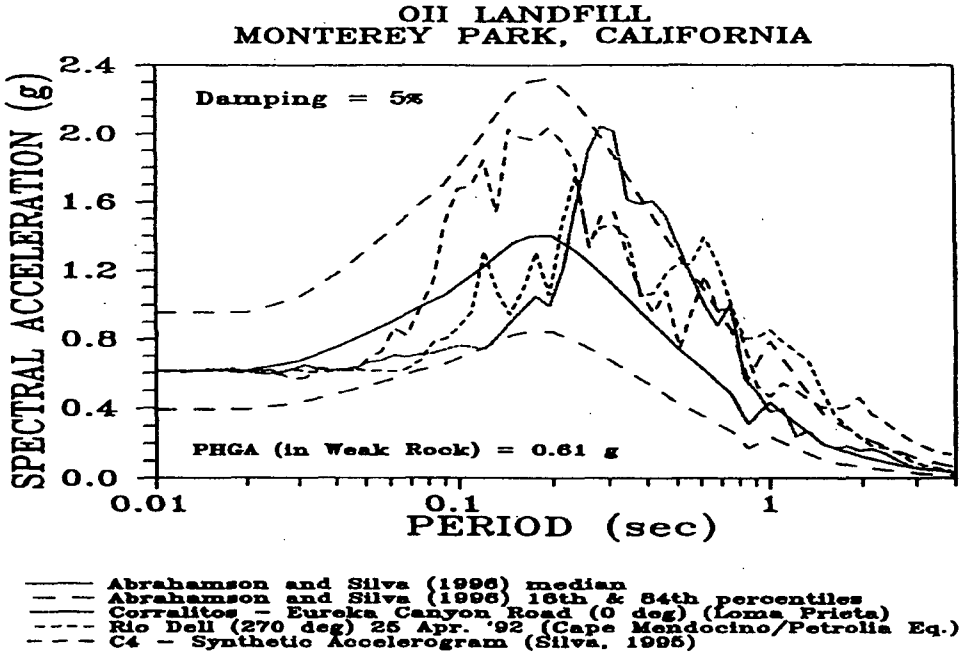

Figure 4-6: Real Spectra vs. Smoothed Spectra

4.4 ENERGY CONTENT

The *energy content* of the acceleration time history provides another means of characterizing strong ground motions. The energy content of the motion is proportional to the square of the acceleration. In engineering practice, the energy content of the motion is typically expressed in terms of either the *root-mean-square* (RMS) and duration of the acceleration time history or the *Arias intensity*, I_A. The RMS of the acceleration time history is the square root of the square of the acceleration integrated over the duration of the motion and divided by the duration:

$$RMSA = \sqrt{\frac{1}{t_f}\int_0^{t_f}[a(t)]^2\,dt} \qquad (4\text{-}1)$$

where RMSA is the RMS of the acceleration time history, *a(t)* is the acceleration time history, and t_f is the duration of strong ground shaking. The RMSA represents an average acceleration for the time history over the duration of strong shaking. The square of the RMSA multiplied by the duration of the motion is directly proportional to the energy content of the motion.

The value of the RMSA depends upon the definition of the duration of the motion. For instance, if the duration of the motion is defined such that it extends into the quiet period beyond the end of strong shaking, the RMSA value will be "diluted" by the quiet period at the end of the record. However, as the energy content of the motion is unchanged, the product of the RMSA and duration will remain constant. As the RMSA is not used as frequently as peak ground acceleration in engineering practice, RMSA attenuation relationships are not developed or revised as frequently as peak acceleration attenuation relationships. Figure 4-7 presents an attenuation relationship for RMSA at rock sites in the western United States developed by Kavazanjian, *et al.* (1985a) using the significant duration (Trifunac and Brady, 1975) defined in the next Section of this Chapter.

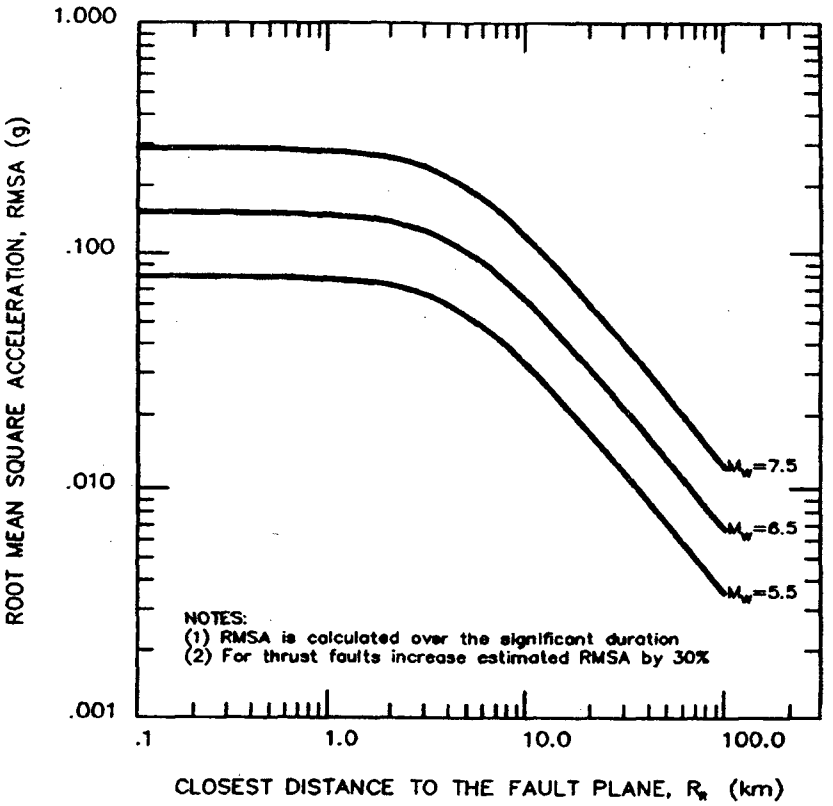

Figure 4-7: Attenuation of the Root Mean Square Acceleration. (Kavazanjian, *et al.*, 1985a, reprinted by permission of ASCE)

The *Arias intensity*, I_A, is proportional to the square of the acceleration integrated over the entire acceleration time history, a(t):

$$I_A = \frac{\pi}{2g}\int_0^{t_f}[a(t)]^2 dt \qquad (4\text{-}2)$$

where g is the acceleration of gravity and t_f is the duration of strong shaking. Arias (1969) showed that this integral is a measure of the total energy of the accelerogram. Arias intensity may be related to the RMSA as follows:

$$I_A = \frac{\pi}{2g}(RMSA)^2 \cdot t_f \qquad (4\text{-}3)$$

Figure 4-8 presents the attenuation relationship developed by Kayen and Mitchell (1997) for Arias intensity.

The specification of the duration of strong shaking for an acceleration time history can be somewhat arbitrary, as relatively low intensity motions may persist for a long time towards the end of the record. If the defined duration of strong motion is increased to include such low intensity motions, the Arias

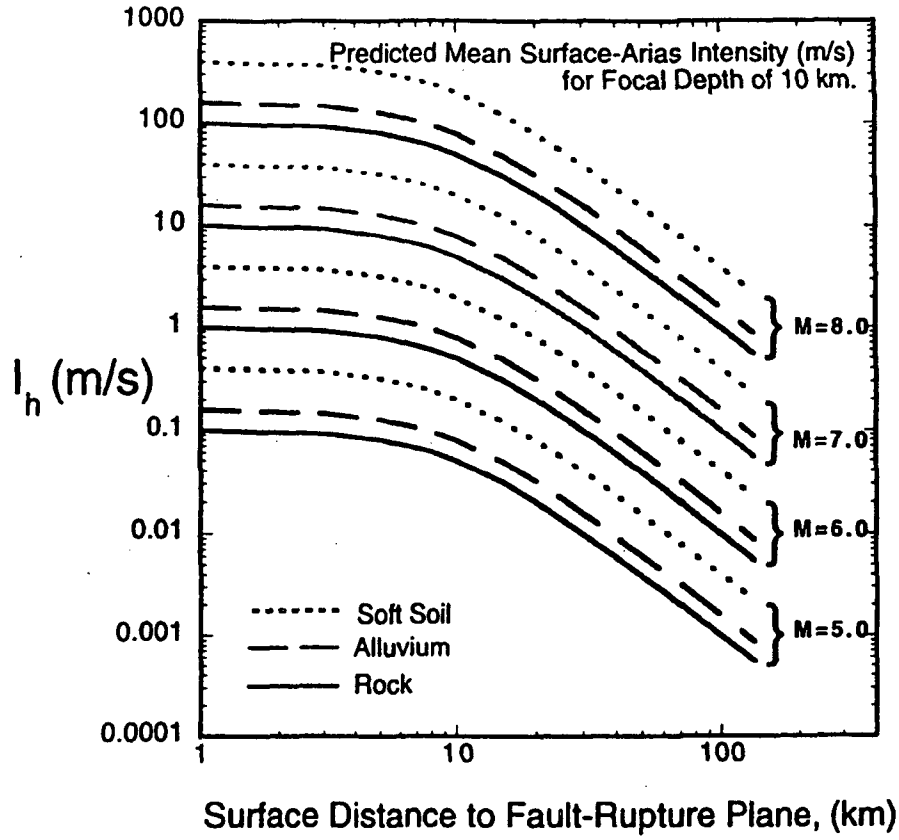

Figure 4-8: Arias Intensity Attenuation Relationship (Kayen and Mitchell, 1997)

intensity will remain essentially constant but the RMSA will decrease (as discussed above). Therefore, some investigators prefer Arias intensity to RMSA as a measure of energy content because the Arias intensity of a strong motion record is a more definite, essentially fixed value while the RMSA depends upon the definition of the duration of strong ground motion. A definition that results in a longer duration will result in a lower RMSA, but I_A will remain essentially unchanged.

Husid (1969) proposed plotting the evolution of the Arias intensity for an accelerogram versus time to study the evolution of energy release for the strong motion record. Figure 4-9 presents the acceleration time history recorded at Aloha Avenue in Saratoga during the 1989 M_w 6.9 Loma Prieta earthquake and the corresponding Husid plot.

Arias intensity and/or RMSA and duration are useful parameters in selecting time histories for geotechnical analysis. This is particularly true if a *seismic deformation analysis* is to be performed, as the deformation potential of a strong motion record is directly proportional to the energy content, which can be expressed as a function of either Arias intensity or the product of the RMSA and duration of the record.

4.5 DURATION

The duration of shaking is important to the response of a soil deposit and/or overlying structures if the materials are susceptible to cyclic pore pressure generation, loss of strength or stiffness during cyclic

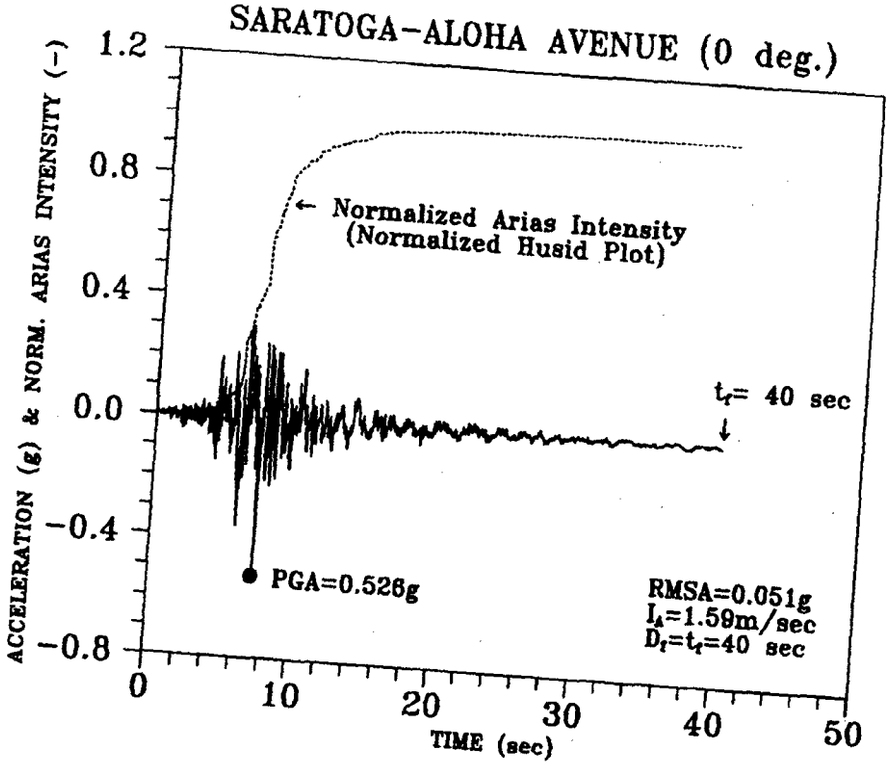

Figure 4-9: Accelerogram Recorded During the 1989 Loma Prieta Earthquake.

loading, or other forms of cumulative damage (e.g., permanent seismic deformation). Duration is often neglected or treated indirectly in evaluating the dynamic response of structures, but is usually implicitly (based upon magnitude) or explicitly accounted for in liquefaction and seismic deformation analyses.

The *bracketed duration of strong motion*, D_b, defined by Bolt (1973) as the elapsed time between the first and last acceleration excursion greater than a specified threshold level, is the definition most often found in strong motion catalogs. Figure 4-10 illustrates calculation of bracketed duration for Saratoga - Aloha Avenue accelerogram and a threshold acceleration of 0.05 g.

For problems dealing with cumulative damage during an earthquake, many engineers find the definition of *significant duration*, D_s, proposed by Trifunac and Brady (1975) to be the most appropriate duration definition. Trifunac and Brady (1975) defined the significant duration as the time interval between 5 and 95 percent of the total Arias intensity on a Husid plot. The Trifunac and Brady definition of duration is illustrated on the Husid plot in Figure 4-11.

The most recent study of significant duration available in the technical literature is by Dobry, *et al.* (1978). These investigators plotted significant duration versus earthquake magnitude for events less than and greater than 25 km from the source. Based upon the summary plot shown on Figure 4-12, these investigators suggested the following design equation for the significant duration at rock sites:

$$D_s = 10^{(0.432M_w - 1.83)} \qquad (4\text{-}4)$$

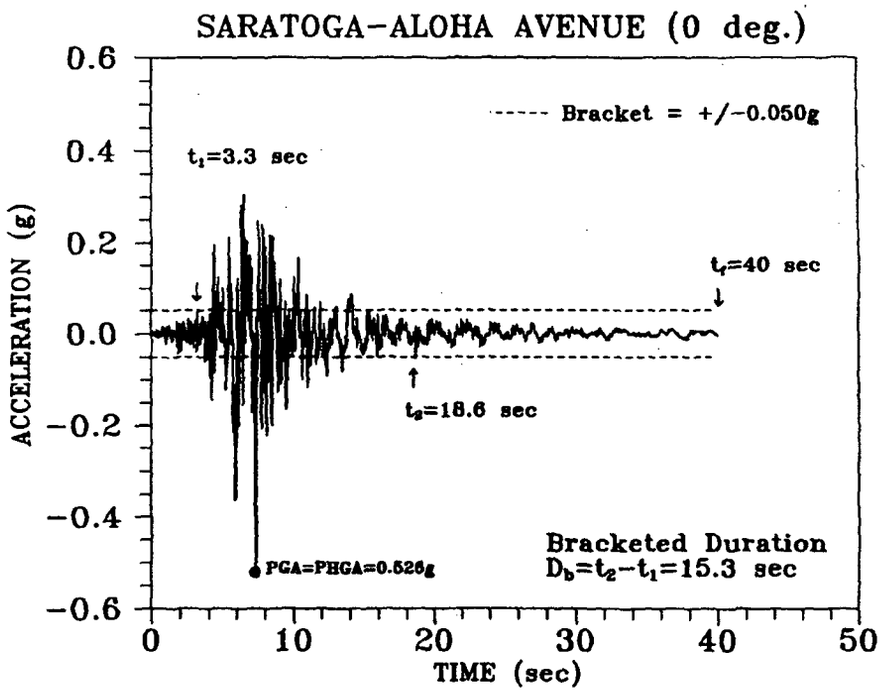

Figure 4-10: Bolt (1973) Duration of Strong Shaking.

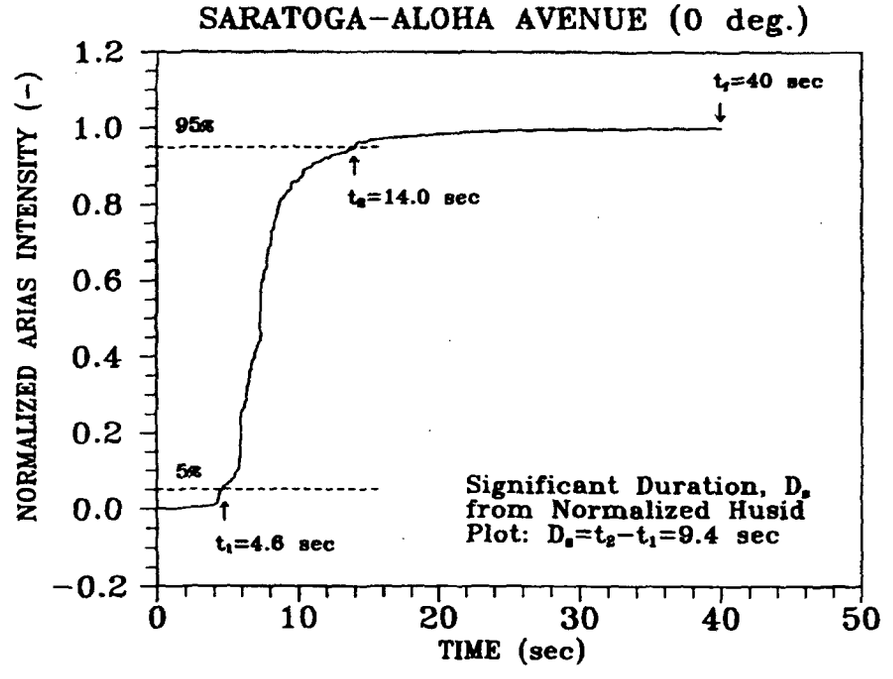

Figure 4-11: Trifunac and Brady (1975) Duration of Strong Shaking.

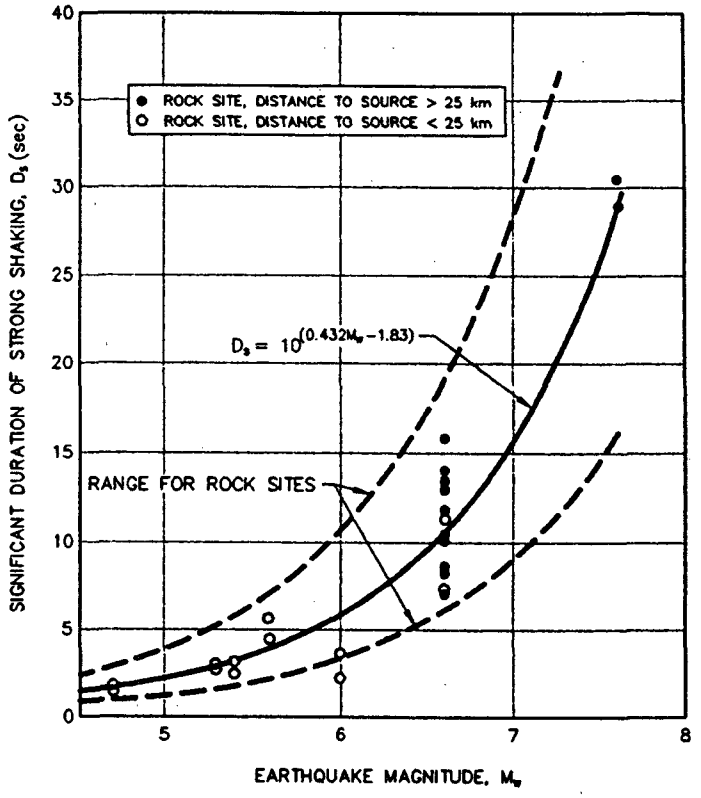

Figure 4-12: Duration Versus Earthquake Magnitude for the Western United States. (Dobry, *et al.*, 1978, reprinted by permission of SSA)

where D_s is the significant duration as defined by Trifunac and Brady (1975) and M_W is the moment magnitude of the design earthquake.

For problems related to soil liquefaction, duration is commonly expressed in terms of the *number of equivalent uniform cycles* (e.g., see Seed, *et al.*, 1975). The number of equivalent uniform cycles is typically expressed as a function of earthquake magnitude to reflect the general increase in duration with increasing magnitude. Recommendations for the number of equivalent uniform cycles as a function of earthquake magnitude for use in liquefaction and seismic settlement analyses are presented in Chapter 8.

4.6 INFLUENCE OF LOCAL SITE CONDITIONS

4.6.1 Local Site Effects

Qualitative reports of the influence of local soil conditions on the intensity of shaking and on the damage induced by earthquake ground motions date back to at least the 1906 San Francisco earthquake (Wood, 1908). Reports of localization of areas of major damage within the same city and of preferential damage to buildings of a certain height within the same local area from the Mexico City earthquake of 1957, the Skopje, Macedonia earthquake of 1963, and the Caracas, Venezuela earthquake of 1967 focused the attention of the engineering community on the influence of local soil conditions on the damage potential of earthquake ground motions.

Back-analysis by Seed (1975) of accelerograms from the moment magnitude M_w 5.3 Daly City (San Francisco) earthquake of 22 March 1957, presented in Figure 4-13, demonstrate the influence of local soil conditions on site response. Figure 4-13 shows peak acceleration, acceleration response spectra, and soil

stratigraphy data at six San Francisco sites approximately the same distance from the source of the 1957 earthquake. The peak acceleration and frequency content of the ground motion recorded at these six sites were dependent on the soil profile beneath each specific site.

At the sites shown in Figure 4-13, the local soil deposits attenuated the peak ground acceleration by a factor of approximately two compared to the bedrock sites. However, the acceleration response spectra for the soil sites clearly show amplification of spectral accelerations at longer periods (periods greater than 0.25 sec) compared to the rock sites. If the bedrock motions had larger spectral accelerations at the longer periods, a characteristic of larger magnitude events and of events from a more distant source, or if the natural period of the local soil deposits more closely matched the predominant period of the bedrock motions, amplification of the peak acceleration could have occurred at the soil sites.

The influence of local ground conditions can also be illustrated using the smoothed acceleration response spectra discussed in Section 4.3. Figure 4-14 presents smoothed acceleration response spectra calculated using the Campbell and Bozorgnia (1994) attenuation relationship for a magnitude 8 event at a distance of 5 km for both soil and rock sites. This figure clearly indicates the tendency for soil site motions to contain a larger proportion of their energy content at longer periods than rock site motions.

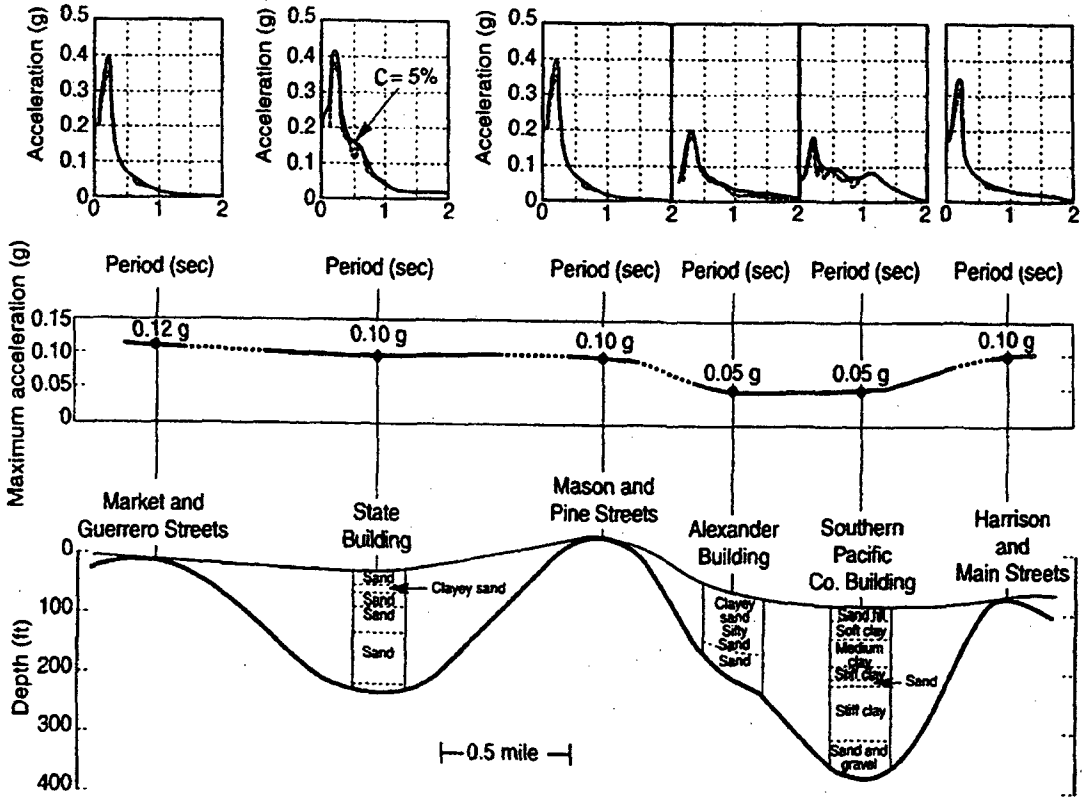

Figure 4-13: Soil Conditions and Characteristics of Recorded Ground Motions, Daly City (San Francisco) M_w 5.3 Earthquake of 1957. (Seed, 1975, reprinted by permission of Chapman and Hall)

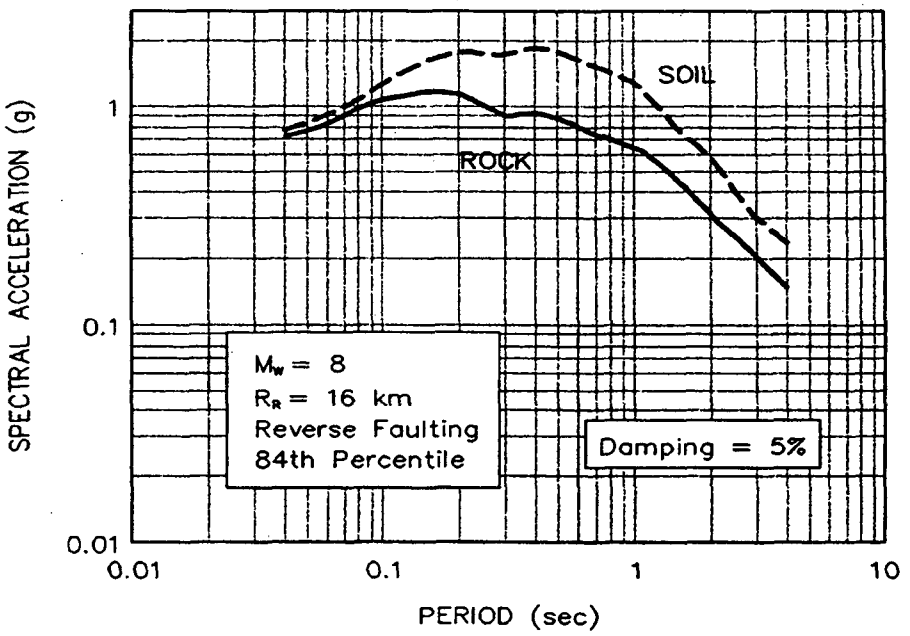

Figure 4-14: Comparison of Soil and Rock Site Acceleration Response Spectra for M_w 8 Event at 5 km. (Campbell and Bozorgnia, 1994, reprinted by permission of EERI)

The Richter Magnitude 8.0 Mexico City earthquake of 1985 provided dramatic evidence of the influence of local soil conditions on earthquake ground motions with respect to both peak ground acceleration and spectral acceleration. Figure 4-15 compares the peak ground acceleration measured at three soft soil sites in Mexico City to the peak acceleration values calculated from a conventional attenuation relationship at the mean plus one standard deviation level. As the figure shows, the peak ground accelerations at the three soft soil sites were significantly greater than the calculated mean plus one standard deviation acceleration values. The peak ground acceleration at one of these sites approached 0.2 g as compared to the mean plus one standard deviation value of 0.08 g for this earthquake, which occurred at a distance of 400 km from Mexico City. Figure 4-16 shows the effect of the local soil conditions at two of these three sites on spectral accelerations. The acceleration response spectra for the two soft clay sites show spectral amplification factors of up to 6 (i.e., a ratio of spectral acceleration to peak ground acceleration of up to 6) at the resonant site period.

4.6.2 Codes and Standards

The influence of local soil conditions on spectral shape may be illustrated using design spectra developed for building codes. For example, the 1994 version of the Uniform Building Code (UBC, 1994), defined three classes of site conditions when defining the shape of the normalized smoothed response spectra for structural design. These three classes of site conditions are rock (Type I), deep, cohesionless or stiff clay soil (Type II), and soft to medium stiff clays and sands (Type III). The smoothed normalized response spectra corresponding to these three site conditions, presented in Figure 4-17, again illustrate the increase in spectral acceleration at long periods for soil site motions compared to rock site motions.

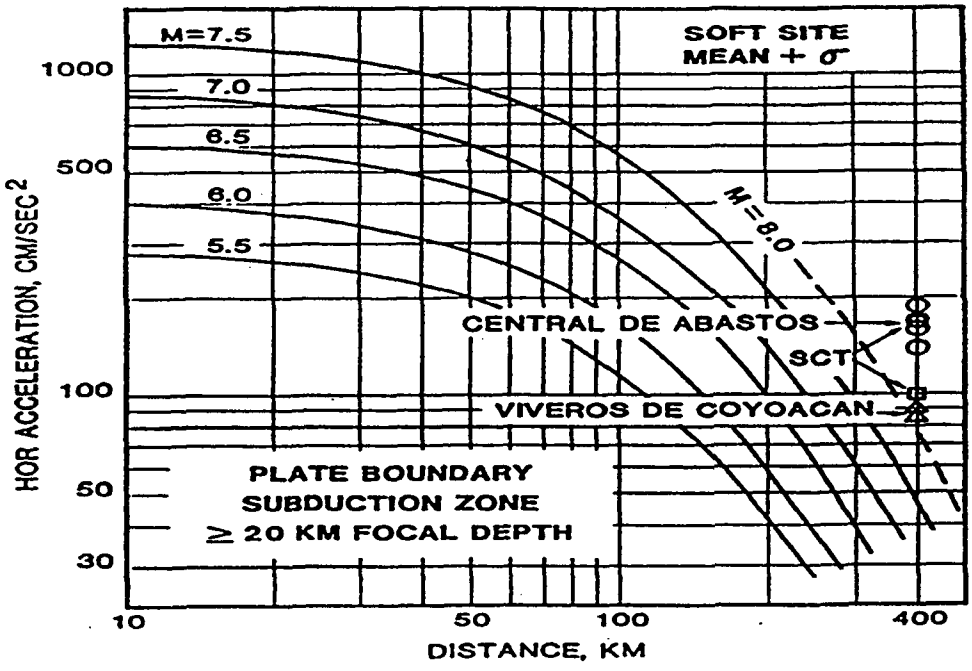

Figure 4-15: PGA Attenuation in 1985 Mexico City Earthquake (Krinitzsky, 1986)

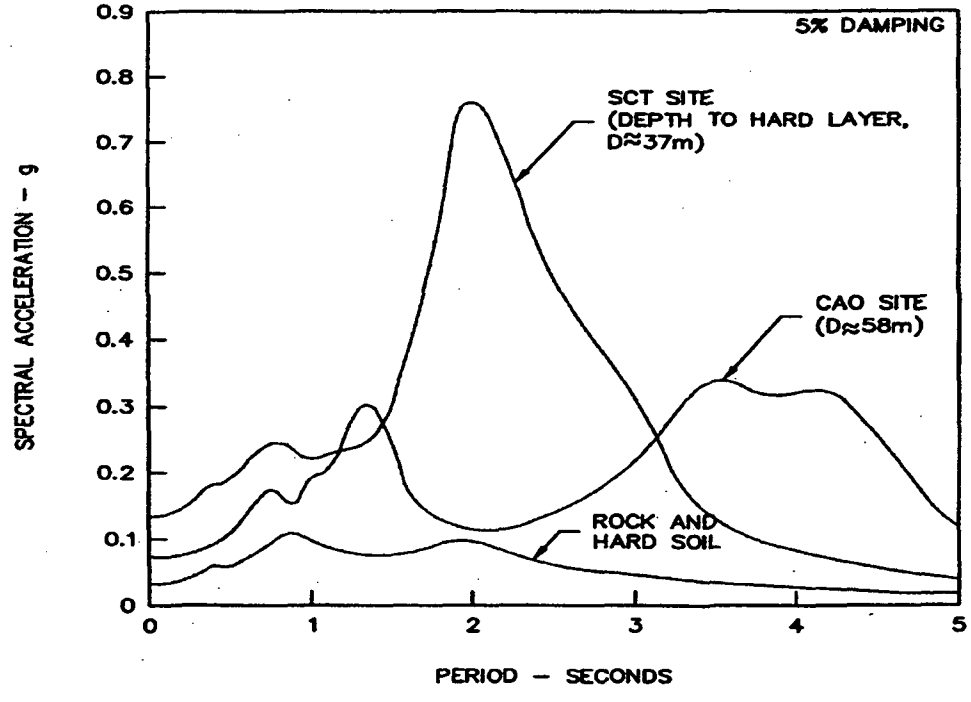

Figure 4-16: Spectral Amplification in 1985 Mexico City Earthquake (Romo and Seed, 1986)

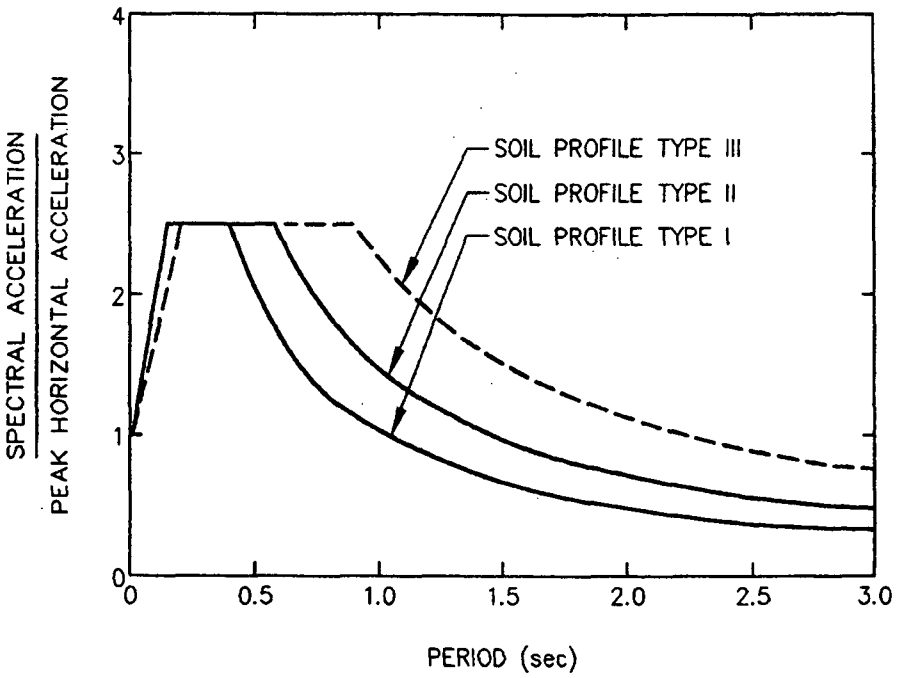

Figure 4-17: Normalized 1994 Uniform Building Code Response Spectra. (UBC, 1994, reproduced from the Uniform Building Code™, copyright© 1994, with the permission of the publisher, the International Conference of Building Officials)

The 1997 version of the UBC has six classes of site conditions and incorporates the effects of near-field ground motion. The six classes of site conditions incorporated in the 1997 UBC, designated S_A through S_F, are defined in Table 4-3 on the basis of the average shear wave velocity in the top 30 meters and other relevant geotechnical characteristics. The acceleration response spectra for classes S_A through S_E are based on Figure 4-18. For site class S_F, a site specific analysis is required to develop the response spectrum. The value of C_a, the spectral acceleration at zero period for the UBC spectra, is equal to the peak ground acceleration with a 10 percent probability of not being exceeded in 50 years. For site classes S_A through S_E, C_a may be taken from Table 4-4 in combination with the use of Figure 3-4 (to determine the Seismic Zone Factor, Z). For site class S_F, a site-specific analysis is required to evaluate C_a. The value of C_V for developing the UBC spectra described by Figure 4-18 is a function of the site class and UBC seismic zone factor (Figure 3-4 and Table 4-5).

For sites close to active faults (i.e. sites in zone 4), the Near Source Factors defined by Tables 4-6 through 4-8 should be applied to C_a and C_V. Vertical spectral accelerations are generally assumed equal to 2/3 of the horizontal spectral accelerations. However, for cases where a Near Source Factor greater than 1.0 is applied to the horizontal spectra, the UBC requires a site-specific analysis to develop the vertical response spectra.

While building code response spectra are useful to illustrate the effect of local soil conditions on ground response, these spectra represent effective spectral accelerations for use in structural design and are not intended to represent smoothed spectra from actual earthquakes. To represent an actual earthquake

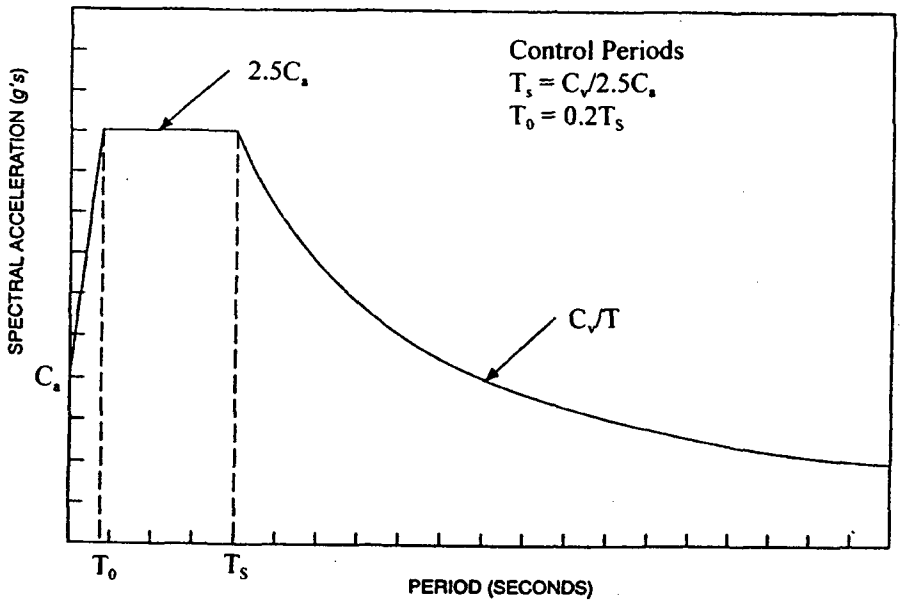

Figure 4-18: 1997 Uniform Building Code Design Response Spectra (UBC, 1997, reproduced from the Uniform Building Code™, copyright© 1997, with the permission of the publisher, the International Conference of Building Officials)

TABLE 4-3
1997 UBC SITE CLASSIFICATION

Designation	Site Class	Shear Wave Velocity[1]	Other Characteristics[2]
S_A	Hard Rock	> 1500 m/s	
S_B	Rock	760 m/s to 1500 m/s	
S_C	Very Dense Soil and Soft Rock	360 m/s to 760 m/s	N > 50, S_u > 100 kPa
S_D	Stiff Soil	180 m/s to 360 m/s	15 < N < 50 50 kPa < S_u < 100 kPa
S_E	Soft Soil	Less than 180 m/s	More than 3m of soil with PI > 20, W_n > 40%, and S_u < 25 kPa
S_F	Special Soils		Collapsible, liquefiable, sensitive soils; More than 3m of peat or highly organic; More than 7.5m of clay with PI > 75; More than 36m of soft to medium clay.

Notes: 1. Average shear wave velocity for upper 30m.
2. N = standard Penetration Test Blow Count
Su = Undrained Shear Strength
PI = Plasticity Index
W_n = Moisture content

TABLE 4-4
SEISMIC COEFFICIENT C_a

Soil Profile Type	Seismic Zone Factor, Z				
	Z = 0.075	Z = 0.15	Z = 0.2	Z = 0.3	Z = 0.4
S_A	0.06	0.12	0.16	0.24	$0.32N_a$
S_B	0.08	0.15	0.20	0.30	$0.40N_a$
S_C	0.09	0.18	0.24	0.33	$0.40N_a$
S_D	0.12	0.22	0.28	0.36	$0.44N_a$
S_E	0.19	0.30	0.34	0.36	$0.36N_a$
S_F	See Footnote 1				

Notes: [1] Site-specific geotechnical investigation and dynamic site response analysis shall be performed to determine seismic coefficients for Soil Profile Type S_F.

TABLE 4-5
SEISMIC COEFFICIENT C_v

Soil Profile Type	Seismic Zone Factor, Z				
	Z = 0.075	Z = 0.15	Z = 0.2	Z = 0.3	Z = 0.4
S_A	0.06	0.12	0.16	0.24	$0.32N_v$
S_B	0.08	0.15	0.20	0.30	$0.40N_v$
S_C	0.13	0.25	0.32	0.45	$0.56N_v$
S_D	0.18	0.32	0.40	0.54	$0.64N_v$
S_E	0.26	0.50	0.64	0.84	$0.96N_v$
S_F	See Footnote 1				

Notes: [1] Site-specific geotechnical investigation and dynamic site response analysis shall be performed to determine seismic coefficients for Soil Profile Type S_F.

TABLE 4-6
SEISMIC SOURCE TYPE[1]

Seismic Source Type	Seismic Source Description	Seismic Source Definition[2]	
		Max. Moment Magnitude, M	Slip Rate, SR (mm/yr)
A	Faults that are capable of producing large magnitude events and that have a high rate of seismic activity	$M \geq 7.0$	$SR \geq 5$
B	All faults other than types A and C	$M \geq 7.0$ $M < 7.0$ $M \geq 6.5$	$SR < 5$ $SR > 2$ $SR < 2$
C	Faults that are not capable of producing large magnitude earthquakes and that have a relatively low rate of seismic activity	$M < 6.5$	$SR \leq 2$

Notes: [1] Subduction sources shall be evaluated on a site-specific basis.
[2] Both maximum moment magnitude and slip rat conditions must be satisfied concurrently when determining the seismic source type.

TABLE 4-7
NEAR-SOURCE FACTOR N_a [1]

Seismic Source Type	Closest Distance to Known Seismic Source [2, 3]		
	≤ 2 km	5 km	≥ 10 km
A	1.5	1.2	1.0
B	1.3	1.0	1.0
C	1.0	1.0	1.0

Notes: [1] The Near-Source Factor may be based on the linear interpolation of values for distances other than those show in the table.
[2] The location and type of seismic sources to be used for design shall be established based on approved geotechnical data.
[3] The closest distance to seismic source shall be taken as the minimum distance between the site and the area described by the vertical projection of the source on the surface. The surface projection need not include portions of the source depths of 10 km or greater. The largest value of the Near-Source Factor considering all sources shall be used for design.

TABLE 4-8
NEAR-SOURCE FACTOR N_v [1]

Seismic Source Type	Closest Distance to Known Seismic Source [2, 3]			
	≤ 2 km	5 km	10 km	≥ 15 km
A	2.0	1.6	1.2	1.0
B	1.6	1.2	1.0	1.0
C	1.0	1.0	1.0	1.0

Notes: [1] The Near-Source Factor may be based on the linear interpolation of values for distances other than those show in the table.
[2] The location and type of seismic sources to be used for design shall be established based on approved geotechnical data.
[3] The closest distance to seismic source shall be taken as the minimum distance between the site and the area described by the vertical projection of the source on the surface. The surface projection need not include portions of the source depths of 10 km or greater. The largest value of the Near-Source Factor considering all sources shall be used for design.

spectrum, the spectrum generated from an attenuation relationship, or the spectrum from seismic site response analysis (see Chapter 6) should be used.

In May 1997, FHWA and the National Center for Earthquake Engineering Research (NCEER) jointly sponsored a workshop on the "National Representation of Seismic Ground Motion for New and Existing Highway Facilities" (Friedland, et. Al, 1997). Among the issues considered at the workshop were:

- Should the USGS maps and UBC code provisions be used for highway facilities;
- Should vertical and near-source ground motions be specified for design; and
- Should spatial variations of ground motions be specified for design?

While building code response spectra are useful to illustrate the effect of local soil conditions on ground Workshop participants concluded that, while the 1996 USGS maps provide the basis for a national portrayal of seismic hazard for highway facilities, design of highway facilities to prevent collapse should consider design ground motions at probabilities lower than 10 percent probability of exceedence in 50 years that is currently in AASHTO and the UBC. The workshop participants recommended to develop seismic hazard maps for highway facilities similar to the 1997 National Earthquake Hazard Reduction Program (NEHRP) provisions for collapse- prevention design of building, wherein the USGS maps for 2% probability of exceedence in 50 years truncated by deterministic peak values in areas of high seismicity was recommended.

Workshop participants concluded that the 1997 UBC spectra, with separate sets of short and long period factors dependant on the intensity of ground shaking, with increased amplification for low levels of shaking, and 1/T decay at long periods, were more appropriate than the current AASHTO provisions for highway facilities design.

Workshop participants also concluded that because the high vertical motions in near-source regions can significantly impact bridge response, vertical ground motions should be specified for certain types of bridges in higher seismic zones. Furthermore, because near-source motions have certain unique characteristics not captured in current UBC or NEHRP spectral shapes, new approaches to specifying near field motions are needed. Workshop participants also recognized that the response of "ordinary" highway bridges is not greatly affected by spatial variations of ground motion, but that spatial variations can be important in some cases and that research is needed to define and address these cases.

4.6.3 Energy and Duration

Local soil conditions can also affect duration and energy content. Energy and durations on soil sites have greater scatter and tend to be longer than durations on rock sites. In fact, the range of energy and durations for rock sites appears to be a lower bound for soil site durations. The FHWA/NCEER workshop participants concluded that energy is a more fundamental parameter, influencing structural response. However, no accepted energy-based design procedures are currently available. For some geotechnical problems, duration may be as important as energy content.

4.6.4 Resonant Site Frequency

Amplification of long period bedrock motions by local soil deposits and constructed dams/embankments and soil retaining systems is now accepted as an important phenomenon that can exert a significant influence on the damage potential of earthquake ground motions. Significant structural damage has been attributed to amplification of both peak acceleration and spectral acceleration by local soil conditions. Amplification of peak acceleration occurs when the resonant frequency of the soil deposits or soil structure is close to the predominant frequencies of the bedrock earthquake motions (the frequencies associated with the peaks of the acceleration response spectra). The *resonant frequency*, f_o, of a horizontal soil layer (deposit) of thickness H can be estimated as a function of the average shear wave velocity of the layer, $(V_s)_{avg}$, using the following equation:

$$f_o = \frac{(V_s)_{avg}}{4H} \tag{4-5}$$

The resonant frequency of a trapezoidal embankment, f_e, can be estimated using a similar equation of the form:

$$f_e = \frac{(V_s)_{avg}}{a_n H} \tag{4-6}$$

where the coefficient a_n varies between 2.4 and 4 as shown in Figure 4-19.

Amplification of the spectral acceleration may occur at soil sites in any earthquake at frequencies around the resonant frequency of the soil deposit. Some of the most significant damage in recent earthquakes

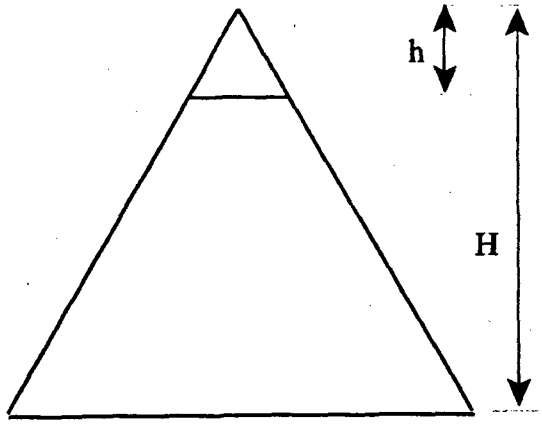

$$\lambda = \frac{h}{H} \qquad f_e = \frac{(V_s)_{avg}}{a_n H}$$

f_e	=	Fundamental Frequency
H-h	=	Height of the Dam/Embankment
V_S	=	Shear Wave Velocity
a_n	=	coefficient

λ	a_n
0.00	2.405
0.03	2.409
0.05	2.416
0.10	2.448
0.15	2.501
0.20	2.574
0.25	2.668
0.30	2.786
0.35	2.930
0.40	3.107
0.45	3.323
0.50	3.588
1.00	4.0

Note: For $0.5 \le \lambda \le 1.0$, a_n may be derived by linear interpolation from $a_n = 3.6$ for $\lambda = 0.5$ to $a_n = 4.0$ for $\lambda = 1.0$.

Figure 4-19: Fundamental Frequency of Trapezoidal Dam/Embankment

(e.g., building damage in Mexico City in the 1985 earthquake and damage to freeway structures in the Loma Prieta earthquake of 1989) has occurred in situations where the predominant frequencies of the bedrock motions and the resonant frequencies of both the local soil deposit and the overlying structure all fell within the same range.

4.7 SELECTION OF REPRESENTATIVE TIME HISTORIES

Earthquake time histories may be required for input to both seismic site response analyses (see Chapter 6) and seismic deformation analyses (see Chapter 7). There are several procedures that can be used to select earthquake ground motions at a site. These procedures include:

- selection of motions previously recorded for similar site conditions during a similar earthquake and at distances comparable to those under consideration;
- selection of generic, publicly available synthetic ground motions generated to represent an event of the target magnitude;
- estimation of a *target spectrum* (a spectrum representative of the design magnitude, site-to-source distance, and local geology (soil or rock) using either an attenuation relationship or a code or standard) and then selection of recorded or synthetic time histories whose special ordinates are either comparable to or envelope those of the target spectrum for the period range of interest; or
- use of simulation techniques to generate a project-specific synthetic time history, starting from the source and propagating the appropriate wave forms to the site to generate a suite of time histories that can then be used to represent the earthquake ground motions at the site of interest.

In selecting a representative time history from the catalog of available records, an attempt should be made to match as many of the relevant characteristics of the design earthquake as possible. Important characteristics that should be considered in selecting a time history include:

- earthquake magnitude;
- source mechanism (e.g., strike slip, dip slip, or oblique faulting);
- focal depth;
- site-to-source distance;
- site geology;
- peak ground acceleration;
- frequency content;
- duration; and
- energy content (RMSA or I_A).

The relative importance of these factors varies from case to case. For instance, if a bedrock record is chosen for use in a site response analysis to model the influence of local soil conditions, site geology will not be particularly important in selection of the input bedrock time history. However, if a soil site record is to be scaled to a specified peak ground acceleration, site geology can be a critical factor in selection of an appropriate time history, as the record must already include any potential influence of local soil conditions on the motion. Scaling of the peak acceleration of a strong motion record by a factor of more than two is not recommended, as the frequency characteristics of ground motions can be directly and indirectly related to the amplitude of the motion. Leeds (1992) and Naeim and Anderson (1993) present comprehensive databases of available strong motion records and their characteristics. These strong motion

records can be obtained in digital form (CD-ROM) from the National Geophysical Data Center (NGDC) in Boulder, Colorado. Also, Tao (1996) provides detailed information on several other sources from which accelerograms can be obtained directly via on-line systems or purchased in a variety of formats.

Due to uncertainties in the selection of a representative earthquake time history, response analyses are usually performed using a suite of time histories rather than a single time history. Engineers commonly use two to five time histories to represent each significant seismic source in a site response analysis. The 1997 UBC requires a minimum of three pairs of time histories from recorded events for time history analysis. For earthquakes in the western United States, it should be possible to find three to five representative time histories that satisfy the above criteria. However, at the present time, there are a limited number of bedrock strong motion records available from earthquakes of magnitude M_w 5.0 or greater in the central and eastern United States or Canada, including:

- eight records from the 1988 Saguenay, Quebec earthquake of magnitude M_w 5.9;
- three records from the 1985 Nahanni; Northwest Territories (Canada) Earthquake of Magnitude M_w 6.7; and
- the Loggie Lodge record with a peak horizontal acceleration of 0.4 g from the 1981 Mirimichi, New Brunswick earthquake of magnitude M_w 5.0.

Therefore, for analysis of sites east of the Rocky Mountains, records from a western United States site, an international recording site or synthetic accelerograms are often used to compile a suite of at least three records for analysis.

Generic, synthetically generated ground motions are available only for a limited number of major faults (fault systems). For example, Jennings, *et al.* (1968) developed the A1 synthetic accelerogram for soil site conditions for an earthquake on the southern segment of the San Andreas fault. Seed and Idriss (1969) developed a synthetic accelerogram for rock sites for an earthquake on the northern segment of the San Andreas fault. The Jennings, *et al.* (1968) A1 accelerogram has an energy content which is larger than the energy content of any accelerogram recorded to date. For this reason, the A1 record is often used to simulate major earthquakes in the Cascadia and New Madrid seismic zones. Appropriate synthetic accelerograms may also be available to the engineer from previous studies and may be used if they are shown to be appropriate for the site. Synthetic earthquake accelerograms for many regions of the country are currently being compiled by the Lamont-Doherty Earth Observatory of Columbia University under the auspices of the Multi-Disciplinary Center for Earthquake Engineering Research (formally National Center for Earthquake Engineering Research, NCEER) and can be downloaded from the NCEER website at "http://nceer.eng.buffalo.edu. A catalog of records representative on northeastern United States seismicity (i.e., Boston) was recently developed for a Federal Emergency Management Agency (FEMA) research project on the performance of steel buildings (Somerville, et. Al, 1998). These records can be downloaded from the Earthquake Engineering Research Center (EERC) website at "http://quiver.eerc.berkeley.edu:8080/studies/system/ ground_motions.html."

The *target spectrum* may be estimated from available attenuation relationships (see Section 4.3). These attenuation relationships, typically developed for a spectral damping of 5 percent, provide estimates of the median spectral ordinates and the log-normal standard deviation about the mean. Representative time histories are selected by trial-and-error on the basis of "reasonable" match with the target spectrum. A "reasonable" match does not necessarily mean that the response spectrum for the candidate record "hugs" the target spectrum. Particularly if a suite of time histories is used, a "reasonable" match only requires that the suite of response spectra averaged together approximates the mean target spectrum. Each individual spectrum may fluctuate within the plus and minus one standard deviation bounds over most of

the period range of interest. Natural and/or generic synthetic time histories can be screened in this type of selection process.

An alternative approach to trial-and-error matching of the target spectrum is computerized generation of a synthetic time history or a suite of time histories whose spectral ordinates provide a reasonable envelope to those of the target spectrum. Existing time histories can also be modified to be spectrum compatible. Several computer programs are available for these tasks (e.g., Gasparin and Vanmarcke, 1976; Ruiz and Penzien, 1969; Silva and Lee, 1987). However, generation of realistic synthetic ground motions is not within the technical expertise of most geotechnical engineering consultants. The simulation programs should only be used by qualified engineering seismologists and earthquake engineers. For this reason, these simulation techniques are beyond the scope of this guidance document.

CHAPTER 8.0
LIQUEFACTION AND SEISMIC SETTLEMENT

8.1 INTRODUCTION

During strong earthquake shaking, loose, saturated cohesionless soil deposits may experience a sudden loss of strength and stiffness, sometimes resulting in loss of bearing capacity, large permanent lateral displacements, and/or seismic settlement of the ground. This phenomenon is called *soil liquefaction.* In the absence of saturated or near-saturation conditions, strong earthquake shaking can induce compaction and settlement of the ground. This phenomenon is called *seismic settlement.*

Liquefaction and/or seismic settlement beneath and in the vicinity of highway facilities can have severe consequences with respect to facility integrity. Localized bearing capacity failures, lateral spreading, and excessive settlements resulting from liquefaction may damage bridges, embankments, and other highway structures. Liquefaction-associated lateral spreading and flow failures and seismically-induced settlement can also affect the overall stability of the roadway. Similarly, excessive total or differential settlement can impact the integrity and/or serviceability of highway facilities. Therefore, a liquefaction and seismic settlement potential assessment is a key element in the seismic design of highways.

This Section outlines the current state-of-the-practice for evaluation of the potential for, and the consequences of (should it occur), soil liquefaction and seismic settlement as they apply to the seismic design of highways. Initial screening criteria to determine whether or not a liquefaction analysis is needed for a particular project are presented in Section 8.2. The simplified procedure for liquefaction potential assessment commonly used in engineering practice is presented in Section 8.3. Methods for performing a liquefaction impact assessment, i.e., to estimate post-liquefaction deformation and stability, are presented in Section 8.4. The simplified procedures for seismic settlement of unsaturated sand evaluation commonly used in engineering practice are presented in Section 8.5. Methods for mitigation of liquefaction and seismic settlement potential and of the consequences of liquefaction are discussed in Section 8.6. Advanced methods for liquefaction potential assessments, including one- and two-dimensional fully-coupled effective stress site response analyses, are briefly discussed in Section 8.3.

8.2 FACTORS AFFECTING LIQUEFACTION SUSCEPTIBILITY

The first step in any liquefaction evaluation is to assess whether the potential for liquefaction exists at the site. A variety of screening techniques exist to distinguish sites that are clearly safe with respect to liquefaction from those sites that require more detailed study (e.g., Dobry, *et al.*, 1980). The following five screening criteria are most commonly used to make this assessment:

- *Geologic age and origin.* Liquefaction potential decreases with increasing age of a soil deposit. Pre-Holocene age soil deposits generally do not liquefy, though liquefaction has occasionally been observed in Pleistocene-age deposits. Table 8-1 presents the liquefaction susceptibility of soil deposits as a function of age and origin (Youd and Perkins, 1978).

- *Fines content and plasticity index.* Liquefaction potential decreases with increasing fines content and increasing plasticity index, PI. Data presented in Figure 8-1 (Ishihara, *et al.*, 1989) show grain size distribution curves of soils known to have liquefied in the past. This data serves as a rough guide for liquefaction potential assessment of cohesionless soils. Soils having greater than 15 percent (by

TABLE 8-1
SUSCEPTIBILITY OF SEDIMENTARY DEPOSITS TO LIQUEFACTION DURING STRONG SHAKING
(After Youd and Perkins, 1978, Reprinted by Permission of ASCE)

Type of Deposit	General Distribution of Cohesionless Sediments in Deposits	Likelihood that Cohesionless Sediments, When Saturated, Would Be Susceptible to Liquefaction (by Age of Deposit)			
		<500 Year	Holocene	Pleistocene	Pre-pleistocene
Continental Deposits					
River channel	Locally variable	Very high	High	Low	Very low
Flood plain	Locally variable	High	Moderate	Low	Very low
Alluvial fan and plain	Widespread	Moderate	Low	Low	Very low
Marine terraces and plains	Widespread	—	Low	Very low	Very low
Delta and fan-delta	Widespread	High	Moderate	Low	Very low
Lacustrine and playa	Variable	High	Moderate	Low	Very low
Colluvium	Variable	High	Moderate	Low	Very low
Talus	Widespread	Low	Low	Very low	Very low
Dunes	Widespread	High	Moderate	Low	Very low
Loess	Variable	High	High	High	Unknown
Glacial till	Variable	Low	Low	Very low	Very low
Tuff	Rare	Low	Low	Very low	Very low
Tephra	Widespread	High	High	Unknown	Unknown
Residual soils	Rare	Low	Low	Very low	Very low
Sebka	Locally variable	High	Moderate	Low	Very low
Coastal Zone					
Delta	Widespread	Very high	High	Low	Very low
Esturine	Locally variable	High	Moderate	Low	Very low
Beach-high wave energy	Widespread	Moderate	Low	Very low	Very low
Beach-low wave energy	Widespread	High	Moderate	Low	Very low
Lagoonal	Locally variable	High	Moderate	Low	Very low
Fore shore	Locally variable	High	Moderate	Low	Very low
Artificial Deposits					
Uncompacted fill	Variable	Very high	—	—	—
Compacted fill	Variable	Low	—	—	—

weight) finer than 0.005 mm, a liquid limit greater than 35 percent, or an in-situ water content less than 0.9 times the liquid limit generally do not liquefy (Seed and Idriss, 1982).

- *Saturation.* Although unsaturated soils have been reported to liquefy, at least 80 to 85 percent saturation is generally deemed to be a necessary condition for soil liquefaction. In many locations, the water table is subject to seasonal oscillation. In general, it is prudent that the highest anticipated seasonal water table elevation be considered for initial screening.

- *Depth below ground surface.* While failures due to liquefaction of end-bearing piles resting on sand layers up to 30 m below the ground surface have been reported, shallow foundations are generally not affected if liquefaction occurs more than 15 m below the ground surface.

- *Soil penetration resistance.* According to the data presented in Seed and Idriss (1982), liquefaction has not been observed in soil deposits having normalized Standard Penetration Test (SPT) blow counts, $(N_1)_{60}$ larger than 22. Marcuson, *et al.* (1990) suggest a normalized SPT value of 30 as the threshold value above which liquefaction will not occur. However, Chinese experience, as quoted in Seed, *et al.* (1983), suggests that in extreme conditions liquefaction is possible in soils having normalized SPT blow counts as high as 40. Shibata and Teparaska (1988), based on a large number of observations, conclude that no liquefaction is possible if normalized Cone Penetration Test (CPT) cone resistance, q_{c1}, is larger than 15 MPa.

If three or more of the above criteria indicate that liquefaction is *not* likely, the potential for liquefaction may be considered to be small enough that a formal liquefaction potential analysis is not required. If, however, based on the above initial screening criteria, the potential for liquefaction of a cohesionless soil layer beneath the site cannot be dismissed, more rigorous analysis of liquefaction potential is needed.

Liquefaction susceptibility maps, derived on the basis of some (or all) of the above listed criteria, are available for many major urban areas in seismic zones (e.g., Kavazanjian, *et al.*, 1985b for San Francisco; Tinsley, *et al.*, 1985 for Los Angeles; Hadj-Hamou and Elton, 1988 for Charleston, South Carolina; Hwang and Lee, 1992 for Memphis). These maps may be useful for preliminary screening analyses for highway routing studies. However, as most new highways are sited outside major urban areas, these types of maps are unlikely to be available for many highway sites. Furthermore, most of these maps do not provide sufficient detail to be useful for site-specific studies or detailed design analyses.

Several attempts have been made to establish threshold criteria for values of seismic shaking that can induce liquefaction (e.g., minimum earthquake magnitude, minimum peak horizontal acceleration, maximum distance from causative fault). Most of these criteria have eventually been shown to be misleading, since even low intensity bedrock ground motions from distant earthquakes can be amplified by local soils to intensity levels strong enough to induce liquefaction, as observations of liquefaction in the 1985 Mexico City and 1989 Loma Prieta earthquakes demonstrate.

Most soil deposits known to have liquefied are sand deposits. However, as indicated on Figure 8-1, some deposits containing gravel particles (> 2 mm size) in a fine grained soil matrix may be susceptible to liquefaction. Discussion of the liquefaction potential of gravel deposits is beyond the scope of this document. The reader is referred to Ishihara (1985), Harder (1988), and Stark and Olson (1995) for a discussion of methods for evaluation of the liquefaction potential of gravels.

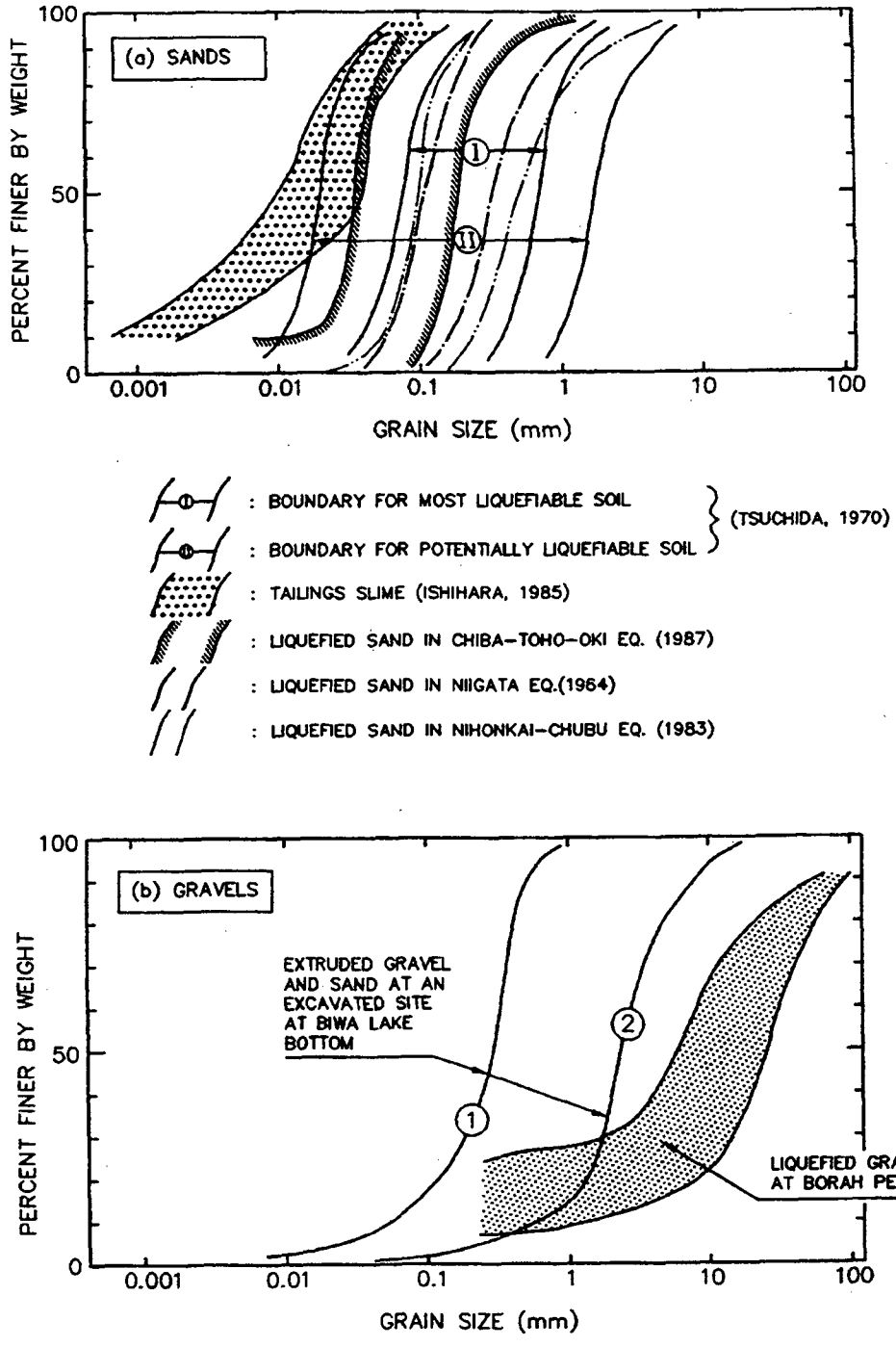

Figure 8-1: Grain Size Distribution Curves of Potentially Liquefiable Soils. (Modified after Ishihara, *et al.*, 1989, reprinted with permission of A.A. Balkema, Old Post Rd., Brookfield, VT 05036)

8.3 EVALUATION OF LIQUEFACTION POTENTIAL

8.3.1 Introduction

Due to the difficulties in obtaining and testing undisturbed representative samples from most potentially liquefiable soil materials, in situ testing is the approach preferred by most engineers for evaluating the liquefaction potential of a soil deposit. Liquefaction potential assessment procedures involving both the SPT and CPT are widely used in practice (e.g., Seed and Idriss, 1982; Ishihara, 1985; Seed and De Alba, 1986; Shibata and Teparaska, 1988; Stark and Olson, 1995). For gravelly soils, the Becker Penetration Test (BPT) is commonly used to evaluate liquefaction potential (Harder and Seed, 1986). Geophysical techniques for measuring shear wave velocity have recently emerged as potential alternatives for liquefaction potential assessment (Tokimatsu, *et al.*, 1991; Youd and Idriss, 1997).

8.3.2 Simplified Procedure

The most common procedure used in engineering practice for the liquefaction potential assessment of sands and silts is the *Simplified Procedure* originally developed by Seed and Idriss (1982). Since its original development, the original Simplified Procedure as proposed by Seed and Idriss has been progressively revised, extended, and refined (Seed, *et al.*, 1983; Seed, *et al.*, 1985; Seed and De Alba, 1986; Liao and Whitman, 1986). The Simplified Procedure may be used with either SPT or CPT data. Recent summaries of the various revisions to the Simplified Procedure are provided by Marcuson, *et al.*, (1990) and Seed and Harder (1990). A 1996 workshop sponsored by the National Center for Earthquake Engineering Research (NCEER) reviewed recent developments on evaluation of liquefaction resistance of soils and arrived consensus on improvements and augmentation to the simplified procedure (Youd and Idriss, 1997). Based primarily on recommendations from these studies, the Simplified Procedure for evaluating liquefaction potential at the site of highway facilities can be performed using the following steps:

Step 1: From borings and soundings, in situ testing and laboratory index tests, develop a detailed understanding of the project site subsurface conditions, including stratigraphy, layer geometry, material properties and their variability, and the areal extent of potential problem zones. Establish the zones to be analyzed and develop idealized, representative sections amenable to analysis. The subsurface data used to develop the representative sections should include the location of the water table, either SPT blow count, N, or tip resistance of a standard CPT cone, q_c, mean grain size, D_{50}, unit weight, and the percentage of fines in the soil (percent by weight passing the U.S. Standard No. 200 sieve).

Step 2: Evaluate the total vertical stress, σ_v, and effective vertical stress, σ_v', for all potentially liquefiable layers within the deposit both at the time of exploration and for design. Vertical and shear stress design values should include the stresses resulting from facility construction. Exploration and design values for vertical total and effective stress may be the same or may differ due to seasonal fluctuations in the water table or changes in local hydrology resulting from project development. Note that for underwater sites, the total weight of water above the mudline should not be included in calculating the total vertical stress. Also evaluate the initial static shear stress on the horizontal plane, τ_{ho}, for design.

Step 3: If results of a site response analysis are not available, evaluate the *stress reduction factor*, r_d as described below. The stress reduction factor is a soil flexibility factor defined as the ratio of the peak shear stress for the soil column, $(\tau_{max})_d$, to that of a rigid body, $(\tau_{max})_r$. There are several ways to obtain r_d. For non-critical projects, the following equations for r_d were recommended by

a panel of experts convened by the National Center for Earthquake Engineering Research (NCEER) in 1996 (Youd and Idriss, 1997):

$$
\begin{aligned}
r_d &= 1.0 - 0.00765\ z && \text{for } z \le 9.15 \text{ m} \\
r_d &= 1.174 - 0.0267\ z && \text{for } 9.15 \text{ m} < z \le 23 \text{ m} \\
r_d &= 0.744 - 0.008\ z && \text{for } 23 < z \le 30 \text{ m} \\
r_d &= 0.5 && \text{for } z > 30 \text{ m}
\end{aligned}
\qquad (8\text{-}1)
$$

where z is the depth below the ground surface in meters. Mean values of r_d calculated from Equation 8-1 are plotted in Figure 8-2 along with the range of data proposed by seed and Idriss (1971).

For critical projects warranting a site-specific response analysis, or if results of a site response analysis (see Chapter 6) are available, the maximum earthquake-induced shear stress at depth z, τ_{max}, can be directly obtained from the results of the site response analysis. In this case, it may be convenient to calculate r_d from the site response results for use in spreadsheet calculations using the following equation:

$$
r_d = \frac{(\tau_{max})_{@depth=z}}{(\sigma_v)_{@depth=z} \cdot (a_{max}/g)_{@surface}} \qquad (8\text{-}2)
$$

where σ_v is the total shear stress at depth z, a_{max} is the peak ground surface acceleration, and g is the acceleration of gravity. The parameters σ_v and a_{max} are also directly calculated by most site response computer programs described in Chapter 6.

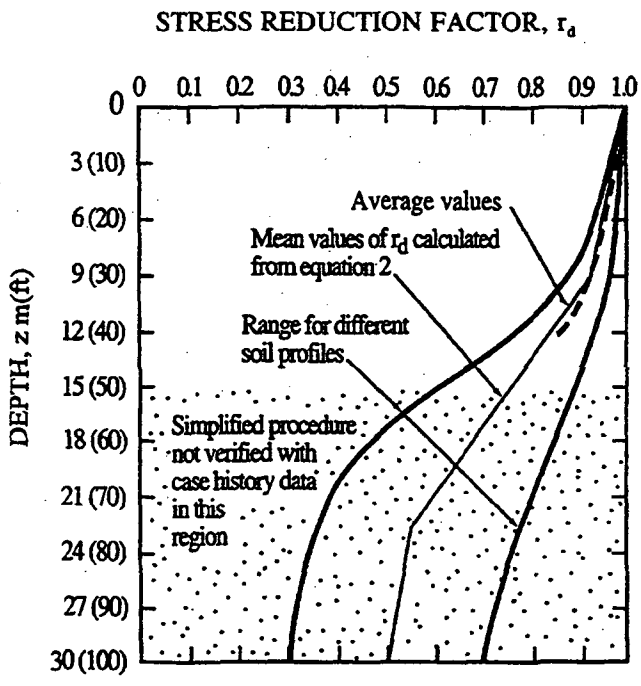

Figure 8-2: Stress Reduction Factor, r_d, Versus Depth Curves Developed by Seed and Idriss (1971) with Added Mean Value Lines from Equation 8-1.

Use of τ_{max} from site response analysis (or use of the results of a site response analysis to evaluate r_d) is considered to be generally more reliable than any of the simplified approaches to estimate r_d, and is strongly recommended for sites that are marginal with respect to liquefaction potential (i.e., sites where the factor of safety for liquefaction is close to 1.0).

Step 4: Calculate the *critical stress ratio induced by the design earthquake,* CSR_{EQ}, as:

$$CSR_{EQ} = 0.65\ (a_{max}/g)\ r_d\ (\sigma_v/\sigma_v') \tag{8-3a}$$

If the results of a seismic site response analysis are available, CSR_{EQ} can be evaluated from τ_{max} as:

$$CSR_{EQ} = 0.65\ \tau_{max}/\sigma_v' \tag{8-3b}$$

Note that the ratio τ_{max}/σ_v' corresponds to the peak average acceleration denoted by k_{max} in Chapter 6.

Step 5: Evaluate the *standardized* SPT blow count, N_{60}, using the procedure presented in Chapter 5.

Step 6: Calculate the normalized and standardized SPT blow count, $(N_1)_{60}$, using the procedure presented in Chapter 5

Step 7: Evaluate the critical stress ratio $CSR_{7.5}$ at which liquefaction is expected to occur during an earthquake of magnitude $M_w = 7.5$ as a function of $(N_1)_{60}$. Use the chart developed by Seed, *et al.* (1985) as modified by NCEER, shown in Figure 8-3, to find $CSR_{7.5}$. It should be noted that this chart was developed using a large database from sites where liquefaction did or did not occur during past earthquakes. The general conditions for the case history data presented in this chart are as follows: (1) all sites evaluated were under level ground condition, (2) the effective overburden pressure for all cases does not exceed 96 kPa, and (3) the magnitude of the earthquakes considered in all cases was in the neighborhood of 7.5.

Step 8: Calculate the *corrected* critical stress ratio resisting liquefaction, CSR_L. CSR_L is calculated as:

$$CSR_L = CSR_{7.5} \cdot k_M \cdot k_\sigma \cdot k_\alpha \tag{8-4}$$

where k_M is the correction factor for earthquake magnitudes other than 7.5, k_σ is the correction factor for stress levels larger than 96 kPa, and k_α is the correction factor for the initial driving static shear stress, τ_{ho}. Previous investigators have derived various recommendations on the magnitude correction factor, K_M, as shown in Figure 8-4. Upon review of all the data, the NCEER workshop participants have recommended a range of K_M values for design and analysis purposes. Their recommendations are presented in Figure 8-4. For effective confining pressures σ'_m larger than 96 kPa, k_σ can be determined from Figure 8-5 (Youd and Idriss, 1997). For σ'_m less than or equal to 96 kPa, no correction is required.

The value of k_α depends on both τ_{ho} and the relative density of the soil, D_r. On sloping ground, or below structures and embankments, τ_{ho} can be estimated using various closed-form elastic solutions (e.g., Poulos and Davis, 1974) or using the results of finite element (static) analyses. Once τ_{ho} and σ_v' are estimated, k_α can be determined from Figure 8-6, originally proposed by Seed

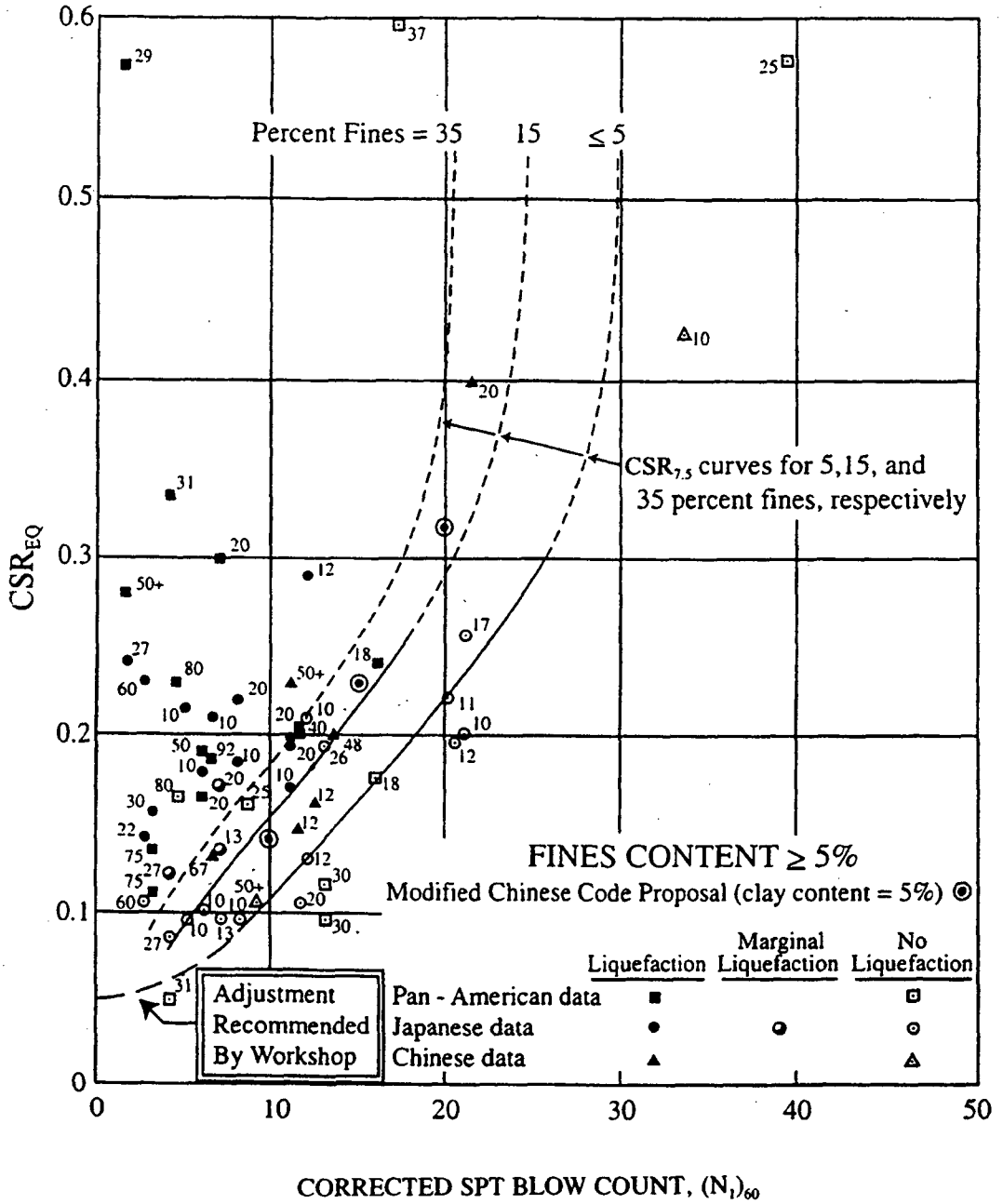

Figure 8-3: Relationship Between Cyclic Stress Ratio Causing Liquefaction and SPT $(N_1)_{60}$ Values for Sands for M = 7.5 Earthquakes (modified From Seed et al., 1985)

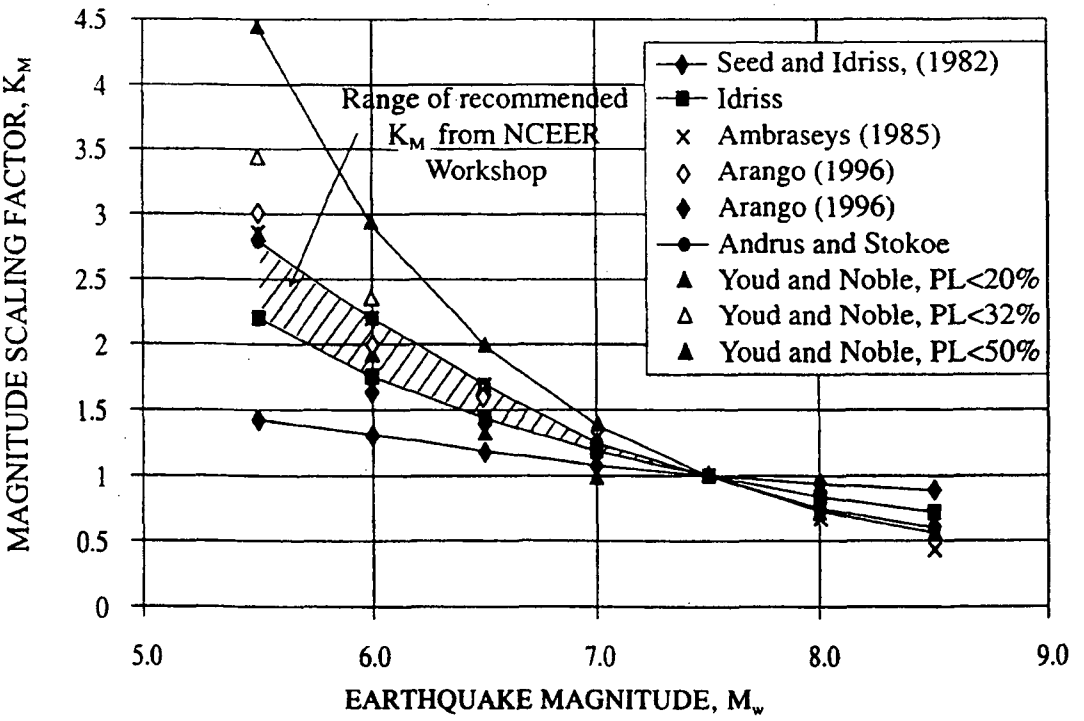

Figure 8-4: Magnitude Scaling Factors Derived by Various Investigators (After Youd and Idriss, 1997)

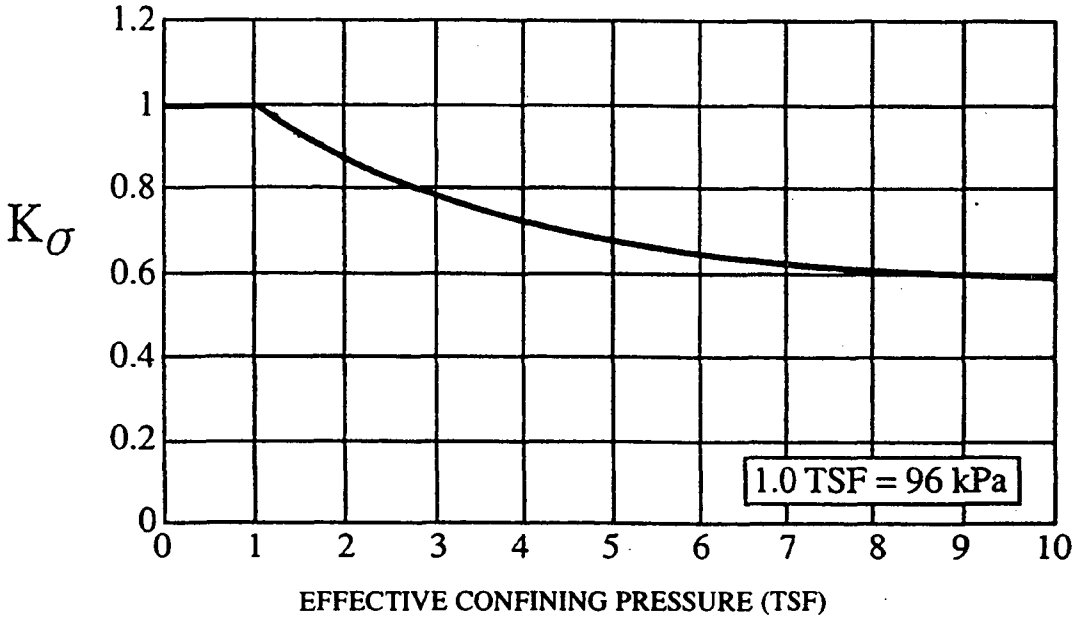

Figure 8-5: Recommended Correction Factor k_σ. (After Youd and Idriss, 1997)

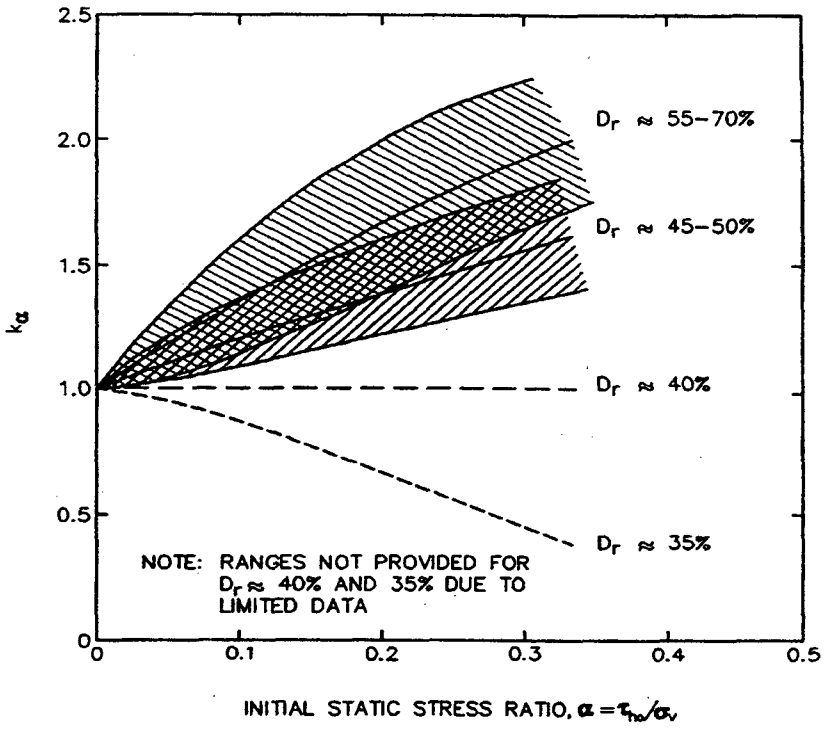

Figure 8-6: Curves for Estimation of Correction Factor, k_α. (Harder, 1988 and Hynes, 1988, as cited in Marcuson, *et al.*, 1990, reprinted by permission of EERI)

(1983) and modified by Harder (1988) and Hynes (1988). However, experts participating in the 1996 NCEER workshop on "Evaluation of Liquefaction Resistance of Soils" (1997) have concluded that due to the wide range of k_α values developed from previous studies and a lack of consistency of the results, general recommendations for use of k_α for design purposes are not advisable at this time. The evaluation of liquefaction resistance beneath sloping ground or embankments is not well understood and further research is required.

The effect of plasticity index on liquefaction resistance has also been reported (Ishihara, 1990). It is generally recognized that liquefaction resistance increases with soil plasticity. For example, many practitioners have been applying a 10 percent increase to the liquefaction resistance for soils with a plasticity index greater than 15 percent. However, a reliable correction relationship could not be formulated at this time due to the lack of data (Youd and Idriss, 1997).

Liquefaction resistance based on SPT (or CPT) measurements could not be reliably estimated for gravelly soils. Large gravel particles tend to increase the penetration resistance of the penetrometer unproportionately. To overcome this difficulty, large-diameter penetrometers have been used by some investigators. The Becker penetration test (BPT) has become the more effective and most widely used of this type of tools. There are correlations between Becker blowcount and SPT blowcount. The correlation proposed by Harder (1997) is recommended for liquefaction evaluation of gravelly soils in cases where Becker penetration testing data are available. Detailed information on the procedure is presented in the NCEER report (Youd and Idriss, 1997). In the absence of Becker penetration testing data, the effects of gravel content can be roughly estimated using the correlation curve shown in Figure 8-7 (Ishihara, 1985). The "Cyclic Strength of Sand

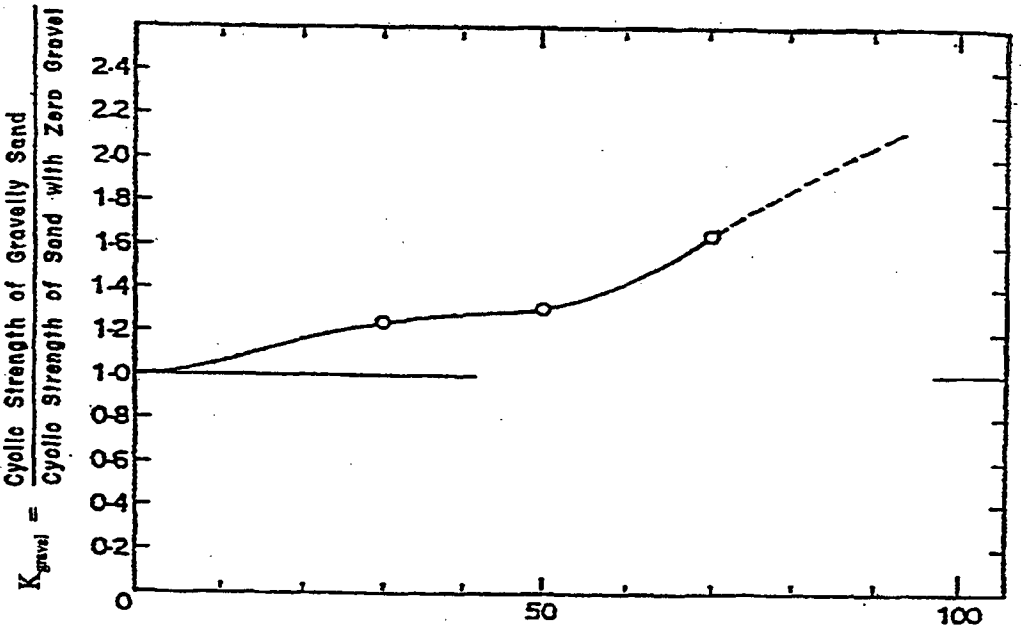

Figure 8-7: Effects of Gravel Content on Liquefaction Resistance of Gravelly Soils (Ishihara, 1985)

with Zero Gravel" cited in the figure should be obtained from the sand layers at the site in the vicinity of the gravelly soil deposit, provided that the sand layers (without gravel) and the gravelly soil layers were formed under the same geological conditions.

Step 9: Calculate the factor of safety against initial liquefaction, FS_L, as:

$$FS_L = \frac{CSR_L}{CSR_{EQ}} \tag{8-5}$$

There is no general agreement on the appropriate minimum factor of safety against liquefaction (NRC, 1985). There are cases where liquefaction-induced instability has occurred prior to complete liquefaction, i.e., with a factor of safety against initial liquefaction greater than 1.0. For regular highway bridge design, it is recommended that a minimum factor of safety of 1.1 against liquefaction be required.

It should be noted that the Simplified Procedure is aimed primarily at moderately strong ground motions ($0.2\ g < a_{max} < 0.5\ g$). If the peak horizontal acceleration is larger than 0.5 g, more sophisticated, truly non-linear effective stress-based analytical approaches may be advisable. Computer programs for evaluation of liquefaction potential as a part of a site response analysis include the one-dimensional response analysis computer program DESRA-2 (Lee and Finn, 1978) and its derivative codes MARDES (Chang, *et al.*, 1991), D-MOD (Matasović, 1993), and SUMDES (Li, *et al.*, 1992) as well as two-dimensional codes such as DYNAFLOW (Prevost, 1981), TARA-3 (Finn, *et al.*, 1986), LINOS (Bardet, 1992), DYSAC2 (Muraleetharan, *et al.*, 1991), and certain adaptations of FLAC (Cundall and Board, 1988) (e.g., Roth and Inel, 1993). These computer programs are briefly discussed in Chapter 6.

An example of a liquefaction analysis performed using the Simplified Procedure is presented in Part II of this document.

8.3.3 Variations on the Simplified Procedure

The principle variations on the simplified procedure used in practice include the use of CPT resistance and shear wave velocity, instead of the normalized SPT blow count to evaluate the critical stress ratio, causing liquefication for a magnitude 7.5 earthquake, $CSR_{7.5}$. Figure 8-8 presents the relationship between corrected CPT tip resistance, q_{c1N}, and $CSR_{7.5}$, where q_{c1N} is evaluated from the tip resistance q_c as follows:

$$q_{c1N} = \left(\frac{P_a}{\sigma'_v}\right)^n \left(\frac{q_c}{P_a}\right) \tag{8-6}$$

where σ'_v is effective overburden pressure, P_a is atmospheric pressure (approximately 100 kPa) and n is an exponent that varies from 0.5 for clean sands, 0.7 for silty sands, and 0.8 for sandy silt.

It should be noted that Figure 8-8 is applicable for clean sands with fines less than 5 %. To correct the normalized penetration resistance, q_{c1N}, of sands with fines greater than 5% to an equivalent clean sand value, $(q_{c1N})_{cs}$ the following relationship is used.

$$(q_{c1N})_{cs} = K_{cs} q_{c1N} \tag{8-7}$$

where K_{cs} varies from 1.0 for fines less than 5%, 1.4 for fines equal to 15%, to 3.35 for fines equal to 35%.

Simplified procedures using field measurements of small-strain shear wave velocity, V_s, to assess liquefaction resistance of granular soils have also been proposed. Figure 8-9 presents the relationship (Youd and Idriss,1997) between $CSR_{7.5}$ and stress-corrected shear wave velocity, V_{s1}, where V_{s1} is calculated as:

$$V_{s1} = V_s \left(\frac{P_a}{\sigma'_v}\right)^{0.25} \tag{8-8}$$

The relationship shown in Figure 8-9 was developed based on data from many field sites (including the field performance data from the 1989 Loma Prieta earthquake) where liquefaction did or did not occur. Similar to the relationships developed using SPT and CPT data, the liquefaction resistance curves in Figure 8-9 are for magnitude 7.5 earthquakes and effective overburden pressures less than about 100 kPa. Appropriate correction factors as discussed in Section 8.3.2 should be applied to account for magnitudes other than 7.5 or effective overburden pressures greater than 100 kPa.

8.4 POST-LIQUEFACTION DEFORMATION AND STABILITY

For soil layers in which the factor of safety against initial liquefaction is unsatisfactory, a liquefaction impact analysis may demonstrate that the site will still perform adequately even if liquefaction occurs. Potential impacts of liquefaction include bearing capacity failure, loss of lateral support for piles, lateral spreading, and post-liquefaction settlement. These are all phenomena associated with large soil strains and

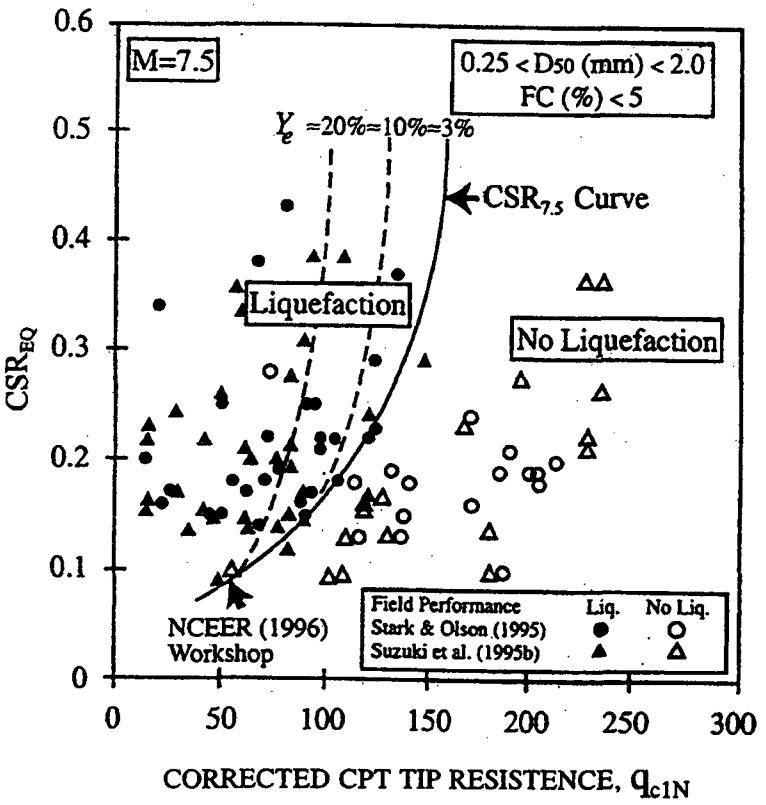

Figure 8-8: Relationship between Cyclic Stress Ratio Causing Liquefaction and CPT Tip Resistance, q_{c1N} for Sands for M = 7.5 (Robertson and Wride, 1997)

ground deformations. Relatively dense soils which liquefy may subsequently harden or stabilize at small deformations and thus have minimal impact on overlying highway structures. Conversely, relatively loose soils that liquefy will tend to collapse resulting in a much greater potential for post-liquefaction deformation. Methods for assessing the impact of liquefaction generally are based upon evaluation of the strain or deformation potential of the liquefiable soil. A liquefaction impact analysis for highway-related projects may consist of the following steps:

Step 1: Calculate the magnitude and distribution of liquefaction-induced settlement by multiplying the post-liquefaction volumetric strain, ε_v, by the thickness of the liquefiable layer, H.

The post-liquefaction volumetric strain can be estimated from the chart presented in Figure 8-10 (Tokimatsu and Seed, 1987). An alternative chart has recently been proposed by Ishihara (1993). Note that both charts were developed for clean sands and tend to overestimate settlements of sandy silts and silts. Application of Ishihara's chart requires translation of normalized SPT blow count $(N_1)_{60}$ values determined in Chapter 5 to Japanese-standard N_J values ($N_J = 0.833\ (N_1)_{60}$; after Ishihara, 1993). The magnitude of liquefaction-induced settlement should be calculated at each SPT or CPT sounding location to evaluate the potential variability in seismic settlement across the project site.

Step 2: Estimate the free-field liquefaction-induced lateral displacement, Δ_L. The empirical equation proposed by Hamada, *et al.* (1987) may be used to estimate Δ_L in meters:

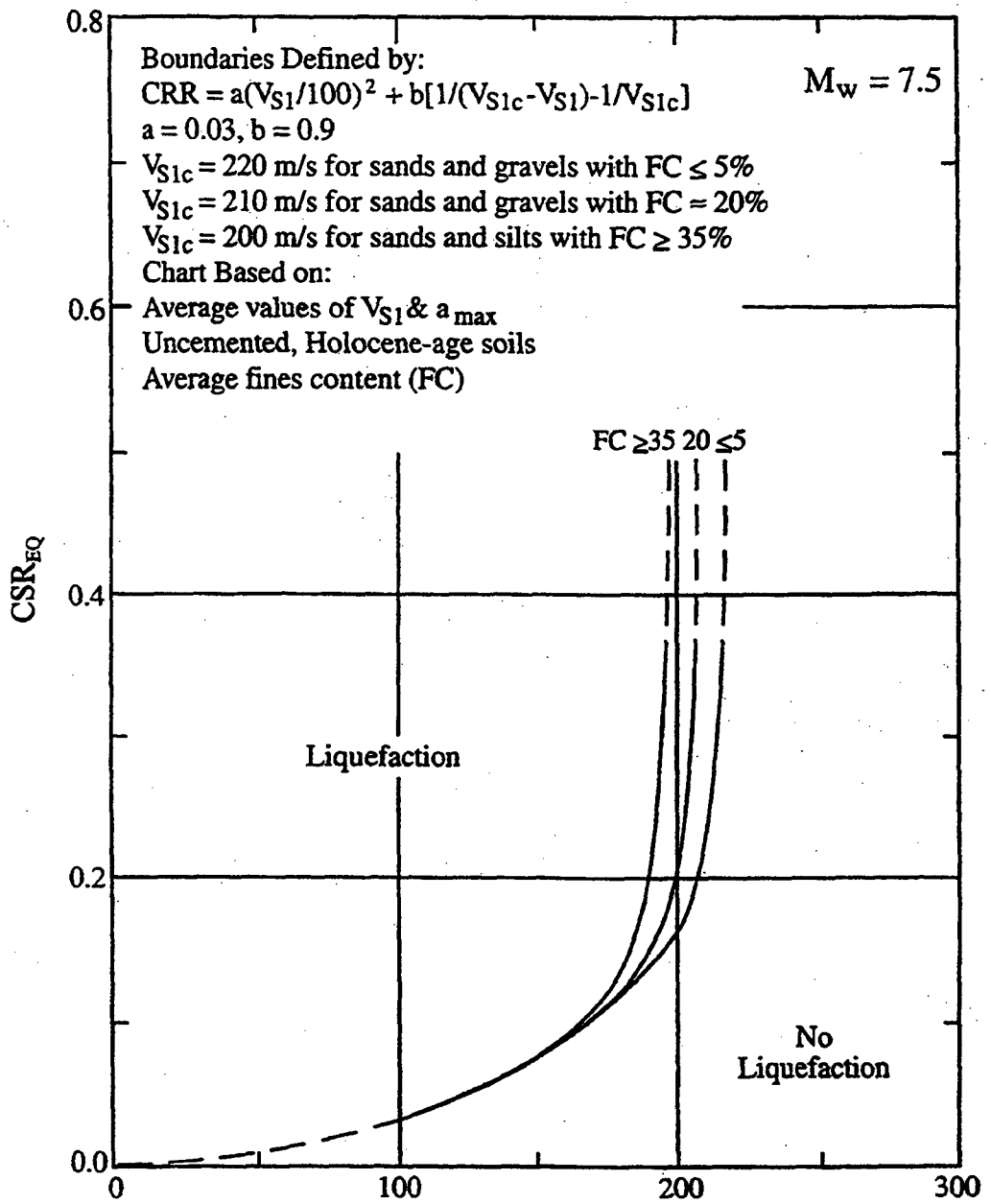

Figure 8-9: Relationship Between Cyclic Stress Ratio Causing Liquefication and Shear Wave Velocity Values, V_{S1}, for Sands for M = 7.5 Earthquakes (Youd and Idriss, 1997)

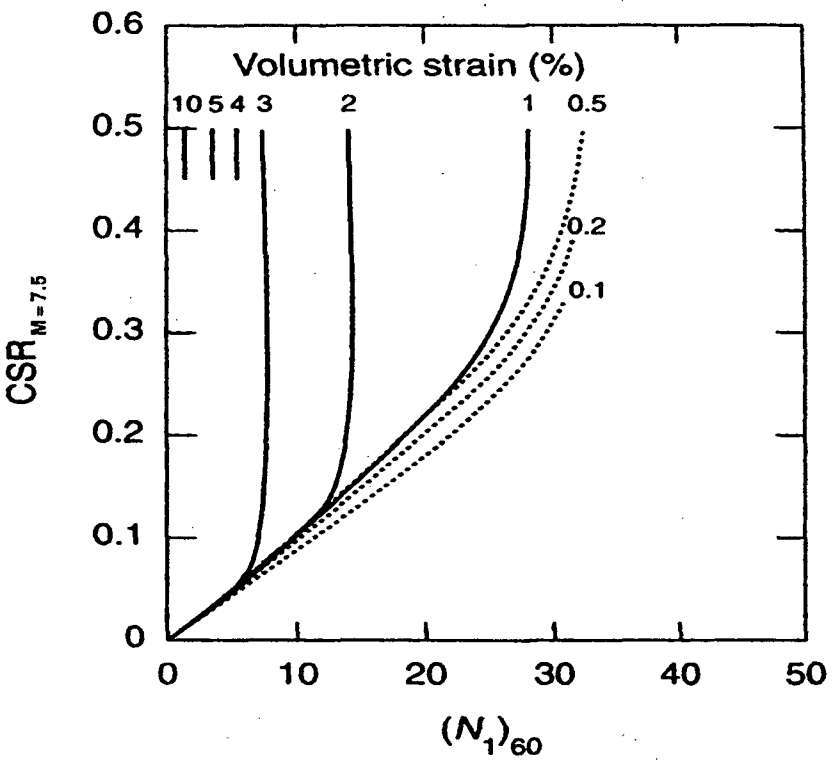

Figure 8-10: Curves for Estimation of Post-Liquefaction Volumetric Strain Using Spt Data and Cyclic Stress Ratio for M_w 7.5 Earthquakes. (Tokimatsu and Seed, 1987, reprinted by permission of ASCE).

$$\Delta_L = 0.75\ (H)^{1/2}\ (S)^{1/3} \qquad (8\text{-}9)$$

where H is the thickness of the liquefied layer in meters and S is the ground slope in percent.

The Hamada, *et al.* (1987) formula in Equation 8-9 is based primarily on Japanese data (for major earthquakes of magnitude 7.5 or greater) on observed liquefaction displacements of very loose sand deposits having a slope, S, less than 10 percent. Therefore, Equation 8-9 should be assumed to provide only a rough upper bound estimate of lateral displacement. Since Equation 8-9 does not reflect either the density, or $(N_1)_{60}$ value, of the liquefiable soil or the depth of the liquefiable layer, it likely provides a conservative estimate of lateral displacement for denser sands or for cases where the soil liquefies at depth. Estimates of lateral displacement obtained using Equation 8-9 may indicate excessive liquefaction-induced lateral displacements in areas of essentially flat ground conditions.

A more accurate empirical procedure for assessing lateral spreading was developed by Bartlett and Youd (1995). This procedure was developed from multiple linear regression analyses of U.S. and Japanese case histories. Two general types of lateral spreading are differentiated according to Bartlett and Youds' study: (1) lateral spread towards a free face, and (2) lateral spread down gentle ground slopes where a free face is absent. The procedure is summarized as follows:

(1) If $(N_1)_{60}$ values are equal to or more than 15, the potential for lateral displacements would be small for earthquakes with magnitudes less than 8.0, and no additional

analyses are warranted.

(2) If $(N_1)_{60}$ values are less than 15, then the evaluation of lateral displacement is performed using the following equations:

For free-face conditions:

$$\text{Log}\Delta_L = -16.366 + 1.178M - 0.927\text{Log } R - 0.013R + 0.657\text{Log } W + 0.348\text{Log } H_{15} + 4.527\text{Log } (100 - F_{15}) - 0.922D50_{15} \quad (8\text{-}10a)$$

For ground slope conditions:

$$\text{Log}\Delta_L = -15.787 + 1.178M - 0.927\text{Log } R - 0.013R + 0.429\text{Log } S + 0.348\text{Log } H_{15} + 4.527\text{Log } (100 - F_{15}) - 0.922D50_{15} \quad (8\text{-}10b)$$

Where:

- Δ_L = Estimated lateral ground displacement in meters
- H_{15} = Cumulative thickness of saturated granular layers with corrected blow counts, $(N_1)_{60}$, less than or equal to 15, in meters.
- $D50_{15}$ = Average mean grain size in granular layer included in H_{15} in mm.
- F_{15} = Average fines content for granular layers included in H_{15} in percent.
- M = Earthquake magnitude (moment magnitude).
- R = Horizontal distance from seismic energy source, in kilometers.
- S = Ground slope, in percent.
- W = Ratio of the height (H) of the free face to the distance (L) from the base of the free face to the point in question, in percent (i.e., 100H/L).

Step 3: In areas of significant ground slope, or in situations when a deep failure surface may pass through the body of the facility or through underlying liquified layers, a flow slide can occur following liquefaction. The potential for flow sliding should be checked using a conventional limit equilibrium approach for slope stability analyses (discussed in Chapter 7) together with residual shear strengths in zones in which liquefaction may occur. Residual shear strengths can be estimated from the penetration resistance values of the soil using the chart proposed by Seed, *et al.* (1988) presented in Figure 5-15. Seed and Harder (1990) and Marcuson, *et al.* (1990) present further guidance for performing a post-liquefaction stability assessment using residual shear strengths.

If liquefaction-induced vertical and/or lateral deformations are large, the integrity of the highway facility may be compromised. The question the engineer must answer is "What magnitude of deformation is too large?" The magnitude of acceptable deformation should be established by the design engineer on a case-by-case basis. Calculated seismic deformations on the order of 0.15 to 0.30 m are generally deemed to be acceptable in current practice for highway embankments in California. For highway system components other than embankments, engineering judgement must be used in determining the allowable level of calculated seismic deformation. For example, components that are designed to be unyielding, such as bridge abutments restrained by batter piles, may have more restrictive deformation requirements than structures which can more easily accommodate foundation deformations. At the current time,

determination of allowable deformations remains a subject requiring considerable engineering judgement.

8.5 SEISMIC SETTLEMENT EVALUATION

Both unsaturated and saturated sands tend to settle and densify when subjected to earthquake shaking. If the sand is saturated and there is no possibility for drainage, so that constant volume conditions are maintained, the primary initial effect of the shaking is the generation of excess pore water pressures. Settlement then occurs as the excess pore pressures dissipate. In unsaturated sands, on the other hand, settlement may occur during the earthquake shaking under conditions of constant effective vertical stress (depending on the degree of saturation). In both cases (saturated and unsaturated soil), however, one result of strong ground shaking is settlement of the soil.

Liquification induced settlement of saturated sand is addressed as part of a post-liquefaction deformation and stability assessment as described in Section 8.4 of this Chapter. A procedure for evaluating the seismic settlement of unsaturated sand, following the general procedure presented in Tokimatsu and Seed (1987), is outlined below.

Seismic settlement analysis of unsaturated sand can be performed using the following steps:

Step 1: From borings and soundings, in situ testing and laboratory index tests, develop a detailed understanding of the project site subsurface conditions, including stratigraphy, layer geometry, material properties and their variability, and the areal extent of potential problem zones. Establish the zones to be analyzed and develop idealized, representative sections amenable to analysis. The subsurface data used to develop the representative sections should include normalized standardized SPT blow counts, $(N_1)_{60}$ (or results of some other test, e.g., the CPT from which $(N_1)_{60}$ can be inferred) and the unit weight of the soil.

Step 2: Evaluate the total vertical stress, σ_v, and the mean normal effective stress, σ'_m, at several layers within the deposit at the time of exploration and for design. The design values should include stresses resulting from highway facility construction. Outside of the highway facility footprint, the exploration and design values are generally the same.

Step 3: Evaluate the stress reduction factor, r_d, using one of the approaches presented in step 3 of Section 8.3 of this Chapter.

Step 4: Evaluate γ_{eff} (G_{eff} /G_{max}) using the Tokimatsu and Seed (1987) equation:

$$\gamma_{eff}\,(G_{eff} / G_{max}) = (0.65 \cdot a_{max} \cdot \sigma_v \cdot r_d)/(g \cdot G_{max}) \qquad (8\text{-}11)$$

where γ_{eff} (G_{eff}/G_{max}) is a *hypothetical effective shear stress factor*, a_{max} is the peak ground surface acceleration, g is the acceleration of gravity, and G_{max} is the shear modulus of the soil at small strain. Note that $G_{max} = \rho \cdot V_s^2$, where V_s is the shear wave velocity and ρ is the mass density of the soil. Alternatively, G_{max} (in kPa) can be evaluated from the correlation given below (Seed and Idriss, 1970):

$$G_{max} = 4{,}400[(N_1)_{60}]^{1/3}\ (\sigma'_m)^{1/2} \qquad (8\text{-}12)$$

where $(N_1)_{60}$ is the normalized standardized SPT blow count defined before and σ'_m is mean normal effective stress in kPa. For unsaturated sands, σ'_m can be estimated using Equation 5-12.

However, for most practical purposes, the approximation $\sigma'_m \approx 0.65\ \sigma'_v$ will suffice.

Step 5: Evaluate γ_{eff} as a function of γ_{eff} (G_{eff}/G_{max}) and σ_m using the chart reproduced in Figure 8-11.

Step 6: Assuming that $\gamma_{eff} \approx \gamma_c$, where γ_c is the cyclic shear strain, evaluate the volumetric strain due to compaction, ε_c, for an earthquake of magnitude 7.5 (15 cycles) using the chart reproduced in Figure 8-12.

Step 7: Correct for earthquake (moment) magnitude other than M_w 7.5 using the correction factors reproduced in Table 8-2.

Step 8: Multiply the volumetric strain due to compaction for each layer by two to correct for the multidirectional shaking effect, as recommended by Tokimatsu and Seed (1987), to get the representative volumetric strain for each layer.

Step 9: Calculate seismic settlements of each layer by multiplying the layer thickness by the representative volumetric strain evaluated in Step 8. Sum up the layer settlements to obtain the total seismic settlement for the analyzed profile.

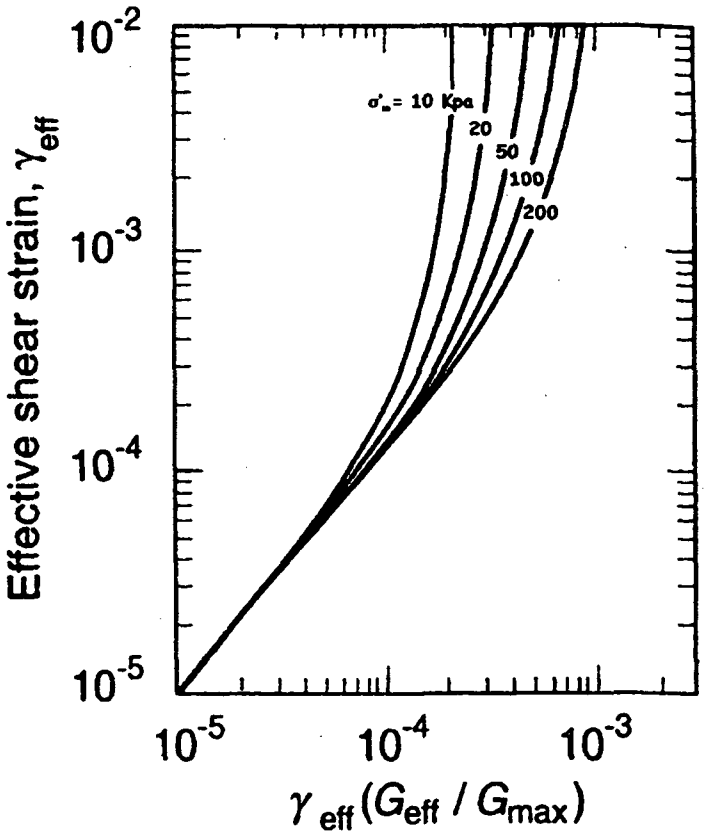

Figure 8-11: Plot for Determination of Earthquake-Induced Shear Strain in Sand Deposits. (Tokimatsu and Seed, 1987, reprinted by permission of ASCE)

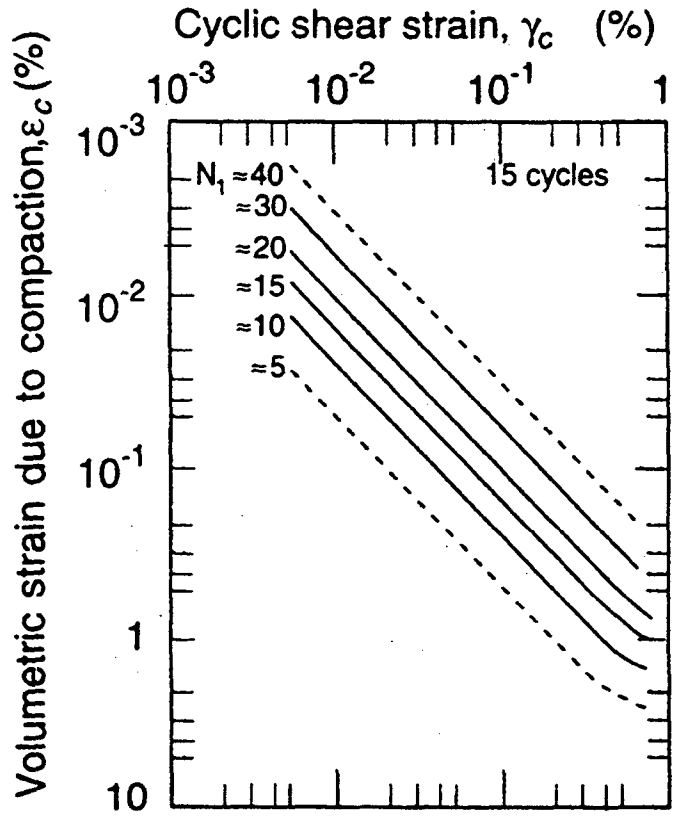

Figure 8-12: Relationship Between Volumetric Strain, Cyclic Shear Strain, and Penetration Resistance for Unsaturated Sands. (Tokimatsu and Seed, 1987, reprinted by permission of ASCE)

TABLE 8-2
INFLUENCE OF EARTHQUAKE MAGNITUDE
ON VOLUMETRIC STRAIN RATIO FOR DRY SANDS
(After Tokimatsu and Seed, 1987, Reprinted by Permission of ASCE)

Earthquake Magnitude	Number of Representative Cycles at 0.65 τ_{max}	Volumetric Strain Ratio $\varepsilon_{C,N}/\varepsilon_{C,N}=15$
8.5	26	1.25
7.5	15	1.0
6.75	10	0.85
6	5	0.6
5.25	2-3	0.4

Considerable judgement is required when evaluating the performance of a highway facility based on an estimate of seismic settlement. The magnitude of calculated seismic settlement should be considered primarily as an indication of whether settlements are relatively small (several centimeters) or relatively large (several meters). A more precise evaluation of seismic settlement is not within the capabilities of conventional engineering analyses using the simplified methods presented herein.

8.6 LIQUEFACTION MITIGATION

If the seismic impact analyses presented in Sections 8.4 and 8.5 yield unacceptable deformations, consideration may be given to performing a more sophisticated liquefaction potential assessment and to evaluation of liquefaction potential mitigation measures. Generally, the engineer has the following options: (1) proceed with a more advanced analysis technique; (2) design the facility to resist the anticipated deformations; (3) remediate the site to reduce the anticipated deformations to acceptable levels; or (4) choose an alternative site. If a more advanced analysis still indicates unacceptable impacts from liquefaction, the engineer must still consider options (2) through (4). These options may require additional subsurface investigation, advanced laboratory testing, more sophisticated numerical modeling, and, in rare cases, physical modeling. Discussion of these techniques is beyond the scope of this document.

Options that may be considered when designing to resist anticipated deformation include the use of ductile pile foundations, reinforced earth, structural walls, or buttress fills keyed into non-liquefiable strata to resist the effects of lateral spreading. These techniques are described in detail elsewhere (e.g., Kramer and Holtz, 1991).

A variety of techniques exist to remediate potentially liquefiable soils and mitigate the liquefaction hazard. Table 8-3 presents a summary of methods for improvement of liquefiable soil foundation conditions (NRC, 1985). The cost of foundation improvement can vary over an order of magnitude, depending on site conditions (e.g., adjacent sensitive structures) and the nature and geometry of the liquefiable soils. Remediation costs can vary from as low as several thousand dollars per acre for dynamic compaction of shallow layers of clean sands in open areas to upwards of $100,000 per acre for deep layers of silty soils adjacent to sensitive structures. Liquefaction remediation measures must be evaluated on a case-by-case basis to determine their economic viability.

The results of a number of post-earthquake settlement measurements made on Port Island and Rokko Island following the 1995 Kobe Earthquake in relation to site treatment methods are presented in Figure 8-13 (Yasuda, et al, 1995). The soil profile on these islands is typically 12 to 20 m of loose, hydraulically filled, decomposed granite sand underlain by several meters of soft, compressible alluvial clay. It should be noted that sand drains and preloading were used for the purpose of precompressing the soft clay for reducing future long term settlements under static loads. The results shown in Figure 8-13 suggest that sand drains and preloading, although have some beneficial effects on the liquefaction resistance, are not effective methods in preventing liquefaction from occuring. To mitigate liquefaction risk of loose, grannular soils, proper methods of ground treatment have to be applied.

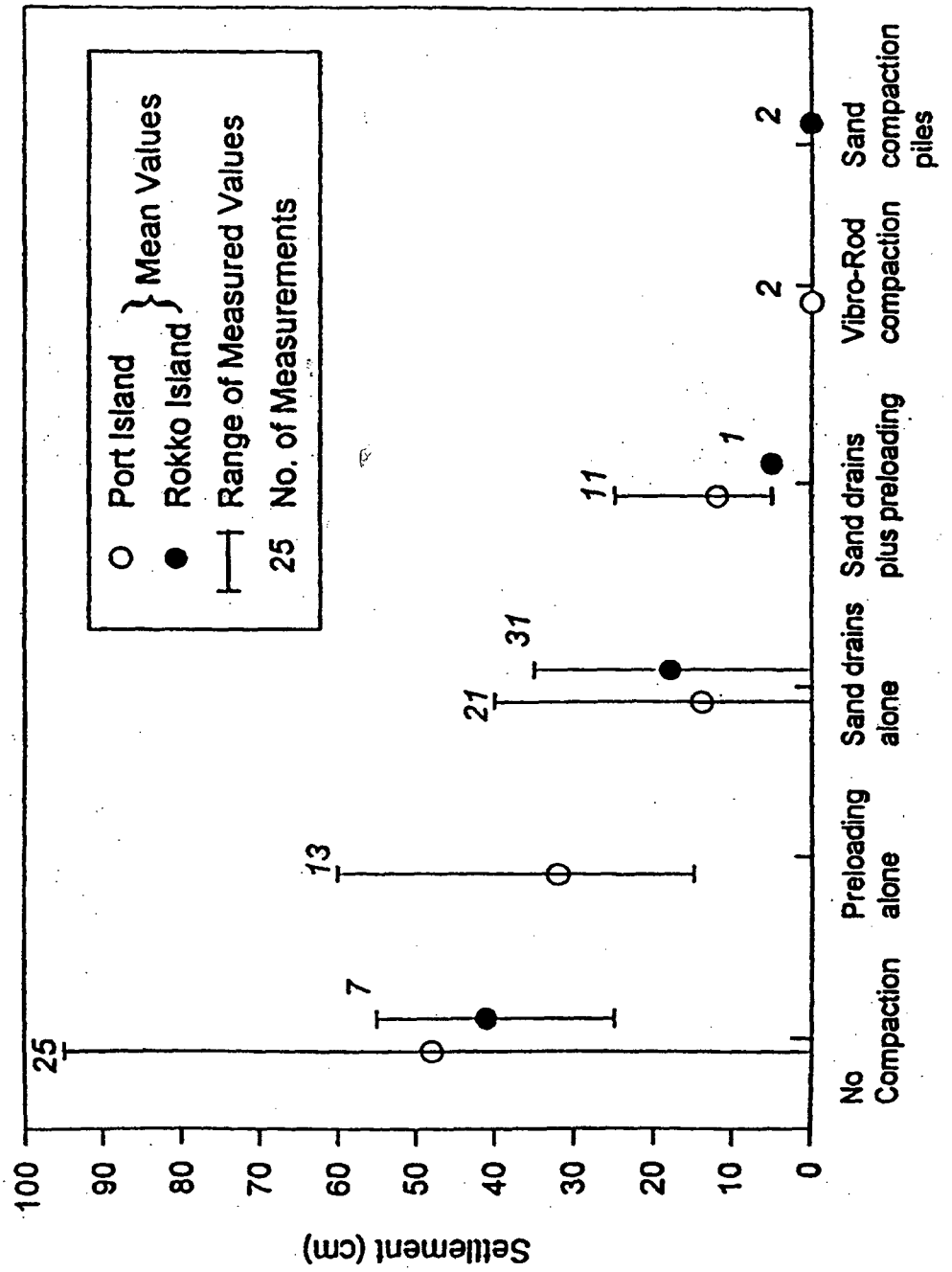

Figure 8-13: Post-Earthquake Settlements at Two Port Sites due to the 1995 Kobe Earthquake (Yasuda, et. al, 1995).

TABLE 8-3 IMPROVEMENT TECHNIQUES FOR LIQUEFIABLE SOIL FOUNDATION CONDITIONS (AFTER NRC, 1985)

Method	Principle	Most Suitable Soil Conditions/Types	Maximum Effective Treatment Depth	Economical Size of Treated Area	Ideal Properties of Treated Material*	Applications**	Case†	Relative Costs
In-Situ Deep Compaction								
(1) Blasting	Shock waves and vibrations cause limited liquefaction, displacement, *remolding and settlement to higher* density.	Saturated, clean sands; partly *saturated sands and* silts after flooding.	>40 m Solymar (1984)	Any Size	Can obtain relative densities of 70-80%; *may get variable* density; time-dependent strength gain.	Induce liquefaction in controlled and limited stages and increase relative density to potentially non-*liquefiable range.*	2 3	Low
(2) Vibratory Probe (a) Terraprobe (b) Vibro-Rods (c) Vibro-Wing	Densification by vibration; liquefaction-induced settlement and settlement in dry soil under overburden to produce a higher density.	Saturated or dry clean sand; sand.	20 m routinely (ineffective above 3-4 m depth) >30 m sometimes Mitchell (1981) Vibro-Wing-40 m Broms and Hansson (1984)	>1,000 m²	Can obtain relative densities of 80% or more. Ineffective in some sands.	Induce liquefaction in controlled and limited stages and increase relative density to potentially non-liquefiable range. Has been shown ineffective in preventing liquefaction.	2 3	Moderate
(3) Vibro-Compaction (a) Vibroflot (b) Vibro-Composer System (c) Soil Vibratory stabilizing method	Densification by vibration and compaction of backfill material of sand or gravel.	Cohesionless soils with less than 20% fines.	>30 m Solymar et al. (1984)	>1,000 m²	Can obtain high relative densities (over 85%), good uniformity.	Induce liquefaction in controlled and limited stages and increase relative densities to nonliquefiable condition. Is used extensively to prevent liquefaction. The dense column of backfill provides (a) vertical support, (b) drains to relieve pore water pressure and (c) shear resistance in horizontal and inclined directions. Used to stabilize slopes and strengthen potential failure surfaces or slip circles.	1 2 Δ‡	Low to moderate
(4) Compaction Soils	Densification by displacement of pile volume and by vibration during driving, increase in lateral effective earth pressure.	Loose sandy soils; partly saturated clayey soils; loess.	>20 m Nataraja and Cook (1983)	>1,000 m²	Can obtain high densities, good uniformity. Relative densities of more than 80%.	Useful in soils with fines. Increases relative densities to nonliquefiable range. Is used to prevent liquefaction. Provides shear resistance in horizontal and inclined directions. Useful to stabilize slopes and strengthen potential failure surfaces or slip circles.	1 2 3	Moderate to High
(5) Heavy Tamping (dynamic compaction)	Repeated application of high-intensity impacts at surface.	Cohesionless soils best, other types can also be improved.	30 m (possibly deeper) Ménard and Broise (1975)	>3,300 m²	Can obtain high relative densities, reasonable uniformity. Relative densities of 80% or more.	Suitable for some soils with fines; usable above and below water. In cohesionless soils, induces liquefaction in controlled and limited stages and increases relative density to potentially nonliquefiable range. Is used to prevent liquefaction.	2 3	Low

* SP, SW, or SM soils which have average relative density equal to or greater than 85 percent and the minimum relative density not less than 80 percent are in general not susceptible to liquefaction (TM 5-818-1). D'Appolonia (1970) stated that for soil within the zone of influence and confinement of the structure foundation, the relative density should not be less than 70 percent. Therefore, a criterion may be used that relative density increase into the 70-90 percent range is in general considered to prevent liquefaction. These properties of treated materials and applications occur only under ideal conditions of soil, moisture, and method application. The methods and properties achieved are not applicable and will not occur in all soils.

** Applications and results of the improvement methods are dependent on: (a) soil profiles, types, and conditions, (b) site conditions, (c) earthquake loading, (d) structure type and condition, and (e) material and equipment availability. Combinations of the methods will most likely provide the best and most stable solution.

† Site conditions have been classified into three cases; Case 1 is for beneath structures, Case 2 is for the not-under-water free field adjacent to a structure, and Case 3 is for the under-water free field adjacent to a structure.

‡ Δ means the method has potential use for Case 3 with special techniques required which would increase the cost.

TABLE 8-3 IMPROVEMENT TECHNIQUES FOR LIQUEFIABLE SOIL FOUNDATION CONDITIONS (AFTER NRC, 1985)

Method	Principle	Most Suitable Soil Conditions/Types	Maximum Effective Treatment Depth	Economical Size of Treated Area	Ideal Properties of Treated Material*	Applications**	Case†	Relative Costs
In-Situ Deep Compaction								
(6) Displacement/ Compaction Grout	Highly viscous grout acts as radical hydraulic jack when pumped in under high pressure.	All soils.	Unlimited	Small	Grout bulbs within compressed soil matrix. Soil mass as a whole is strengthened.	Increase in soil relative density and horizontal effective stress. Reduce liquefaction potential. Stabilize the ground against movement.	1 2 3	Low to Moderate
Compression								
(7) Surcharge/Buttress	The weight of a surcharge/buttress increases the liquefaction resistance by increasing the effective confining pressures in the foundation.	Can be placed on any soil surface.	—	$>1{,}000\ m^2$	Increase strength and reduce compressibility.	Increase the effective confining pressure in a liquefiable layer. Can be used in conjunction with vertical and horizontal drains to relieve pore pressure. Reduce liquefaction potential. Useful to prevent movements of a structure and for slope stability.	2 3	Moderate if vertical drains used.
Pore-Water Pressure Relief								
(8) Drains (a) Gravel (b) Sand (c) Wick (d) Wells (for permanent dewatering)	Relief of excess pore-water pressure to prevent liquefaction. (Wick drains have comparable permeability to sand drains). Primarily gravel drains; sand/wick drains may supplement gravel drain or relieve existing excess pore water pressure. Permanent dewatering with pumps.	Sand, silt, clay.	Gravel and Sand >30 m Depth limited by vibratory equipment Wick >45 m Morrison (1982)	$>1{,}500\ m^2$ Any size for wick.	Pore-water pressure relief will prevent liquefaction.	Prevent liquefaction by gravel drains. Sand and gravel drains are installed vertically; however, wick drains can be installed at any angle. Dewatering will prevent liquefaction but not seismically-induced settlements.	Gravel and Sand 2 Δ† Wick 1 2 3	Dewatering very expensive.
(9) Particulate Grouting	Penetration grouting - fill soil pores with soil, cement, and/or clay.	Medium to coarse sand and gravel.	Unlimited	Small	Impervious, high strength with cement grout. Voids filled so they cannot collapse under cyclic loading	Eliminate liquefaction danger. Slope stabilization. Could potentially be used to confine an area of liquefiable soil so that liquefied soil could not flow out of the area.	1 2 3	Lowest of Grout Methods

* SP, SW, or SM soils which have average relative density equal to or greater than 85 percent and the minimum relative density not less than 80 percent are in general not susceptible to liquefaction (TM 5-818-1). D'Appolonia (1970) stated that for soil within the zone of influence and confinement of the structure foundation, the relative density should not be less than 70 percent. Therefore, a criterion may be used that relative density increase into the 70-90 percent range is in general considered to prevent liquefaction. These properties of treated materials and applications occur only under ideal conditions of soil, moisture, and method application. The methods and properties achieved are not applicable and will not occur in all soils.

** Applications and results of the improvement methods are dependent on: (a) soil profiles, types, and conditions, (b) site conditions, (c) earthquake loading, (d) structure type and condition, and (e) material and equipment availability. Combinations of the methods will most likely provide the best and most stable solution.

† Site conditions have been classified into three cases; Case 1 is for beneath structures, Case 2 is for the not-under-water free field adjacent to a structure, and Case 3 is for the under-water free field adjacent to a structure.

† Δ means the method has potential use for Case 3 with special techniques required which would increase the cost.

TABLE 8-3 IMPROVEMENT TECHNIQUES FOR LIQUEFIABLE SOIL FOUNDATION CONDITIONS (AFTER NRC, 1985)

Method	Principle	Most Suitable Soil Conditions/Types	Maximum Effective Treatment Depth	Economical Size of Treated Area	Ideal Properties of Treated Material*	Applications**	Case†	Relative Costs
(10) Chemical Grouting	Solutions of two or more chemicals react in soil pores to form a gel or a solid precipitate.	Medium silts and coarser.	Unlimited	Small	Impervious, low to high strength. Voids filled so they cannot collapse under cyclic loading.	Eliminate liquefaction danger. Slope stabilization. Could potentially be used to confine an area of liquefiable soil so that liquefied soil could not flow out of the area. Good water shutoff.	1 2 3	High
(11) Pressure-Injected Lime	Penetration grouting - fill soil pores with lime.	Medium to coarse sand and gravel.	Unlimited	Small	Impervious to some degree. No significant strength increase. Collapse of voids under cyclic loading reduced.	Reduce liquefaction potential.	1 2 3	Low
Pore-Water Pressure Relief								
(12) Electrokinetic Injection	Stabilizing chemicals move into and fill soil pores by electro-osmosis or colloids into pores by electro-phoresis.	Saturated sands, silts, silty clays.	Unknown	Small	Increased strength, reduced compressibility, voids filled so they cannot collapse under cyclic loading.	Reduce liquefaction potential.	1 2 3	Expensive
(13) Jet Grouting	High-speed jets at depth excavate, inject, and mix a stabilizer with soil to form columns or panels.	Sands, silts, clays.	Unknown	Small	Solidified columns and walls.	Slope stabilization by providing shear resistance in horizontal and inclined directions which strengthens potential failure surfaces or slip circles. A wall could be used to confine an area of liquefiable soil so that liquefied soil could not flow out of the area.	1 2 3	High
Admixture Stabilization								
(14) Mix-in-Place Piles and Walls	Lime, cement, or asphalt introduced through rotating auger or special in-place mixer.	Sands, silts, clays, all soft or loose inorganic soils.	>20 m (60 m obtained in Japan) Mitchell (1981)	Small	Solidified soil piles or walls of relatively high strength.	Slope stabilization by providing shear resistance in horizontal and inclined directions which strengthens potential failure surfaces or slip circles. A wall could be used to confine an area of liquefiable soil so that liquefied soil could not flow out of the area.	1 2 3	High

* SP, SW, or SM soils which have average relative density equal to or greater than 85 percent and the minimum relative density not less than 80 percent are in general not susceptible to liquefaction (TM 5-818-1). D'Appolonia (1970) stated that for soil within the zone of influence and confinement of the structure foundation, the relative density should not be less than 70 percent. Therefore, a criterion may be used that relative density increase into the 70-90 percent range is in general considered to prevent liquefaction. These properties of treated materials and applications occur only under ideal conditions of soil, moisture, and method application. The methods and properties achieved are not applicable and will not occur in all soils.

** Applications and results of the improvement methods are dependent on: (a) soil profiles, types, and conditions, (b) site conditions, (c) earthquake loading, (d) structure type and condition, and (e) material and equipment availability. Combinations of the methods will most likely provide the best and most stable solution.

† Site conditions have been classified into three cases; Case 1 is for beneath structures, Case 2 is for the not-under-water free field adjacent to a structure, and Case 3 is for the under-water free field adjacent to a structure.

TABLE 8-3 IMPROVEMENT TECHNIQUES FOR LIQUEFIABLE SOIL FOUNDATION CONDITIONS (AFTER NRC, 1985)

Method	Principle	Most Suitable Soil Conditions/Types	Maximum Effective Treatment Depth	Economical Size of Treated Area	Ideal Properties of Treated Material*	Applications**	Case†	Relative Costs
Thermal Stabilization								
(15) In-Situ Vitrification	Melts soil in place to create an obsidian-like vitreous material.	All soils and rock.	>30 m Verbal from Battrelle Laboratories	Unknown	Solidified soil piles or walls of high strength. Impervious; more durable than granite or marble; compressive strength, 9-11 ksi; splitting tensile strength, 1-2 ksi	Slope stabilization by providing shear resistance in horizontal and inclined directions which strengths potential failure surfaces or slip circles. A wall could be used to confine an area of liquefiable soil so that liquefied soil could not flow out of the area.	1 2 3	Moderate
Soil Reinforcement								
(16) Vitro-Replacement Stone and Sand Columns (a) Grouted (b) Not Grouted	Hole jetted into fine-grained soil and backfilled with densely compacted gravel or sand hole formed in cohesionless soils by vibro techniques and compaction of backfilled gravel or sand. For grouted columns, voids filled with a grout.	Sands, silts, clays.	>30 m Limited by vibratory equipment.	>1,500 m^3 Fine-grained soils >1,000 m^2	Increased vertical and horizontal load carrying capacity. Density increase in cohesionless soils. Shorter drainage paths.	Provides: (a) vertical support, (b) drains to relieve pore water pressure, and (c) shear resistance in horizontal and inclined direction. used to stabilize slopes and strengthen potential failure surfaces or slip circles. For grouted columns, no drainage provided but increased shear resistance. In cohesionless soil, density increase reduces liquefaction potential.	1 2 Δ†	Moderate
(17) Root Piles, Soil Nailing	Small-diameter inclusions used to carry tension, shear, compression.	All soils.	Unknown.	Unknown	Reinforced zone of soil behaves as a coherent mass.	Slope stability by providing shear resistance in horizontal and inclined directions to strengthen potential failure surfaces or slip circles. Both vertical and angled placement of the piles and nails.	1 2 3	Moderate to High

* SP, SW, or SM soils which have average relative density equal to or greater than 85 percent and the minimum relative density not less than 80 percent are in general not susceptible to liquefaction (TM 5-818-1). D'Appolonia (1970) stated that for soil within the zone of influence and confinement of the structure foundation, the relative density should not be less than 70 percent. Therefore, a criterion may be used that relative density increase into the 70-90 percent range is in general considered to prevent liquefaction. These properties of treated materials and applications occur only under ideal conditions of soil, moisture, and method application. The methods and properties achieved are not applicable and will not occur in all soils.

** Applications and results of the improvement methods are dependent on: (a) soil profiles, types, and conditions, (b) site conditions, (c) earthquake loading, (d) structure type and condition, and (e) material and equipment availability. Combinations of the methods will most likely provide the best and most stable solution.

† Site conditions have been classified into three cases; Case 1 is for beneath structures, Case 2 is for the not-under-water free field adjacent to a structure, and Case 3 is for the under-water free field adjacent to a structure.

† Δ means the method has potential use for Case 3 with special techniques required which would increase the cost.

CHAPTER 5

SITE CHARACTERIZATION

5.1 INTRODUCTION

This chapter describes the site characterization information required to evaluate the geotechnical parameters used for the seismic design of highway facilities. It is assumed that the basic geological, geotechnical, and hydrological investigations required for the general design of the structure under consideration have been (or will be) conducted according to the state of practice. The goal of site characterization for seismic design is to develop the subsurface profile and soil property information necessary for seismic analyses. Soil parameters required for seismic analyses include the initial (small strain) dynamic shear modulus, equivalent viscous damping ratio, shear modulus reduction and equivalent viscous damping characteristics, cyclic shear strength parameters, and liquefaction resistance parameters.

Three broad categories of site investigation activities can be included in a seismic site exploration program. The first category is conventional geotechnical site exploration, including a drilling program followed by laboratory testing on undisturbed or remolded samples. The second category is in situ testing, wherein the parameters that describe dynamic soil properties are estimated in situ using penetrometers and other types of probes and in situ testing devices. The third category is geophysical exploration.

The remainder of this chapter will describe the relevant soil parameters for seismic site characterization, their importance for seismic analyses, and the available evaluation techniques.

5.2 SUBSURFACE PROFILE DEVELOPMENT

5.2.1 General

As for all geotechnical engineering analyses, seismic analysis requires knowledge of the subsurface profile, or stratigraphy, at the site under study. The required stratigraphic information includes information on the water level, the soil stratigraphic profile, and the underlying bedrock. Stratigraphy can be obtained using classical investigation techniques (drilling and sampling), in situ tests, or geophysical means.

As in any geotechnical analysis, identification and quantification of relatively thin, weak layers can be an important part of seismic site characterization. However, the "weak" layer in a seismic analysis may differ from the "weak" layer in a static analysis. For instance, a saturated sand layer considered a suitable foundation material with respect to static loads may be susceptible to liquefaction under earthquake loads and thus becomes a weak layer in a seismic analysis. In other

cases, such as soft material between beds of rock or stiff soil on a hillside, the same material that is a weak material for static analyses also represents a potential problem under earthquake loads.

5.2.2 Water Level

The groundwater level (or levels) should be established during a seismic site investigation. Groundwater may play an important role in seismic analysis, particularly if the soil deposits are liquefiable. Seasonal variability in the water level should be considered in developing the stratigraphic profile and performing liquefaction potential analyses.

Groundwater level information is often obtained by observation of the depth to which water accumulates in an open borehole. However, water level observations in boreholes may be unreliable due to a variety of factors, including:

- insufficient time for equilibrium in borings in fine-grained soils;
- artesian pressures in confined aquifers; and
- perched water tables in coarser soils overlying fine-grained deposits.

Furthermore, borehole observations do not, in general, permit observations of seasonal fluctuations in water levels. Piezometers or observation wells installed in a borehole provide a much more reliable means of monitoring water levels in the subsurface. In deposits where layers of fine-grained soils are present and multiple water levels are suspected, multiple-point piezometers can be installed in a single borehole or multiple boreholes can be fit with single point piezometers.

A cone penetrometer (CPT) with pore pressure measuring capabilities, referred to as a piezocone, can also be used to estimate water level elevations. By holding the cone at a constant elevation and waiting until the pore pressure drops to a constant value, the piezocone can be used to determine the steady state pore pressure at a specified elevation. The potential for perched water tables or confined aquifers can be assessed with the piezocone by combining steady-state pore pressure readings at several elevations with stratigraphic information developed from the tip and sleeve resistance of the cone.

Geophysical stratigraphic profiling methods are generally not used to evaluate the depth to groundwater. Geophysical methods used to evaluate soil stratigraphy are often based upon shear wave or Rayleigh wave velocity and thus are generally insensitive to the water level. Some resistivity methods (e.g., down hole resistivity surveys) can detect the presence of water in the soil pores but cannot measure the pressure in the water. Therefore, in a fine-grained soil, such methods can neither distinguish between soil above the water table saturated by capillarity and soil below the water table nor measure an artesian pressure in a confined aquifer.

5.2.3 Soil Stratigraphy

The subsurface investigation should provide a detailed description of the soil stratigraphy at the site, including the thickness and elevation of the different layers. Potentially liquefiable soils should be clearly identified and quantified by one of the methods described later in this chapter. Both conventional boring and sampling and in situ testing using the CPT offer the possibility of development of a continuous soil profile in which layers as small as 75 mm can be identified. Thin continuous layers of weak or potentially liquefiable soil encountered between beds of more competent soil may prove to be the critical plane in seismic slope stability analyses. Borings offer the advantage of recovery of a sample for visual classification and, if desired, laboratory testing. In a boring in which continuous Standard Penetration Tests (SPT) sampling is performed, layers of soil can be visually identified from the sample recovered from the split spoon to develop a continuous stratigraphic profile. However, the SPT blow count, the primary measurement of cohesionless soil strength and consistency obtained using the SPT, generally applies only to the gross behavior of a relatively large 300 mm interval of the boring and thus cannot be used to characterize the liquefaction susceptibility of thin lenses of soil visually identified in the split-spoon sample. In the CPT, the resistance of the tip and sleeve of the cone to penetration can be used to develop continuous profiles of the shear strength of the soil that are applicable to layers as thin as 75 mm.

Geophysical methods will provide information on the stratigraphy of the soil with respect to the measured geophysical property. The measured geophysical property may be a physical property of direct interest in a seismic analysis (e.g., shear wave velocity) or may be correlated to a physical property of interest (e.g., electrical resistivity and water level). The ability of geophysical methods to resolve layering in the ground varies among the available methods and, in general, decreases with depth unless a down hole method is used (in which case a boring or in situ probe is required).

5.2.4 Depth to Bedrock

Ideally, the soil profile developed for a seismic analysis should extend to *competent bedrock*, where competent bedrock is defined as material with a shear wave velocity of at least 700 m/s, and the physical properties of the soil over the entire interval between the ground surface and competent bedrock should be defined. However, if competent bedrock is not reachable at a reasonable depth, the depth over which the physical properties of the soil for seismic analyses are defined should be at least 30 m. Furthermore, the depth to which the soil profile is developed should be at least as deep as required for conventional geotechnical analyses.

5.3 REQUIRED SOIL PARAMETERS

5.3.1 General

At a minimum, a seismic analysis requires the same parameters used to describe soil properties for static analyses of earth structures and foundations. During the course of a typical geotechnical investigation, the following information is obtained:

- soil classification and index parameters;
- unit weight of the soil; and
- compressibility and shear strength parameters of the soil.

For seismic design purposes, a series of other soil parameters and properties may need to be evaluated. For a seismic analysis, these may include:

- a measure of the relative density of the soil;
- shear wave velocity;
- cyclic stress-strain behavior; and
- peak and residual shear strength.

5.3.2 Relative Density

Measures of both the absolute and relative density of the soil skeleton are required for seismic analysis. The absolute density is usually expressed in terms of unit weight. The unit weight of the soil is used to calculate the total and effective vertical stresses for liquefaction and slope stability analyses. Unit weight is also an important parameter in dynamic response and stability analyses, as the inertia force of an element of soil is equal to the acceleration times the total weight. Total unit weight may be assessed on the basis of measured values from undisturbed samples, or from the water content and specific gravity of saturated soil.

Relative density is an important parameter with respect to the potential for soil liquefaction and seismically-induced settlement of cohesionless soils. The relative density is a measure of the relative consistency of the soil.

Mathematically, relative density, D_r, is related to the maximum density (γ_{max}) or minimum void ratio e_{min} (the densest state to which the material can be compacted) and the minimum density (γ_{min}) or maximum void ratio e_{max} (the loosest state the material can attain) by:

$$D_r = \frac{e_{max} - e_o}{e_{max} - e_{min}} = \frac{1 - \gamma_{min}/\gamma_o}{1 - \gamma_{min}/\gamma_{max}} 100\% \qquad (5\text{-}1)$$

where e_o is the in situ void ratio of the material and γ_o is the in situ unit weight. Dry unit weights are used for γ_o, γ_{min}, and γ_{max}. The relative density is an important parameter with respect to

liquefaction and seismic settlement potential because it is related to the potential for a granular material to decrease in volume when subjected to disturbance.

Relative density is rarely measured directly. Generally, an index of the relative density is measured in situ. Commonly used indices of the relative density, or relative consistency, of soil in situ are the SPT blow count, N, and the normalized tip and sleeve resistance of the CPT probe, q_{cl}, and f_s, respectively. Table 4 presents the Terzaghi and Peck (1948) relationship between relative density and SPT blow count for sandy soils. Several of the indices used to evaluate relative density in situ have, in turn, been directly correlated to liquefaction and seismic settlement potential, often eliminating the need for direct evaluation of relative density in a seismic analyses.

Table 4. Relative density of sandy soils (after Terzaghi and Peck, 1948).

Relative Density, D_r (%)	**Penetration Resistance, N (blows/300mm)**	**Descriptive Term**
0-15	0-4	Very Loose
15-35	5-10	Loose
35-65	11-30	Medium
65-85	31-50	Dense
85-100	> 50	Very Dense

Note: See also figure 37 for an alternative N-D_r correlation.

5.3.3 Shear Wave Velocity

The shear wave velocity of a soil is used to establish the stiffness of the soil at small strains. The small strain (initial) shear modulus of a soil, G_{max}, is related to the shear wave velocity, V_s, and the mass density, ρ, of the soil by the equation:

$$G_{max} = \rho \cdot V_s^2 \tag{5-2}$$

Mass density of the soil is related to the total unit weight of the soil, γ_t, by the acceleration of gravity, g:

$$\rho = \frac{\gamma_t}{g} \tag{5-3}$$

The mass density of most soils can be reasonably estimated from soil classification and location relative to the water table. Therefore, measurement of shear wave velocity can provide a reliable means for evaluating the small strain shear modulus of the soil if the stratigraphic profile is known.

Small strain (initial) Young's modulus, E_{max}, is related to small strain shear modulus as a function of Poisson's ratio, ν, by the theory of elasticity:

$$E_{max} = 2(1+\nu)G_{max} \tag{5-4}$$

For practical purposes, Poisson's ratio of soil can be assumed equal to 0.35 for sands and 0.45 for clays. Alternatively, if results of geophysical measurements are available, the following equation may be used to estimate ν.

$$\nu = 1 - \frac{1}{2(1-(V_s/V_p)^2)} \tag{5-5}$$

where V_s and V_p are shear and compressional wave velocities, respectively. Young's modulus can also be evaluated from the compressional wave velocity and mass density of the soil. Consequently an efficient and reliable means of obtaining the small-strain elasticity properties of the soil is through the measurement of shear and compressional wave velocities.

5.3.4 Cyclic Stress-Strain Behavior

During an earthquake, a soil deposit is subjected to a complex system of stresses and strains resulting from the ground motions induced by the earthquake. In general, these stresses and strains will be cyclical due to the vibrational nature of the earthquake loading. To evaluate the seismic response of the soil deposit, it is necessary to estimate how it responds to this cyclic loading.

The earthquake-induced stresses and strains that produce the most damage in soils are generally considered to be due to cyclic shearing of the soil. Shear waves propagate primarily upward near the ground surface. Therefore, most geotechnical earthquake engineering analyses assume that earthquake ground motions are generated by vertically-propagating shear waves.

The cyclic stresses induced on a soil element by a vertically-propagating shear wave are schematically presented in figure 34. The stress-strain response of soil to this type of cyclic loading is commonly characterized by a *hysteresis loop*. A typical hysteresis loop is shown on figure 35. Various constitutive models have been developed to characterize soil hysteresis loops. The most common model used to represent the hysteretic behavior of soil in seismic analysis is the *equivalent-linear* model (Seed and Idriss, 1970). Various non-linear constitutive models (Kondner and Zelasko, 1963; Martin, 1975; Matasović and Vucetic, 1993) have also been developed to represent hysteretic

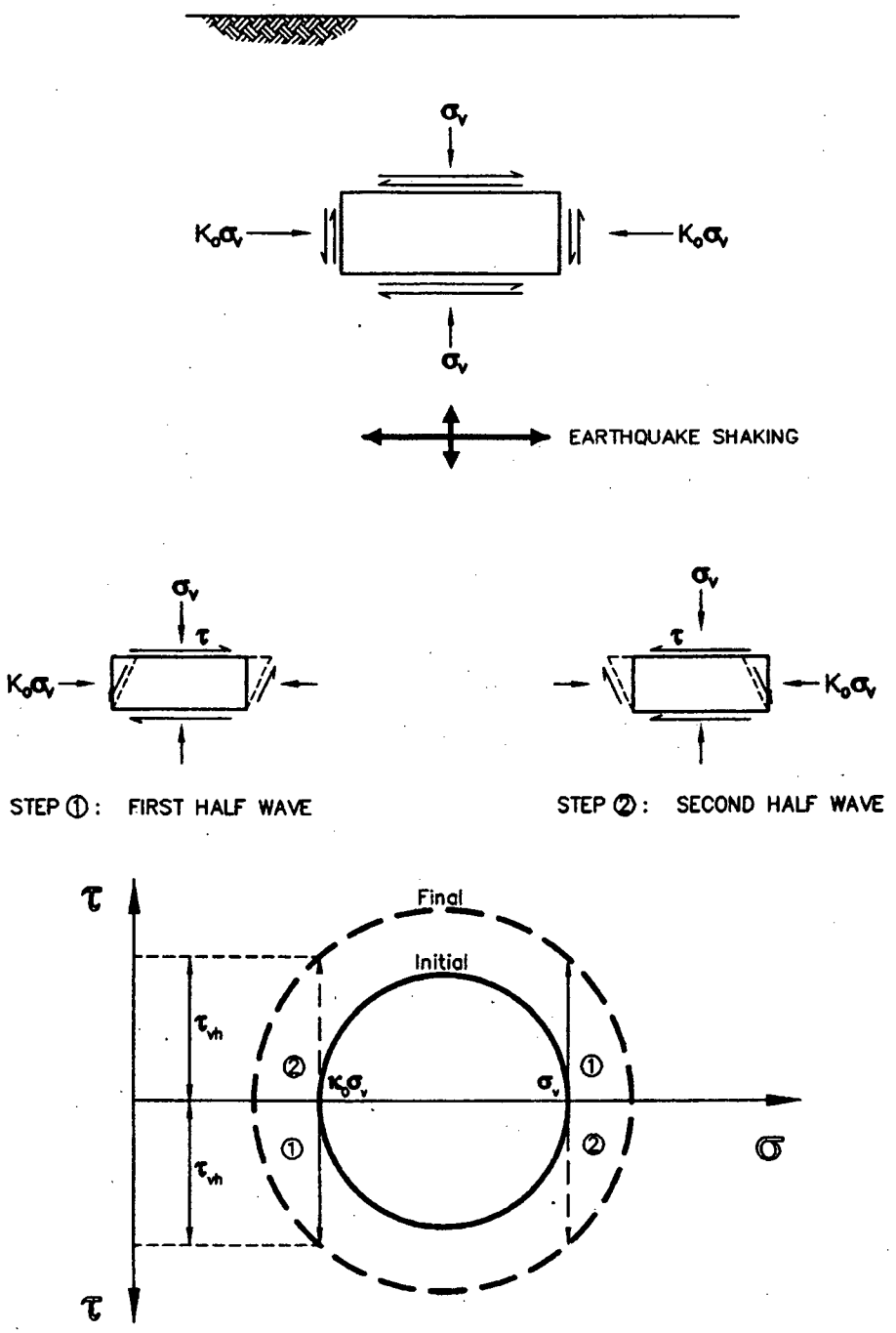

Figure 34. Stresses induced in a soil element by vertically propogating shear wave.

soil behavior. Detailed discussion of non-linear constitutive models for the hysteretic behavior of soil is beyond the scope of this document.

The equivalent-linear model represents non-linear hysteretic soil behavior using an equivalent shear modulus, G, equal to the slope of the line connecting the tips of the hysteresis loop and an equivalent viscous damping ratio proportional to the enclosed area of the loop. The equivalent modulus and damping ratio are strain-dependent. The strain dependence of the equivalent modulus and damping ratio are described by the *modulus reduction* and *damping curves* shown on figure 36. The equivalent viscous damping ratio is evaluated from the area of the hysteresis loop as schematically shown on figure 35. Modulus reduction and damping curves strictly apply only to uniform cyclic loading. However, these curves are typically also used to model the soil behavior under irregular (non-uniform) cyclic loading generated by earthquakes.

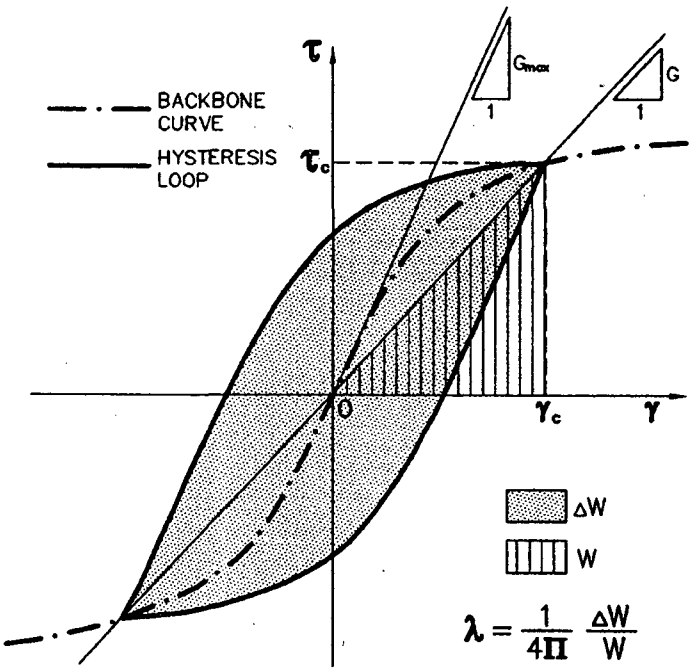

Figure 35. Hysteretic stress-strain response of soil subjected to cyclic loading.

Cyclic loading can break the bonds between soil particles and rearrange the particles into a denser state. In a dry soil, this rearrangement will be manifested as compression of the soil and will result in seismic settlement. If the soil is saturated, volume change cannot occur instantaneously and the load carried by the soil skeleton is transferred to the pore water as the particles are rearranged. If the rearrangement is sufficient in magnitude, the soil skeleton can shed all of the load to the pore water, resulting in a pore pressure equal to the overburden pressure, complete loss of shear strength, and, consequently, liquefaction of the soil.

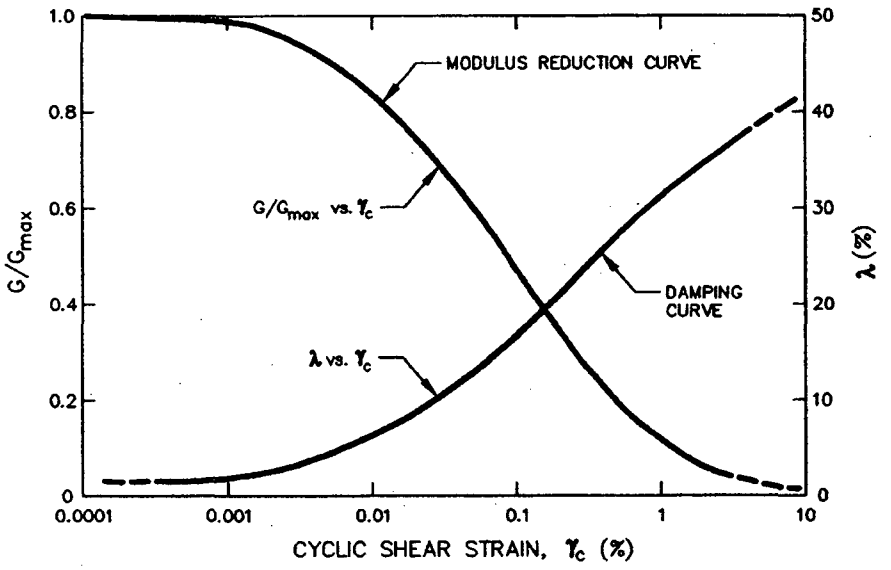

Figure 36. Shear modulus reduction and equivalent viscous damping ratio curves.

5.3.5 Peak and Residual Shear Strength

Peak and residual shear strengths are important elements in the evaluation of seismic stability. The peak shear strength refers to the maximum shearing resistance an element of soil can sustain during and after cyclic loading. The peak shear strength may be used to calculate the *yield acceleration* of a soil (the horizontal acceleration above which permanent seismic deformations begin to accumulate) if the buildup of seismically-induced pore pressures is not anticipated. Residual shear strength refers to shear strength of the soil after significant static and/or cyclic shearing has occurred. Residual shear strength is often used to evaluate stability and calculate the accumulation of permanent seismic deformation in a post-liquefaction stability and deformation analysis for a foundation or earth structure.

While there is some limited information to indicate that the shear strength of soil increases with increasing strain rate, the peak shear strength of soil subjected to cyclic loading is generally assumed to be less than or equal to the peak static strength. If the soil is dry, the drained shear strength may be used. If the soil is saturated, even if the soil is relatively free draining, the undrained shear strength should be used for seismic analyses because of the rapid nature of earthquake loading.

Residual shear strength is used to represent the post-peak strength of the soil subsequent to both monotonic and cyclic loading. Many soils and geosynthetic interfaces show a marked decrease in shearing resistance when subjected to relatively large monotonic shear strains. If the seismic design philosophy for a foundation or earth structure calls for allowing the peak strength to be exceeded as long as cumulative deformations remain within a range defined as acceptable, the residual shear strength after monotonic loading is typically used to assess the post-deformation stability. The yield

acceleration calculated using the residual shear strength can be used to assess cumulative seismic deformations on a conservative basis.

5.4 EVALUATION OF SOIL PROPERTIES

5.4.1 General

The key dynamic soil parameters required to perform a seismic response analysis are the shear wave velocity, modulus reduction and damping curves, peak and residual shear strength, and the parameters needed to evaluate soil liquefaction potential. A value for Poisson's ratio may also be required. These parameters can either be directly evaluated from laboratory test results or in situ test results or indirectly evaluated by correlation with index properties of soils. Laboratory tests generally provide the most direct means of evaluating soil parameters for seismic analyses. However, laboratory tests are subject to limitations on the recovery and testing of representative samples as well as on the testing itself. For some parameters (e.g., shear wave velocity), field testing provides a reliable and cost effective means of evaluation. However, in many cases, empirical correlation with index parameters and in situ test results is the most practical means of evaluating soil parameters for seismic analyses. Sometimes, for particular geographical areas and soils (e.g., Piedmont region residual soils, Borden et al., 1996) typical dynamic soil parameters have been established.

5.4.2 In Situ Testing for Soil Profiling

5.4.2.1 Standard Penetration Testing (SPT)

Probably the most common in situ test used in geotechnical practice, the SPT, measures the resistance to penetration of a standard split-spoon sampler in a boring. The test method is rapid and yields useful data, although there are many factors that affect the results. The procedure used to perform the SPT is codified under ASTM Standard D 1586. The SPT consists of driving a standard split barrel sampler with a 63.5 kg hammer dropping 762 mm in a free fall which theoretically delivers 60 percent of the energy to the drill rod. The (uncorrected) SPT blow count, N, is the result of the test.

Although widely recognized as an unsophisticated test, the SPT is performed routinely worldwide and, when performed properly, yields useful results. Extensive work has been conducted to understand the limitations of the test and develop reliable correction factors accounting for the influence of vertical stress, soil gradation, hammer efficiency, and other factors on test results. Correction factors to normalize and standardize the value of the SPT blow count, N, are discussed in chapter 8. Corrected SPT blow count values can be used to:

- estimate the relative density of sand;
- estimate shear strength parameters of cohesionless soils;
- estimate bearing capacity;
- evaluate seismic settlement potential of sands;

- evaluate liquefaction potential of saturated sands; and
- estimate the shear modulus at very low strain.

Hammer efficiency is a key factor in evaluating SPT blow count. Values of hammer efficiency, defined as the energy delivered to the sampler divided by the theoretical kinetic energy of the free-falling weight, measured in the field vary from 30 to 90 percent, with an average value of 60 percent, depending on the equipment, the operator, and other site-specific conditions. Field and analytical data indicate that the blow count is directly proportional to the energy delivered to the split spoon sampler (Seed et al., 1985). Measurement of efficiency made on the same day using the same equipment and operator has been known to vary by a factor of two. A two- to three-fold variation in efficiency will result in a two- to three-fold variation in blow count in a uniform soil. To mitigate this problem, i.e., to be able to relatively accurately standardize the blow count to correspond to the average efficiency of 60 percent, several companies have developed systems for measuring the energy delivered to the rods or split spoon sampler by the hammer. The services of these companies are available on a commercial basis and should seriously be considered for major projects or where liquefaction potential assessment is a critical issue.

Most soil mechanics text books contain correlations relating SPT blow counts to soil shear strength and foundation bearing capacity (e.g., Bowles, 1988). As discussed in chapter 5.3.2 and presented in table 4, SPT blow counts may also be used to estimate relative density of sand. Figure 37 presents a correlation between overburden pressure, relative density, and SPT blow count developed by Marcuson and Bieganousky (1977) for clean sand.

The use of SPT blow counts to evaluate soil liquefaction potential is described in detail in chapter 8.

5.4.2.2 Cone Penetration Testing (CPT)

The CPT test involves pushing a standard dimension conical probe into the ground at a constant rate and measuring the resistance of the tip of the cone and along the side of the cone to penetration. The cone tip resistance, q_c, combined with the friction ratio, f_s (the ratio between the side resistance and point resistance of the cone), has been shown to be strongly correlated to soil type and soil strength. In recent years, cone penetration testing probes have been fitted with pore pressure cells (piezocones) to measure pore pressure during penetrations and pore pressure dissipation after penetration, facilitating in situ measurement of consolidation properties and water table depth. The CPT can also be fitted with a geophone for use in "down hole" seismic profiling to determine shear wave velocity.

CPT testing is codified as ASTM Standard D 3441. Recommendations for CPT testing are also provided by FHWA (1992). The CPT is relatively easy to perform and provides a continuous profile of soil stratigraphy that can be invaluable in identifying the extent of liquefiable soils at a site.

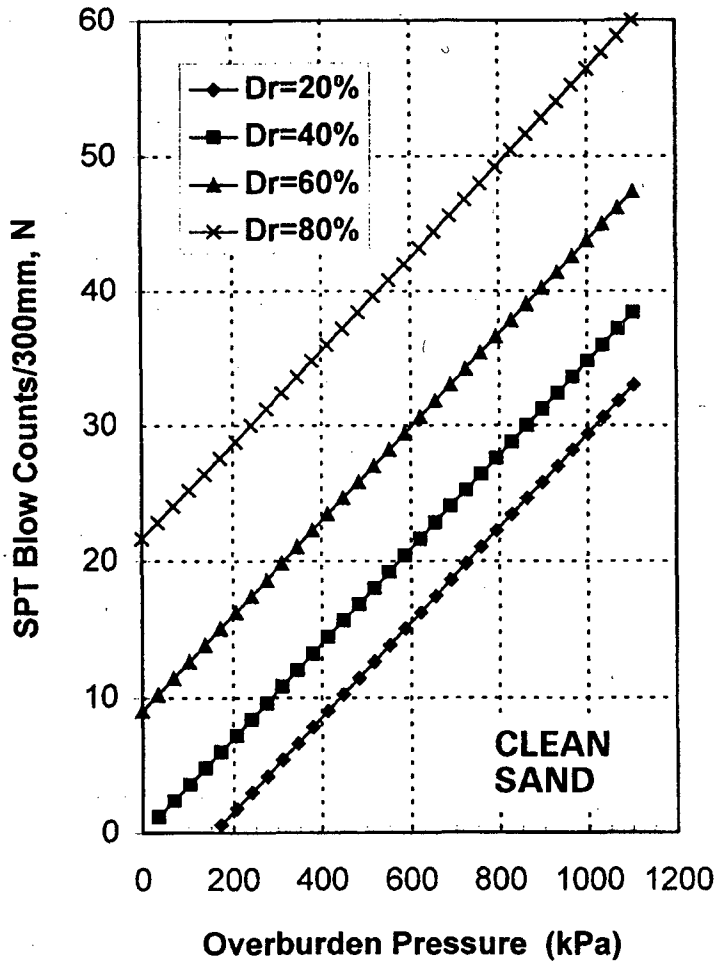

Figure 37. SPT-relative density correlation (after Marcuson and Bieganousky, 1977, reprinted by permission of ASCE).

Figure 38 shows a typical soil classification system based on cone penetration resistance readings. Data from the CPT can also be used to establish allowable bearing capacity and for pile design. In addition, correlations between SPT *N* values and CPT cone resistance have been developed to allow for the use of CPT data with relationships between SPT values and dynamic soil properties (e.g., liquefaction potential). Figure 39 presents the Martin (1992) chart which illustrates the relationship between cone resistance and SPT *N* values. Cone resistance has also been correlated to undrained shear strength, angle of internal friction, and relative density (Bowles, 1988; Meigh, 1987; Schmertmann, 1975).

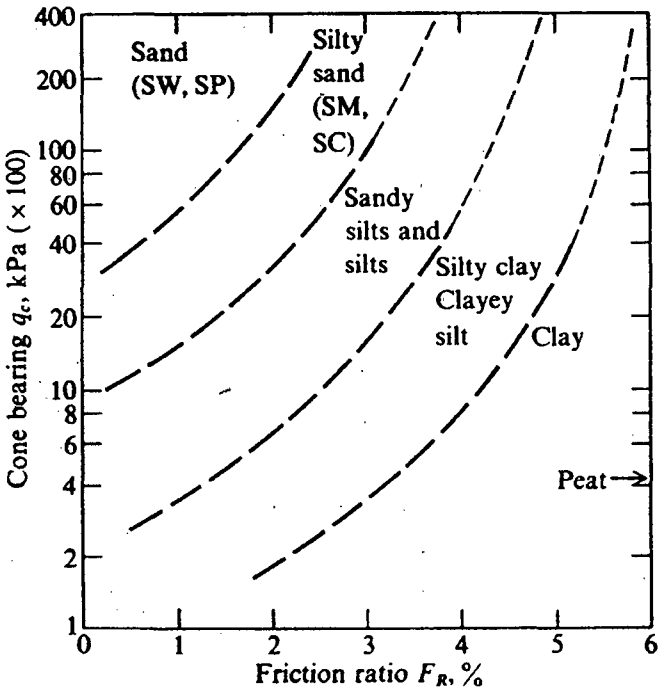

Figure 38. Soil Classification system based on the CPT (Douglas and Olsen, 1981, reprinted by permission of ASCE).

5.4.3 Soil Density

The total density of soil is usually expressed in terms of total unit weight. Typical values of the total unit weight are generally adequate for use in engineering analysis. If a higher degree of accuracy is required, unit weight can be evaluated from measurements made on undisturbed samples. In saturated cohesive soils, unit weight can be evaluated from the water content and the specific gravity.

Relative density, D_r, is rarely measured directly for geotechnical engineering purposes. Instead, an index of the relative density, usually the SPT blow count or the CPT resistance, is measured. Figure 37 presents one relationship between SPT blow count and the relative density of a clean sand.

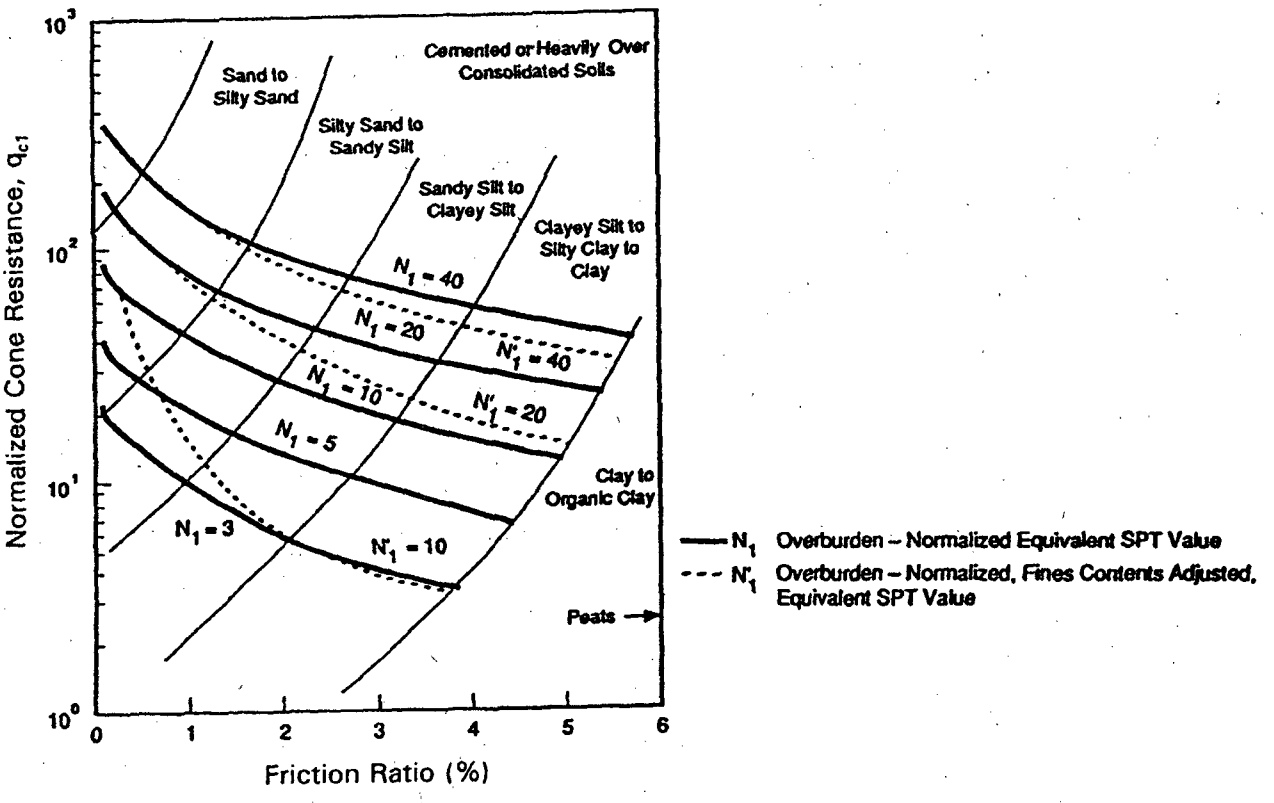

Figure 39. CPT-soil behavior - SPT correlation chart (Martin, 1992, reprinted by permission of ASCE).

5.4.4 Shear Wave Velocity

5.4.4.1 General

In general, shear wave velocity is directly measured in the field. However, shear wave velocity can also be estimated based upon soil type and consistency or by using the empirical correlations for small strain shear modulus described in section 5.4.5.2 in conjunction with the soil density and equation 5-2.

Shear wave velocity, or small strain shear modulus, can be evaluated in the laboratory using resonant column tests, as noted in section 5.4.5. However, field geophysical measurements are used more commonly and reliably to estimate shear wave velocity.

Geophysical measurements of in situ wave velocities are typically based on measuring the wave travel time along a known propagation path. From knowledge of distance and travel time, the

velocity is obtained. Wave velocity may be measured from intrusive methods such as boreholes and CPT soundings (seismic cone) or non-intrusively using seismic reflection, refraction, and surface wave profiling.

5.4.4.2 Geophysical Surveys

Geophysical techniques for subsurface exploration are described in detail by Woods (1994). Geophysical techniques commonly used in geotechnical practice are briefly summarized in the following paragraphs. Two general types of techniques are available to measure shear wave velocities in the field:

- intrusive techniques whereby measurements are made using probes and sensors that are lowered in boreholes or pushed into the ground; and
- non-intrusive techniques whereby the measurements are made from the ground surface.

Borehole Surveys

In a borehole seismic survey, one or more boreholes are drilled into the soil to the desired depth of exploration. Wave sources and/or receivers are then lowered into the boreholes to perform the desired tests. There are three approaches to borehole seismic surveys:

- *Up Hole Surveys*: Geophones are laid out on the surface in an array around the borehole. The energy source is set off within the borehole at successively decreasing depths starting at the bottom of the hole. The travel times from the source to the surface are analyzed to evaluate wave velocity versus depth. The energy source is usually either explosives or a mechanical pulse instrument composed of a stationary part and a hammer held against the side of the borehole by a pneumatic or hydraulic bladder.
- *Down Hole Surveys*: In a down hole survey, the energy source is located on the surface and the detector, or geophone, is placed in the borehole. The travel time is measured with the geophone placed at progressively increasing depth to evaluate the wave velocity profile.
- *Cross Hole Survey*: In a cross hole survey, the energy source is located in one boring and the detector (or detectors) is placed at the same depth as the energy source in one or more surrounding boreholes at a known spacing. Travel time between source and receiver is measured to determine the wave velocity.

The cross hole technique is generally the preferred technique for a borehole survey as it offers the highest resolution and greatest accuracy. However, cross hole measurements require a very precise evaluation of the distance between the energy source and the detector. An inclinometer reading is generally performed in the boreholes used in a cross hole survey to correct the results for deviation

of the boreholes from verticality. Cross hole geophysical testing is codified in ASTM Standard D 4428.

Seismic Refraction and Seismic Reflection Methods

Seismic refraction and reflection exploration surveys are conducted from the surface and do not require boreholes. The resolution of the methods is relatively poor and decreases with depth. These methods are most suitable as a means of identifying the depth to competent rock and the location of prominent soil horizons that have a large contrast in density and stiffness compared to the overlying soil.

Spectral Analysis of Surface Waves (SASW)

Spectral Analysis of Surface Waves (SASW) is a non-intrusive geophysical technique used primarily for evaluating subsurface shear wave velocity profiles. SASW testing evaluates shear wave velocity indirectly by direct measurement of Rayleigh, or surface wave, velocity. Rayleigh wave velocity is related to shear wave velocity by Poisson's ratio. The two velocities are usually within 5 percent of each other for most soils. SASW results are representative of the average properties of a relatively large mass of material, mitigating the potential for misleading results due to non-homogeneity. SASW can be a very cost-effective method of investigation. The ease and rapidity of field measurements and automated algorithms for data processing and inversion allow for evaluation of subsurface conditions at a relatively large number of points at a fraction of the cost of conventional intrusive exploration techniques.

A schematic representation of SASW testing is presented in figure 40. Excitation at the ground surface is used to generate the Rayleigh, or surface, waves at various frequencies. By spectral analysis of the ground surface response (velocity or acceleration) at two points a known distance apart, the Rayleigh wave velocity can be obtained at discrete frequencies. Usually, an inversion process (trial and error) is used to determine the velocity profile. At sites where wave velocity increases gradually with depth, the velocity profile may be determined directly from the field data. The depth over which reliable measurements can be made depends upon the energy and frequency content of the source excitation and the consistency of the subgrade material. Measurements are not affected by the depth to the water table.

The concept of measuring the velocity of Rayleigh waves of different frequencies to determine the profile of shear wave velocity with depth was first proposed by Jones (1962), in Great Britain, for pavement surveys and by Ballard (1964), at the Waterways Experiment Station in Vicksburg, Mississippi, for geotechnical analyses. These investigators used impact loading as the source excitation and developed an analysis based upon the assumption of a uniform, homogeneous layer. Stokoe and Nazarian (1985) at the University of Texas, Austin, extended the analysis to consider multi-layered media. These investigators also used a surface impact as the source excitation and thus reliable measurements were typically limited to maximum depths on the order of 10 meters by the relatively low energy content of the excitation at relatively long wave lengths.

Satoh and his co-workers (1991) in Japan developed an electro-magnetic controlled vibrator for use as the source excitation. Large (2000 kg) mass, Controlled Source Spectral Analysis of Surface

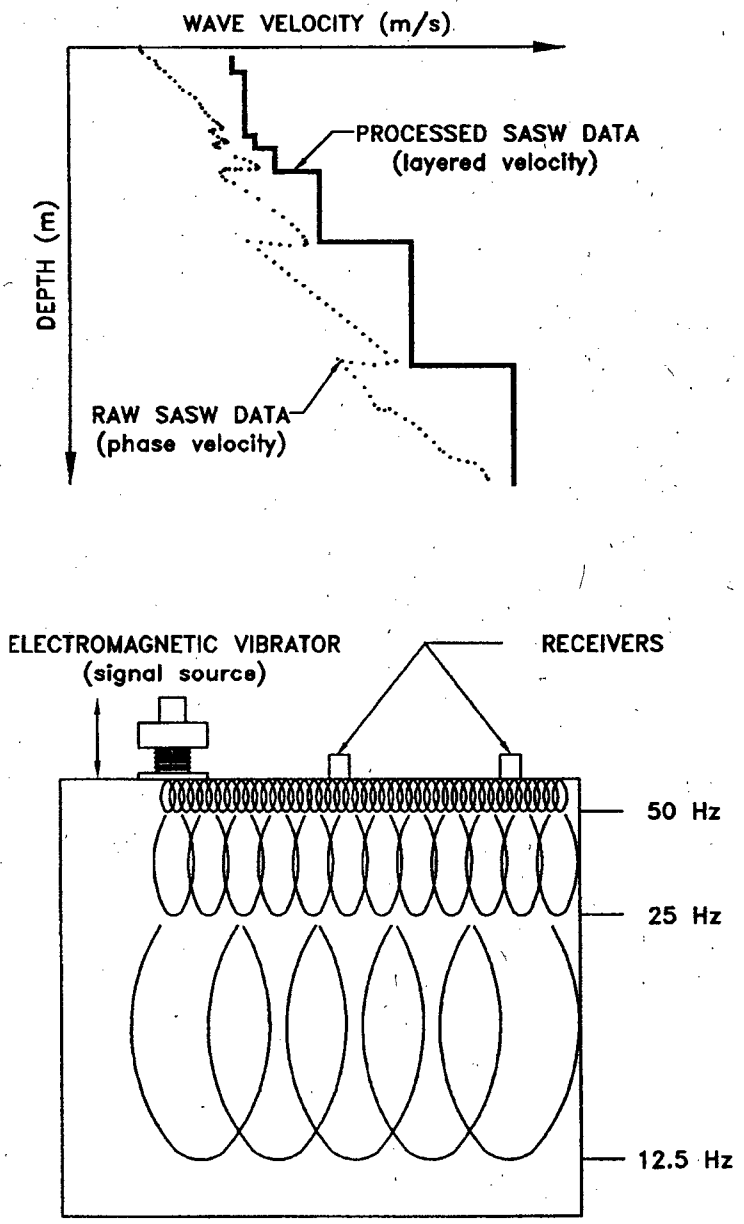

Figure 40. Schematics of SASW testing (Kavazanjian et al., 1994).

Waves (CSSASW) equipment capable of penetrating over 100 meters below the ground surface has recently been developed. Comparisons between SASW and down hole velocity measurements have been made (Nazarian and Stokoe, 1984) and show good agreement between the two methods.

5.4.4.3 Compressional Wave Velocity

Compressional wave velocity may sometimes be required for seismic analyses. Compressional wave velocity can be directly measured in a bore hole survey or in a laboratory test. Alternatively, the compressional wave velocity can be calculated from the shear wave velocity and Poisson's ratio using equation 5-5.

5.4.5 Evaluation of Cyclic Stress-Strain Parameters

5.4.5.1 Laboratory Testing

Laboratory testing for evaluation of cyclic stress-strain parameters of soil is appealing to many engineers because direct measurements are made of the hysteretic stress-strain behavior of soils. However, cyclic laboratory testing is subject to a variety of constraints, including:

- difficulty in reproducing field stresses (or strains);
- difficulty in recovering and testing undisturbed cohesionless soil samples; and
- the time and expense associated with cyclic laboratory testing.

A summary of the different types of cyclic laboratory tests used in geotechnical practice and their advantages and limitations follows. More details on cyclic laboratory testing can be found in Kramer (1996).

Cyclic Direct Simple Shear Test

The cyclic direct simple shear (CyDSS) test may provide the most accurate representation of the stress state resulting from a vertically propagating shear wave in a horizontally layered soil deposit of any laboratory test. The simple shear device consists either of a rectangle box made of hinged plates or a cylindrical wire-reinforced membrane which surrounds the sample and restrains the sample from deforming laterally during the test. The apparatus includes either an arrangement for applying a constant vertical load or for maintaining a constant sample height while measuring the vertical load and a mechanism for applying a horizontal cyclic shear load. The sample is usually formed directly in the simple shear device. However, undisturbed samples of cohesive soil or frozen sand can be tested in the devices that use wire-reinforced membranes.

Cyclic Triaxial Test

The cyclic triaxial test was developed for geotechnical purposes by Seed and his co-workers at the University of California at Berkeley in the 1960s and has been used extensively to evaluate cyclic behavior of soils. The device consists of a regular triaxial cell and a cyclic, often sinusoidal loading machine attached to the loading piston. The sample is isotropically consolidated in the triaxial cell and then subjected to a cyclic axial load in extension and compression. The primary drawback of the cyclic triaxial tests is that it does not provide a good representation of the stress state induced in the ground by an earthquake (see figure 34). The main difference in cyclic triaxial test stress conditions compared to the field conditions are: (1) the laboratory soil sample is isotropically consolidated, whereas the soil is under a K_o condition in the field; (2) in the field there is a continuous reorientation of the principal stresses whereas in the triaxial test, the reorientation angle is either 0 or 90 degrees; (3) the cyclic shear stress is applied on a horizontal plane in the field but on a 45 degree plane in the triaxial test; and (4) the mean normal stress in the field is constant while the mean normal stress in the laboratory varies cyclically.

Torsional Simple Shear Test

In order to overcome some of the limitations of the CyDSS and triaxial tests, Ishibashi and Sherif (1974) developed a torsional simple shear test. The sample is "doughnut-like" in shape with outer to inner radius and outer to inner height ratios of about two. This doughnut-like shape ensures a relatively uniform shear strain on the horizontal plane throughout the sample. The torsional simple shear test offers several advantages over CyDSS and cyclic triaxial tests:

- simulates closely the field stress (strain) conditions like the CyDSS;
- it is possible to apply vertical and horizontal stresses independently; and
- permits the octahedral normal stress to remain unchanged during the test.

There are also some disadvantages associated with this test:

- interpretation of the results is rather complicated and the definition of liquefaction (Ishibashi and Sherif, 1974) does not permit correlation of torsional simple shear results with those of other tests;

- mobilization of enough interface shear between the sample and the top and bottom plates to prevent slippage may be difficult, however steel pins cast into porous stones will provide good contact between the sample and the plates; and

- the shape of the sample makes the device impractical for use in conventional practice, particularly for undisturbed samples.

Resonant Column Test

The resonant column test for determining dynamic properties of soils is based on the theory of wave propagation in rods. Either compression or shear waves can be propagated through the soil specimen in resonant column testing. Solid or hollow specimens can be used in the apparatus.

Either a sinusoidal torque or a vertical compressional load is applied to the top of the sample through the top cap. The deformation of the top of the specimen is measured. The excitation frequency is adjusted until the specimen resonates. The wave velocity or modulus is computed from the resonant frequency and the geometric properties of the sample and driving apparatus. Damping is determined by switching off the current to the driving coil at resonance and recording the amplitude of decay of the vibrations. The decay of the amplitude with time is used to determine the *logarithmic decrement* (the percentage decay over one log cycle of time), which is directly related to the viscous damping ratio.

The primary problem associated with using resonant column tests to measure dynamic soil properties is that the test is generally limited to small to intermediate shear strains by the applied force requirements and resonant frequencies. Furthermore, at larger strains, hollow samples must be used to maintain a relatively constant shear strain across the sample. For these reasons, resonant column testing is primarily used to estimate small strain shear modulus. However, it can also be used to determine modulus reduction and equivalent viscous damping in intermediate strain range.

5.4.5.2 Use of Empirical Correlations

Parameters describing the cyclic soil properties required for a dynamic analyses include the initial (small strain) damping, λ, the initial (small strain) shear modulus at small shear strain, G_{max}, and the modulus reduction and damping curves for the soil. Small strain damping is difficult to evaluate. Therefore, an equivalent viscous damping ratio of 2 to 5 percent is commonly assumed in equivalent-linear analyses, while a viscous damping of 0.5 to 1 percent is commonly assumed in non-linear analyses. The small strain shear modulus, commonly referred to as the *initial shear modulus*, G_{max}, can be obtained from site-specific investigations or by using empirical correlations with index soil properties. Geophysical methods for establishing G_{max} were previously described. Table 5 presents the typical range of G_{max} for several generic soil types.

Table 5. Typical values of initial shear modulus

Type of Soil	**Initial Shear Modulus, G_{max} (kPa)**
Soft Clays	2,750 - 13,750
Firm Clays	6,900 - 34,500
Silty Sands	27,600 - 138,000
Dense Sands and Gravel	69,000 - 345,000

The parameter G_{max} has been empirically related to both the SPT N value and CPT point resistance, q_c. Correlations with SPT results by Seed et al. (1984) and Imai and Tonouchi (1982) and with CPT results by Mayne and Rix (1993) are presented in table 6.

Following the initial work of Hardin and Drnevich (1972), many researchers developed empirical relationships to estimate G_{max} of the following general form:

$$G_{max} = A\ \sigma'^{½}_{m}\ OCR^{k}\ f(e) \tag{5-6}$$

where $f(e)$ is some function of the void ratio, e, OCR is the overconsolidation ratio, A is a normalizing constant, k is the power factor, and σ'_m is the mean normal effective stress obtained as:

$$\sigma'_m = \left[\frac{1+2K_o}{3}\right] \sigma'_v \tag{5-7}$$

where σ'_v is the vertical effective stress and K_o is the coefficient of lateral earth pressure at rest.

Seed and Idriss (1970) developed a series of curves relating G_{max} to relative density and mean normal effective stress through a coefficient, $(K_2)_{max}$:

$$G_{max} = 1000\ (K_2)_{max}\ (\sigma'_m)^{½} \text{ in psf} \tag{5-8}$$

$$G_{max} = 220\ (K_2)_{max}\ (\sigma'_m)^{½} \text{ in psf} \tag{5-9}$$

where $(K_2)_{max}$ is a function of relative density and soil type (see table 6). This approach has been further extended to estimate stress-dependent modulus reduction curves for sandy soils using the strain dependent parameter K_2 instead of $(K_2)_{max}$. An example of a curve relating K_2 to shear strain is shown in figure 41. Iwasaki et al. (1978) found that the mean normal effective stress is the predominant factor that governs the modulus reduction of cohesionless soils and developed stress dependent curves shown in figure 42. Note that the authors did not provide damping curves.

Vucetic and Dobry (1991) have shown that the relationships between modulus reduction and cyclic shear strain and between equivalent viscous damping and cyclic shear strain can, with a relatively high degree of confidence, be reduced to a set of curves that depend on the plasticity index, PI, of the soil. The Vucetic and Dobry modulus reduction and damping curves are presented in figure 43. Note that the curves for PI equal to zero apply to sands, gravels, and other cohesionless soil. The Vucetic and Dobry PI = 0 damping curve may be used in conjunction with the Iwasaki et al. (1978) stress-dependent modulus reduction curve to characterize the dynamic behavior of sandy soils.

Table 6. Correlations for estimating initial shear modulus.

Reference	Correlation	Units	Limitation
Seed et al. (1984)	$G_{max} = 220\ (K_2)_{max}\ (\sigma'_m)^{1/2}$ $(K_2)_{max} \approx 20(N_1)_{60}^{1/3}$	kPa	$(K_2)_{max} \approx 30$ for very loose sands and 75 for very dense sands; $\approx$ 80-180 for dense well graded gravels; Limited to cohesionless soils
Imai and Tonouchi (1982)	$G_{max} = 15{,}560\ N_{60}^{0.68}$	kPa	Limited to cohesionless soils
Hardin (1978)	$G_{max} = \frac{625}{(0.3 + 0.7\ e_o^2)}(P_a \cdot \sigma'_m)^{0.5}\ OCR^k$	kPa(1)	Limited to cohesive soils P_a = atmopsheric pressure
Jamiolkowski et al. (1991)	$G_{max} = \frac{625}{e_o^{1.3}}(P_a \cdot \sigma'_m)^{0.5}\ OCR^k$	kPa(1)	Limited to cohesive soils P_a = atmopsheric pressure
Mayne and Rix (1993)	$G_{max} = 99.5(P_a)^{0.305}(q_c)^{0.695}/(e_o)^{1.13}$	kPa(2)	Limited to cohesive soils P_a = atmopsheric pressure

Notes: (1) P_a and σ'_m in kPa
(2) P_a and q_c in kPa

The modulus reduction curves shown on figures 41, 42, and 43 end at a shear strain level of 1 percent. In areas of high seismicity (e.g., California) cyclic strains in soils may exceed 1 percent. If necessary, modulus reduction curves can be extended to shear strain levels larger than 1 percent using a procedure developed by CALTRANS and elaborated upon in Jackura (1992).

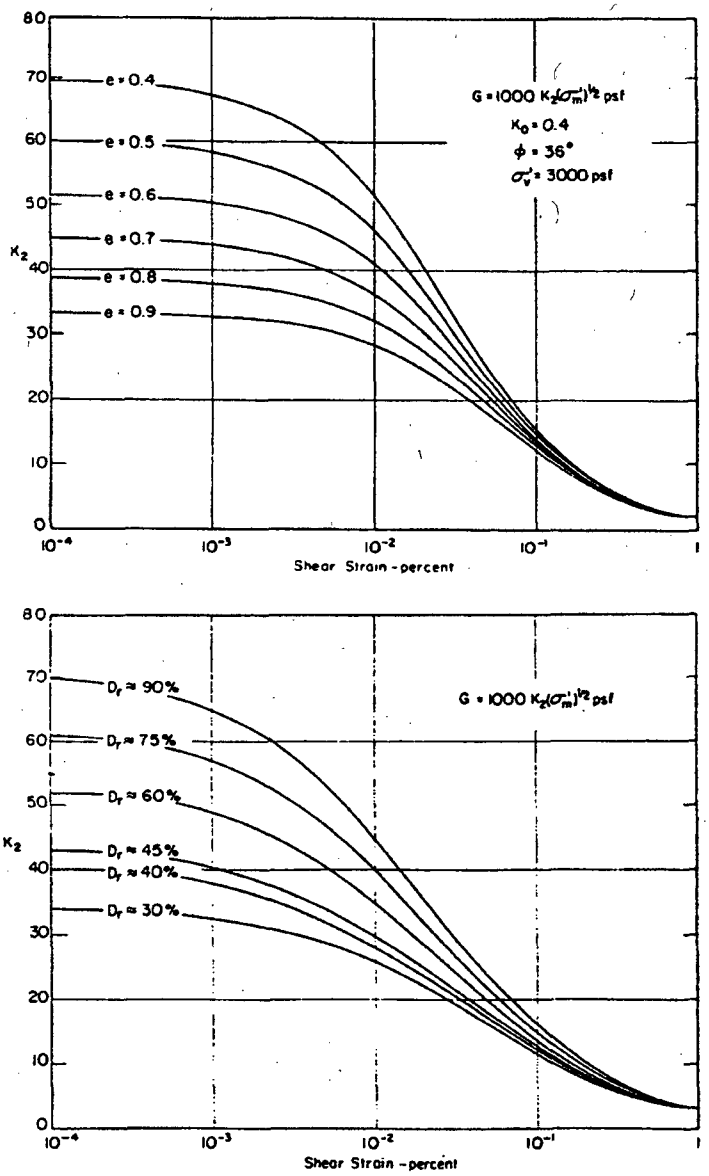

Figure 41. Shear modulus reduction curves for sands (Seed and Idriss, 1970, reprinted by permission of ASCE).

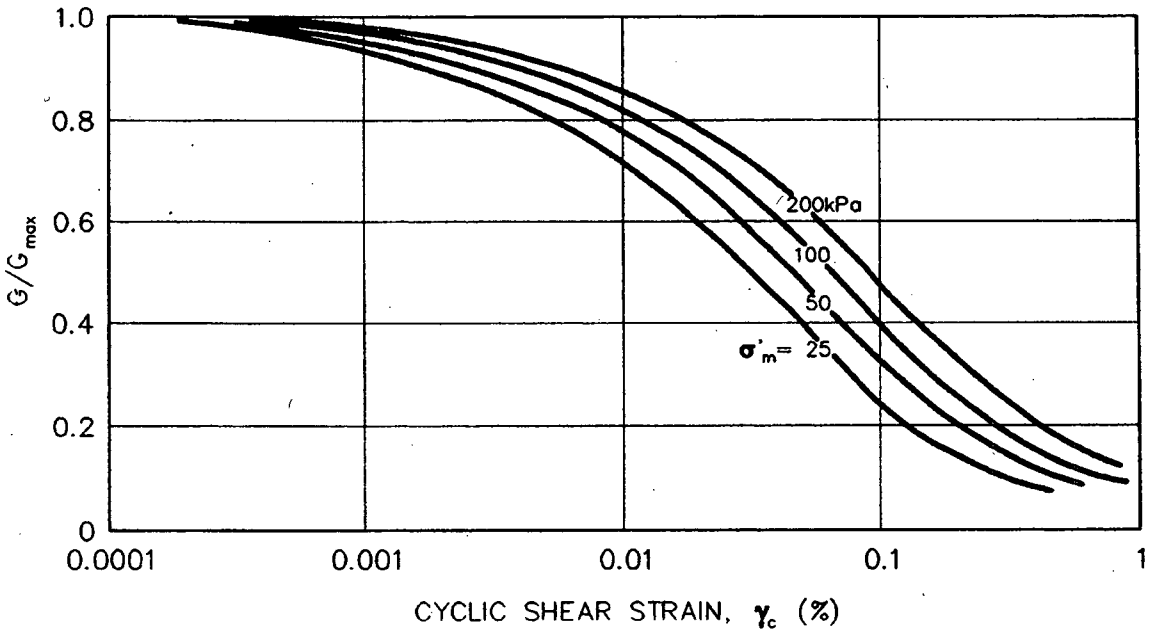

Figure 42. Shear modulus reduction curves for sands (Iwasaki et al., 1978, reprinted by permission of Japanese Society of Soil Mechanics and Foundation Engineering).

5.4.6 Peak and Residual Shear Strength

The peak shear strength of soil not subject to strength degradation under cyclic loading may be evaluated using conventional methods, including laboratory and in situ testing and correlations with soil index properties. A key difference in seismic problems compared to static problems is that undrained strength parameters are typically used for the strength of saturated soils subjected to cyclic loading, even for cohesionless soils (e.g., sands, gravels) because of the relatively rapid rate of earthquake loading.

The dynamic undrained shear strength of a soil may be influenced by the amplitude of the cyclic deviator stress, the number of applied loading cycles, and the plasticity of the soil. For saturated cohesionless soils, even relatively modest cyclic shear stresses can lead to pore pressure rise and a significant loss of undrained strength. However, Makdisi and Seed (1978) point out that substantial permanent strains may be produced by cyclic loading of clay soils to stresses near the yield stress, while essentially elastic behavior is observed for large numbers of (>100) cycles of loading at cyclic shear stresses of up to 80 percent of the undrained strength. Therefore, these investigators recommend the use of 80 percent of the undrained strength as the "dynamic yield strength" for soils that exhibit small increases in pore pressure during cyclic loading, such as clayey materials, and partially saturated cohesionless soils.

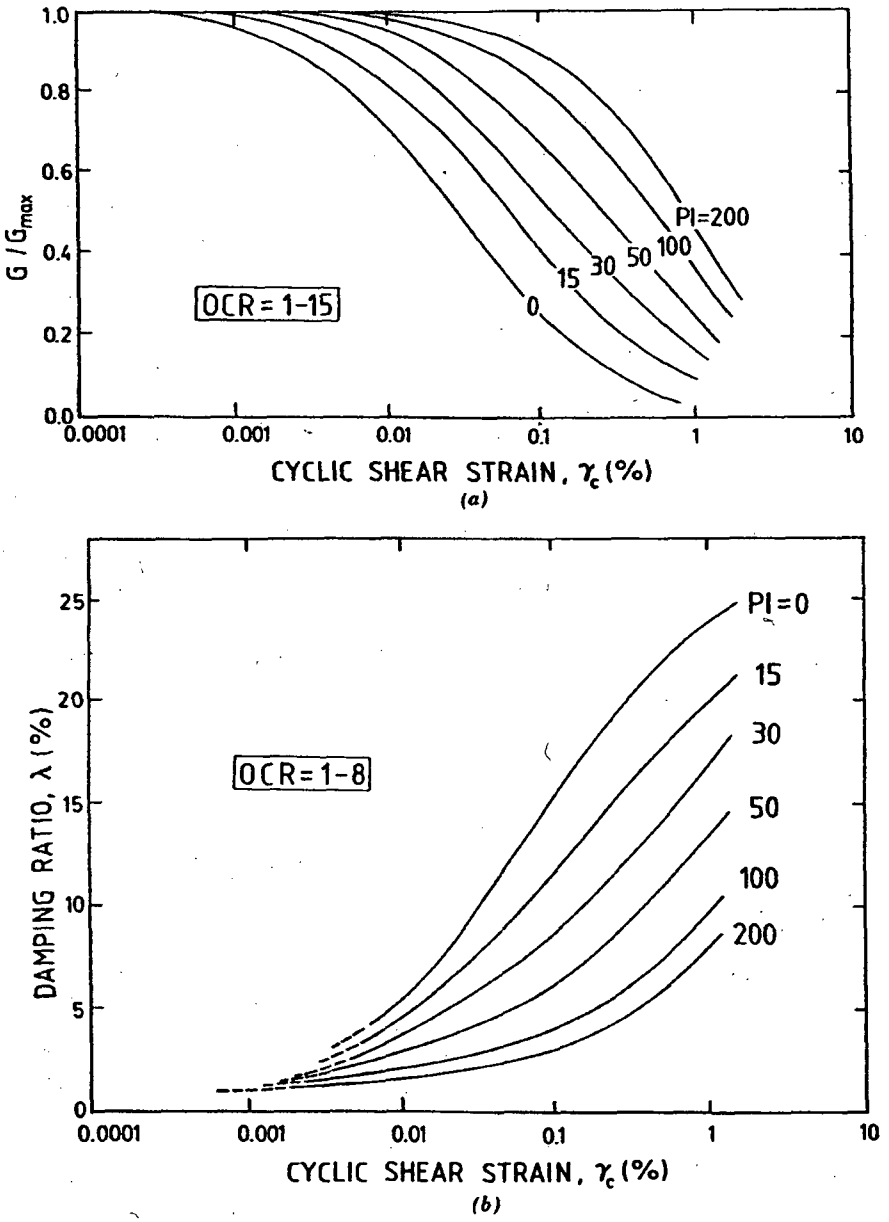

Figure 43. Shear modulus reduction and damping ratio as a function of shear strain and soil plasticity index (Vucetic and Dobry, 1991, reprinted by permission of ASCE).

Evaluation of the potential for shear strength reduction in a saturated or almost saturated cohesionless soil (low plasticity silt, sand, or gravel) subjected to dynamic loading may require sophisticated cyclic laboratory testing. Alternatively, a residual strength may be assigned to the soil based upon either undrained laboratory tests or in situ test results.

The residual shear strength after cyclic loading is of critical importance in assessing the post-liquefaction stability of a foundation or earth structure. Saturated soils which liquefy typically possess some "residual" shear strength even when in the liquefied state. In initially loose soils, this residual strength may be very small and of little consequence. In initially dense soils, particularly in dense granular soils which tend to dilate, or expand in volume, when sheared, this residual strength can be significant and of great consequence in acting as a stabilizing force subsequent to liquefaction.

Evaluation of residual shear strength from laboratory tests is not typically recommended due to the difficulties associated with testing. Use of residual strengths derived from in situ testing is, in general, considered more reliable than use of laboratory test results. However, use of residual strengths in assessments of the pseudo-static factor of safety and/or yield acceleration can result in very conservative values (Marcuson et al., 1990), as discussed in chapter 7.

The *steady-state* shear strength, S_{su}, governs the behavior of liquefied soil. Poulos et al. (1985) proposed a methodology for evaluation of the in situ S_{su} based on obtaining high-quality soil samples with minimal disturbance. The high-quality samples were tested in the laboratory and the laboratory strengths were then adjusted for field conditions using specially developed techniques to correct the resulting laboratory S_{su} values for effects of void ratio changes due to sampling, handling, and test set-up. Due to the very high sensitivity of S_{su} to even small changes in void ratio, the laboratory techniques proposed by Poulos et al. presently do not appear to represent a reliable basis for engineering analyses unless very conservative assumptions and high factors of safety are employed to account for the considerable uncertainties involved.

Because of difficulties in measuring steady-state strength in laboratory, Seed (1987) proposed an alternate technique for evaluation of in situ undrained residual shear strength based on the results of SPT testing. He back analyzed a number of liquefaction-induced failures from which residual strength could be calculated for soil zones in which SPT data was available, and proposed a correlation between *residual strength*, S_r, and $(N_1)_{60\text{-}cs}$. $(N_1)_{60\text{-}cs}$ is a "corrected" normalized standardized SPT blow count, as discussed in chapter 5.4.2.1, with a correction, N_{corr}, for fines content to generate an equivalent "clean sand" blow count as:

$$(N_1)_{60-cs} = (N_1)_{60} + N_{corr} \qquad (5\text{-}10)$$

where N_{corr} is a function of percent of fines. Recommendations for selecting N_{corr} are given in the insert of figure 44. Since there is no guarantee that all the conditions for steady-state of deformation were satisfied in the case histories used to develop figure 44, the term residual strength is used instead of steady-strength strength. Note that the fines correction on figure 44 is <u>not</u> the same "fines" correction as is used in the liquefaction susceptibility analyses (see, e.g., figure 58).

Figure 44 presents an updated and revised version of the Seed (1987) residual shear strength correlation developed by Seed and Harder (1990). Due to scatter and uncertainty and the limited number of case studies back analyzed to date, it is recommended that the lower-bound curve and the average $(N_1)_{60\text{-}cs}$ from all borings be used to estimate S_r. If lower bound, rather than average, $(N_1)_{60\text{-}cs}$ values are used, S_r may reasonably be estimated based upon the average of the lower and upper bound curves in figure 44.

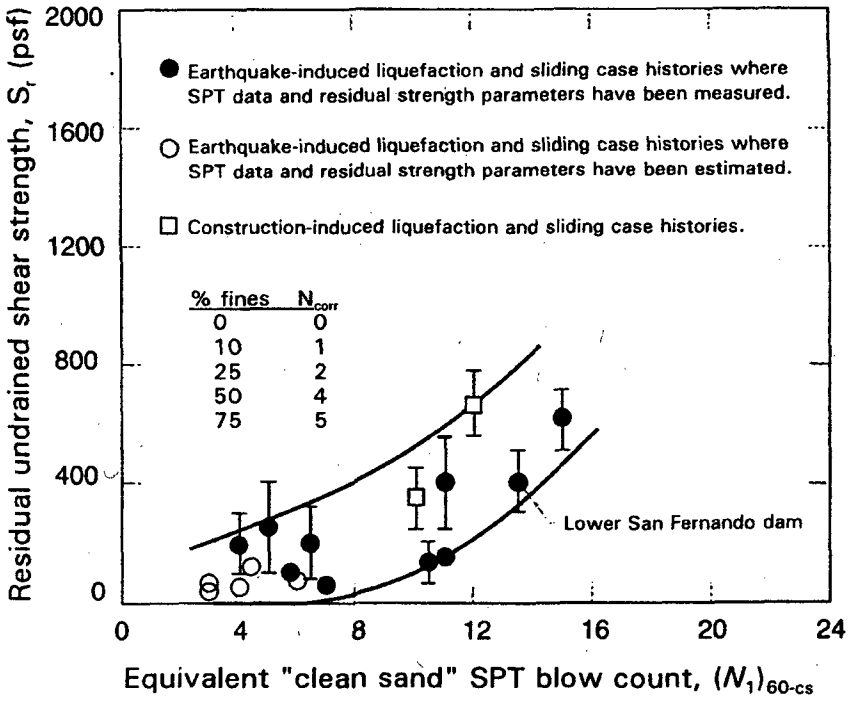

Figure 44. Relationship between corrected "clean sand" blow count $(N_1)_{60\text{-}cs}$ and undrained residual strength (S_r) from case studies (Seed and Harder, 1990).

ATTACHMENT I
Settlement Calculations

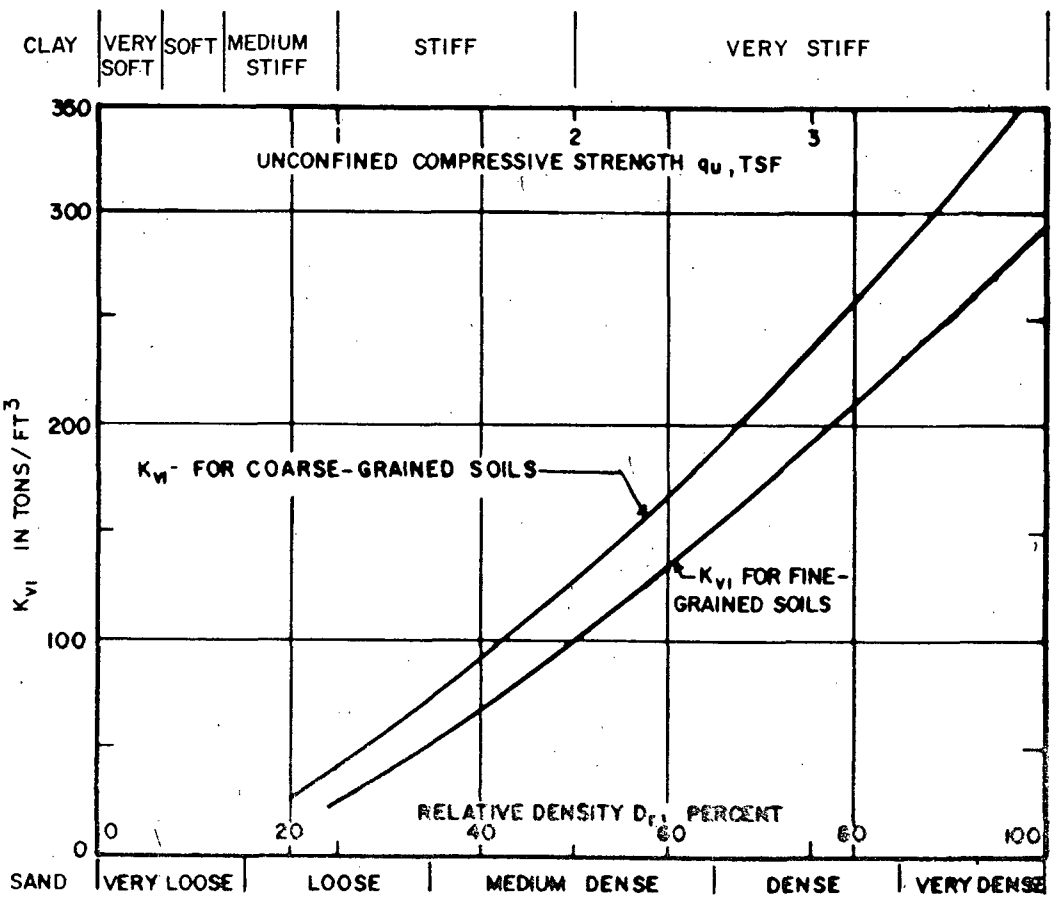

DEFINITIONS

ΔH_i = IMMEDIATE SETTLEMENT OF FOOTING

q = FOOTING UNIT LOAD IN tsf

B = FOOTING WIDTH

D = DEPTH OF FOOTING BELOW GROUND SURFACE

K_{v1} = MODULUS OF VERTICAL SUBGRADE REACTION

COARSE-GRAINED SOILS

(MODULUS OF ELASTICITY INCREASING LINEARLY WITH DEPTH)

SHALLOW FOOTINGS $D \leq B$

FOR $B \leq 20$ FT:

$$\Delta H_i = \frac{4\, q\, B^2}{K_{v1}\,(B+1)^2}$$

FOR $B \geq 40$ FT:

$$\Delta H_i = \frac{2\, q\, B^2}{K_{v1}\,(B+1)^2}$$

INTERPOLATE FOR INTERMEDIATE VALUES OF B

DEEP FOUNDATION $D \geq 5B$

FOR $B \leq 20$ FT:

$$\Delta H_i = \frac{2\, q\, B^2}{K_{v1}\,(B+1)^2}$$

NOTES: 1. NONPLASTIC SILT IS ANALYZED AS COARSE-GRAINED SOIL WITH MODULUS OF ELASTICITY INCREASING LINEARLY WITH DEPTH.

2. VALUES OF K_{v1} SHOWN FOR COARSE-GRAINED SOILS APPLY TO DRY OR MOIST MATERIAL WITH THE GROUNDWATER LEVEL AT A DEPTH OF AT LEAST 1.5B BELOW BASE OF FOOTING. IF GROUNDWATER IS AT BASE OF FOOTING, USE $K_{v1}/2$ IN COMPUTING SETTLEMENT

3. FOR CONTINUOUS FOOTINGS MULTIPLY THE SETTLEMENT COMPUTED FOR WIDTH "B" BY 2.

FIGURE 6

Instantaneous Settlement of Isolated Footings on Coarse-Grained Soils

SHEET NO. 1 OF

PROJECT NO.

DATE 8/1/09

BY SL

CHK'D CMJ

SUBJECT SMC DECOMMISSIONING

SETTLEMENT CALCULATIONS

RELATIVE DENSITY - D_r = 60%

K_{V1} - MODULUS OF VERTICAL SUBGRADE REACTION (FIG 6)
= 125 TONS/FT^2

q = FOOTING UNIT LOAD (tsf) = 1.875 tsf

B = FOOTING WIDTH = 170 ft.

ΔH_i = IMMEDIATE SETTLEMENT

$$\Delta H_i = \frac{2qB^2}{\frac{K_{V1}}{2}(B+1)^2}$$

$$\Delta H_i = \frac{2(1875)(170)^2}{\frac{125}{2}(170+1)^2} = 0.059 \text{ ft}$$

FOR CONTINUOUS FOOTING MULTIPLY RESULT BY 2

ΔH_i = 0.059 ft x 2 = 0.12 ft

ΔH_i = 1.4 inches

A

ATTACHMENT J
Static Stability Model Analyses

JANBU #1 STATIC CIRCULAR

Geometry and Boundary Conditions

Problem: SMC Newfield Decommissioning - Section A-A' - FS Min = 2.225

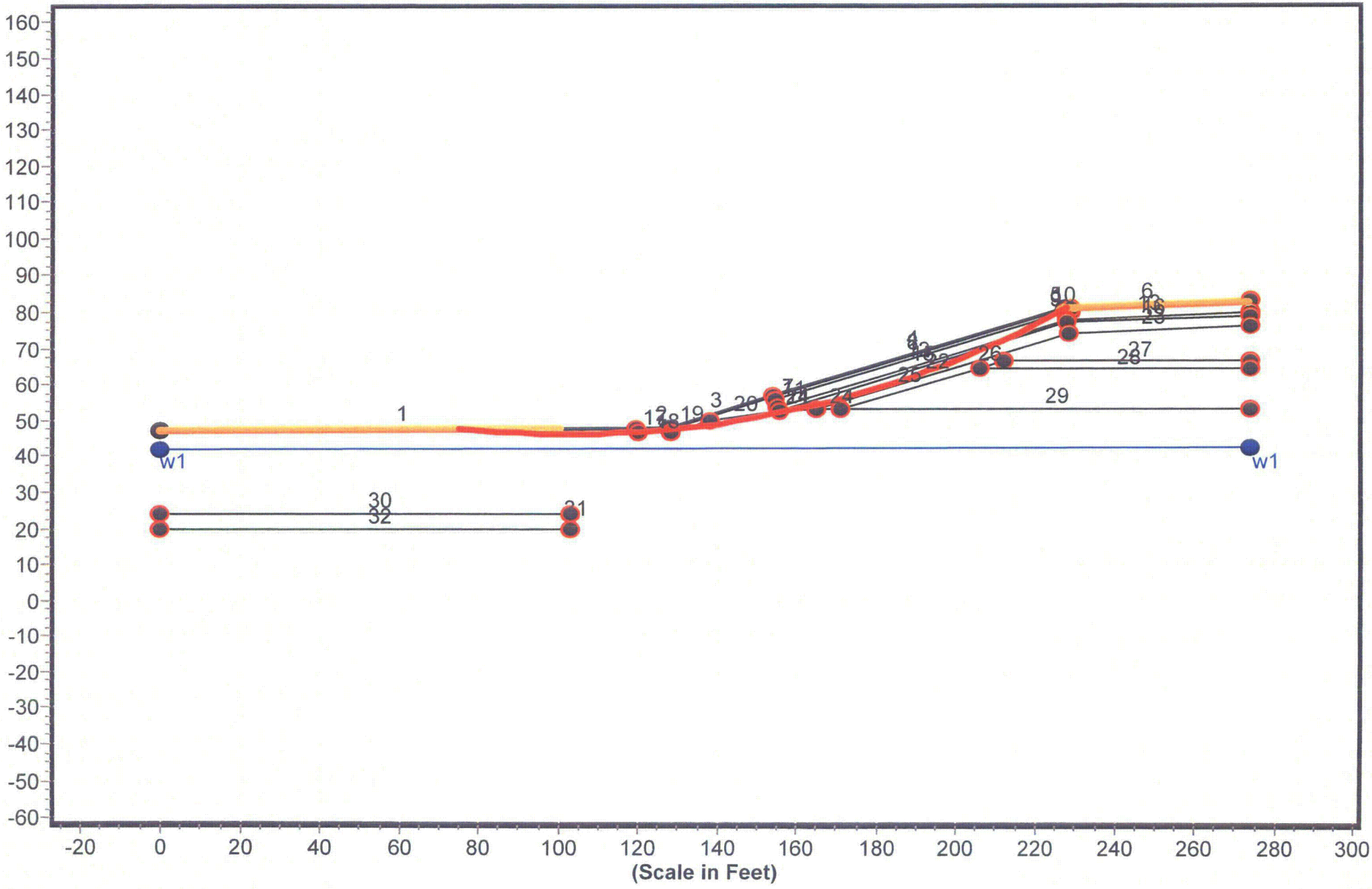

Geometry and Boundary Conditions

Problem: SMC Newfield Decommissioning - Section A-A' - FS Min = 2.225

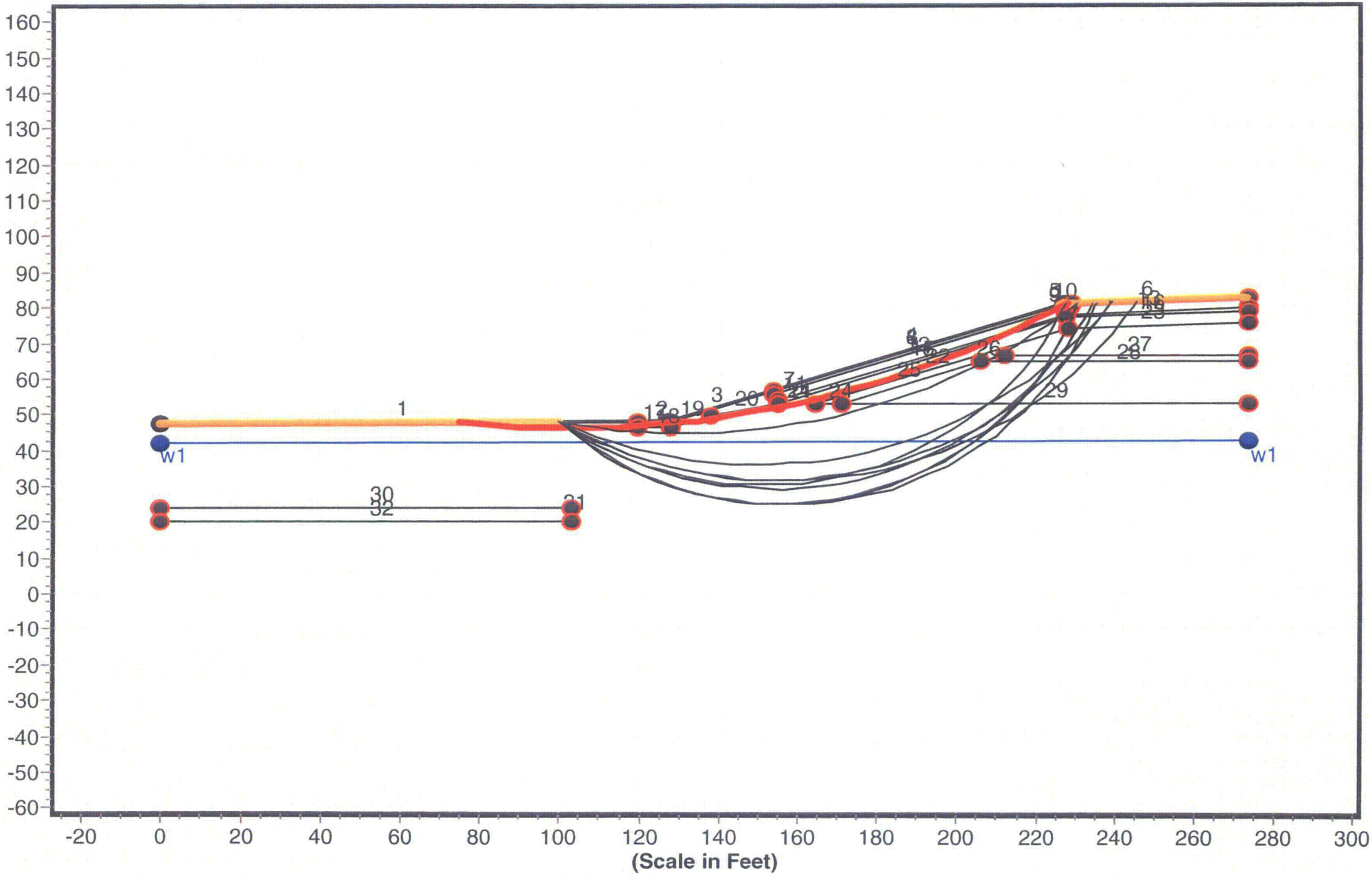

Geometry and Boundary Conditions
Problem: SMC Newfield Decommissioning - Section A-A' - FS Min = 2.225

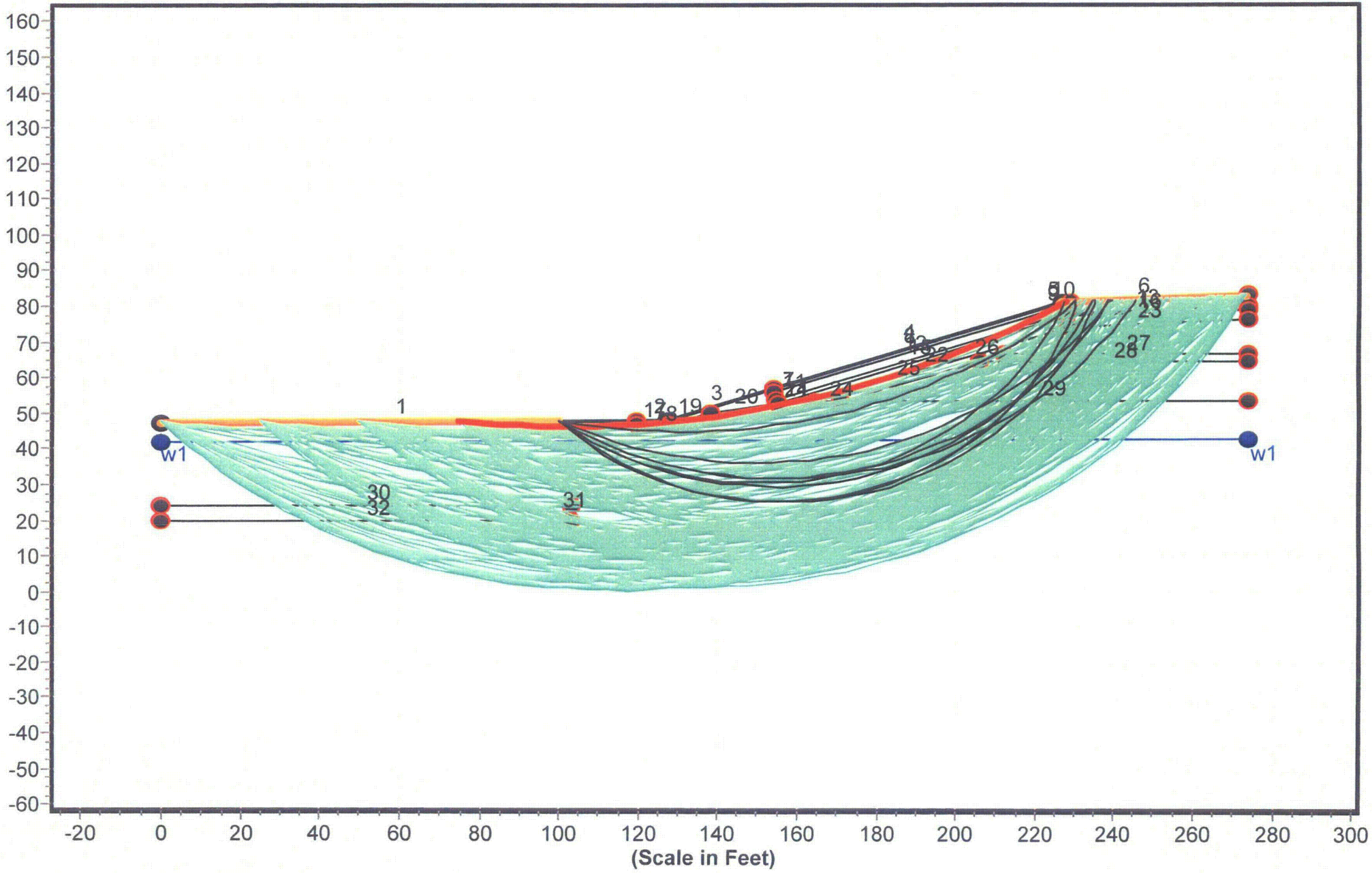

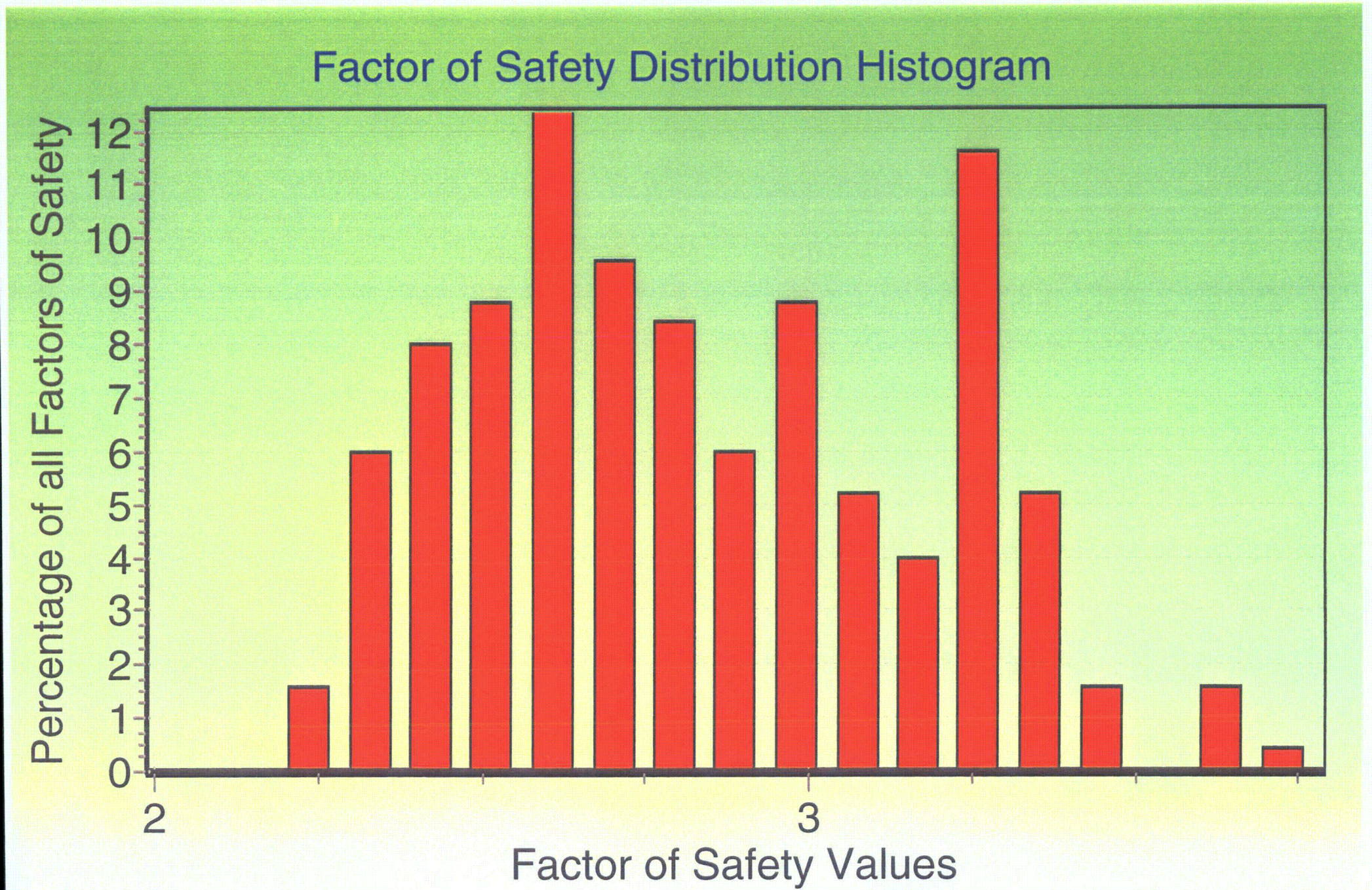
Factor of Safety Distribution Histogram
Percentage of all Factors of Safety
0
1
2
3
4
5
6
7
8
9
10
11
12
2
3
Factor of Safety Values

Janbu Circular #1 Results.txt
** PCSTABL6 **

by
Purdue University

1

--Slope Stability Analysis--
Simplified Janbu, Simplified Bishop
or Spencer's Method of Slices

Run Date:
Time of Run:
Run By:
Input Data Filename: run.in
Output Filename: result.out
Unit: ENGLISH
Plotted Output Filename: result.plt

PROBLEM DESCRIPTION SMC Newfield Decommissioning - Section A -A'

BOUNDARY COORDINATES

6 Top Boundaries
32 Total Boundaries

Boundary No.	X-Left (ft)	Y-Left (ft)	X-Right (ft)	Y-Right (ft)	Soil Type Below Bnd
1	0.00	47.40	119.50	48.00	7
2	119.50	48.00	127.50	48.00	1
3	127.50	48.00	153.90	56.80	1
4	153.90	56.80	226.90	81.10	1
5	226.90	81.10	228.90	81.20	1
6	228.90	81.20	273.60	83.00	2
7	153.90	56.80	154.20	55.80	1
8	154.20	55.80	227.10	80.10	2
9	227.10	80.10	228.80	80.20	2
10	228.80	80.20	228.90	81.20	2
11	154.20	55.80	154.80	53.90	1
12	154.80	53.90	227.40	78.10	1
13	227.40	78.10	273.60	80.00	1
14	154.80	53.90	155.20	52.60	1
15	155.20	52.60	227.60	77.10	3
16	227.60	77.10	273.60	79.00	3
17	119.50	48.00	119.60	46.40	7
18	119.60	46.40	127.80	46.40	7
19	127.80	46.40	137.90	49.80	7
20	137.90	49.80	155.20	52.60	7
21	155.20	52.60	164.60	53.00	7
22	164.60	53.00	228.20	74.10	4
23	228.20	74.10	273.60	76.00	4
24	164.60	53.00	171.00	53.00	7
25	171.00	53.00	205.80	64.60	6
26	205.80	64.60	211.80	66.60	5

27	211.80	66.60	273.60	66.60	5
28	205.80	64.60	273.60	64.60	6
29	171.00	53.00	273.60	53.00	7
30	0.00	24.00	103.10	24.00	8
31	103.00	20.00	103.10	24.00	7
32	0.00	20.00	103.10	20.00	7

1

ISOTROPIC SOIL PARAMETERS

8 Type(s) of Soil

Soil Type No.	Total Unit Wt. (pcf)	Saturated Unit Wt. (pcf)	Cohesion Intercept (psf)	Friction Angle (deg)	Pore Pressure Param.	Pressure Constant (psf)	Piez. Surface No.
1	135.0	140.0	0.0	40.0	0.00	0.0	0
2	135.0	140.0	0.0	35.0	0.00	0.0	0
3	125.0	130.0	250.0	15.0	0.00	0.0	0
4	125.0	135.0	0.0	32.0	0.00	0.0	0
5	135.0	140.0	0.0	38.0	0.00	0.0	0
6	135.0	140.0	0.0	40.0	0.00	0.0	0
7	115.0	130.0	0.0	33.0	0.00	0.0	1
8	130.0	140.0	300.0	20.0	0.00	0.0	1

1

1 PIEZOMETRIC SURFACE(S) HAVE BEEN SPECIFIED

Unit Weight of Water = 62.40

Piezometric Surface No. 1 Specified by 2 Coordinate Points

Point No.	X-Water (ft)	Y-Water (ft)
1	0.00	41.70
2	273.60	42.50

1

A Critical Failure Surface Searching Method, Using A Random Technique For Generating Circular Surfaces, Has Been Specified.

250 Trial Surfaces Have Been Generated.

50 Surfaces Initiate From Each Of 5 Points Equally Spaced Along The Ground Surface Between X = 0.00 ft.
and X = 100.00 ft.

Each Surface Terminates Between X = 226.00 ft.
and X = 273.00 ft.

Unless Further Limitations Were Imposed, The Minimum Elevation At Which A Surface Extends Is Y = 0.00 ft.

5.00 ft. Line Segments Define Each Trial Failure Surface.

Restrictions Have Been Imposed Upon The Angle Of Initiation. The Angle Has Been Restricted Between The Angles Of -45.0 And -5.0 deg.

1

Following Are Displayed The Ten Most Critical Of The Trial Failure Surfaces Examined. They Are Ordered - Most Critical First.

* * Safety Factors Are Calculated By The Modified Janbu Method * *

Failure Surface Specified By 33 Coordinate Points

Point No.	X-Surf (ft)	Y-Surf (ft)
1	75.00	47.78
2	79.97	47.25
3	84.96	46.84
4	89.95	46.52
5	94.94	46.31
6	99.94	46.20
7	104.94	46.20
8	109.94	46.30
9	114.93	46.50
10	119.93	46.81
11	124.91	47.22
12	129.88	47.73
13	134.84	48.35
14	139.79	49.07
15	144.72	49.89
16	149.64	50.81
17	154.53	51.84
18	159.40	52.97
19	164.25	54.19
20	169.07	55.52
21	173.86	56.95
22	178.62	58.48
23	183.35	60.10
24	188.04	61.83
25	192.70	63.65
26	197.32	65.56
27	201.90	67.57
28	206.43	69.68
29	210.92	71.88
30	215.37	74.17
31	219.76	76.56
32	224.10	79.03
33	227.62	81.14

*** 2.225 ***

Individual data on the 46 slices

Slice No.	Width (ft)	Weight (lbs)	Water Force Top (lbs)	Water Force Bot (lbs)	Force Norm (lbs)	Force Tan (lbs)	Earthquake Force Hor (lbs)	Earthquake Force Ver (lbs)	Surcharge Load (lbs)
1	5.0	156.4	0.0	0.0	0.0	0.0	0.0	0.0	0.0
2	5.0	440.4	0.0	0.0	0.0	0.0	0.0	0.0	0.0
3	5.0	666.0	0.0	0.0	0.0	0.0	0.0	0.0	0.0
4	5.0	832.5	0.0	0.0	0.0	0.0	0.0	0.0	0.0
5	5.0	939.3	0.0	0.0	0.0	0.0	0.0	0.0	0.0
6	5.0	986.2	0.0	0.0	0.0	0.0	0.0	0.0	0.0
7	5.0	973.0	0.0	0.0	0.0	0.0	0.0	0.0	0.0
8	5.0	899.8	0.0	0.0	0.0	0.0	0.0	0.0	0.0
9	4.6	707.8	0.0	0.0	0.0	0.0	0.0	0.0	0.0
10	0.1	11.5	0.0	0.0	0.0	0.0	0.0	0.0	0.0
11	0.3	56.8	0.0	0.0	0.0	0.0	0.0	0.0	0.0
12	5.0	664.6	0.0	0.0	0.0	0.0	0.0	0.0	0.0
13	2.6	227.1	0.0	0.0	0.0	0.0	0.0	0.0	0.0
14	2.4	253.8	0.0	0.0	0.0	0.0	0.0	0.0	0.0
15	3.0	549.9	0.0	0.0	0.0	0.0	0.0	0.0	0.0
16	2.0	501.3	0.0	0.0	0.0	0.0	0.0	0.0	0.0
17	3.1	941.3	0.0	0.0	0.0	0.0	0.0	0.0	0.0
18	1.9	689.9	0.0	0.0	0.0	0.0	0.0	0.0	0.0
19	4.9	2190.0	0.0	0.0	0.0	0.0	0.0	0.0	0.0
20	4.9	2698.9	0.0	0.0	0.0	0.0	0.0	0.0	0.0
21	4.3	2712.2	0.0	0.0	0.0	0.0	0.0	0.0	0.0
22	0.3	203.0	0.0	0.0	0.0	0.0	0.0	0.0	0.0
23	0.3	226.1	0.0	0.0	0.0	0.0	0.0	0.0	0.0
24	0.3	184.5	0.0	0.0	0.0	0.0	0.0	0.0	0.0
25	0.4	276.9	0.0	0.0	0.0	0.0	0.0	0.0	0.0
26	3.2	2307.2	0.0	0.0	0.0	0.0	0.0	0.0	0.0
27	1.0	741.6	0.0	0.0	0.0	0.0	0.0	0.0	0.0
28	4.8	3772.1	0.0	0.0	0.0	0.0	0.0	0.0	0.0
29	4.8	3949.6	0.0	0.0	0.0	0.0	0.0	0.0	0.0
30	4.8	4057.6	0.0	0.0	0.0	0.0	0.0	0.0	0.0
31	4.8	4097.3	0.0	0.0	0.0	0.0	0.0	0.0	0.0
32	4.7	4069.8	0.0	0.0	0.0	0.0	0.0	0.0	0.0
33	4.7	3976.3	0.0	0.0	0.0	0.0	0.0	0.0	0.0
34	4.7	3818.6	0.0	0.0	0.0	0.0	0.0	0.0	0.0
35	4.6	3598.2	0.0	0.0	0.0	0.0	0.0	0.0	0.0
36	4.6	3317.1	0.0	0.0	0.0	0.0	0.0	0.0	0.0
37	4.5	2977.4	0.0	0.0	0.0	0.0	0.0	0.0	0.0
38	1.7	1015.4	0.0	0.0	0.0	0.0	0.0	0.0	0.0
39	2.8	1560.2	0.0	0.0	0.0	0.0	0.0	0.0	0.0
40	4.0	1897.2	0.0	0.0	0.0	0.0	0.0	0.0	0.0
41	0.5	198.1	0.0	0.0	0.0	0.0	0.0	0.0	0.0
42	4.4	1557.7	0.0	0.0	0.0	0.0	0.0	0.0	0.0
43	4.3	967.9	0.0	0.0	0.0	0.0	0.0	0.0	0.0
44	0.3	38.3	0.0	0.0	0.0	0.0	0.0	0.0	0.0
45	2.5	250.8	0.0	0.0	0.0	0.0	0.0	0.0	0.0
46	0.7	19.3	0.0	0.0	0.0	0.0	0.0	0.0	0.0

Failure Surface Specified By 33 Coordinate Points

Point No.	X-Surf (ft)	Y-Surf (ft)
1	100.00	47.90
2	104.02	44.93
3	108.20	42.19
4	112.54	39.69
5	117.00	37.45
6	121.59	35.46
7	126.29	33.74
8	131.07	32.29
9	135.93	31.12
10	140.85	30.22
11	145.81	29.61
12	150.80	29.28
13	155.80	29.24
14	160.80	29.48
15	165.77	30.00
16	170.70	30.81
17	175.58	31.90
18	180.39	33.27
19	185.12	34.91
20	189.74	36.81
21	194.25	38.98
22	198.62	41.40
23	202.85	44.06
24	206.92	46.96
25	210.82	50.09
26	214.54	53.44
27	218.06	56.99
28	221.36	60.74
29	224.45	64.67
30	227.31	68.78
31	229.94	73.03
32	232.31	77.43
33	234.17	81.41

*** 2.259 ***

1

Failure Surface Specified By 32 Coordinate Points

Point No.	X-Surf (ft)	Y-Surf (ft)
1	100.00	47.90
2	104.03	44.94
3	108.23	42.23
4	112.59	39.77
5	117.08	37.59
6	121.70	35.68
7	126.43	34.05
8	131.25	32.71
9	136.14	31.67
10	141.08	30.92
11	146.06	30.47
12	151.06	30.32

13	156.06	30.48
14	161.04	30.93
15	165.98	31.69
16	170.87	32.75
17	175.68	34.09
18	180.41	35.73
19	185.02	37.65
20	189.52	39.84
21	193.87	42.30
22	198.06	45.02
23	202.09	47.99
24	205.93	51.19
25	209.56	54.63
26	212.98	58.27
27	216.18	62.12
28	219.14	66.15
29	221.85	70.35
30	224.30	74.71
31	226.48	79.21
32	227.27	81.12

*** 2.261 ***

Failure Surface Specified By 34 Coordinate Points

Point No.	X-Surf (ft)	Y-Surf (ft)
1	100.00	47.90
2	104.22	45.23
3	108.58	42.77
4	113.06	40.55
5	117.65	38.56
6	122.33	36.81
7	127.10	35.30
8	131.94	34.04
9	136.83	33.04
10	141.78	32.29
11	146.75	31.79
12	151.75	31.55
13	156.75	31.57
14	161.74	31.85
15	166.71	32.39
16	171.65	33.18
17	176.54	34.23
18	181.36	35.53
19	186.12	37.08
20	190.79	38.87
21	195.36	40.89
22	199.82	43.16
23	204.15	45.65
24	208.36	48.36
25	212.41	51.28
26	216.31	54.41
27	220.04	57.74
28	223.60	61.25
29	226.97	64.94
30	230.14	68.81

31	233.11	72.83
32	235.87	77.00
33	238.41	81.31
34	238.56	81.59

*** 2.269 ***

1

Failure Surface Specified By 33 Coordinate Points

Point No.	X-Surf (ft)	Y-Surf (ft)
1	100.00	47.90
2	104.50	45.72
3	109.10	43.75
4	113.78	41.99
5	118.53	40.45
6	123.35	39.13
7	128.23	38.02
8	133.15	37.14
9	138.11	36.49
10	143.09	36.06
11	148.09	35.86
12	153.09	35.89
13	158.08	36.15
14	163.06	36.63
15	168.01	37.34
16	172.92	38.28
17	177.78	39.44
18	182.59	40.82
19	187.33	42.41
20	191.99	44.23
21	196.56	46.25
22	201.03	48.48
23	205.40	50.91
24	209.66	53.54
25	213.79	56.36
26	217.78	59.36
27	221.64	62.54
28	225.34	65.90
29	228.89	69.42
30	232.28	73.10
31	235.49	76.93
32	238.53	80.91
33	239.01	81.61

*** 2.287 ***

Failure Surface Specified By 34 Coordinate Points

Point No.	X-Surf (ft)	Y-Surf (ft)

1	100.00	47.90
2	103.65	44.49
3	107.51	41.31
4	111.57	38.39
5	115.80	35.73
6	120.20	33.35
7	124.74	31.25
8	129.40	29.45
9	134.17	27.95
10	139.03	26.76
11	143.95	25.88
12	148.92	25.32
13	153.92	25.08
14	158.91	25.15
15	163.90	25.55
16	168.85	26.26
17	173.74	27.29
18	178.56	28.63
19	183.28	30.28
20	187.89	32.22
21	192.36	34.46
22	196.68	36.97
23	200.83	39.76
24	204.80	42.80
25	208.56	46.10
26	212.10	49.63
27	215.41	53.37
28	218.48	57.32
29	221.28	61.46
30	223.82	65.77
31	226.07	70.23
32	228.04	74.83
33	229.70	79.55
34	230.19	81.25

*** 2.298 ***

1

Failure Surface Specified By 35 Coordinate Points

Point No.	X-Surf (ft)	Y-Surf (ft)
1	100.00	47.90
2	103.70	44.53
3	107.59	41.40
4	111.67	38.51
5	115.92	35.87
6	120.32	33.49
7	124.85	31.39
8	129.51	29.57
9	134.27	28.04
10	139.11	26.80
11	144.02	25.86
12	148.98	25.22
13	153.97	24.88
14	158.97	24.85

15	163.96	25.12
16	168.93	25.70
17	173.85	26.57
18	178.71	27.75
19	183.49	29.22
20	188.17	30.98
21	192.73	33.03
22	197.16	35.34
23	201.45	37.93
24	205.56	40.77
25	209.50	43.85
26	213.23	47.17
27	216.76	50.71
28	220.07	54.46
29	223.14	58.41
30	225.97	62.54
31	228.54	66.83
32	230.84	71.26
33	232.86	75.83
34	234.61	80.52
35	234.89	81.44

*** 2.299 ***

Failure Surface Specified By 34 Coordinate Points

Point No.	X-Surf (ft)	Y-Surf (ft)
1	100.00	47.90
2	103.64	44.47
3	107.49	41.29
4	111.54	38.35
5	115.77	35.68
6	120.16	33.29
7	124.69	31.18
8	129.35	29.36
9	134.12	27.85
10	138.97	26.65
11	143.89	25.76
12	148.86	25.19
13	153.85	24.93
14	158.85	25.00
15	163.83	25.39
16	168.78	26.09
17	173.68	27.11
18	178.50	28.44
19	183.22	30.08
20	187.83	32.02
21	192.31	34.24
22	196.63	36.75
23	200.79	39.54
24	204.76	42.58
25	208.52	45.87
26	212.07	49.39
27	215.38	53.13
28	218.45	57.08
29	221.26	61.22

30	223.80	65.53
31	226.06	69.99
32	228.02	74.59
33	229.69	79.30
34	230.24	81.25

*** 2.300 ***

1

Failure Surface Specified By 29 Coordinate Points

Point No.	X-Surf (ft)	Y-Surf (ft)
1	100.00	47.90
2	104.91	46.94
3	109.84	46.14
4	114.80	45.51
5	119.78	45.04
6	124.77	44.73
7	129.77	44.59
8	134.77	44.62
9	139.77	44.80
10	144.75	45.16
11	149.73	45.68
12	154.68	46.36
13	159.61	47.21
14	164.50	48.21
15	169.37	49.38
16	174.19	50.71
17	178.96	52.20
18	183.68	53.85
19	188.35	55.65
20	192.95	57.60
21	197.48	59.70
22	201.95	61.95
23	206.34	64.35
24	210.64	66.89
25	214.86	69.58
26	218.99	72.40
27	223.02	75.35
28	226.96	78.44
29	230.31	81.26

*** 2.308 ***

Failure Surface Specified By 35 Coordinate Points

Point No.	X-Surf (ft)	Y-Surf (ft)
1	100.00	47.90
2	104.28	45.31

3	108.67	42.92
4	113.17	40.75
5	117.78	38.80
6	122.47	37.07
7	127.24	35.57
8	132.07	34.29
9	136.96	33.26
10	141.90	32.46
11	146.87	31.89
12	151.86	31.57
13	156.86	31.48
14	161.85	31.64
15	166.84	32.04
16	171.80	32.67
17	176.72	33.54
18	181.60	34.65
19	186.41	35.99
20	191.16	37.56
21	195.83	39.36
22	200.40	41.38
23	204.87	43.61
24	209.23	46.06
25	213.47	48.72
26	217.57	51.57
27	221.54	54.62
28	225.35	57.86
29	229.00	61.27
30	232.48	64.86
31	235.79	68.61
32	238.91	72.51
33	241.85	76.56
34	244.58	80.75
35	245.23	81.86

*** 2.313 ***

1

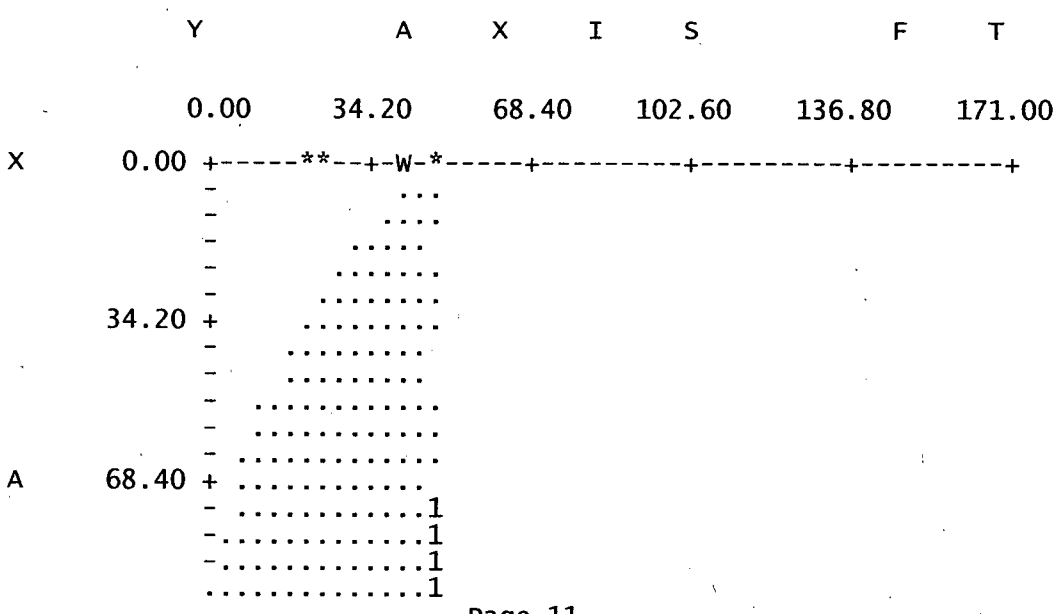

```
                 .............1
X     102.60     ......**.....21
                 ............241
                 ..........66291
                 ..........2259*
                 .........625.9*
                 .........235.91
I     136.80     ........6245.91*
                 ........62.5.911
                 .......6.25..9.1
                 -......6.25...9***
                 -......6.2.5..91
                 -......6.2.5..9*1
S     171.00   + ......6235..9*1
               - ......623.5..9.1
               - .......6235...9.1
               -  ......6.23...9.1
               -  .......62355..9.1
               -   ......76233..9911
      205.20   +    .......7223...*1
               -     .......64233.*91
               -      ........72233991
               -      .........7422.311
               -        ........07422***
               -         .........004522
F     239.40   +          ..........00.4
               -            ...........0
               -             ...........
               -               .........
               -                 .......
               -                   ....
T     273.60   +          W  *   *  ***
```

Janbu Circular #1 Results.txt
** PCSTABL6 **

by
Purdue University

1

--Slope Stability Analysis--
Simplified Janbu, Simplified Bishop
or Spencer's Method of Slices

Run Date:
Time of Run:
Run By:
Input Data Filename: run.in
Output Filename: result.out
Unit: ENGLISH
Plotted Output Filename: result.plt

PROBLEM DESCRIPTION SMC Newfield Decommissioning - Section A -A'

BOUNDARY COORDINATES

6 Top Boundaries
32 Total Boundaries

Boundary No.	X-Left (ft)	Y-Left (ft)	X-Right (ft)	Y-Right (ft)	Soil Type Below Bnd
1	0.00	47.40	119.50	48.00	7
2	119.50	48.00	127.50	48.00	1
3	127.50	48.00	153.90	56.80	1
4	153.90	56.80	226.90	81.10	1
5	226.90	81.10	228.90	81.20	1
6	228.90	81.20	273.60	83.00	2
7	153.90	56.80	154.20	55.80	1
8	154.20	55.80	227.10	80.10	2
9	227.10	80.10	228.80	80.20	2
10	228.80	80.20	228.90	81.20	2
11	154.20	55.80	154.80	53.90	1
12	154.80	53.90	227.40	78.10	1
13	227.40	78.10	273.60	80.00	1
14	154.80	53.90	155.20	52.60	1
15	155.20	52.60	227.60	77.10	3
16	227.60	77.10	273.60	79.00	3
17	119.50	48.00	119.60	46.40	7
18	119.60	46.40	127.80	46.40	7
19	127.80	46.40	137.90	49.80	7
20	137.90	49.80	155.20	52.60	7
21	155.20	52.60	164.60	53.00	7
22	164.60	53.00	228.20	74.10	4
23	228.20	74.10	273.60	76.00	4
24	164.60	53.00	171.00	53.00	7
25	171.00	53.00	205.80	64.60	6
26	205.80	64.60	211.80	66.60	5

27	211.80	66.60	273.60	66.60	5
28	205.80	64.60	273.60	64.60	6
29	171.00	53.00	273.60	53.00	7
30	0.00	24.00	103.10	24.00	8
31	103.00	20.00	103.10	24.00	7
32	0.00	20.00	103.10	20.00	7

1

ISOTROPIC SOIL PARAMETERS

8 Type(s) of Soil

Soil Type No.	Total Unit Wt. (pcf)	Saturated Unit Wt. (pcf)	Cohesion Intercept (psf)	Friction Angle (deg)	Pore Pressure Param.	Pressure Constant (psf)	Piez. Surface No.
1	135.0	140.0	0.0	40.0	0.00	0.0	0
2	135.0	140.0	0.0	35.0	0.00	0.0	0
3	125.0	130.0	250.0	15.0	0.00	0.0	0
4	125.0	135.0	0.0	32.0	0.00	0.0	0
5	135.0	140.0	0.0	38.0	0.00	0.0	0
6	135.0	140.0	0.0	40.0	0.00	0.0	0
7	115.0	130.0	0.0	33.0	0.00	0.0	1
8	130.0	140.0	300.0	20.0	0.00	0.0	1

1

1 PIEZOMETRIC SURFACE(S) HAVE BEEN SPECIFIED

Unit Weight of Water = 62.40

Piezometric Surface No. 1 Specified by 2 Coordinate Points

Point No.	X-Water (ft)	Y-Water (ft)
1	0.00	41.70
2	273.60	42.50

1

A Critical Failure Surface Searching Method, Using A Random Technique For Generating Circular Surfaces, Has Been Specified.

250 Trial Surfaces Have Been Generated.

50 Surfaces Initiate From Each Of 5 Points Equally Spaced Along The Ground Surface Between X = 0.00 ft.
and X = 100.00 ft.

Each Surface Terminates Between X = 226.00 ft.
and X = 273.00 ft.

Unless Further Limitations Were Imposed, The Minimum Elevation At Which A Surface Extends Is Y = 0.00 ft.

5.00 ft. Line Segments Define Each Trial Failure Surface.

Restrictions Have Been Imposed Upon The Angle Of Initiation. The Angle Has Been Restricted Between The Angles Of -45.0 And -5.0 deg.

1

Following Are Displayed The Ten Most Critical Of The Trial Failure Surfaces Examined. They Are Ordered - Most Critical First.

* * Safety Factors Are Calculated By The Modified Janbu Method * *

Failure Surface Specified By 33 Coordinate Points

Point No.	X-Surf (ft)	Y-Surf (ft)
1	75.00	47.78
2	79.97	47.25
3	84.96	46.84
4	89.95	46.52
5	94.94	46.31
6	99.94	46.20
7	104.94	46.20
8	109.94	46.30
9	114.93	46.50
10	119.93	46.81
11	124.91	47.22
12	129.88	47.73
13	134.84	48.35
14	139.79	49.07
15	144.72	49.89
16	149.64	50.81
17	154.53	51.84
18	159.40	52.97
19	164.25	54.19
20	169.07	55.52
21	173.86	56.95
22	178.62	58.48
23	183.35	60.10
24	188.04	61.83
25	192.70	63.65
26	197.32	65.56
27	201.90	67.57
28	206.43	69.68
29	210.92	71.88
30	215.37	74.17
31	219.76	76.56
32	224.10	79.03
33	227.62	81.14

*** 2.225 ***

Individual data on the 46 slices

Slice No.	Width (ft)	Weight (lbs)	Water Force Top (lbs)	Water Force Bot (lbs)	Force Norm (lbs)	Force Tan (lbs)	Earthquake Force Hor (lbs)	Earthquake Force Ver (lbs)	Surcharge Load (lbs)
1	5.0	156.4	0.0	0.0	0.0	0.0	0.0	0.0	0.0
2	5.0	440.4	0.0	0.0	0.0	0.0	0.0	0.0	0.0
3	5.0	666.0	0.0	0.0	0.0	0.0	0.0	0.0	0.0
4	5.0	832.5	0.0	0.0	0.0	0.0	0.0	0.0	0.0
5	5.0	939.3	0.0	0.0	0.0	0.0	0.0	0.0	0.0
6	5.0	986.2	0.0	0.0	0.0	0.0	0.0	0.0	0.0
7	5.0	973.0	0.0	0.0	0.0	0.0	0.0	0.0	0.0
8	5.0	899.8	0.0	0.0	0.0	0.0	0.0	0.0	0.0
9	4.6	707.8	0.0	0.0	0.0	0.0	0.0	0.0	0.0
10	0.1	11.5	0.0	0.0	0.0	0.0	0.0	0.0	0.0
11	0.3	56.8	0.0	0.0	0.0	0.0	0.0	0.0	0.0
12	5.0	664.6	0.0	0.0	0.0	0.0	0.0	0.0	0.0
13	2.6	227.1	0.0	0.0	0.0	0.0	0.0	0.0	0.0
14	2.4	253.8	0.0	0.0	0.0	0.0	0.0	0.0	0.0
15	3.0	549.9	0.0	0.0	0.0	0.0	0.0	0.0	0.0
16	2.0	501.3	0.0	0.0	0.0	0.0	0.0	0.0	0.0
17	3.1	941.3	0.0	0.0	0.0	0.0	0.0	0.0	0.0
18	1.9	689.9	0.0	0.0	0.0	0.0	0.0	0.0	0.0
19	4.9	2190.0	0.0	0.0	0.0	0.0	0.0	0.0	0.0
20	4.9	2698.9	0.0	0.0	0.0	0.0	0.0	0.0	0.0
21	4.3	2712.2	0.0	0.0	0.0	0.0	0.0	0.0	0.0
22	0.3	203.0	0.0	0.0	0.0	0.0	0.0	0.0	0.0
23	0.3	226.1	0.0	0.0	0.0	0.0	0.0	0.0	0.0
24	0.3	184.5	0.0	0.0	0.0	0.0	0.0	0.0	0.0
25	0.4	276.9	0.0	0.0	0.0	0.0	0.0	0.0	0.0
26	3.2	2307.2	0.0	0.0	0.0	0.0	0.0	0.0	0.0
27	1.0	741.6	0.0	0.0	0.0	0.0	0.0	0.0	0.0
28	4.8	3772.1	0.0	0.0	0.0	0.0	0.0	0.0	0.0
29	4.8	3949.6	0.0	0.0	0.0	0.0	0.0	0.0	0.0
30	4.8	4057.6	0.0	0.0	0.0	0.0	0.0	0.0	0.0
31	4.8	4097.3	0.0	0.0	0.0	0.0	0.0	0.0	0.0
32	4.7	4069.8	0.0	0.0	0.0	0.0	0.0	0.0	0.0
33	4.7	3976.3	0.0	0.0	0.0	0.0	0.0	0.0	0.0
34	4.7	3818.6	0.0	0.0	0.0	0.0	0.0	0.0	0.0
35	4.6	3598.2	0.0	0.0	0.0	0.0	0.0	0.0	0.0
36	4.6	3317.1	0.0	0.0	0.0	0.0	0.0	0.0	0.0
37	4.5	2977.4	0.0	0.0	0.0	0.0	0.0	0.0	0.0
38	1.7	1015.4	0.0	0.0	0.0	0.0	0.0	0.0	0.0
39	2.8	1560.2	0.0	0.0	0.0	0.0	0.0	0.0	0.0
40	4.0	1897.2	0.0	0.0	0.0	0.0	0.0	0.0	0.0
41	0.5	198.1	0.0	0.0	0.0	0.0	0.0	0.0	0.0
42	4.4	1557.7	0.0	0.0	0.0	0.0	0.0	0.0	0.0
43	4.3	967.9	0.0	0.0	0.0	0.0	0.0	0.0	0.0
44	0.3	38.3	0.0	0.0	0.0	0.0	0.0	0.0	0.0
45	2.5	250.8	0.0	0.0	0.0	0.0	0.0	0.0	0.0
46	0.7	19.3	0.0	0.0	0.0	0.0	0.0	0.0	0.0

Failure Surface Specified By 33 Coordinate Points

Point No.	X-Surf (ft)	Y-Surf (ft)
1	100.00	47.90
2	104.02	44.93
3	108.20	42.19
4	112.54	39.69
5	117.00	37.45
6	121.59	35.46
7	126.29	33.74
8	131.07	32.29
9	135.93	31.12
10	140.85	30.22
11	145.81	29.61
12	150.80	29.28
13	155.80	29.24
14	160.80	29.48
15	165.77	30.00
16	170.70	30.81
17	175.58	31.90
18	180.39	33.27
19	185.12	34.91
20	189.74	36.81
21	194.25	38.98
22	198.62	41.40
23	202.85	44.06
24	206.92	46.96
25	210.82	50.09
26	214.54	53.44
27	218.06	56.99
28	221.36	60.74
29	224.45	64.67
30	227.31	68.78
31	229.94	73.03
32	232.31	77.43
33	234.17	81.41

*** 2.259 ***

1

Failure Surface Specified By 32 Coordinate Points

Point No.	X-Surf (ft)	Y-Surf (ft)
1	100.00	47.90
2	104.03	44.94
3	108.23	42.23
4	112.59	39.77
5	117.08	37.59
6	121.70	35.68
7	126.43	34.05
8	131.25	32.71
9	136.14	31.67
10	141.08	30.92
11	146.06	30.47
12	151.06	30.32

13	156.06	30.48
14	161.04	30.93
15	165.98	31.69
16	170.87	32.75
17	175.68	34.09
18	180.41	35.73
19	185.02	37.65
20	189.52	39.84
21	193.87	42.30
22	198.06	45.02
23	202.09	47.99
24	205.93	51.19
25	209.56	54.63
26	212.98	58.27
27	216.18	62.12
28	219.14	66.15
29	221.85	70.35
30	224.30	74.71
31	226.48	79.21
32	227.27	81.12

*** 2.261 ***

Failure Surface Specified By 34 Coordinate Points

Point No.	X-Surf (ft)	Y-Surf (ft)
1	100.00	47.90
2	104.22	45.23
3	108.58	42.77
4	113.06	40.55
5	117.65	38.56
6	122.33	36.81
7	127.10	35.30
8	131.94	34.04
9	136.83	33.04
10	141.78	32.29
11	146.75	31.79
12	151.75	31.55
13	156.75	31.57
14	161.74	31.85
15	166.71	32.39
16	171.65	33.18
17	176.54	34.23
18	181.36	35.53
19	186.12	37.08
20	190.79	38.87
21	195.36	40.89
22	199.82	43.16
23	204.15	45.65
24	208.36	48.36
25	212.41	51.28
26	216.31	54.41
27	220.04	57.74
28	223.60	61.25
29	226.97	64.94
30	230.14	68.81

31	233.11	72.83
32	235.87	77.00
33	238.41	81.31
34	238.56	81.59

*** 2.269 ***

1

Failure Surface Specified By 33 Coordinate Points

Point No.	X-Surf (ft)	Y-Surf (ft)
1	100.00	47.90
2	104.50	45.72
3	109.10	43.75
4	113.78	41.99
5	118.53	40.45
6	123.35	39.13
7	128.23	38.02
8	133.15	37.14
9	138.11	36.49
10	143.09	36.06
11	148.09	35.86
12	153.09	35.89
13	158.08	36.15
14	163.06	36.63
15	168.01	37.34
16	172.92	38.28
17	177.78	39.44
18	182.59	40.82
19	187.33	42.41
20	191.99	44.23
21	196.56	46.25
22	201.03	48.48
23	205.40	50.91
24	209.66	53.54
25	213.79	56.36
26	217.78	59.36
27	221.64	62.54
28	225.34	65.90
29	228.89	69.42
30	232.28	73.10
31	235.49	76.93
32	238.53	80.91
33	239.01	81.61

*** 2.287 ***

Failure Surface Specified By 34 Coordinate Points

Point No.	X-Surf (ft)	Y-Surf (ft)

1	100.00	47.90
2	103.65	44.49
3	107.51	41.31
4	111.57	38.39
5	115.80	35.73
6	120.20	33.35
7	124.74	31.25
8	129.40	29.45
9	134.17	27.95
10	139.03	26.76
11	143.95	25.88
12	148.92	25.32
13	153.92	25.08
14	158.91	25.15
15	163.90	25.55
16	168.85	26.26
17	173.74	27.29
18	178.56	28.63
19	183.28	30.28
20	187.89	32.22
21	192.36	34.46
22	196.68	36.97
23	200.83	39.76
24	204.80	42.80
25	208.56	46.10
26	212.10	49.63
27	215.41	53.37
28	218.48	57.32
29	221.28	61.46
30	223.82	65.77
31	226.07	70.23
32	228.04	74.83
33	229.70	79.55
34	230.19	81.25

*** 2.298 ***

1

Failure Surface Specified By 35 Coordinate Points

Point No.	X-Surf (ft)	Y-Surf (ft)
1	100.00	47.90
2	103.70	44.53
3	107.59	41.40
4	111.67	38.51
5	115.92	35.87
6	120.32	33.49
7	124.85	31.39
8	129.51	29.57
9	134.27	28.04
10	139.11	26.80
11	144.02	25.86
12	148.98	25.22
13	153.97	24.88
14	158.97	24.85

15	163.96	25.12
16	168.93	25.70
17	173.85	26.57
18	178.71	27.75
19	183.49	29.22
20	188.17	30.98
21	192.73	33.03
22	197.16	35.34
23	201.45	37.93
24	205.56	40.77
25	209.50	43.85
26	213.23	47.17
27	216.76	50.71
28	220.07	54.46
29	223.14	58.41
30	225.97	62.54
31	228.54	66.83
32	230.84	71.26
33	232.86	75.83
34	234.61	80.52
35	234.89	81.44

*** 2.299 ***

Failure Surface Specified By 34 Coordinate Points

Point No.	X-Surf (ft)	Y-Surf (ft)
1	100.00	47.90
2	103.64	44.47
3	107.49	41.29
4	111.54	38.35
5	115.77	35.68
6	120.16	33.29
7	124.69	31.18
8	129.35	29.36
9	134.12	27.85
10	138.97	26.65
11	143.89	25.76
12	148.86	25.19
13	153.85	24.93
14	158.85	25.00
15	163.83	25.39
16	168.78	26.09
17	173.68	27.11
18	178.50	28.44
19	183.22	30.08
20	187.83	32.02
21	192.31	34.24
22	196.63	36.75
23	200.79	39.54
24	204.76	42.58
25	208.52	45.87
26	212.07	49.39
27	215.38	53.13
28	218.45	57.08
29	221.26	61.22

30	223.80	65.53
31	226.06	69.99
32	228.02	74.59
33	229.69	79.30
34	230.24	81.25

*** 2.300 ***

1

Failure Surface Specified By 29 Coordinate Points

Point No.	X-Surf (ft)	Y-Surf (ft)
1	100.00	47.90
2	104.91	46.94
3	109.84	46.14
4	114.80	45.51
5	119.78	45.04
6	124.77	44.73
7	129.77	44.59
8	134.77	44.62
9	139.77	44.80
10	144.75	45.16
11	149.73	45.68
12	154.68	46.36
13	159.61	47.21
14	164.50	48.21
15	169.37	49.38
16	174.19	50.71
17	178.96	52.20
18	183.68	53.85
19	188.35	55.65
20	192.95	57.60
21	197.48	59.70
22	201.95	61.95
23	206.34	64.35
24	210.64	66.89
25	214.86	69.58
26	218.99	72.40
27	223.02	75.35
28	226.96	78.44
29	230.31	81.26

*** 2.308 ***

Failure Surface Specified By 35 Coordinate Points

Point No.	X-Surf (ft)	Y-Surf (ft)
1	100.00	47.90
2	104.28	45.31

3	108.67	42.92
4	113.17	40.75
5	117.78	38.80
6	122.47	37.07
7	127.24	35.57
8	132.07	34.29
9	136.96	33.26
10	141.90	32.46
11	146.87	31.89
12	151.86	31.57
13	156.86	31.48
14	161.85	31.64
15	166.84	32.04
16	171.80	32.67
17	176.72	33.54
18	181.60	34.65
19	186.41	35.99
20	191.16	37.56
21	195.83	39.36
22	200.40	41.38
23	204.87	43.61
24	209.23	46.06
25	213.47	48.72
26	217.57	51.57
27	221.54	54.62
28	225.35	57.86
29	229.00	61.27
30	232.48	64.86
31	235.79	68.61
32	238.91	72.51
33	241.85	76.56
34	244.58	80.75
35	245.23	81.86

*** 2.313 ***

1

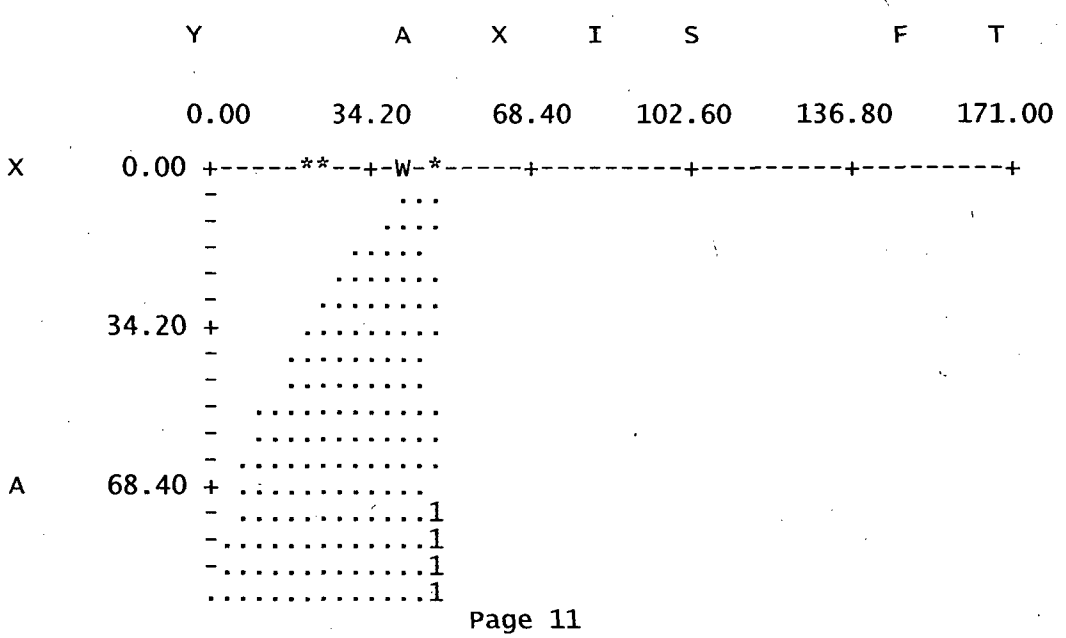

```
                .............1
X     102.60    ......**.....21
                ............241
                ...........66291
                ..........2259*
                .........625.9*
                .........235.91
I     136.80    ........6245.91*
                ........62.5.911
                .......6.25..9.1
                -......6.25...9***
                -......6.2.5..91
                -......6.2.5..9*1
S     171.00 +  ......6235..9*1
                -  ......623.5..9.1
                -  .......6235...9.1
                -   ......6.23...9.1
                -   .......62355..9.1
                -    ......76233..9911
      205.20 +     .......7223...*1
                -     .......64233.*91
                -      ........72233991
                -      .........7422.311
                -        ........07422***
                -         .........004522
F     239.40 +           ..........00.4
                -            ...........0
                -             ...........
                -               .........
                -                 .......
                -                   ....
T     273.60 +           W  *   *  ***
```

BISHOP #1 STATIC CIRCULAR

Geometry and Boundary Conditions
Problem: SMC Newfield Decommissioning - Section A-A' - FS Min = 2.261

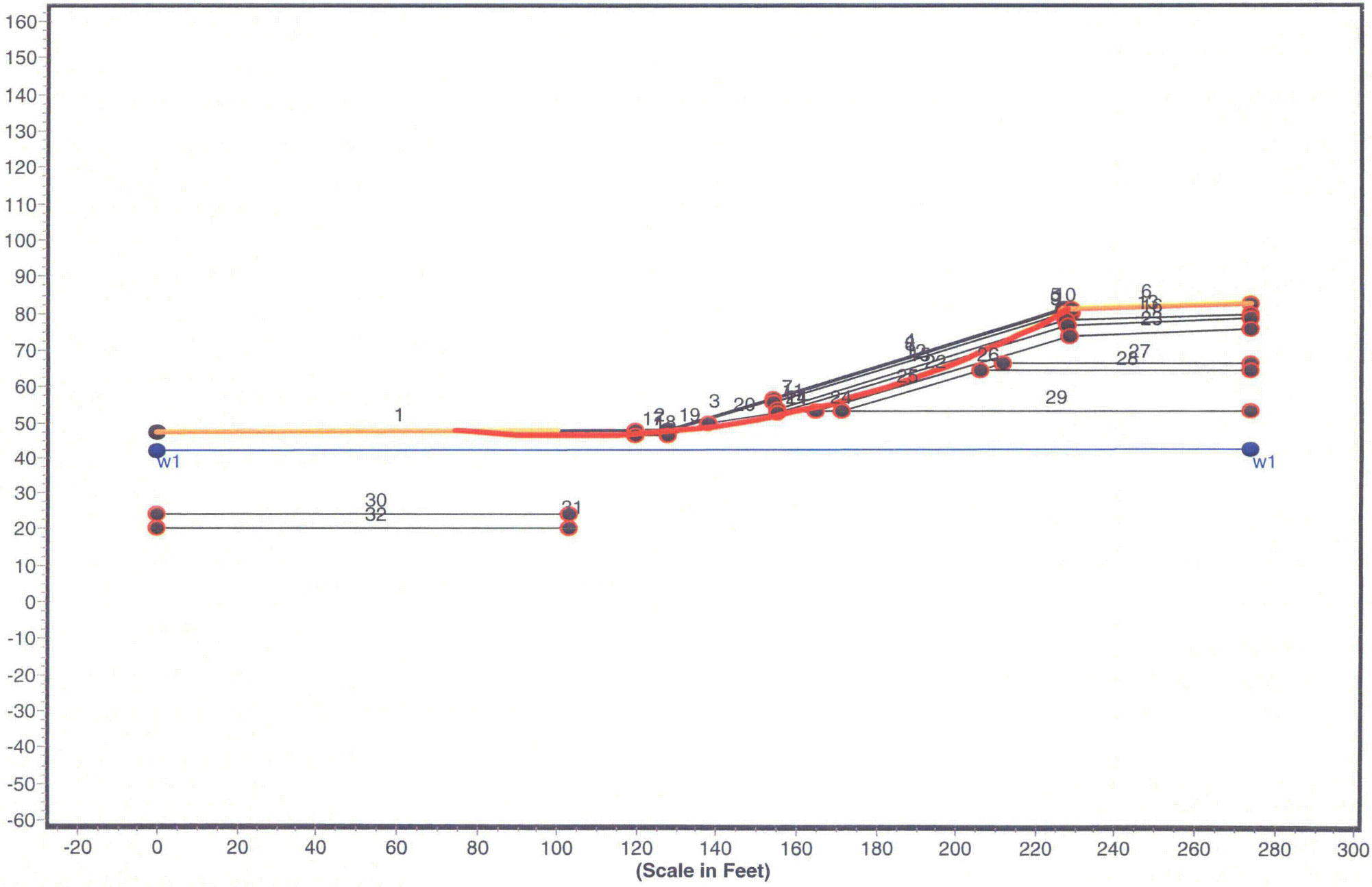

Geometry and Boundary Conditions

Problem: SMC Newfield Decommissioning - Section A-A' - FS Min = 2.261

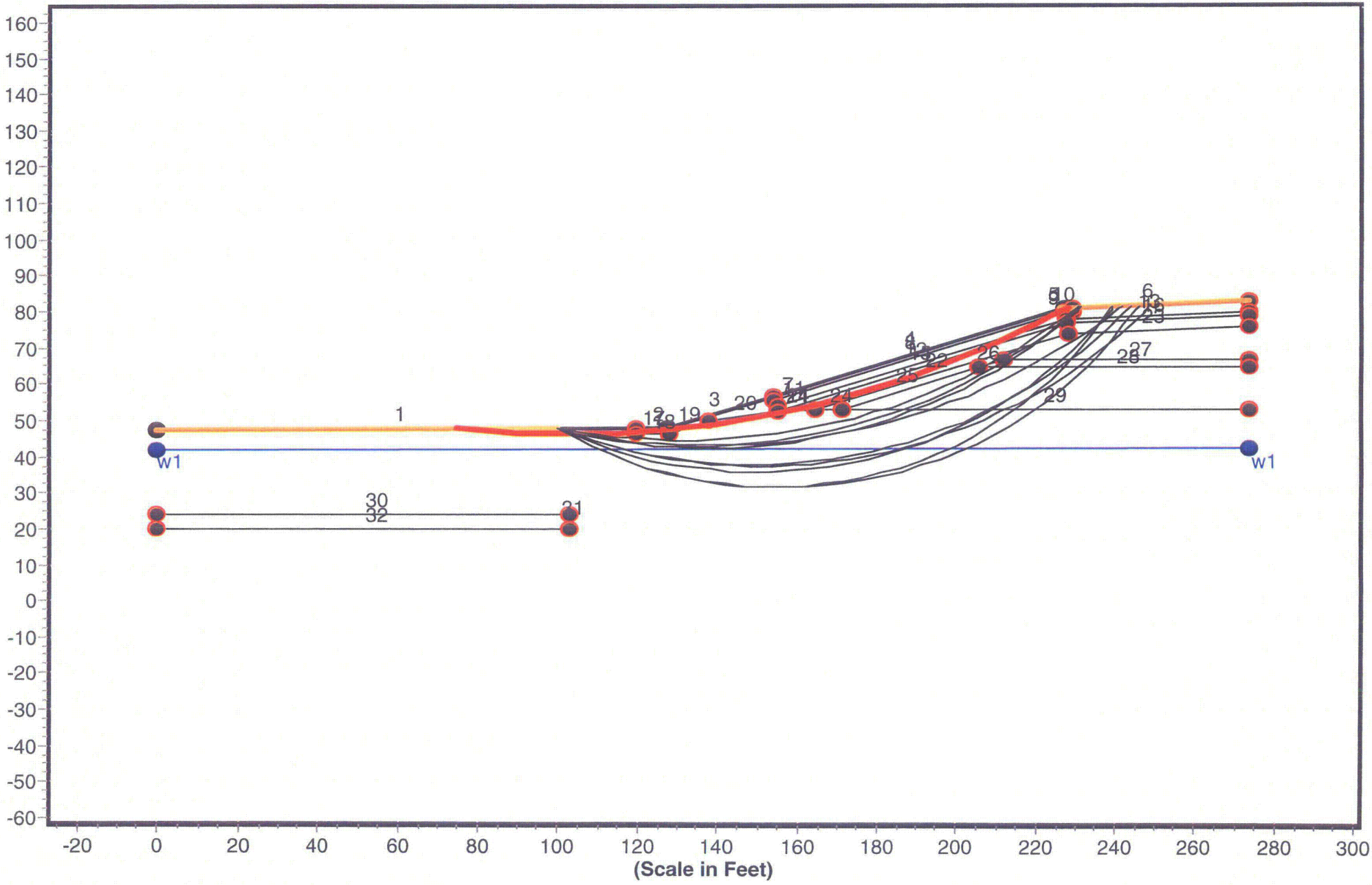

Geometry and Boundary Conditions
Problem: SMC Newfield Decommissioning - Section A-A' - FS Min = 2.261

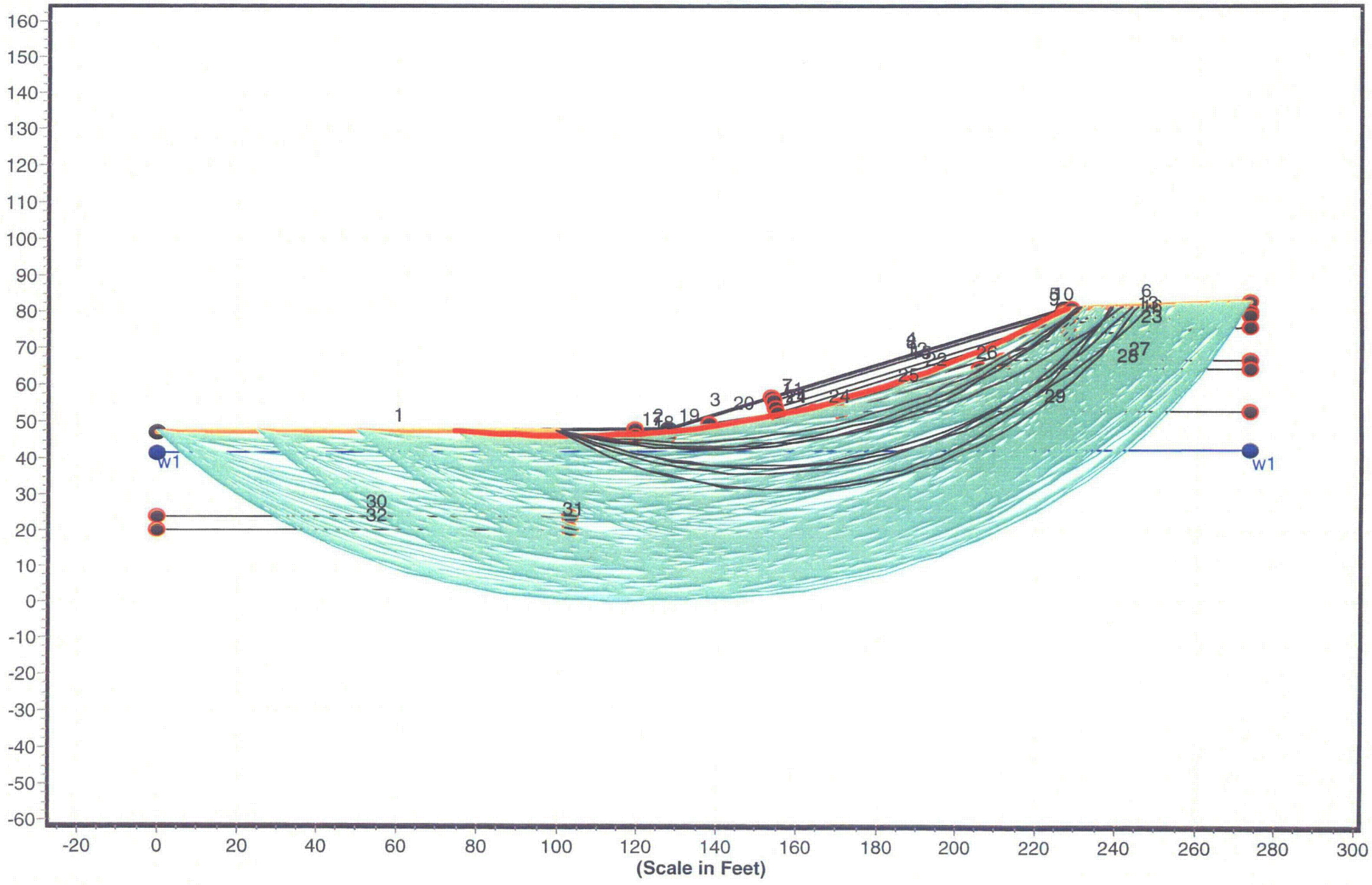

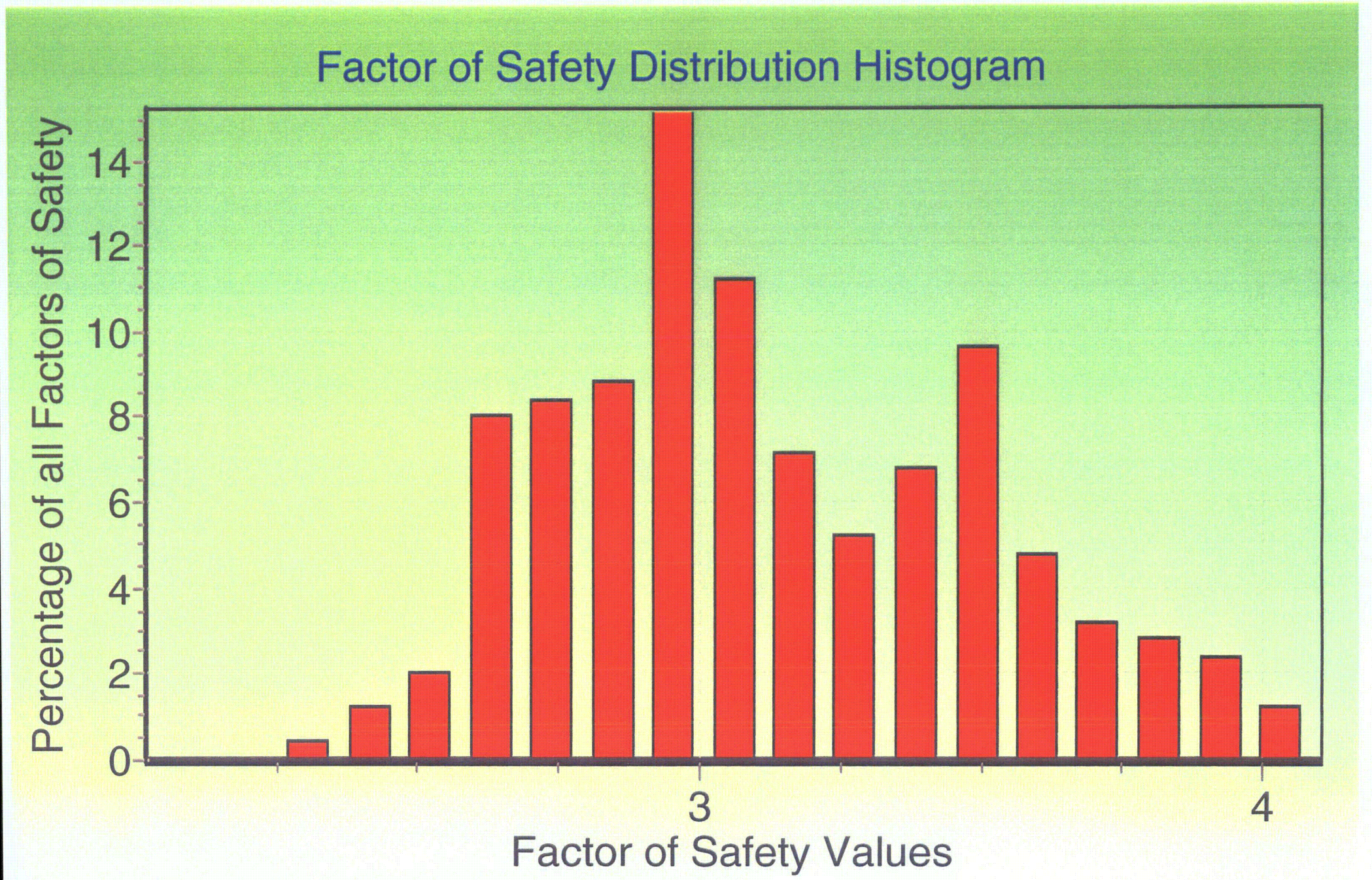
Factor of Safety Distribution Histogram
Percentage of all Factors of Safety
0
2
4
6
8
10
12
14
3
4
Factor of Safety Values

SMC Bishop Circular Results #1.txt
** PCSTABL6 **

by
Purdue University

1

--Slope Stability Analysis--
Simplified Janbu, Simplified Bishop
or Spencer's Method of Slices

Run Date:
Time of Run:
Run By:
Input Data Filename: run.in
Output Filename: result.out
Unit: ENGLISH
Plotted Output Filename: result.plt

PROBLEM DESCRIPTION SMC Newfield Decommissioning - Section A -A'

BOUNDARY COORDINATES

6 Top Boundaries
32 Total Boundaries

Boundary No.	X-Left (ft)	Y-Left (ft)	X-Right (ft)	Y-Right (ft)	Soil Type Below Bnd
1	0.00	47.40	119.50	48.00	7
2	119.50	48.00	127.50	48.00	1
3	127.50	48.00	153.90	56.80	1
4	153.90	56.80	226.90	81.10	1
5	226.90	81.10	228.90	81.20	1
6	228.90	81.20	273.60	83.00	2
7	153.90	56.80	154.20	55.80	1
8	154.20	55.80	227.10	80.10	2
9	227.10	80.10	228.80	80.20	2
10	228.80	80.20	228.90	81.20	2
11	154.20	55.80	154.80	53.90	1
12	154.80	53.90	227.40	78.10	1
13	227.40	78.10	273.60	80.00	1
14	154.80	53.90	155.20	52.60	1
15	155.20	52.60	227.60	77.10	3
16	227.60	77.10	273.60	79.00	3
17	119.50	48.00	119.60	46.40	7
18	119.60	46.40	127.80	46.40	7
19	127.80	46.40	137.90	49.80	7
20	137.90	49.80	155.20	52.60	7
21	155.20	52.60	164.60	53.00	7
22	164.60	53.00	228.20	74.10	4
23	228.20	74.10	273.60	76.00	4
24	164.60	53.00	171.00	53.00	7
25	171.00	53.00	205.80	64.60	6
26	205.80	64.60	211.80	66.60	5

27	211.80	66.60	273.60	66.60	5
28	205.80	64.60	273.60	64.60	6
29	171.00	53.00	273.60	53.00	7
30	0.00	24.00	103.10	24.00	8
31	103.00	20.00	103.10	24.00	7
32	0.00	20.00	103.10	20.00	7

1

ISOTROPIC SOIL PARAMETERS

8 Type(s) of Soil

Soil Type No.	Total Unit Wt. (pcf)	Saturated Unit Wt. (pcf)	Cohesion Intercept (psf)	Friction Angle (deg)	Pore Pressure Param.	Pressure Constant (psf)	Piez. Surface No.
1	135.0	140.0	0.0	40.0	0.00	0.0	0
2	135.0	140.0	0.0	35.0	0.00	0.0	0
3	125.0	130.0	250.0	15.0	0.00	0.0	0
4	125.0	135.0	0.0	32.0	0.00	0.0	0
5	135.0	140.0	0.0	38.0	0.00	0.0	0
6	135.0	140.0	0.0	40.0	0.00	0.0	0
7	115.0	130.0	0.0	33.0	0.00	0.0	1
8	130.0	140.0	300.0	20.0	0.00	0.0	1

1

1 PIEZOMETRIC SURFACE(S) HAVE BEEN SPECIFIED

Unit Weight of Water = 62.40

Piezometric Surface No. 1 Specified by 2 Coordinate Points

Point No.	X-Water (ft)	Y-Water (ft)
1	0.00	41.70
2	273.60	42.50

1

A Critical Failure Surface Searching Method, Using A Random Technique For Generating Circular Surfaces, Has Been Specified.

250 Trial Surfaces Have Been Generated.

50 Surfaces Initiate From Each Of 5 Points Equally Spaced Along The Ground Surface Between X = 0.00 ft.
and X = 100.00 ft.

Each Surface Terminates Between X = 226.00 ft.
and X = 273.60 ft.

Unless Further Limitations Were Imposed, The Minimum Elevation At Which A Surface Extends Is Y = 0.00 ft.

5.00 ft. Line Segments Define Each Trial Failure Surface.

Restrictions Have Been Imposed Upon The Angle Of Initiation. The Angle Has Been Restricted Between The Angles Of -45.0 And -5.0 deg.

1

Following Are Displayed The Ten Most Critical Of The Trial Failure Surfaces Examined. They Are Ordered - Most Critical First.

* * Safety Factors Are Calculated By The Modified Bishop Method * *

Failure Surface Specified By 33 Coordinate Points

Point No.	X-Surf (ft)	Y-Surf (ft)
1	75.00	47.78
2	79.97	47.25
3	84.96	46.84
4	89.95	46.52
5	94.94	46.31
6	99.94	46.20
7	104.94	46.20
8	109.94	46.30
9	114.93	46.50
10	119.93	46.81
11	124.91	47.22
12	129.88	47.73
13	134.84	48.35
14	139.79	49.07
15	144.72	49.89
16	149.64	50.81
17	154.53	51.84
18	159.40	52.96
19	164.25	54.19
20	169.07	55.52
21	173.86	56.95
22	178.62	58.48
23	183.35	60.10
24	188.05	61.82
25	192.70	63.64
26	197.32	65.56
27	201.90	67.57
28	206.43	69.68
29	210.92	71.88
30	215.37	74.17
31	219.76	76.55
32	224.11	79.03
33	227.63	81.14

Circle Center At X = 102.6 ; Y = 287.2 and Radius, 241.0

*** 2.261 ***

Individual data on the 46 slices

Slice No.	Width (ft)	Weight (lbs)	Water Force Top (lbs)	Water Force Bot (lbs)	Force Norm (lbs)	Force Tan (lbs)	Earthquake Force Hor (lbs)	Earthquake Force Ver (lbs)	Surcharge Load (lbs)
1	5.0	156.4	0.0	0.0	0.0	0.0	0.0	0.0	0.0
2	5.0	440.5	0.0	0.0	0.0	0.0	0.0	0.0	0.0
3	5.0	666.1	0.0	0.0	0.0	0.0	0.0	0.0	0.0
4	5.0	832.5	0.0	0.0	0.0	0.0	0.0	0.0	0.0
5	5.0	939.3	0.0	0.0	0.0	0.0	0.0	0.0	0.0
6	5.0	986.2	0.0	0.0	0.0	0.0	0.0	0.0	0.0
7	5.0	973.1	0.0	0.0	0.0	0.0	0.0	0.0	0.0
8	5.0	899.9	0.0	0.0	0.0	0.0	0.0	0.0	0.0
9	4.6	708.0	0.0	0.0	0.0	0.0	0.0	0.0	0.0
10	0.1	11.6	0.0	0.0	0.0	0.0	0.0	0.0	0.0
11	0.3	56.8	0.0	0.0	0.0	0.0	0.0	0.0	0.0
12	5.0	664.9	0.0	0.0	0.0	0.0	0.0	0.0	0.0
13	2.6	227.2	0.0	0.0	0.0	0.0	0.0	0.0	0.0
14	2.4	254.0	0.0	0.0	0.0	0.0	0.0	0.0	0.0
15	3.0	549.4	0.0	0.0	0.0	0.0	0.0	0.0	0.0
16	2.0	502.2	0.0	0.0	0.0	0.0	0.0	0.0	0.0
17	3.1	941.6	0.0	0.0	0.0	0.0	0.0	0.0	0.0
18	1.9	690.1	0.0	0.0	0.0	0.0	0.0	0.0	0.0
19	4.9	2190.5	0.0	0.0	0.0	0.0	0.0	0.0	0.0
20	4.9	2699.5	0.0	0.0	0.0	0.0	0.0	0.0	0.0
21	4.3	2712.7	0.0	0.0	0.0	0.0	0.0	0.0	0.0
22	0.3	203.0	0.0	0.0	0.0	0.0	0.0	0.0	0.0
23	0.3	226.2	0.0	0.0	0.0	0.0	0.0	0.0	0.0
24	0.3	184.5	0.0	0.0	0.0	0.0	0.0	0.0	0.0
25	0.4	276.9	0.0	0.0	0.0	0.0	0.0	0.0	0.0
26	3.2	2313.5	0.0	0.0	0.0	0.0	0.0	0.0	0.0
27	1.0	736.2	0.0	0.0	0.0	0.0	0.0	0.0	0.0
28	4.8	3773.1	0.0	0.0	0.0	0.0	0.0	0.0	0.0
29	4.8	3950.7	0.0	0.0	0.0	0.0	0.0	0.0	0.0
30	4.8	4058.9	0.0	0.0	0.0	0.0	0.0	0.0	0.0
31	4.8	4098.7	0.0	0.0	0.0	0.0	0.0	0.0	0.0
32	4.7	4071.3	0.0	0.0	0.0	0.0	0.0	0.0	0.0
33	4.7	3978.0	0.0	0.0	0.0	0.0	0.0	0.0	0.0
34	4.7	3820.4	0.0	0.0	0.0	0.0	0.0	0.0	0.0
35	4.6	3600.1	0.0	0.0	0.0	0.0	0.0	0.0	0.0
36	4.6	3319.2	0.0	0.0	0.0	0.0	0.0	0.0	0.0
37	4.5	2979.7	0.0	0.0	0.0	0.0	0.0	0.0	0.0
38	1.7	1032.1	0.0	0.0	0.0	0.0	0.0	0.0	0.0
39	2.8	1546.0	0.0	0.0	0.0	0.0	0.0	0.0	0.0
40	4.0	1910.3	0.0	0.0	0.0	0.0	0.0	0.0	0.0
41	0.4	187.7	0.0	0.0	0.0	0.0	0.0	0.0	0.0
42	4.4	1560.6	0.0	0.0	0.0	0.0	0.0	0.0	0.0
43	4.3	970.9	0.0	0.0	0.0	0.0	0.0	0.0	0.0
44	0.3	41.3	0.0	0.0	0.0	0.0	0.0	0.0	0.0
45	2.5	249.7	0.0	0.0	0.0	0.0	0.0	0.0	0.0
46	0.7	19.9	0.0	0.0	0.0	0.0	0.0	0.0	0.0

Failure Surface Specified By 29 Coordinate Points

Point No.	X-Surf (ft)	Y-Surf (ft)
1	100.00	47.90
2	104.91	46.94
3	109.84	46.14
4	114.80	45.51
5	119.78	45.04
6	124.77	44.73
7	129.77	44.59
8	134.77	44.61
9	139.77	44.80
10	144.75	45.16
11	149.73	45.68
12	154.68	46.36
13	159.61	47.20
14	164.50	48.21
15	169.37	49.38
16	174.19	50.71
17	178.96	52.19
18	183.68	53.84
19	188.35	55.64
20	192.95	57.59
21	197.49	59.69
22	201.95	61.94
23	206.34	64.34
24	210.65	66.88
25	214.87	69.56
26	219.00	72.38
27	223.03	75.33
28	226.96	78.42
29	230.35	81.26

Circle Center At X = 131.5 ; Y = 196.0 and Radius, 151.4

*** 2.393 ***

1

Failure Surface Specified By 30 Coordinate Points

Point No.	X-Surf (ft)	Y-Surf (ft)
1	100.00	47.90
2	104.86	46.71
3	109.75	45.70
4	114.68	44.86
5	119.64	44.20
6	124.62	43.72
7	129.61	43.42
8	134.61	43.30
9	139.60	43.36
10	144.60	43.60
11	149.58	44.01
12	154.55	44.61

13	159.49	45.38
14	164.39	46.33
15	169.27	47.46
16	174.09	48.76
17	178.87	50.24
18	183.59	51.88
19	188.25	53.70
20	192.84	55.68
21	197.36	57.82
22	201.80	60.13
23	206.15	62.59
24	210.41	65.21
25	214.57	67.98
26	218.63	70.90
27	222.58	73.96
28	226.42	77.16
29	230.15	80.50
30	230.96	81.28

Circle Center At X = 135.5 ; Y = 182.3 and Radius, 139.0

*** 2.421 ***

Failure Surface Specified By 30 Coordinate Points

Point No.	X-Surf (ft)	Y-Surf (ft)
1	100.00	47.90
2	104.82	46.56
3	109.68	45.40
4	114.58	44.42
5	119.52	43.63
6	124.49	43.04
7	129.47	42.62
8	134.46	42.40
9	139.46	42.37
10	144.46	42.53
11	149.45	42.88
12	154.42	43.42
13	159.37	44.15
14	164.28	45.07
15	169.16	46.17
16	173.99	47.46
17	178.77	48.92
18	183.49	50.57
19	188.14	52.40
20	192.72	54.41
21	197.23	56.58
22	201.64	58.93
23	205.96	61.44
24	210.19	64.12
25	214.31	66.95
26	218.32	69.94
27	222.21	73.08
28	225.98	76.36
29	229.62	79.79
30	231.10	81.29

Circle Center At X = 137.8 ; Y = 173.7 and Radius, 131.4

*** 2.438 ***

1

Failure Surface Specified By 32 Coordinate Points

Point No.	X-Surf (ft)	Y-Surf (ft)
1	100.00	47.90
2	104.87	46.76
3	109.77	45.78
4	114.70	44.95
5	119.66	44.28
6	124.63	43.76
7	129.62	43.41
8	134.61	43.21
9	139.61	43.17
10	144.61	43.30
11	149.60	43.57
12	154.58	44.01
13	159.55	44.61
14	164.49	45.36
15	169.41	46.27
16	174.29	47.34
17	179.14	48.56
18	183.95	49.93
19	188.71	51.46
20	193.42	53.14
21	198.08	54.96
22	202.67	56.93
23	207.20	59.05
24	211.66	61.31
25	216.05	63.71
26	220.35	66.25
27	224.58	68.92
28	228.72	71.73
29	232.76	74.67
30	236.71	77.73
31	240.57	80.92
32	241.46	81.71

Circle Center At X = 138.3 ; Y = 200.5 and Radius, 157.3

*** 2.475 ***

Failure Surface Specified By 33 Coordinate Points

Point No.	X-Surf (ft)	Y-Surf (ft)

1	100.00	47.90
2	104.50	45.72
3	109.10	43.75
4	113.78	41.99
5	118.53	40.45
6	123.35	39.12
7	128.23	38.02
8	133.15	37.14
9	138.11	36.48
10	143.09	36.05
11	148.09	35.85
12	153.09	35.88
13	158.08	36.13
14	163.06	36.61
15	168.01	37.32
16	172.92	38.25
17	177.78	39.41
18	182.59	40.78
19	187.33	42.38
20	191.99	44.18
21	196.57	46.20
22	201.04	48.43
23	205.41	50.85
24	209.67	53.48
25	213.80	56.29
26	217.80	59.29
27	221.66	62.47
28	225.37	65.82
29	228.93	69.34
30	232.32	73.01
31	235.54	76.84
32	238.58	80.81
33	239.14	81.61

Circle Center At X = 150.0 ; Y = 145.5 and Radius, 109.7

*** 2.496 ***

1

Failure Surface Specified By 33 Coordinate Points

Point No.	X-Surf (ft)	Y-Surf (ft)
1	100.00	47.90
2	104.64	46.03
3	109.34	44.35
4	114.12	42.85
5	118.94	41.55
6	123.82	40.45
7	128.74	39.54
8	133.69	38.83
9	138.66	38.32
10	143.65	38.01
11	148.65	37.90
12	153.65	37.99
13	158.64	38.28
14	163.62	38.77

15	168.57	39.46
16	173.49	40.35
17	178.37	41.44
18	183.20	42.72
19	187.98	44.20
20	192.69	45.86
21	197.34	47.72
22	201.90	49.76
23	206.38	51.98
24	210.77	54.38
25	215.05	56.95
26	219.23	59.69
27	223.30	62.60
28	227.25	65.67
29	231.07	68.90
30	234.75	72.28
31	238.30	75.80
32	241.71	79.46
33	243.70	81.80

Circle Center At X = 148.9 ; Y = 162.3 and Radius, 124.4

*** 2.511 ***

Failure Surface Specified By 34 Coordinate Points

Point No.	X-Surf (ft)	Y-Surf (ft)
1	100.00	47.90
2	104.63	46.01
3	109.33	44.30
4	114.09	42.77
5	118.90	41.42
6	123.77	40.27
7	128.67	39.31
8	133.61	38.53
9	138.58	37.95
10	143.56	37.56
11	148.56	37.37
12	153.56	37.37
13	158.56	37.57
14	163.54	37.96
15	168.51	38.54
16	173.45	39.32
17	178.35	40.28
18	183.22	41.44
19	188.03	42.78
20	192.79	44.31
21	197.49	46.03
22	202.12	47.93
23	206.67	50.00
24	211.13	52.25
25	215.51	54.67
26	219.78	57.26
27	223.96	60.01
28	228.02	62.93
29	231.97	66.00

30	235.79	69.22
31	239.49	72.59
32	243.05	76.09
33	246.47	79.74
34	248.43	81.99

Circle Center At X = 151.0 ; Y = 165.9 and Radius, 128.6

*** 2.549 ***

1

Failure Surface Specified By 34 Coordinate Points

Point No.	X-Surf (ft)	Y-Surf (ft)
1	100.00	47.90
2	104.22	45.23
3	108.58	42.77
4	113.06	40.55
5	117.65	38.56
6	122.33	36.81
7	127.10	35.30
8	131.93	34.04
9	136.83	33.03
10	141.78	32.28
11	146.75	31.78
12	151.74	31.54
13	156.74	31.56
14	161.74	31.83
15	166.71	32.37
16	171.65	33.16
17	176.54	34.20
18	181.37	35.49
19	186.12	37.04
20	190.79	38.82
21	195.36	40.84
22	199.83	43.10
23	204.16	45.59
24	208.37	48.29
25	212.43	51.21
26	216.33	54.33
27	220.07	57.66
28	223.63	61.17
29	227.01	64.86
30	230.18	68.71
31	233.16	72.73
32	235.93	76.90
33	238.47	81.20
34	238.68	81.59

Circle Center At X = 153.9 ; Y = 128.3 and Radius, 96.8

*** 2.552 ***

Failure Surface Specified By 35 Coordinate Points

Point No.	X-Surf (ft)	Y-Surf (ft)
1	100.00	47.90
2	104.28	45.31
3	108.67	42.92
4	113.17	40.75
5	117.77	38.80
6	122.47	37.07
7	127.23	35.56
8	132.07	34.29
9	136.96	33.25
10	141.89	32.44
11	146.86	31.88
12	151.85	31.55
13	156.85	31.46
14	161.85	31.61
15	166.83	32.00
16	171.79	32.63
17	176.72	33.50
18	181.59	34.60
19	186.41	35.93
20	191.16	37.50
21	195.83	39.29
22	200.41	41.30
23	204.88	43.53
24	209.25	45.97
25	213.49	48.62
26	217.60	51.46
27	221.57	54.50
28	225.39	57.73
29	229.05	61.14
30	232.54	64.72
31	235.85	68.46
32	238.98	72.36
33	241.93	76.40
34	244.67	80.58
35	245.43	81.87

Circle Center At X = 156.2 ; Y = 135.7 and Radius, 104.2

*** 2.576 ***

1

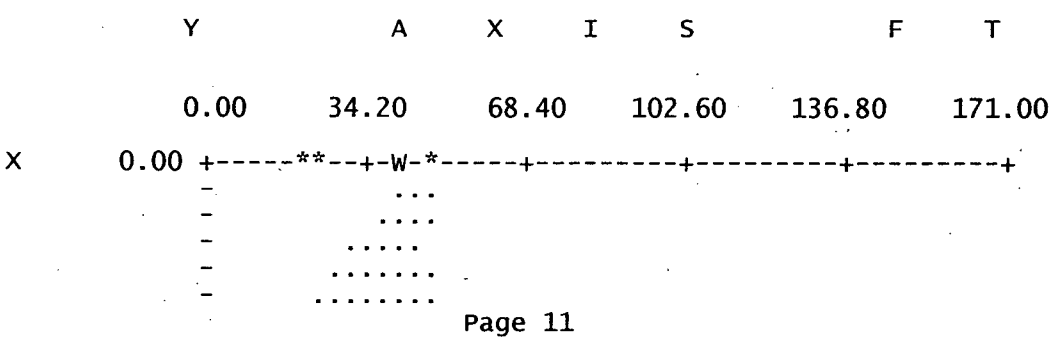

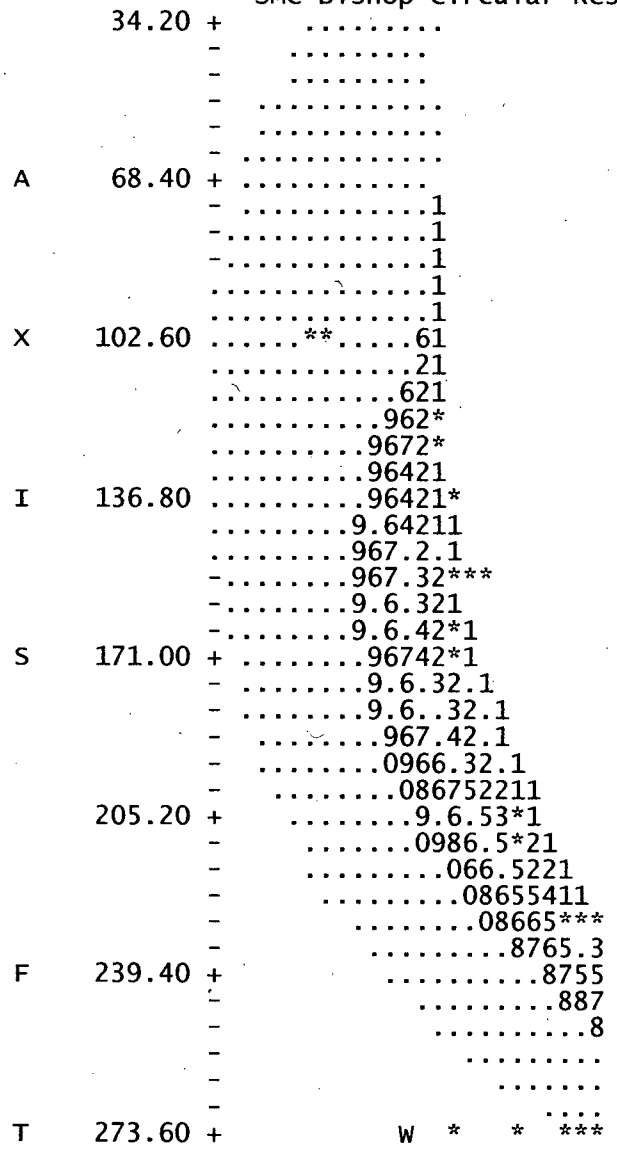
34.20
A 68.40
X 102.60
I 136.80
S 171.00
205.20
F 239.40
T 273.60

SPENCER #1 STATIC SLICES

Geometry and Boundary Conditions

Problem: SMC Newfield Decommissioning - Section A-A' - FS Min = 2.275

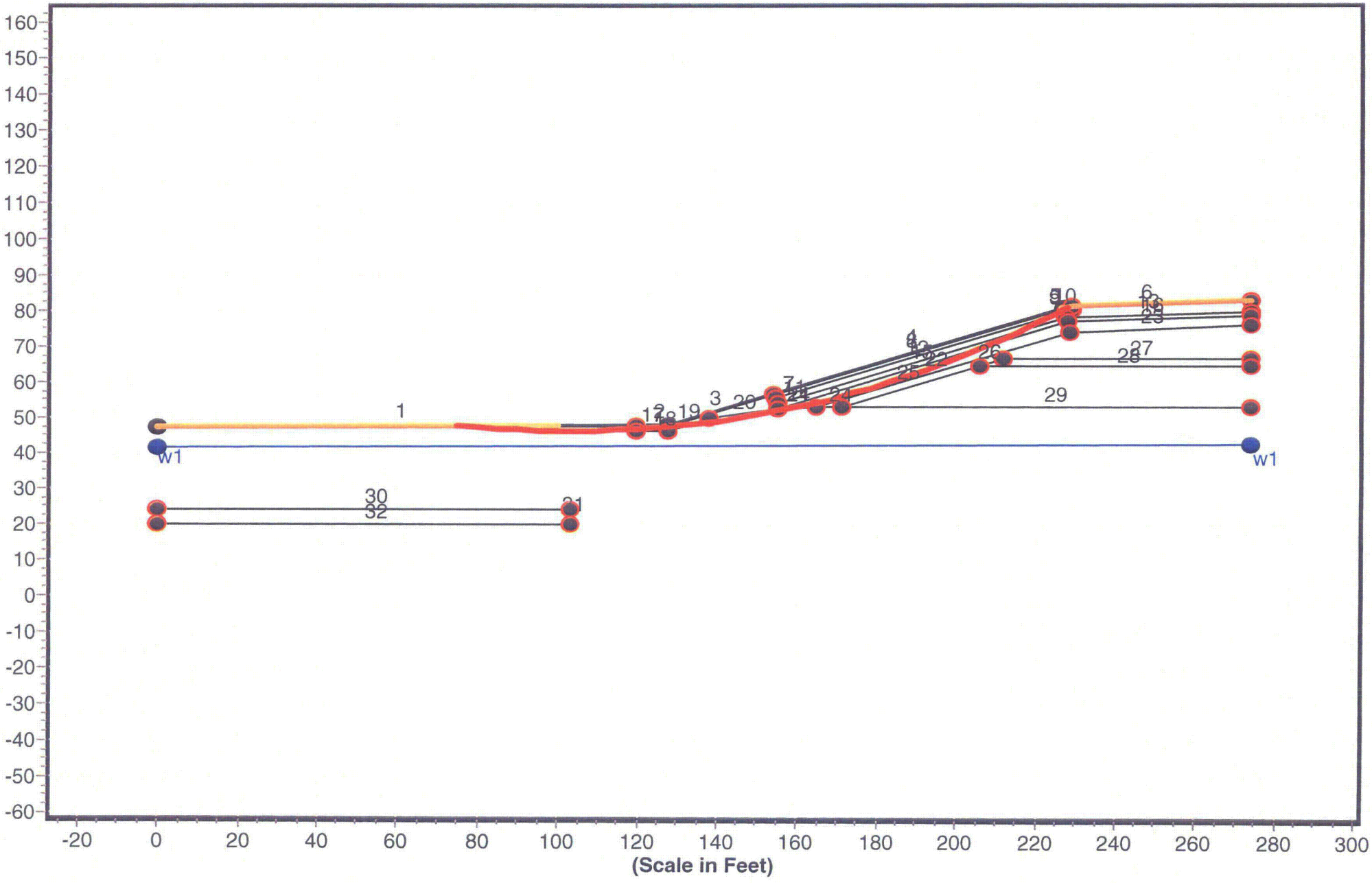

Geometry and Boundary Conditions

Problem: SMC Newfield Decommissioning - Section A-A' - FS Min = 2.275

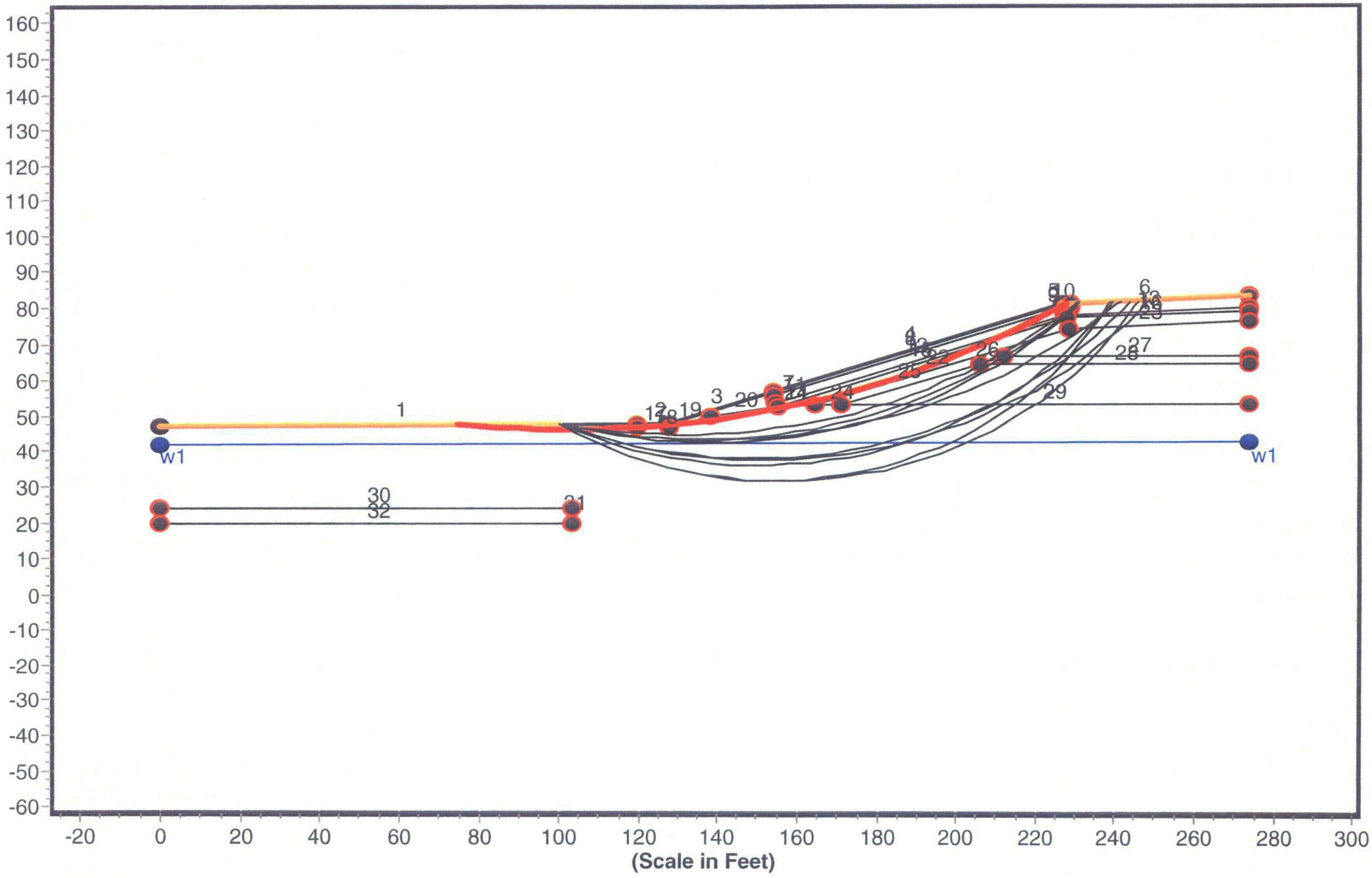

Geometry and Boundary Conditions

Problem: SMC Newfield Decommissioning - Section A-A' - FS Min = 2.275

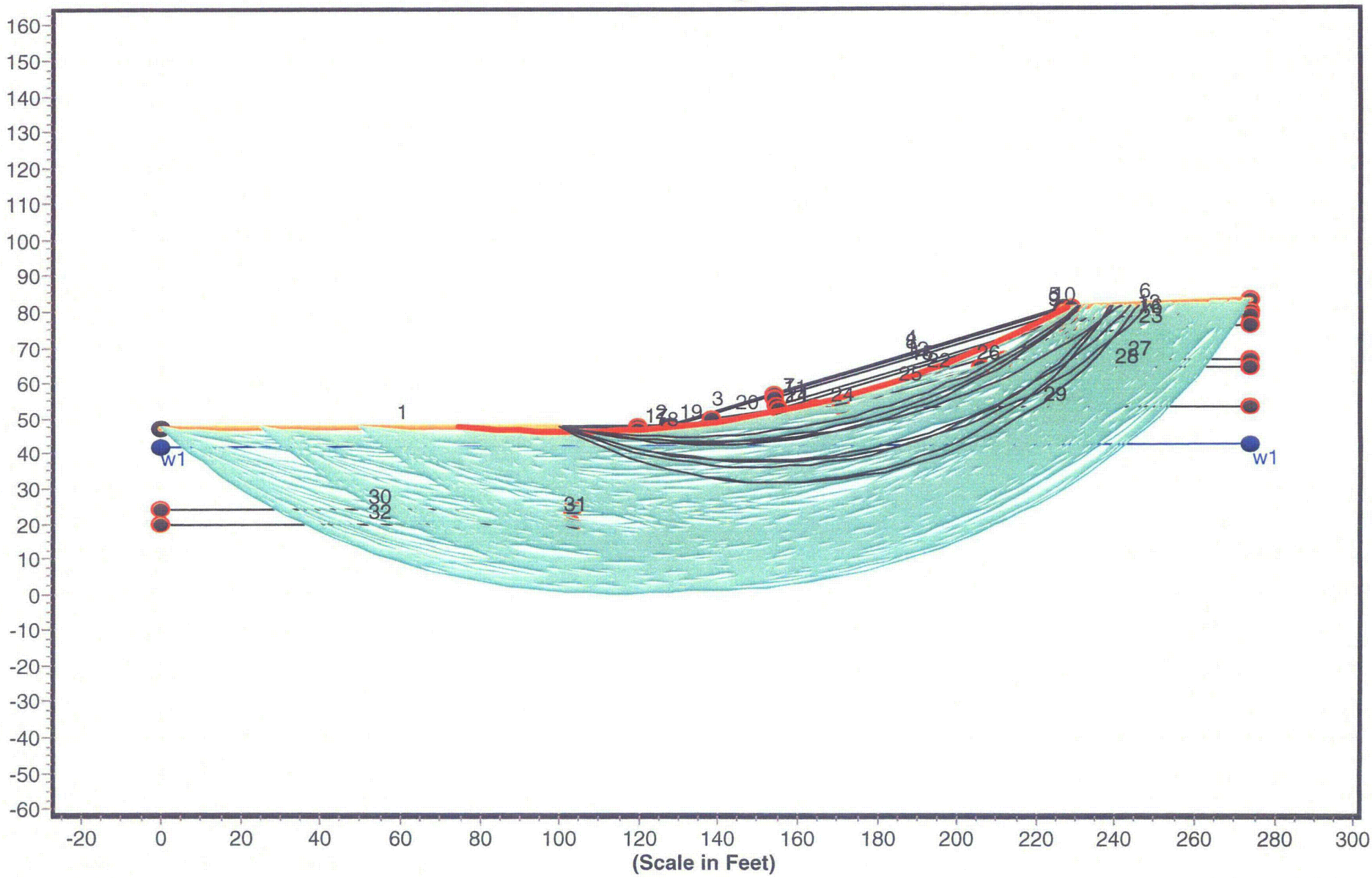

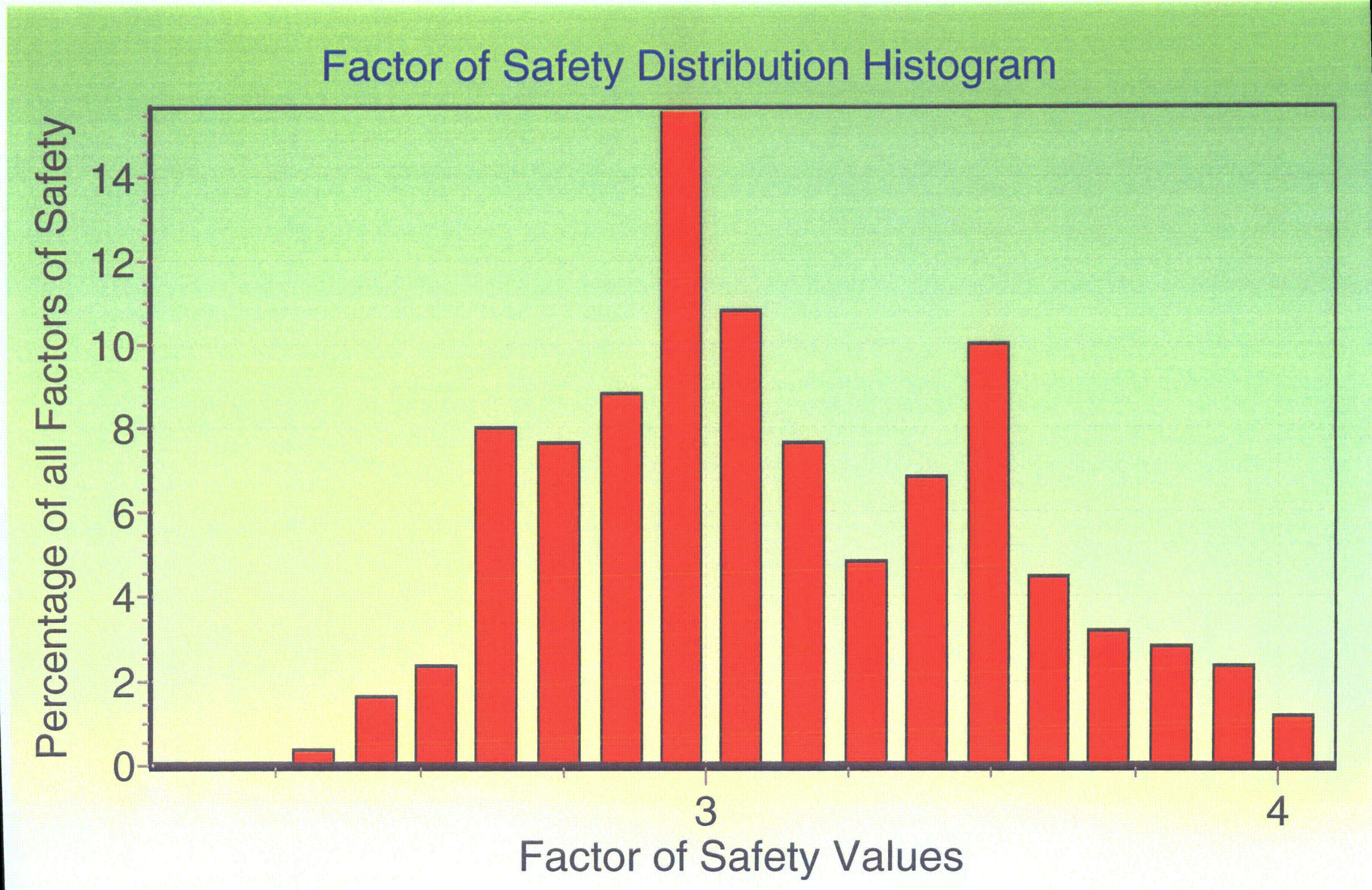
Factor of Safety Distribution Histogram
Percentage of all Factors of Safety
0
2
4
6
8
10
12
14
3
4
Factor of Safety Values

Spencer #1 Results.txt
** PCSTABL6 **

by
Purdue University

1

--Slope Stability Analysis--
Simplified Janbu, Simplified Bishop
or Spencer`s Method of Slices

Run Date:
Time of Run:
Run By:
Input Data Filename: run.in
Output Filename: result.out
Unit: ENGLISH
Plotted Output Filename: result.plt

PROBLEM DESCRIPTION SMC Newfield Decommissioning - Section A -A'

BOUNDARY COORDINATES

6 Top Boundaries
32 Total Boundaries

Boundary No.	X-Left (ft)	Y-Left (ft)	X-Right (ft)	Y-Right (ft)	Soil Type Below Bnd
1	0.00	47.40	119.50	48.00	7
2	119.50	48.00	127.50	48.00	1
3	127.50	48.00	153.90	56.80	1
4	153.90	56.80	226.90	81.10	1
5	226.90	81.10	228.90	81.20	1
6	228.90	81.20	273.60	83.00	2
7	153.90	56.80	154.20	55.80	1
8	154.20	55.80	227.10	80.10	2
9	227.10	80.10	228.80	80.20	2
10	228.80	80.20	228.90	81.20	2
11	154.20	55.80	154.80	53.90	1
12	154.80	53.90	227.40	78.10	1
13	227.40	78.10	273.60	80.00	1
14	154.80	53.90	155.20	52.60	1
15	155.20	52.60	227.60	77.10	3
16	227.60	77.10	273.60	79.00	3
17	119.50	48.00	119.60	46.40	7
18	119.60	46.40	127.80	46.40	7
19	127.80	46.40	137.90	49.80	7
20	137.90	49.80	155.20	52.60	7
21	155.20	52.60	164.60	53.00	7
22	164.60	53.00	228.20	74.10	4
23	228.20	74.10	273.60	76.00	4
24	164.60	53.00	171.00	53.00	7
25	171.00	53.00	205.80	64.60	6
26	205.80	64.60	211.80	66.60	5

27	211.80	66.60	273.60	66.60	5
28	205.80	64.60	273.60	64.60	6
29	171.00	53.00	273.60	53.00	7
30	0.00	24.00	103.10	24.00	8
31	103.00	20.00	103.10	24.00	7
32	0.00	20.00	103.10	20.00	7

1

ISOTROPIC SOIL PARAMETERS

8 Type(s) of Soil

Soil Type No.	Total Unit Wt. (pcf)	Saturated Unit Wt. (pcf)	Cohesion Intercept (psf)	Friction Angle (deg)	Pore Pressure Param.	Pressure Constant (psf)	Piez. Surface No.
1	135.0	140.0	0.0	40.0	0.00	0.0	0
2	135.0	140.0	0.0	35.0	0.00	0.0	0
3	125.0	130.0	250.0	15.0	0.00	0.0	0
4	125.0	135.0	0.0	32.0	0.00	0.0	0
5	135.0	140.0	0.0	38.0	0.00	0.0	0
6	135.0	140.0	0.0	40.0	0.00	0.0	0
7	115.0	130.0	0.0	33.0	0.00	0.0	1
8	130.0	140.0	300.0	20.0	0.00	0.0	1

1

1 PIEZOMETRIC SURFACE(S) HAVE BEEN SPECIFIED

Unit Weight of Water = 62.40

Piezometric Surface No. 1 Specified by 2 Coordinate Points

Point No.	X-Water (ft)	Y-Water (ft)
1	0.00	41.70
2	273.60	42.50

1

A Critical Failure Surface Searching Method, Using A Random Technique For Generating Circular Surfaces, Has Been Specified.

250 Trial Surfaces Have Been Generated.

50 Surfaces Initiate From Each Of 5 Points Equally Spaced Along The Ground Surface Between X = 0.00 ft.
and X = 100.00 ft.

Each Surface Terminates Between X = 226.00 ft.
and X = 273.00 ft.

Unless Further Limitations Were Imposed, The Minimum Elevation At Which A Surface Extends Is Y = 0.00 ft.

5.00 ft. Line Segments Define Each Trial Failure Surface.

Restrictions Have Been Imposed Upon The Angle Of Initiation. The Angle Has Been Restricted Between The Angles Of -45.0 And -5.0 deg.

1

Following Are Displayed The Ten Most Critical Of The Trial Failure Surfaces Examined. They Are Ordered - Most Critical First.

* * Safety Factors Are Calculated By Spencer's Method * *

Number of convergent trials 250
Number of non convergent trials 0

Failure Surface Specified By 33 Coordinate Points

Point No.	X-Surf (ft)	Y-Surf (ft)
1	75.00	47.78
2	79.97	47.25
3	84.96	46.84
4	89.95	46.52
5	94.94	46.31
6	99.94	46.20
7	104.94	46.20
8	109.94	46.30
9	114.93	46.50
10	119.93	46.81
11	124.91	47.22
12	129.88	47.73
13	134.84	48.35
14	139.79	49.07
15	144.72	49.89
16	149.64	50.81
17	154.53	51.84
18	159.40	52.97
19	164.25	54.19
20	169.07	55.52
21	173.86	56.95
22	178.62	58.48
23	183.35	60.10
24	188.04	61.83
25	192.70	63.65
26	197.32	65.56
27	201.90	67.57
28	206.43	69.68
29	210.92	71.88
30	215.37	74.17
31	219.76	76.56

32	224.10	79.03
33	227.62	81.14

*** Factor of Safety = 2.275 ***

Individual data on the 46 slices

Slice No.	Width (ft)	Weight (lbs)	Water Force Top (lbs)	Water Force Bot (lbs)	Force Norm (lbs)	Force Tan (lbs)	Earthquake Force Hor (lbs)	Earthquake Force Ver (lbs)	Surcharge Load (lbs)
1	5.0	156.4	0.0	0.0	0.0	0.0	0.0	0.0	0.0
2	5.0	440.4	0.0	0.0	0.0	0.0	0.0	0.0	0.0
3	5.0	666.0	0.0	0.0	0.0	0.0	0.0	0.0	0.0
4	5.0	832.5	0.0	0.0	0.0	0.0	0.0	0.0	0.0
5	5.0	939.3	0.0	0.0	0.0	0.0	0.0	0.0	0.0
6	5.0	986.2	0.0	0.0	0.0	0.0	0.0	0.0	0.0
7	5.0	973.0	0.0	0.0	0.0	0.0	0.0	0.0	0.0
8	5.0	899.8	0.0	0.0	0.0	0.0	0.0	0.0	0.0
9	4.6	707.8	0.0	0.0	0.0	0.0	0.0	0.0	0.0
10	0.1	11.5	0.0	0.0	0.0	0.0	0.0	0.0	0.0
11	0.3	56.8	0.0	0.0	0.0	0.0	0.0	0.0	0.0
12	5.0	664.6	0.0	0.0	0.0	0.0	0.0	0.0	0.0
13	2.6	227.1	0.0	0.0	0.0	0.0	0.0	0.0	0.0
14	2.4	253.8	0.0	0.0	0.0	0.0	0.0	0.0	0.0
15	3.0	549.9	0.0	0.0	0.0	0.0	0.0	0.0	0.0
16	2.0	501.3	0.0	0.0	0.0	0.0	0.0	0.0	0.0
17	3.1	941.3	0.0	0.0	0.0	0.0	0.0	0.0	0.0
18	1.9	689.9	0.0	0.0	0.0	0.0	0.0	0.0	0.0
19	4.9	2190.0	0.0	0.0	0.0	0.0	0.0	0.0	0.0
20	4.9	2698.9	0.0	0.0	0.0	0.0	0.0	0.0	0.0
21	4.3	2712.2	0.0	0.0	0.0	0.0	0.0	0.0	0.0
22	0.3	203.0	0.0	0.0	0.0	0.0	0.0	0.0	0.0
23	0.3	226.1	0.0	0.0	0.0	0.0	0.0	0.0	0.0
24	0.3	184.5	0.0	0.0	0.0	0.0	0.0	0.0	0.0
25	0.4	276.9	0.0	0.0	0.0	0.0	0.0	0.0	0.0
26	3.2	2307.2	0.0	0.0	0.0	0.0	0.0	0.0	0.0
27	1.0	741.6	0.0	0.0	0.0	0.0	0.0	0.0	0.0
28	4.8	3772.1	0.0	0.0	0.0	0.0	0.0	0.0	0.0
29	4.8	3949.6	0.0	0.0	0.0	0.0	0.0	0.0	0.0
30	4.8	4057.6	0.0	0.0	0.0	0.0	0.0	0.0	0.0
31	4.8	4097.3	0.0	0.0	0.0	0.0	0.0	0.0	0.0
32	4.7	4069.8	0.0	0.0	0.0	0.0	0.0	0.0	0.0
33	4.7	3976.3	0.0	0.0	0.0	0.0	0.0	0.0	0.0
34	4.7	3818.6	0.0	0.0	0.0	0.0	0.0	0.0	0.0
35	4.6	3598.2	0.0	0.0	0.0	0.0	0.0	0.0	0.0
36	4.6	3317.1	0.0	0.0	0.0	0.0	0.0	0.0	0.0
37	4.5	2977.4	0.0	0.0	0.0	0.0	0.0	0.0	0.0
38	1.7	1015.4	0.0	0.0	0.0	0.0	0.0	0.0	0.0
39	2.8	1560.2	0.0	0.0	0.0	0.0	0.0	0.0	0.0
40	4.0	1897.2	0.0	0.0	0.0	0.0	0.0	0.0	0.0
41	0.5	198.1	0.0	0.0	0.0	0.0	0.0	0.0	0.0
42	4.4	1557.7	0.0	0.0	0.0	0.0	0.0	0.0	0.0
43	4.3	967.9	0.0	0.0	0.0	0.0	0.0	0.0	0.0
44	0.3	38.3	0.0	0.0	0.0	0.0	0.0	0.0	0.0
45	2.5	250.8	0.0	0.0	0.0	0.0	0.0	0.0	0.0
46	0.7	19.3	0.0	0.0	0.0	0.0	0.0	0.0	0.0

Failure Surface Specified By 29 Coordinate Points

Point No.	X-Surf (ft)	Y-Surf (ft)
1	100.00	47.90
2	104.91	46.94
3	109.84	46.14
4	114.80	45.51
5	119.78	45.04
6	124.77	44.73
7	129.77	44.59
8	134.77	44.62
9	139.77	44.80
10	144.75	45.16
11	149.73	45.68
12	154.68	46.36
13	159.61	47.21
14	164.50	48.21
15	169.37	49.38
16	174.19	50.71
17	178.96	52.20
18	183.68	53.85
19	188.35	55.65
20	192.95	57.60
21	197.48	59.70
22	201.95	61.95
23	206.34	64.35
24	210.64	66.89
25	214.86	69.58
26	218.99	72.40
27	223.02	75.35
28	226.96	78.44
29	230.31	81.26

*** Factor of Safety = 2.394 ***

1

Failure Surface Specified By 30 Coordinate Points

Point No.	X-Surf (ft)	Y-Surf (ft)
1	100.00	47.90
2	104.86	46.71
3	109.75	45.70
4	114.68	44.86
5	119.64	44.20
6	124.62	43.72
7	129.61	43.42
8	134.61	43.30
9	139.61	43.36
10	144.60	43.60
11	149.58	44.02
12	154.55	44.61
13	159.49	45.39
14	164.39	46.34

15	169.27	47.47
16	174.09	48.77
17	178.87	50.25
18	183.59	51.89
19	188.25	53.71
20	192.84	55.69
21	197.36	57.84
22	201.79	60.14
23	206.14	62.61
24	210.40	65.23
25	214.56	68.00
26	218.62	70.92
27	222.57	73.98
28	226.41	77.19
29	230.13	80.53
30	230.92	81.28

*** Factor of Safety = 2.420 ***

Failure Surface Specified By 30 Coordinate Points

Point No.	X-Surf (ft)	Y-Surf (ft)
1	100.00	47.90
2	104.82	46.56
3	109.68	45.40
4	114.58	44.42
5	119.52	43.63
6	124.49	43.04
7	129.47	42.63
8	134.46	42.41
9	139.46	42.38
10	144.46	42.54
11	149.45	42.89
12	154.42	43.43
13	159.37	44.16
14	164.28	45.07
15	169.16	46.18
16	173.99	47.46
17	178.77	48.93
18	183.49	50.59
19	188.14	52.42
20	192.72	54.42
21	197.22	56.60
22	201.64	58.95
23	205.96	61.46
24	210.18	64.14
25	214.30	66.97
26	218.31	69.96
27	222.20	73.10
28	225.97	76.39
29	229.61	79.81
30	231.06	81.29

*** Factor of Safety = 2.435 ***

1

Failure Surface Specified By 32 Coordinate Points

Point No.	X-Surf (ft)	Y-Surf (ft)
1	100.00	47.90
2	104.87	46.76
3	109.77	45.78
4	114.70	44.95
5	119.66	44.28
6	124.63	43.77
7	129.62	43.41
8	134.61	43.22
9	139.61	43.18
10	144.61	43.30
11	149.60	43.59
12	154.59	44.03
13	159.55	44.62
14	164.49	45.38
15	169.41	46.29
16	174.29	47.36
17	179.14	48.59
18	183.95	49.96
19	188.71	51.49
20	193.42	53.17
21	198.07	55.00
22	202.66	56.98
23	207.19	59.10
24	211.65	61.37
25	216.03	63.77
26	220.34	66.31
27	224.56	68.99
28	228.69	71.81
29	232.73	74.75
30	236.68	77.82
31	240.53	81.01
32	241.31	81.70

*** Factor of Safety = 2.471 ***

Failure Surface Specified By 33 Coordinate Points

Point No.	X-Surf (ft)	Y-Surf (ft)
1	100.00	47.90
2	104.50	45.72
3	109.10	43.75
4	113.78	41.99
5	118.53	40.45
6	123.35	39.13
7	128.23	38.02
8	133.15	37.14

9	138.11	36.49
10	143.09	36.06
11	148.09	35.86
12	153.09	35.89
13	158.08	36.15
14	163.06	36.63
15	168.01	37.34
16	172.92	38.28
17	177.78	39.44
18	182.59	40.82
19	187.33	42.41
20	191.99	44.23
21	196.56	46.25
22	201.03	48.48
23	205.40	50.91
24	209.66	53.54
25	213.79	56.36
26	217.78	59.36
27	221.64	62.54
28	225.34	65.90
29	228.89	69.42
30	232.28	73.10
31	235.49	76.93
32	238.53	80.91
33	239.01	81.61

*** Factor of Safety = 2.491 ***

1

Failure Surface Specified By 33 Coordinate Points

Point No.	X-Surf (ft)	Y-Surf (ft)
1	100.00	47.90
2	104.64	46.03
3	109.34	44.35
4	114.12	42.85
5	118.94	41.55
6	123.82	40.45
7	128.74	39.54
8	133.69	38.83
9	138.66	38.32
10	143.65	38.02
11	148.65	37.91
12	153.65	38.00
13	158.64	38.30
14	163.62	38.79
15	168.57	39.49
16	173.49	40.38
17	178.37	41.48
18	183.20	42.76
19	187.97	44.24
20	192.69	45.91
21	197.33	47.77
22	201.89	49.82
23	206.37	52.05
24	210.75	54.45

25	215.03	57.03
26	219.21	59.78
27	223.27	62.70
28	227.21	65.77
29	231.03	69.01
30	234.71	72.39
31	238.25	75.92
32	241.65	79.59
33	243.53	81.79

*** Factor of Safety = 2.505 ***

Failure Surface Specified By 34 Coordinate Points

Point No.	X-Surf (ft)	Y-Surf (ft)
1	100.00	47.90
2	104.63	46.01
3	109.33	44.30
4	114.09	42.77
5	118.90	41.43
6	123.77	40.27
7	128.67	39.31
8	133.62	38.54
9	138.58	37.96
10	143.57	37.58
11	148.56	37.39
12	153.56	37.39
13	158.56	37.59
14	163.54	37.99
15	168.51	38.57
16	173.45	39.36
17	178.35	40.33
18	183.22	41.49
19	188.03	42.84
20	192.79	44.38
21	197.48	46.10
22	202.10	48.00
23	206.65	50.09
24	211.11	52.34
25	215.48	54.77
26	219.76	57.37
27	223.92	60.13
28	227.98	63.05
29	231.92	66.13
30	235.74	69.36
31	239.43	72.73
32	242.98	76.25
33	246.40	79.90
34	248.19	81.98

*** Factor of Safety = 2.543 ***

1

Failure Surface Specified By 34 Coordinate Points

Point No.	X-Surf (ft)	Y-Surf (ft)
1	100.00	47.90
2	104.22	45.23
3	108.58	42.77
4	113.06	40.55
5	117.65	38.56
6	122.33	36.81
7	127.10	35.30
8	131.94	34.04
9	136.83	33.04
10	141.78	32.29
11	146.75	31.79
12	151.75	31.55
13	156.75	31.57
14	161.74	31.85
15	166.71	32.39
16	171.65	33.18
17	176.54	34.23
18	181.36	35.53
19	186.12	37.08
20	190.79	38.87
21	195.36	40.89
22	199.82	43.16
23	204.15	45.65
24	208.36	48.36
25	212.41	51.28
26	216.31	54.41
27	220.04	57.74
28	223.60	61.25
29	226.97	64.94
30	230.14	68.81
31	233.11	72.83
32	235.87	77.00
33	238.41	81.31
34	238.56	81.59

*** Factor of Safety = 2.549 ***

Failure Surface Specified By 35 Coordinate Points

Point No.	X-Surf (ft)	Y-Surf (ft)
1	100.00	47.90
2	104.28	45.31
3	108.67	42.92
4	113.17	40.75
5	117.78	38.80
6	122.47	37.07
7	127.24	35.57
8	132.07	34.29
9	136.96	33.26

10	141.90	32.46
11	146.87	31.89
12	151.86	31.57
13	156.86	31.48
14	161.85	31.64
15	166.84	32.04
16	171.80	32.67
17	176.72	33.54
18	181.60	34.65
19	186.41	35.99
20	191.16	37.56
21	195.83	39.36
22	200.40	41.38
23	204.87	43.61
24	209.23	46.06
25	213.47	48.72
26	217.57	51.57
27	221.54	54.62
28	225.35	57.86
29	229.00	61.27
30	232.48	64.86
31	235.79	68.61
32	238.91	72.51
33	241.85	76.56
34	244.58	80.75
35	245.23	81.86

*** Factor of Safety = 2.572 ***

1

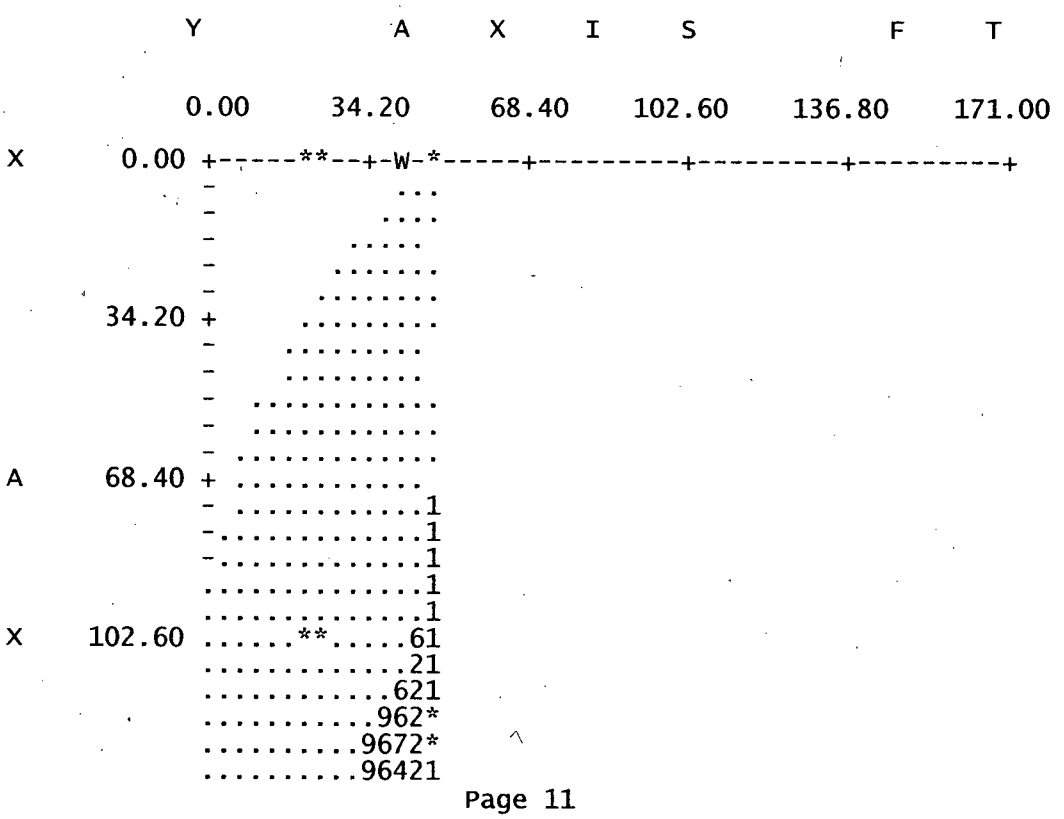

```
I     136.80 ..........96421*
             .........9.64211
             .........967.2.1
             -........967.32***
             -........9.6.321
             -........9.6.42*1
S     171.00 + ........967.2*1
             - ........9.6.32.1
             - ........9.67.32.1
             -  ........967.42.1
             -  ........0966.32.1
             -   ........086752211
      205.20 +    ........9.6.53*1
             -     .......0986.5*21
             -      ........066.5221
             -      .........08655411
             -        ........08665***
             -         .........876593
F     239.40 +          ..........8755
             -            .........887
             -             ..........8
             -               .........
             -                ........
             -                  ....
T     273.60 +           W  *   *  ***
```

JANBU #3 STATIC CIRCULAR

Geometry and Boundary Conditions
Problem: SMC Newfield Decommissioning - Section A-A' - FS Min = 2.191

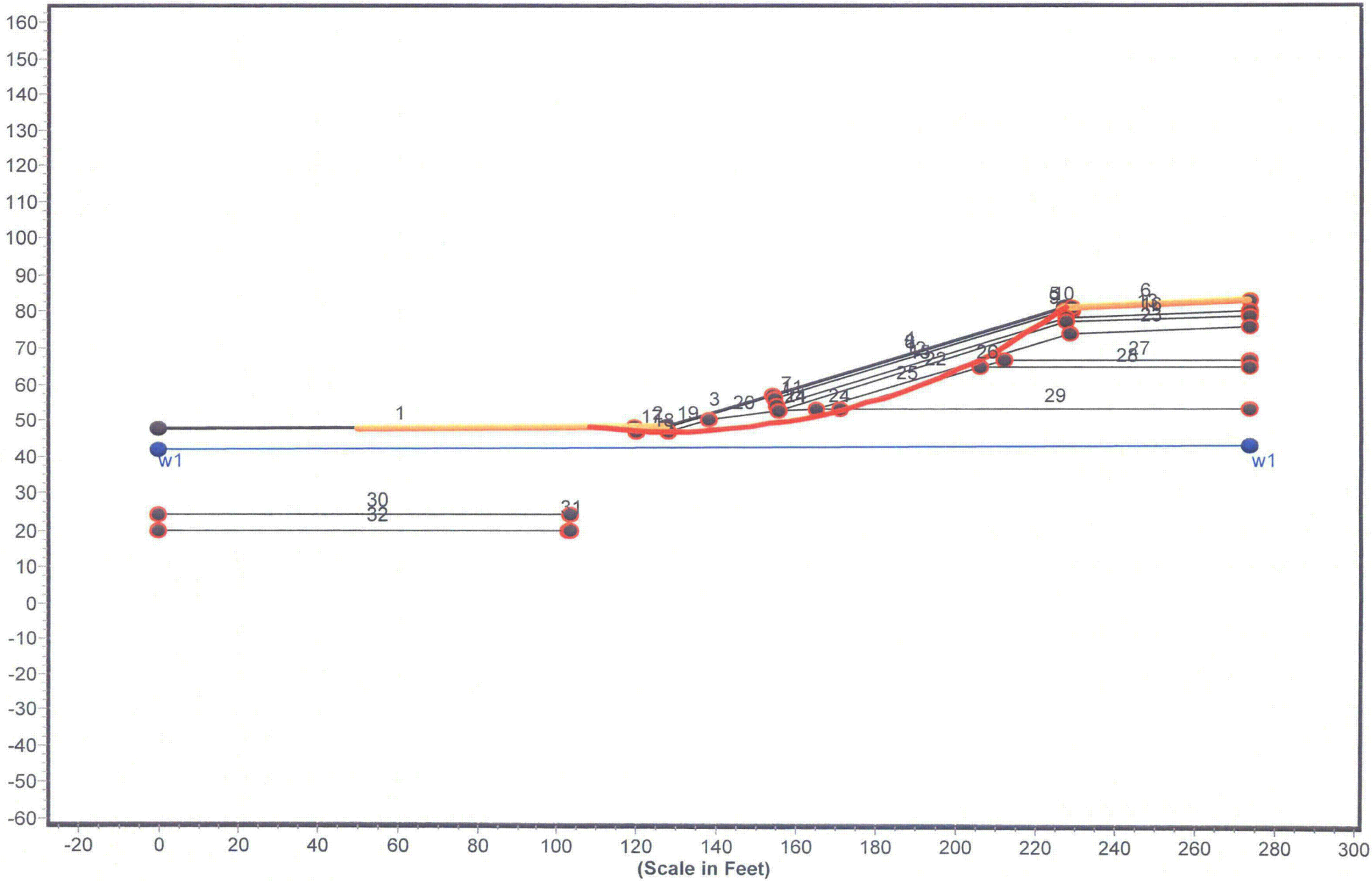

Geometry and Boundary Conditions

Problem: SMC Newfield Decommissioning - Section A-A' - FS Min = 2.191

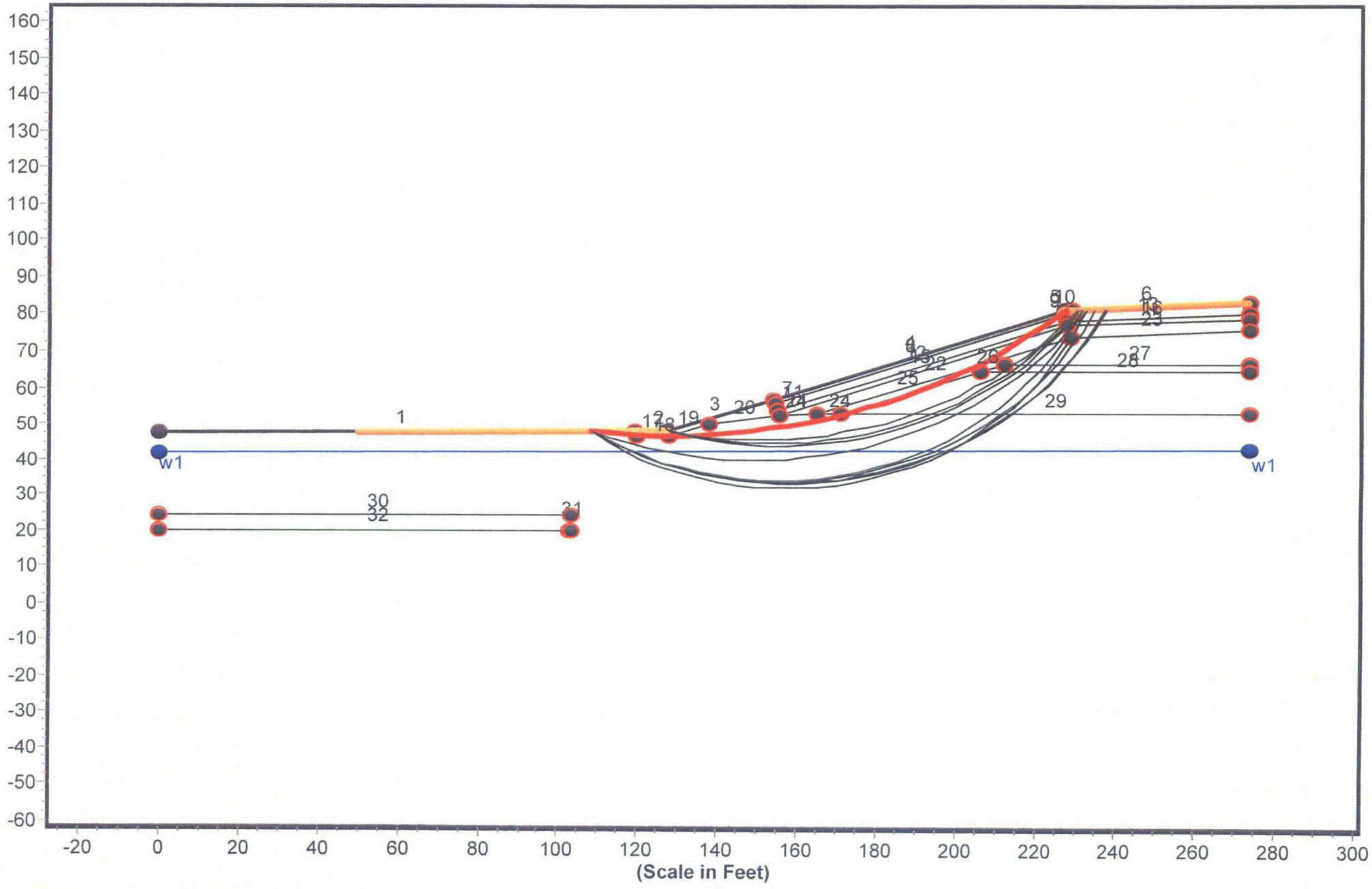

Geometry and Boundary Conditions
Problem: SMC Newfield Decommissioning - Section A-A' - FS Min = 2.191

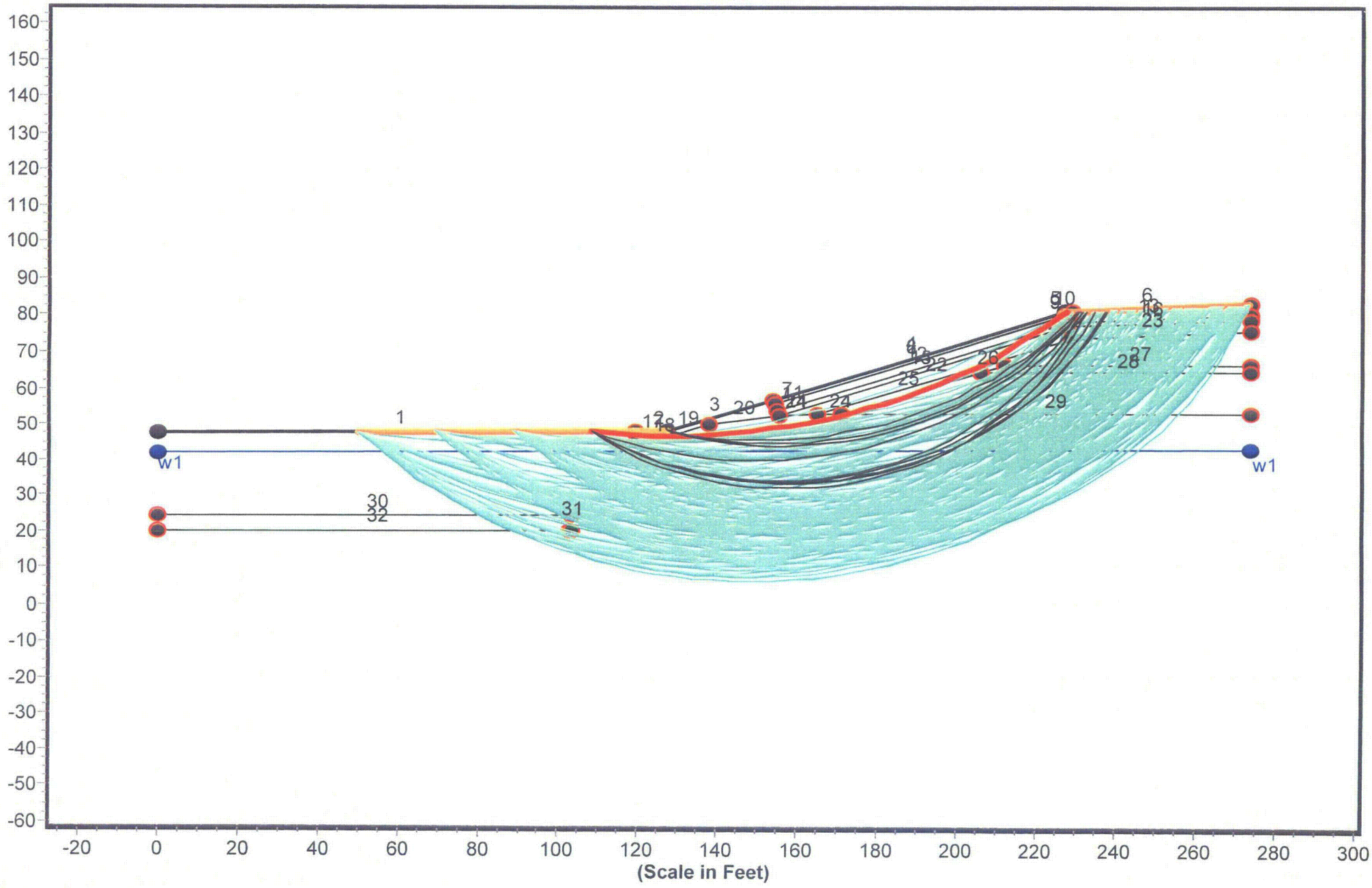

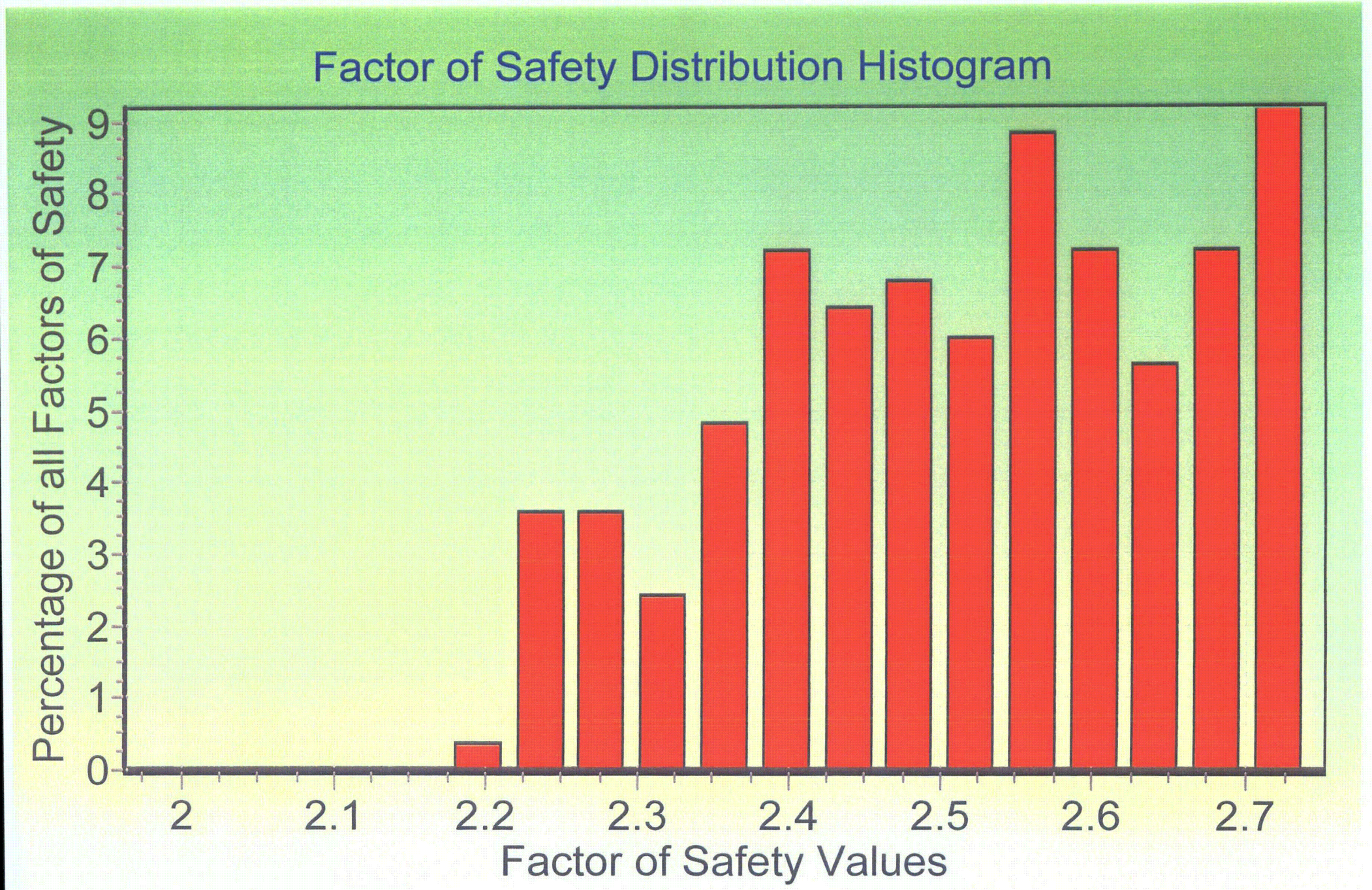
Factor of Safety Distribution Histogram
Percentage of all Factors of Safety
0
1
2
3
4
5
6
7
8
9
2
2.1
2.2
2.3
2.4
2.5
2.6
2.7
Factor of Safety Values

Janbu Circular #3 Results.txt
** PCSTABL6 **

by
Purdue University

1

--Slope Stability Analysis--
Simplified Janbu, Simplified Bishop
or Spencer's Method of Slices

Run Date:
Time of Run:
Run By:
Input Data Filename: run.in
Output Filename: result.out
Unit: ENGLISH
Plotted Output Filename: result.plt

PROBLEM DESCRIPTION SMC Newfield Decommissioning - Section A -A'

BOUNDARY COORDINATES

6 Top Boundaries
32 Total Boundaries

Boundary No.	X-Left (ft)	Y-Left (ft)	X-Right (ft)	Y-Right (ft)	Soil Type Below Bnd
1	0.00	47.40	119.50	48.00	7
2	119.50	48.00	127.50	48.00	1
3	127.50	48.00	153.90	56.80	1
4	153.90	56.80	226.90	81.10	1
5	226.90	81.10	228.90	81.20	1
6	228.90	81.20	273.60	83.00	2
7	153.90	56.80	154.20	55.80	1
8	154.20	55.80	227.10	80.10	2
9	227.10	80.10	228.80	80.20	2
10	228.80	80.20	228.90	81.20	2
11	154.20	55.80	154.80	53.90	1
12	154.80	53.90	227.40	78.10	1
13	227.40	78.10	273.60	80.00	1
14	154.80	53.90	155.20	52.60	1
15	155.20	52.60	227.60	77.10	3
16	227.60	77.10	273.60	79.00	3
17	119.50	48.00	119.60	46.40	7
18	119.60	46.40	127.80	46.40	7
19	127.80	46.40	137.90	49.80	7
20	137.90	49.80	155.20	52.60	7
21	155.20	52.60	164.60	53.00	7
22	164.60	53.00	228.20	74.10	4
23	228.20	74.10	273.60	76.00	4
24	164.60	53.00	171.00	53.00	7
25	171.00	53.00	205.80	64.60	6
26	205.80	64.60	211.80	66.60	5

27	211.80	66.60	273.60	66.60	5
28	205.80	64.60	273.60	64.60	6
29	171.00	53.00	273.60	53.00	7
30	0.00	24.00	103.10	24.00	8
31	103.00	20.00	103.10	24.00	7
32	0.00	20.00	103.10	20.00	7

1

ISOTROPIC SOIL PARAMETERS

8 Type(s) of Soil

Soil Type No.	Total Unit Wt. (pcf)	Saturated Unit Wt. (pcf)	Cohesion Intercept (psf)	Friction Angle (deg)	Pore Pressure Param.	Pressure Constant (psf)	Piez. Surface No.
1	135.0	140.0	0.0	40.0	0.00	0.0	0
2	135.0	140.0	0.0	35.0	0.00	0.0	0
3	125.0	130.0	250.0	15.0	0.00	0.0	0
4	125.0	135.0	0.0	32.0	0.00	0.0	0
5	135.0	140.0	0.0	38.0	0.00	0.0	0
6	135.0	140.0	0.0	40.0	0.00	0.0	0
7	115.0	130.0	0.0	33.0	0.00	0.0	1
8	130.0	140.0	300.0	20.0	0.00	0.0	1

1

1 PIEZOMETRIC SURFACE(S) HAVE BEEN SPECIFIED

Unit Weight of Water = 62.40

Piezometric Surface No. 1 Specified by 2 Coordinate Points

Point No.	X-Water (ft)	Y-Water (ft)
1	0.00	41.70
2	273.60	42.50

1

A Critical Failure Surface Searching Method, Using A Random Technique For Generating Circular Surfaces, Has Been Specified.

250 Trial Surfaces Have Been Generated.

50 Surfaces Initiate From Each Of 5 Points Equally Spaced Along The Ground Surface Between X = 50.00 ft.
and X = 127.50 ft.

Each Surface Terminates Between X = 226.00 ft.
and X = 273.00 ft.

Unless Further Limitations Were Imposed, The Minimum Elevation At Which A Surface Extends Is Y = 0.00 ft.

5.00 ft. Line Segments Define Each Trial Failure Surface.

Restrictions Have Been Imposed Upon The Angle Of Initiation. The Angle Has Been Restricted Between The Angles Of -45.0 And -5.0 deg.

1

Following Are Displayed The Ten Most Critical Of The Trial Failure Surfaces Examined. They Are Ordered - Most Critical First.

* * Safety Factors Are Calculated By The Modified Janbu Method * *

Failure Surface Specified By 27 Coordinate Points

Point No.	X-Surf (ft)	Y-Surf (ft)
1	108.13	47.94
2	113.10	47.42
3	118.08	47.05
4	123.08	46.84
5	128.08	46.78
6	133.08	46.87
7	138.07	47.12
8	143.06	47.52
9	148.03	48.07
10	152.98	48.78
11	157.90	49.64
12	162.80	50.65
13	167.66	51.81
14	172.49	53.11
15	177.27	54.57
16	182.01	56.18
17	186.69	57.92
18	191.32	59.82
19	195.89	61.85
20	200.39	64.02
21	204.82	66.33
22	209.18	68.78
23	213.47	71.36
24	217.67	74.07
25	221.79	76.91
26	225.81	79.87
27	227.41	81.13

*** 2.191 ***

Individual data on the 44 slices

Slice No.	Width (ft)	Weight (lbs)	Water Force Top (lbs)	Water Force Bot (lbs)	Force Norm (lbs)	Force Tan (lbs)	Earthquake Force Hor (lbs)	Earthquake Force Ver (lbs)	Surcharge Load (lbs)
1	5.0	156.4	0.0	0.0	0.0	0.0	0.0	0.0	0.0
2	5.0	426.4	0.0	0.0	0.0	0.0	0.0	0.0	0.0
3	1.4	158.6	0.0	0.0	0.0	0.0	0.0	0.0	0.0
4	0.1	8.0	0.0	0.0	0.0	0.0	0.0	0.0	0.0
5	3.5	516.0	0.0	0.0	0.0	0.0	0.0	0.0	0.0
6	4.4	709.7	0.0	0.0	0.0	0.0	0.0	0.0	0.0
7	0.6	103.0	0.0	0.0	0.0	0.0	0.0	0.0	0.0
8	0.9	186.6	0.0	0.0	0.0	0.0	0.0	0.0	0.0
9	4.1	1246.6	0.0	0.0	0.0	0.0	0.0	0.0	0.0
10	4.8	2198.7	0.0	0.0	0.0	0.0	0.0	0.0	0.0
11	0.2	92.8	0.0	0.0	0.0	0.0	0.0	0.0	0.0
12	5.0	3099.4	0.0	0.0	0.0	0.0	0.0	0.0	0.0
13	5.0	3850.4	0.0	0.0	0.0	0.0	0.0	0.0	0.0
14	4.9	4501.9	0.0	0.0	0.0	0.0	0.0	0.0	0.0
15	0.9	908.0	0.0	0.0	0.0	0.0	0.0	0.0	0.0
16	0.3	298.7	0.0	0.0	0.0	0.0	0.0	0.0	0.0
17	0.6	603.2	0.0	0.0	0.0	0.0	0.0	0.0	0.0
18	0.4	406.5	0.0	0.0	0.0	0.0	0.0	0.0	0.0
19	2.7	2833.7	0.0	0.0	0.0	0.0	0.0	0.0	0.0
20	4.9	5485.0	0.0	0.0	0.0	0.0	0.0	0.0	0.0
21	1.8	2117.0	0.0	0.0	0.0	0.0	0.0	0.0	0.0
22	3.1	3702.0	0.0	0.0	0.0	0.0	0.0	0.0	0.0
23	3.3	4165.7	0.0	0.0	0.0	0.0	0.0	0.0	0.0
24	1.1	1355.5	0.0	0.0	0.0	0.0	0.0	0.0	0.0
25	0.4	541.2	0.0	0.0	0.0	0.0	0.0	0.0	0.0
26	4.8	6180.9	0.0	0.0	0.0	0.0	0.0	0.0	0.0
27	4.7	6153.3	0.0	0.0	0.0	0.0	0.0	0.0	0.0
28	4.7	6016.5	0.0	0.0	0.0	0.0	0.0	0.0	0.0
29	4.1	5067.2	0.0	0.0	0.0	0.0	0.0	0.0	0.0
30	0.6	707.4	0.0	0.0	0.0	0.0	0.0	0.0	0.0
31	4.6	5444.9	0.0	0.0	0.0	0.0	0.0	0.0	0.0
32	4.5	5032.3	0.0	0.0	0.0	0.0	0.0	0.0	0.0
33	4.4	4535.7	0.0	0.0	0.0	0.0	0.0	0.0	0.0
34	0.0	41.8	0.0	0.0	0.0	0.0	0.0	0.0	0.0
35	4.3	3919.2	0.0	0.0	0.0	0.0	0.0	0.0	0.0
36	4.3	3314.5	0.0	0.0	0.0	0.0	0.0	0.0	0.0
37	3.1	1999.4	0.0	0.0	0.0	0.0	0.0	0.0	0.0
38	1.1	601.9	0.0	0.0	0.0	0.0	0.0	0.0	0.0
39	2.2	1061.0	0.0	0.0	0.0	0.0	0.0	0.0	0.0
40	1.9	729.8	0.0	0.0	0.0	0.0	0.0	0.0	0.0
41	3.5	846.3	0.0	0.0	0.0	0.0	0.0	0.0	0.0
42	0.5	65.4	0.0	0.0	0.0	0.0	0.0	0.0	0.0
43	1.1	91.0	0.0	0.0	0.0	0.0	0.0	0.0	0.0
44	0.5	12.9	0.0	0.0	0.0	0.0	0.0	0.0	0.0

Failure Surface Specified By 30 Coordinate Points

Point No.	X-Surf (ft)	Y-Surf (ft)
1	108.13	47.94
2	112.38	45.31
3	116.78	42.94
4	121.31	40.83

5	125.96	38.99
6	130.71	37.43
7	135.54	36.14
8	140.44	35.15
9	145.39	34.44
10	150.38	34.03
11	155.37	33.91
12	160.37	34.08
13	165.35	34.55
14	170.29	35.31
15	175.18	36.36
16	180.00	37.69
17	184.73	39.31
18	189.36	41.20
19	193.87	43.36
20	198.25	45.78
21	202.47	48.45
22	206.53	51.37
23	210.41	54.52
24	214.10	57.89
25	217.59	61.48
26	220.86	65.26
27	223.90	69.23
28	226.70	73.37
29	229.26	77.67
30	231.13	81.29

*** 2.218 ***

1

Failure Surface Specified By 24 Coordinate Points

Point No.	X-Surf (ft)	Y-Surf (ft)
1	127.50	48.00
2	132.41	47.04
3	137.35	46.31
4	142.33	45.81
5	147.32	45.55
6	152.32	45.53
7	157.32	45.73
8	162.30	46.17
9	167.25	46.85
10	172.17	47.76
11	177.04	48.90
12	181.85	50.26
13	186.59	51.85
14	191.25	53.66
15	195.82	55.69
16	200.29	57.92
17	204.65	60.37
18	208.89	63.02
19	213.00	65.87
20	216.98	68.90
21	220.80	72.12
22	224.48	75.51
23	227.98	79.08

24	229.92	81.24

*** 2.226 ***

Failure Surface Specified By 31 Coordinate Points

Point No.	X-Surf (ft)	Y-Surf (ft)
1	108.13	47.94
2	112.22	45.07
3	116.48	42.45
4	120.89	40.10
5	125.44	38.03
6	130.11	36.24
7	134.88	34.73
8	139.73	33.52
9	144.65	32.61
10	149.61	32.01
11	154.60	31.71
12	159.60	31.71
13	164.59	32.02
14	169.55	32.64
15	174.47	33.56
16	179.32	34.77
17	184.08	36.29
18	188.75	38.09
19	193.29	40.17
20	197.70	42.53
21	201.96	45.15
22	206.04	48.03
23	209.95	51.16
24	213.65	54.52
25	217.14	58.10
26	220.41	61.88
27	223.44	65.86
28	226.22	70.02
29	228.74	74.33
30	230.99	78.80
31	232.07	81.33

*** 2.227 ***

1

Failure Surface Specified By 24 Coordinate Points

Point No.	X-Surf (ft)	Y-Surf (ft)
1	127.50	48.00
2	132.36	46.81
3	137.27	45.87
4	142.22	45.17

5	147.20	44.73
6	152.20	44.54
7	157.20	44.60
8	162.19	44.91
9	167.15	45.47
10	172.09	46.29
11	176.97	47.35
12	181.80	48.65
13	186.55	50.20
14	191.23	51.98
15	195.80	54.00
16	200.27	56.25
17	204.62	58.72
18	208.83	61.40
19	212.91	64.29
20	216.84	67.39
21	220.60	70.68
22	224.20	74.15
23	227.61	77.80
24	230.54	81.27

*** 2.227 ***

Failure Surface Specified By 31 Coordinate Points

Point No.	X-Surf (ft)	Y-Surf (ft)
1	108.13	47.94
2	112.40	45.36
3	116.82	43.02
4	121.37	40.93
5	126.02	39.10
6	130.77	37.54
7	135.60	36.25
8	140.50	35.23
9	145.44	34.49
10	150.42	34.03
11	155.42	33.85
12	160.41	33.95
13	165.40	34.33
14	170.36	35.00
15	175.27	35.94
16	180.11	37.16
17	184.89	38.65
18	189.57	40.41
19	194.14	42.43
20	198.60	44.70
21	202.92	47.22
22	207.08	49.98
23	211.09	52.97
24	214.92	56.18
25	218.57	59.60
26	222.02	63.23
27	225.25	67.04
28	228.27	71.02
29	231.05	75.18
30	233.60	79.48

31	234.62	81.43

*** 2.229 ***

1

Failure Surface Specified By 25 Coordinate Points

Point No.	X-Surf (ft)	Y-Surf (ft)
1	127.50	48.00
2	132.32	46.66
3	137.20	45.57
4	142.13	44.74
5	147.09	44.17
6	152.09	43.87
7	157.09	43.83
8	162.08	44.05
9	167.06	44.54
10	172.00	45.29
11	176.90	46.30
12	181.73	47.57
13	186.50	49.10
14	191.17	50.87
15	195.75	52.88
16	200.21	55.14
17	204.54	57.63
18	208.74	60.34
19	212.79	63.28
20	216.68	66.42
21	220.40	69.76
22	223.94	73.30
23	227.28	77.02
24	230.42	80.90
25	230.69	81.27

*** 2.230 ***

Failure Surface Specified By 32 Coordinate Points

Point No.	X-Surf (ft)	Y-Surf (ft)
1	108.13	47.94
2	112.38	45.32
3	116.77	42.93
4	121.29	40.79
5	125.92	38.91
6	130.65	37.28
7	135.46	35.92
8	140.34	34.83
9	145.28	34.02
10	150.25	33.47

11	155.24	33.21
12	160.24	33.22
13	165.23	33.51
14	170.20	34.08
15	175.13	34.92
16	180.00	36.04
17	184.81	37.42
18	189.53	39.07
19	194.15	40.98
20	198.66	43.15
21	203.04	45.56
22	207.28	48.21
23	211.36	51.09
24	215.28	54.19
25	219.02	57.51
26	222.58	61.03
27	225.93	64.74
28	229.07	68.63
29	231.98	72.69
30	234.67	76.91
31	237.12	81.27
32	237.25	81.54

*** 2.243 ***

1

Failure Surface Specified By 32 Coordinate Points

Point No.	X-Surf (ft)	Y-Surf (ft)
1	108.13	47.94
2	112.40	45.34
3	116.81	42.99
4	121.34	40.87
5	125.98	39.02
6	130.72	37.42
7	135.54	36.08
8	140.42	35.01
9	145.36	34.21
10	150.33	33.69
11	155.32	33.44
12	160.32	33.46
13	165.31	33.77
14	170.28	34.34
15	175.21	35.19
16	180.08	36.31
17	184.88	37.70
18	189.60	39.35
19	194.23	41.25
20	198.74	43.41
21	203.12	45.82
22	207.36	48.46
23	211.46	51.33
24	215.39	54.42
25	219.14	57.73
26	222.70	61.24
27	226.07	64.94

28	229.22	68.81
29	232.16	72.86
30	234.87	77.06
31	237.34	81.41
32	237.41	81.54

*** 2.244 ***

Failure Surface Specified By 29 Coordinate Points

Point No.	X-Surf (ft)	Y-Surf (ft)
1	108.13	47.94
2	112.78	46.12
3	117.52	44.52
4	122.32	43.14
5	127.19	42.00
6	132.11	41.09
7	137.06	40.41
8	142.04	39.98
9	147.04	39.78
10	152.04	39.82
11	157.03	40.09
12	162.00	40.61
13	166.95	41.36
14	171.85	42.35
15	176.70	43.57
16	181.48	45.01
17	186.20	46.69
18	190.82	48.59
19	195.35	50.70
20	199.77	53.03
21	204.08	55.57
22	208.26	58.31
23	212.31	61.25
24	216.21	64.38
25	219.96	67.69
26	223.55	71.17
27	226.96	74.82
28	230.20	78.63
29	232.28	81.34

*** 2.248 ***

1

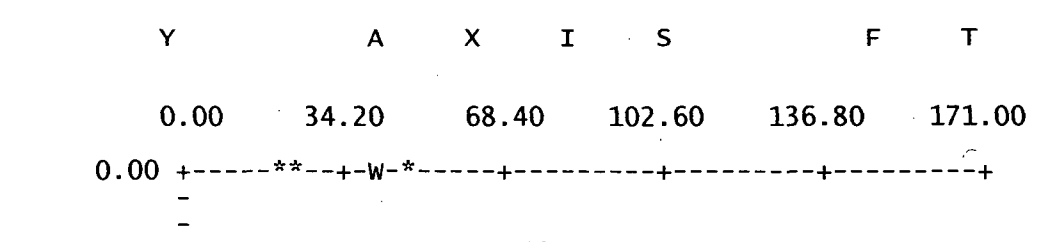

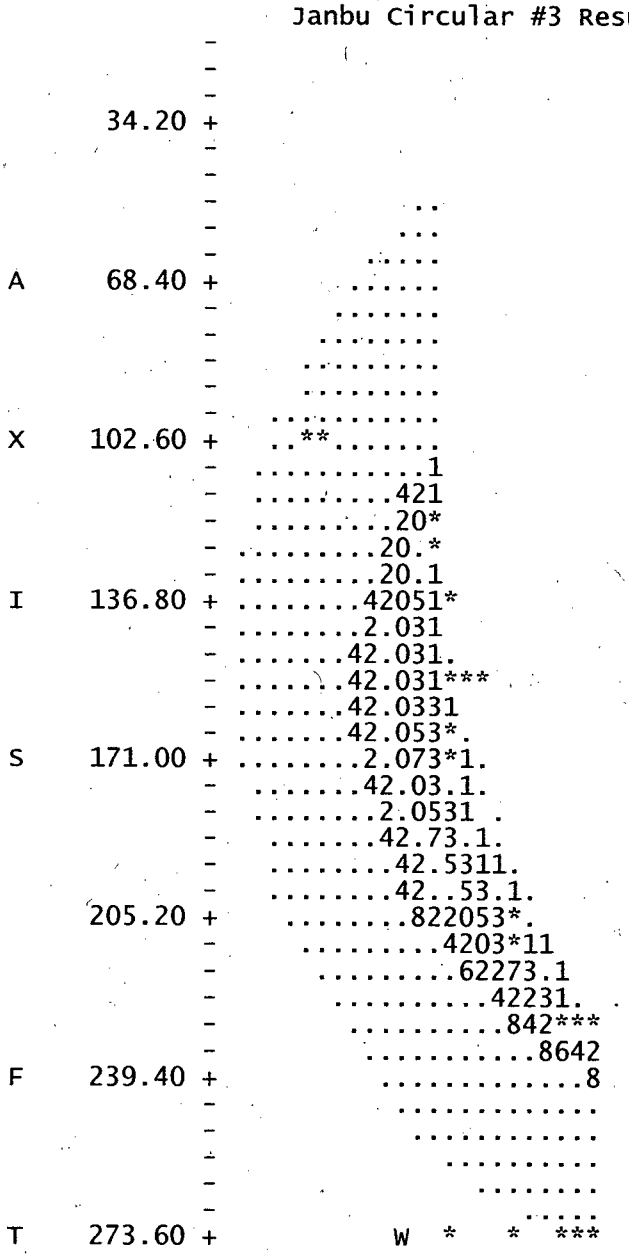
34.20
A 68.40
X 102.60
I 136.80
S 171.00
205.20
F 239.40
T 273.60

BISHOP #3 STATIC CIRCULAR

Geometry and Boundary Conditions

Problem: SMC Newfield Decommissioning - Section A-A' - FS Min = 2.251

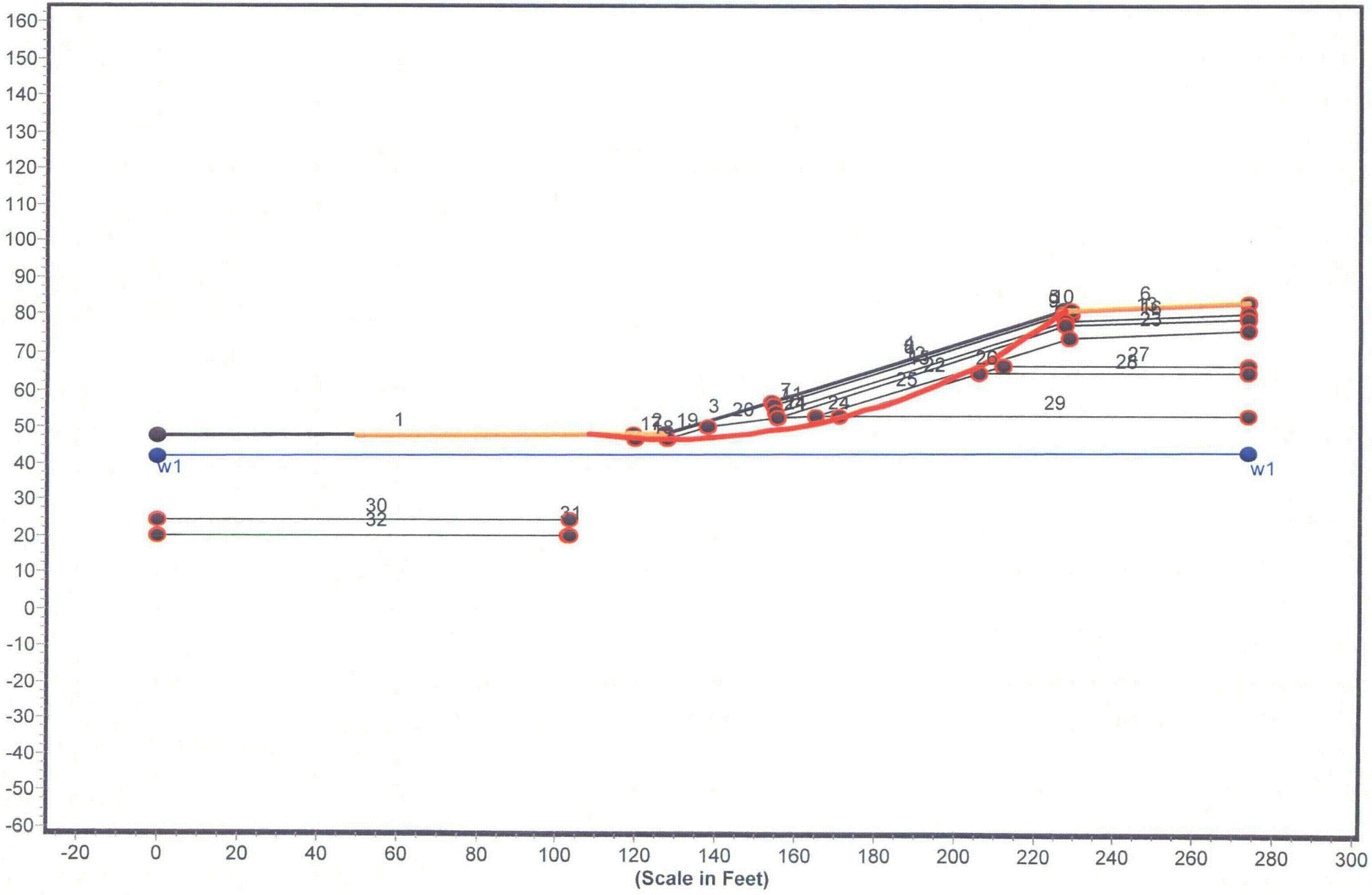

Geometry and Boundary Conditions

Problem: SMC Newfield Decommissioning - Section A-A' - FS Min = 2.251

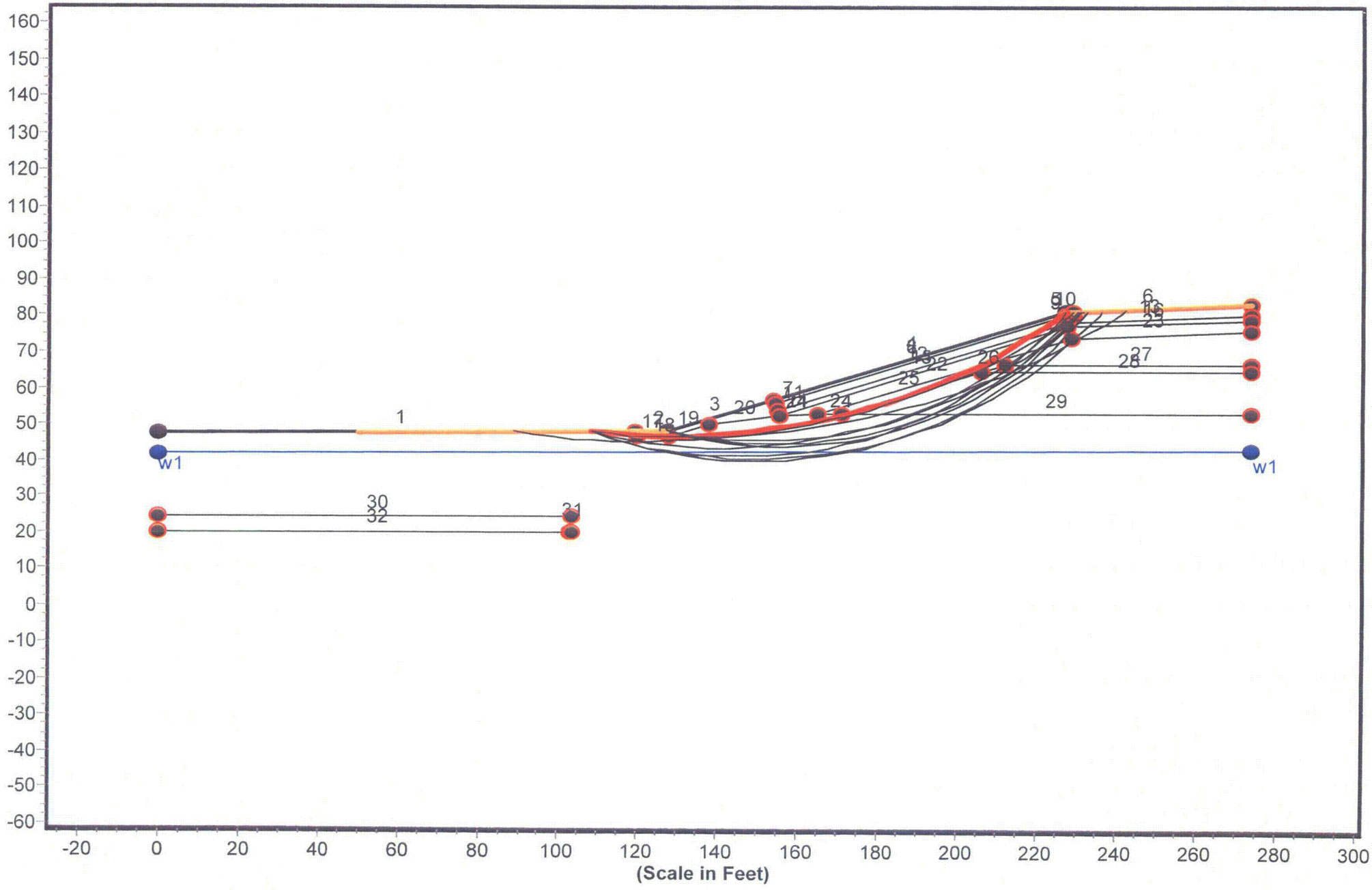

Geometry and Boundary Conditions
Problem: SMC Newfield Decommissioning - Section A-A' - FS Min = 2.251

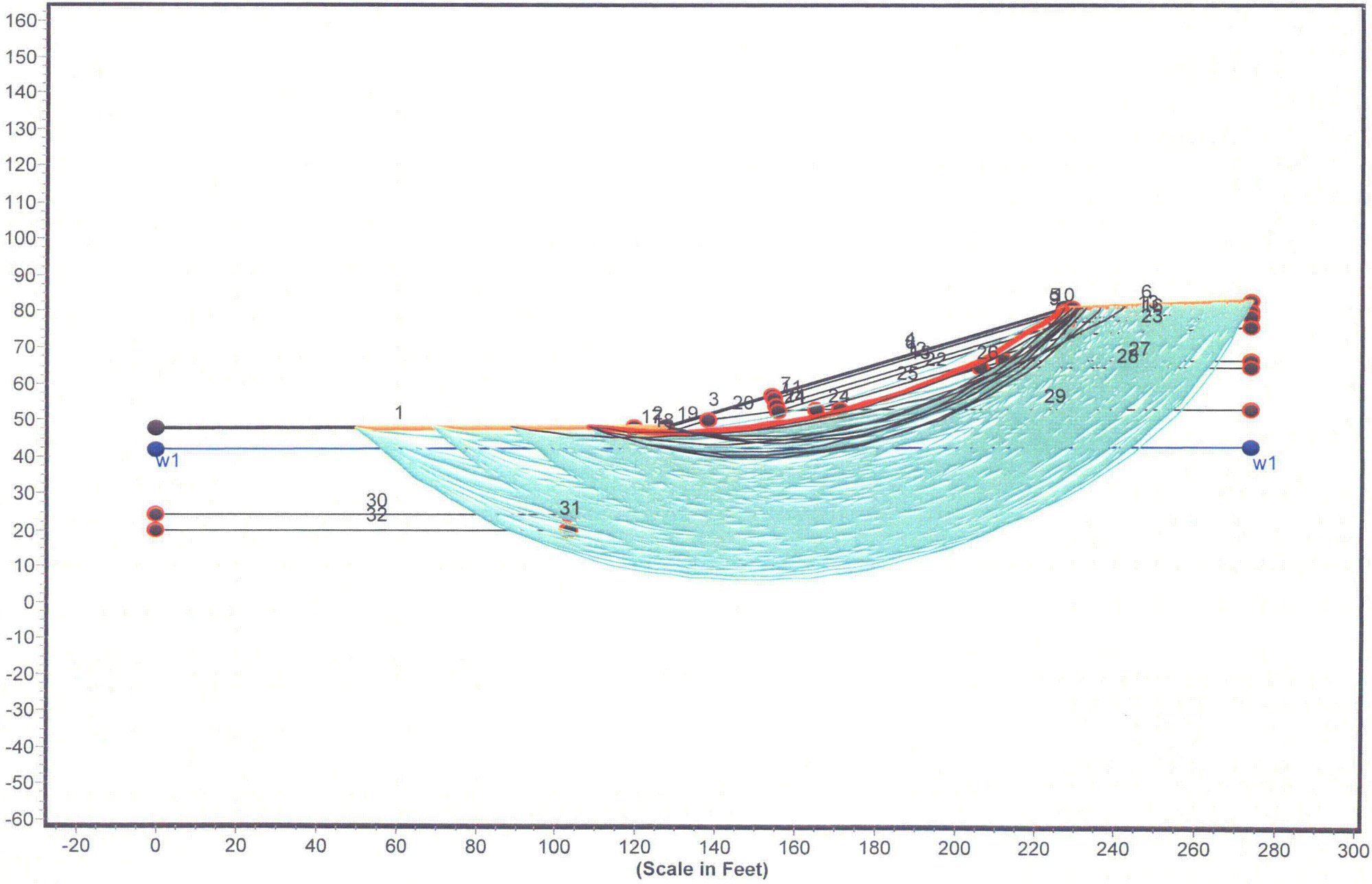

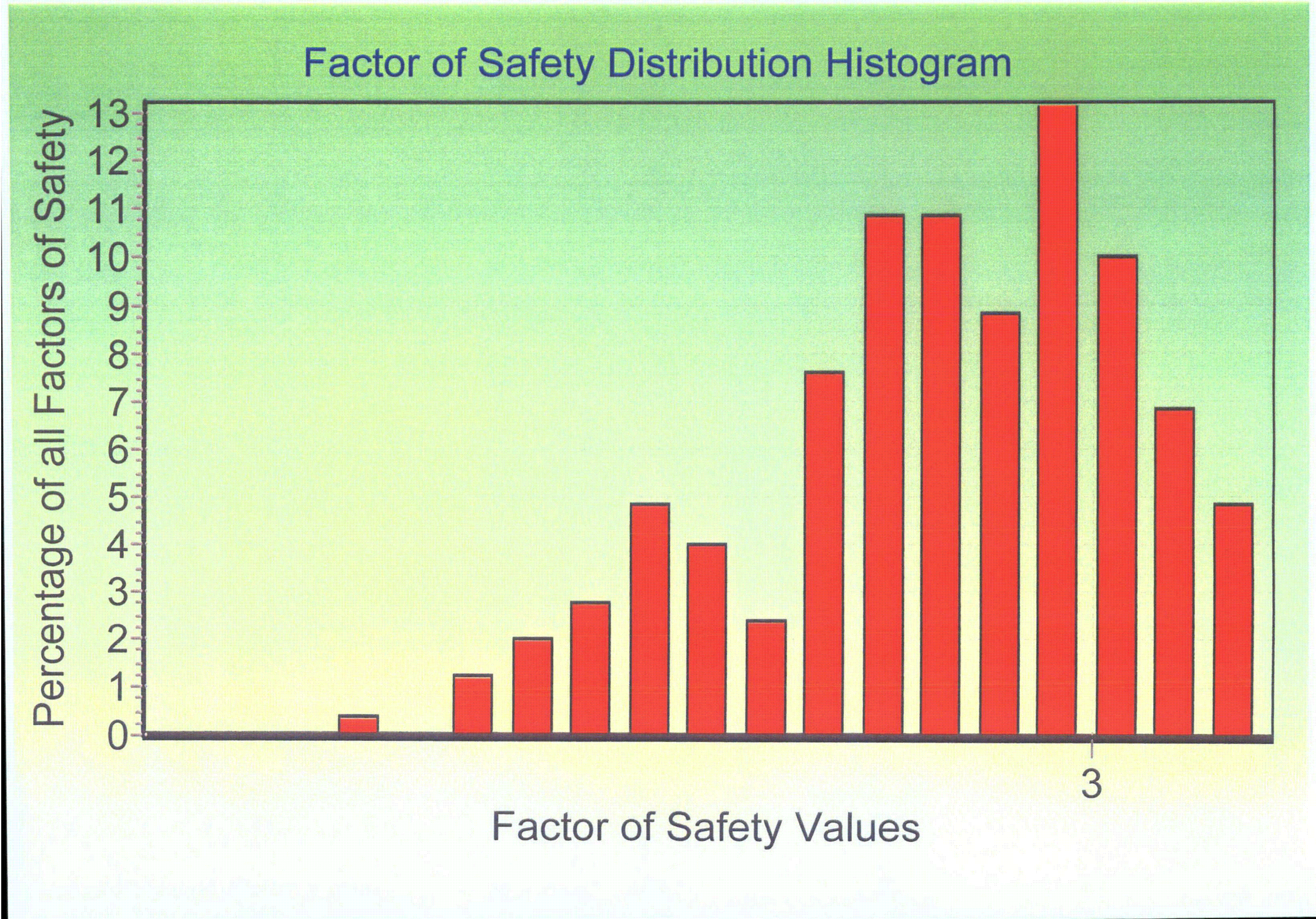
Factor of Safety Distribution Histogram
Percentage of all Factors of Safety
0
1
2
3
4
5
6
7
8
9
10
11
12
13
3
Factor of Safety Values

SMC Bishop Circular Results #3.txt
** PCSTABL6 **

by
Purdue University

1

--Slope Stability Analysis--
Simplified Janbu, Simplified Bishop
or Spencer's Method of Slices

Run Date:
Time of Run:
Run By:
Input Data Filename: run.in
Output Filename: result.out
Unit: ENGLISH
Plotted Output Filename: result.plt

PROBLEM DESCRIPTION SMC Newfield Decommissioning - Section A -A'

BOUNDARY COORDINATES

6 Top Boundaries
32 Total Boundaries

Boundary No.	X-Left (ft)	Y-Left (ft)	X-Right (ft)	Y-Right (ft)	Soil Type Below Bnd
1	0.00	47.40	119.50	48.00	7
2	119.50	48.00	127.50	48.00	1
3	127.50	48.00	153.90	56.80	1
4	153.90	56.80	226.90	81.10	1
5	226.90	81.10	228.90	81.20	1
6	228.90	81.20	273.60	83.00	2
7	153.90	56.80	154.20	55.80	1
8	154.20	55.80	227.10	80.10	2
9	227.10	80.10	228.80	80.20	2
10	228.80	80.20	228.90	81.20	2
11	154.20	55.80	154.80	53.90	1
12	154.80	53.90	227.40	78.10	1
13	227.40	78.10	273.60	80.00	1
14	154.80	53.90	155.20	52.60	1
15	155.20	52.60	227.60	77.10	3
16	227.60	77.10	273.60	79.00	3
17	119.50	48.00	119.60	46.40	7
18	119.60	46.40	127.80	46.40	7
19	127.80	46.40	137.90	49.80	7
20	137.90	49.80	155.20	52.60	7
21	155.20	52.60	164.60	53.00	7
22	164.60	53.00	228.20	74.10	4
23	228.20	74.10	273.60	76.00	4
24	164.60	53.00	171.00	53.00	7
25	171.00	53.00	205.80	64.60	6
26	205.80	64.60	211.80	66.60	5

27	211.80	66.60	273.60	66.60	5
28	205.80	64.60	273.60	64.60	6
29	171.00	53.00	273.60	53.00	7
30	0.00	24.00	103.10	24.00	8
31	103.00	20.00	103.10	24.00	7
32	0.00	20.00	103.10	20.00	7

1

ISOTROPIC SOIL PARAMETERS

8 Type(s) of Soil

Soil Type No.	Total Unit Wt. (pcf)	Saturated Unit Wt. (pcf)	Cohesion Intercept (psf)	Friction Angle (deg)	Pore Pressure Param.	Pressure Constant (psf)	Piez. Surface No.
1	135.0	140.0	0.0	40.0	0.00	0.0	0
2	135.0	140.0	0.0	35.0	0.00	0.0	0
3	125.0	130.0	250.0	15.0	0.00	0.0	0
4	125.0	135.0	0.0	32.0	0.00	0.0	0
5	135.0	140.0	0.0	38.0	0.00	0.0	0
6	135.0	140.0	0.0	40.0	0.00	0.0	0
7	115.0	130.0	0.0	33.0	0.00	0.0	1
8	130.0	140.0	300.0	20.0	0.00	0.0	1

1

1 PIEZOMETRIC SURFACE(S) HAVE BEEN SPECIFIED

Unit Weight of Water = 62.40

Piezometric Surface No. 1 Specified by 2 Coordinate Points

Point No.	X-Water (ft)	Y-Water (ft)
1	0.00	41.70
2	273.60	42.50

1

A Critical Failure Surface Searching Method, Using A Random Technique For Generating Circular Surfaces, Has Been Specified.

250 Trial Surfaces Have Been Generated.

50 Surfaces Initiate From Each Of 5 Points Equally Spaced Along The Ground Surface Between X = 50.00 ft.
and X = 127.50 ft.

Each Surface Terminates Between X = 226.00 ft.
and X = 273.60 ft.

Unless Further Limitations Were Imposed, The Minimum Elevation At Which A Surface Extends Is Y = 0.00 ft.

5.00 ft. Line Segments Define Each Trial Failure Surface.

Restrictions Have Been Imposed Upon The Angle Of Initiation. The Angle Has Been Restricted Between The Angles Of -45.0 And -5.0 deg.

1

Following Are Displayed The Ten Most Critical Of The Trial Failure Surfaces Examined. They Are Ordered - Most Critical First.

* * Safety Factors Are Calculated By The Modified Bishop Method * *

Failure Surface Specified By 27 Coordinate Points

Point No.	X-Surf (ft)	Y-Surf (ft)
1	108.13	47.94
2	113.10	47.42
3	118.08	47.05
4	123.08	46.84
5	128.08	46.78
6	133.08	46.87
7	138.07	47.12
8	143.06	47.52
9	148.03	48.07
10	152.98	48.78
11	157.90	49.63
12	162.80	50.64
13	167.66	51.80
14	172.49	53.11
15	177.27	54.57
16	182.01	56.17
17	186.69	57.92
18	191.32	59.81
19	195.89	61.85
20	200.39	64.02
21	204.82	66.33
22	209.18	68.78
23	213.47	71.36
24	217.67	74.07
25	221.79	76.90
26	225.81	79.87
27	227.42	81.13

Circle Center At X = 127.6 ; Y = 209.2 and Radius, 162.4

*** 2.251 ***

Individual data on the 44 slices

Slice No.	Width (ft)	Weight (lbs)	Water Force Top (lbs)	Water Force Bot (lbs)	Force Norm (lbs)	Force Tan (lbs)	Earthquake Force Hor (lbs)	Earthquake Force Ver (lbs)	Surcharge Load (lbs)
1	5.0	156.4	0.0	0.0	0.0	0.0	0.0	0.0	0.0
2	5.0	426.4	0.0	0.0	0.0	0.0	0.0	0.0	0.0
3	1.4	158.6	0.0	0.0	0.0	0.0	0.0	0.0	0.0
4	0.1	8.0	0.0	0.0	0.0	0.0	0.0	0.0	0.0
5	3.5	516.0	0.0	0.0	0.0	0.0	0.0	0.0	0.0
6	4.4	709.8	0.0	0.0	0.0	0.0	0.0	0.0	0.0
7	0.6	103.0	0.0	0.0	0.0	0.0	0.0	0.0	0.0
8	0.9	186.5	0.0	0.0	0.0	0.0	0.0	0.0	0.0
9	4.1	1246.8	0.0	0.0	0.0	0.0	0.0	0.0	0.0
10	4.8	2198.9	0.0	0.0	0.0	0.0	0.0	0.0	0.0
11	0.2	92.8	0.0	0.0	0.0	0.0	0.0	0.0	0.0
12	5.0	3099.5	0.0	0.0	0.0	0.0	0.0	0.0	0.0
13	5.0	3850.6	0.0	0.0	0.0	0.0	0.0	0.0	0.0
14	4.9	4502.3	0.0	0.0	0.0	0.0	0.0	0.0	0.0
15	0.9	908.0	0.0	0.0	0.0	0.0	0.0	0.0	0.0
16	0.3	298.7	0.0	0.0	0.0	0.0	0.0	0.0	0.0
17	0.6	603.2	0.0	0.0	0.0	0.0	0.0	0.0	0.0
18	0.4	406.5	0.0	0.0	0.0	0.0	0.0	0.0	0.0
19	2.7	2834.0	0.0	0.0	0.0	0.0	0.0	0.0	0.0
20	4.9	5485.6	0.0	0.0	0.0	0.0	0.0	0.0	0.0
21	1.8	2117.1	0.0	0.0	0.0	0.0	0.0	0.0	0.0
22	3.1	3702.6	0.0	0.0	0.0	0.0	0.0	0.0	0.0
23	3.3	4166.0	0.0	0.0	0.0	0.0	0.0	0.0	0.0
24	1.1	1362.3	0.0	0.0	0.0	0.0	0.0	0.0	0.0
25	0.4	534.9	0.0	0.0	0.0	0.0	0.0	0.0	0.0
26	4.8	6182.0	0.0	0.0	0.0	0.0	0.0	0.0	0.0
27	4.7	6154.5	0.0	0.0	0.0	0.0	0.0	0.0	0.0
28	4.7	6018.0	0.0	0.0	0.0	0.0	0.0	0.0	0.0
29	4.1	5109.3	0.0	0.0	0.0	0.0	0.0	0.0	0.0
30	0.5	666.8	0.0	0.0	0.0	0.0	0.0	0.0	0.0
31	4.6	5446.6	0.0	0.0	0.0	0.0	0.0	0.0	0.0
32	4.5	5034.2	0.0	0.0	0.0	0.0	0.0	0.0	0.0
33	4.4	4537.8	0.0	0.0	0.0	0.0	0.0	0.0	0.0
34	0.1	56.9	0.0	0.0	0.0	0.0	0.0	0.0	0.0
35	4.3	3906.3	0.0	0.0	0.0	0.0	0.0	0.0	0.0
36	4.3	3316.9	0.0	0.0	0.0	0.0	0.0	0.0	0.0
37	3.1	2010.0	0.0	0.0	0.0	0.0	0.0	0.0	0.0
38	1.1	593.9	0.0	0.0	0.0	0.0	0.0	0.0	0.0
39	2.2	1068.4	0.0	0.0	0.0	0.0	0.0	0.0	0.0
40	1.9	725.2	0.0	0.0	0.0	0.0	0.0	0.0	0.0
41	3.5	850.8	0.0	0.0	0.0	0.0	0.0	0.0	0.0
42	0.5	63.8	0.0	0.0	0.0	0.0	0.0	0.0	0.0
43	1.1	91.7	0.0	0.0	0.0	0.0	0.0	0.0	0.0
44	0.5	13.3	0.0	0.0	0.0	0.0	0.0	0.0	0.0

Failure Surface Specified By 24 Coordinate Points

Point No.	X-Surf (ft)	Y-Surf (ft)
1	127.50	48.00
2	132.41	47.04

3	137.35	46.31
4	142.33	45.81
5	147.32	45.55
6	152.32	45.52
7	157.32	45.73
8	162.30	46.17
9	167.25	46.85
10	172.17	47.75
11	177.04	48.89
12	181.85	50.25
13	186.59	51.84
14	191.25	53.65
15	195.82	55.68
16	200.29	57.91
17	204.66	60.36
18	208.90	63.01
19	213.01	65.85
20	216.98	68.88
21	220.81	72.10
22	224.48	75.49
23	227.99	79.06
24	229.96	81.24

Circle Center At X = 150.4 ; Y = 151.9 and Radius, 106.4

*** 2.359 ***

1

Failure Surface Specified By 28 Coordinate Points

Point No.	X-Surf (ft)	Y-Surf (ft)
1	108.13	47.94
2	112.97	46.70
3	117.86	45.66
4	122.79	44.81
5	127.75	44.18
6	132.73	43.74
7	137.72	43.51
8	142.72	43.49
9	147.72	43.67
10	152.70	44.05
11	157.67	44.64
12	162.61	45.44
13	167.51	46.43
14	172.36	47.63
15	177.16	49.02
16	181.90	50.61
17	186.57	52.40
18	191.17	54.37
19	195.68	56.53
20	200.09	58.87
21	204.41	61.40
22	208.62	64.09
23	212.71	66.96
24	216.69	70.00
25	220.53	73.19

26	224.25	76.54
27	227.82	80.04
28	228.91	81.20

Circle Center At X = 140.8 ; Y = 165.2 and Radius, 121.7

*** 2.379 ***

Failure Surface Specified By 24 Coordinate Points

Point No.	X-Surf (ft)	Y-Surf (ft)
1	127.50	48.00
2	132.36	46.81
3	137.27	45.87
4	142.22	45.17
5	147.20	44.73
6	152.20	44.54
7	157.20	44.60
8	162.19	44.91
9	167.15	45.47
10	172.09	46.28
11	176.97	47.34
12	181.80	48.65
13	186.56	50.19
14	191.23	51.97
15	195.80	53.99
16	200.27	56.24
17	204.62	58.70
18	208.84	61.38
19	212.92	64.28
20	216.85	67.37
21	220.61	70.66
22	224.21	74.13
23	227.63	77.78
24	230.58	81.27

Circle Center At X = 153.5 ; Y = 143.7 and Radius, 99.2

*** 2.386 ***

1

Failure Surface Specified By 25 Coordinate Points

Point No.	X-Surf (ft)	Y-Surf (ft)
1	127.50	48.00
2	132.32	46.66
3	137.20	45.57
4	142.13	44.74
5	147.09	44.17

6	152.09	43.87
7	157.09	43.83
8	162.08	44.05
9	167.06	44.54
10	172.00	45.29
11	176.90	46.30
12	181.73	47.57
13	186.50	49.09
14	191.17	50.86
15	195.75	52.87
16	200.21	55.13
17	204.55	57.61
18	208.75	60.33
19	212.80	63.26
20	216.69	66.40
21	220.41	69.74
22	223.95	73.27
23	227.29	76.99
24	230.44	80.88
25	230.73	81.27

Circle Center At X = 155.3 ; Y = 138.4 and Radius, 94.6

*** 2.408 ***

Failure Surface Specified By 32 Coordinate Points

Point No.	X-Surf (ft)	Y-Surf (ft)
1	88.75	47.85
2	93.69	47.07
3	98.65	46.43
4	103.62	45.92
5	108.61	45.54
6	113.60	45.29
7	118.60	45.18
8	123.60	45.20
9	128.60	45.35
10	133.59	45.63
11	138.57	46.05
12	143.54	46.60
13	148.50	47.28
14	153.43	48.09
15	158.34	49.04
16	163.22	50.11
17	168.08	51.31
18	172.90	52.64
19	177.68	54.10
20	182.42	55.69
21	187.12	57.40
22	191.77	59.23
23	196.37	61.19
24	200.92	63.27
25	205.41	65.46
26	209.84	67.78
27	214.21	70.22
28	218.51	72.76

29	222.74	75.43
30	226.90	78.20
31	230.99	81.08
32	231.27	81.30

Circle Center At X = 120.4 ; Y = 233.4 and Radius, 188.3

*** 2.422 ***

1

Failure Surface Specified By 28 Coordinate Points

Point No.	X-Surf (ft)	Y-Surf (ft)
1	108.13	47.94
2	112.83	46.26
3	117.62	44.81
4	122.47	43.59
5	127.37	42.61
6	132.31	41.86
7	137.29	41.35
8	142.28	41.09
9	147.28	41.06
10	152.28	41.28
11	157.26	41.74
12	162.21	42.44
13	167.12	43.37
14	171.98	44.54
15	176.78	45.95
16	181.50	47.58
17	186.14	49.44
18	190.69	51.52
19	195.13	53.82
20	199.45	56.33
21	203.65	59.05
22	207.71	61.97
23	211.63	65.08
24	215.39	68.37
25	218.99	71.84
26	222.42	75.48
27	225.66	79.29
28	227.07	81.11

Circle Center At X = 145.3 ; Y = 144.5 and Radius, 103.5

*** 2.428 ***

Failure Surface Specified By 29 Coordinate Points

Point No.	X-Surf (ft)	Y-Surf (ft)

1	108.13	47.94
2	112.78	46.12
3	117.52	44.52
4	122.32	43.14
5	127.19	42.00
6	132.11	41.09
7	137.06	40.41
8	142.04	39.97
9	147.04	39.77
10	152.04	39.81
11	157.03	40.09
12	162.00	40.60
13	166.95	41.35
14	171.85	42.34
15	176.70	43.55
16	181.49	45.00
17	186.20	46.67
18	190.82	48.57
19	195.35	50.68
20	199.78	53.01
21	204.09	55.55
22	208.27	58.29
23	212.32	61.22
24	216.22	64.35
25	219.97	67.65
26	223.56	71.14
27	226.98	74.79
28	230.22	78.59
29	232.34	81.34

Circle Center At X = 148.7 ; Y = 144.6 and Radius, 104.9

*** 2.433 ***

1

Failure Surface Specified By 30 Coordinate Points

Point No.	X-Surf (ft)	Y-Surf (ft)
1	108.13	47.94
2	112.82	46.23
3	117.59	44.73
4	122.42	43.44
5	127.31	42.37
6	132.23	41.51
7	137.19	40.88
8	142.18	40.47
9	147.17	40.28
10	152.17	40.31
11	157.17	40.56
12	162.14	41.03
13	167.10	41.73
14	172.01	42.64
15	176.88	43.77
16	181.70	45.12
17	186.45	46.68
18	191.12	48.45

19	195.72	50.42
20	200.22	52.60
21	204.62	54.97
22	208.91	57.54
23	213.08	60.30
24	217.13	63.24
25	221.04	66.35
26	224.80	69.64
27	228.42	73.09
28	231.89	76.70
29	235.18	80.45
30	236.01	81.49

Circle Center At X = 149.0 ; Y = 152.7 and Radius, 112.5

*** 2.442 ***

Failure Surface Specified By 30 Coordinate Points

Point No.	X-Surf (ft)	Y-Surf (ft)
1	108.13	47.94
2	113.09	47.37
3	118.07	46.93
4	123.06	46.62
5	128.06	46.44
6	133.06	46.40
7	138.06	46.48
8	143.05	46.70
9	148.04	47.06
10	153.02	47.54
11	157.98	48.16
12	162.92	48.90
13	167.85	49.78
14	172.74	50.79
15	177.61	51.93
16	182.45	53.19
17	187.25	54.59
18	192.02	56.11
19	196.74	57.75
20	201.41	59.52
21	206.04	61.41
22	210.62	63.43
23	215.14	65.57
24	219.60	67.82
25	224.00	70.19
26	228.34	72.68
27	232.61	75.28
28	236.81	77.99
29	240.94	80.82
30	242.20	81.74

Circle Center At X = 132.3 ; Y = 235.1 and Radius, 188.7

*** 2.451 ***

1

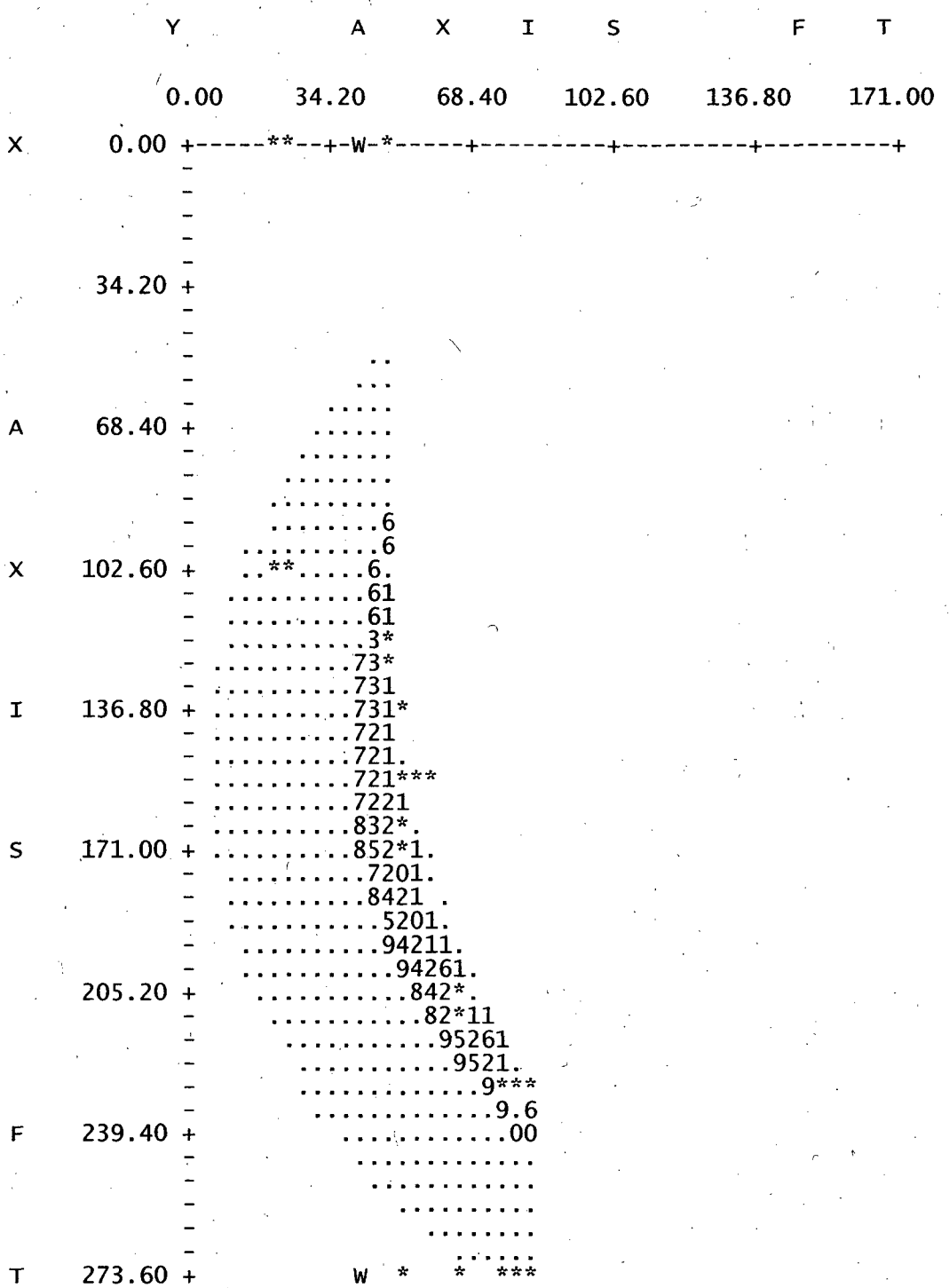
Y A X I S F T
0.00 34.20 68.40 102.60 136.80 171.00
X 0.00
34.20
A 68.40
X 102.60
I 136.80
S 171.00
205.20
F 239.40
T 273.60

SPENCER #3 STATIC SLICES

Geometry and Boundary Conditions

Problem: SMC Newfield Decommissioning - Section A-A' - FS Min = 2.262

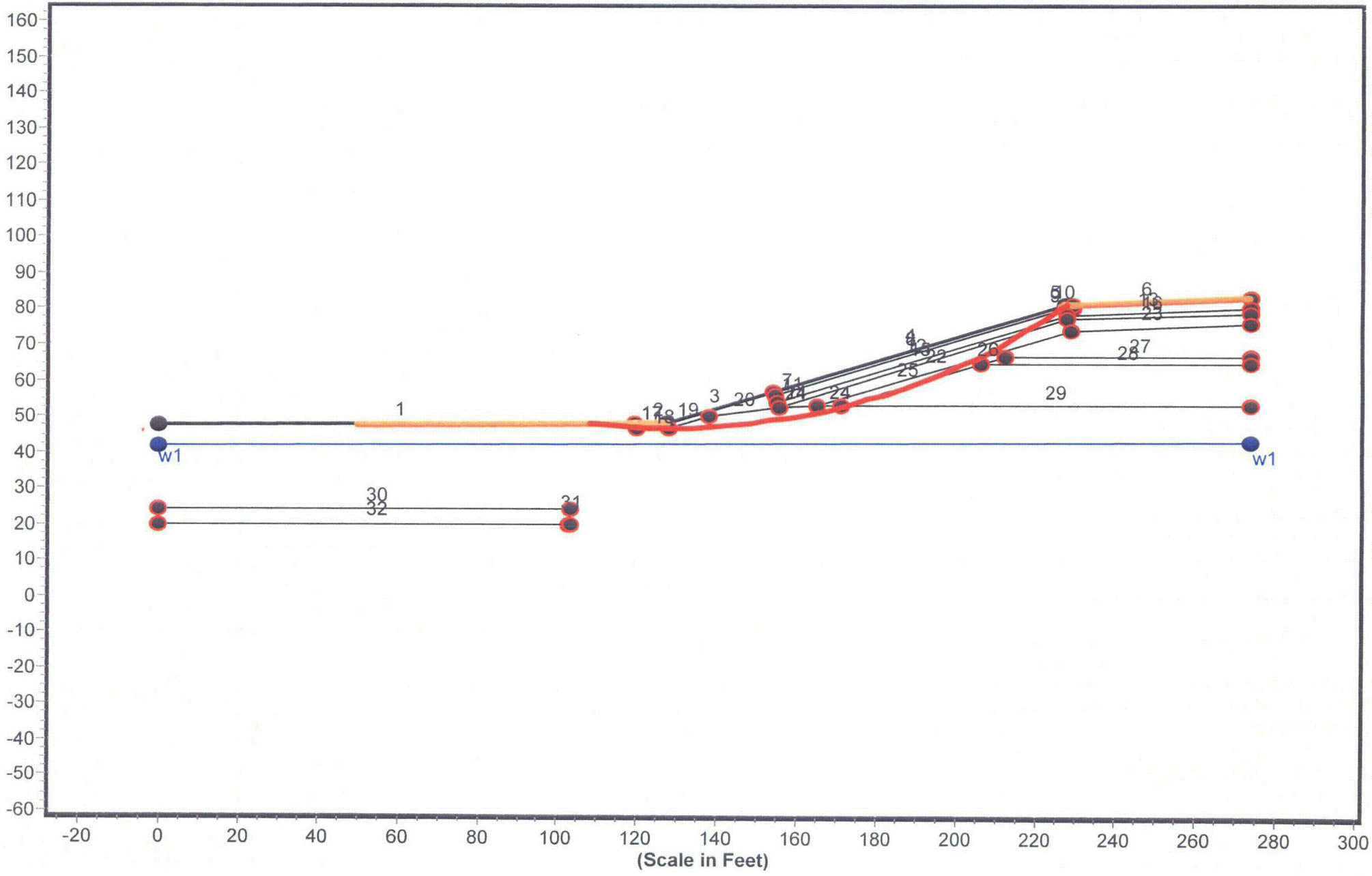

Geometry and Boundary Conditions

Problem: SMC Newfield Decommissioning - Section A-A' - FS Min = 2.262

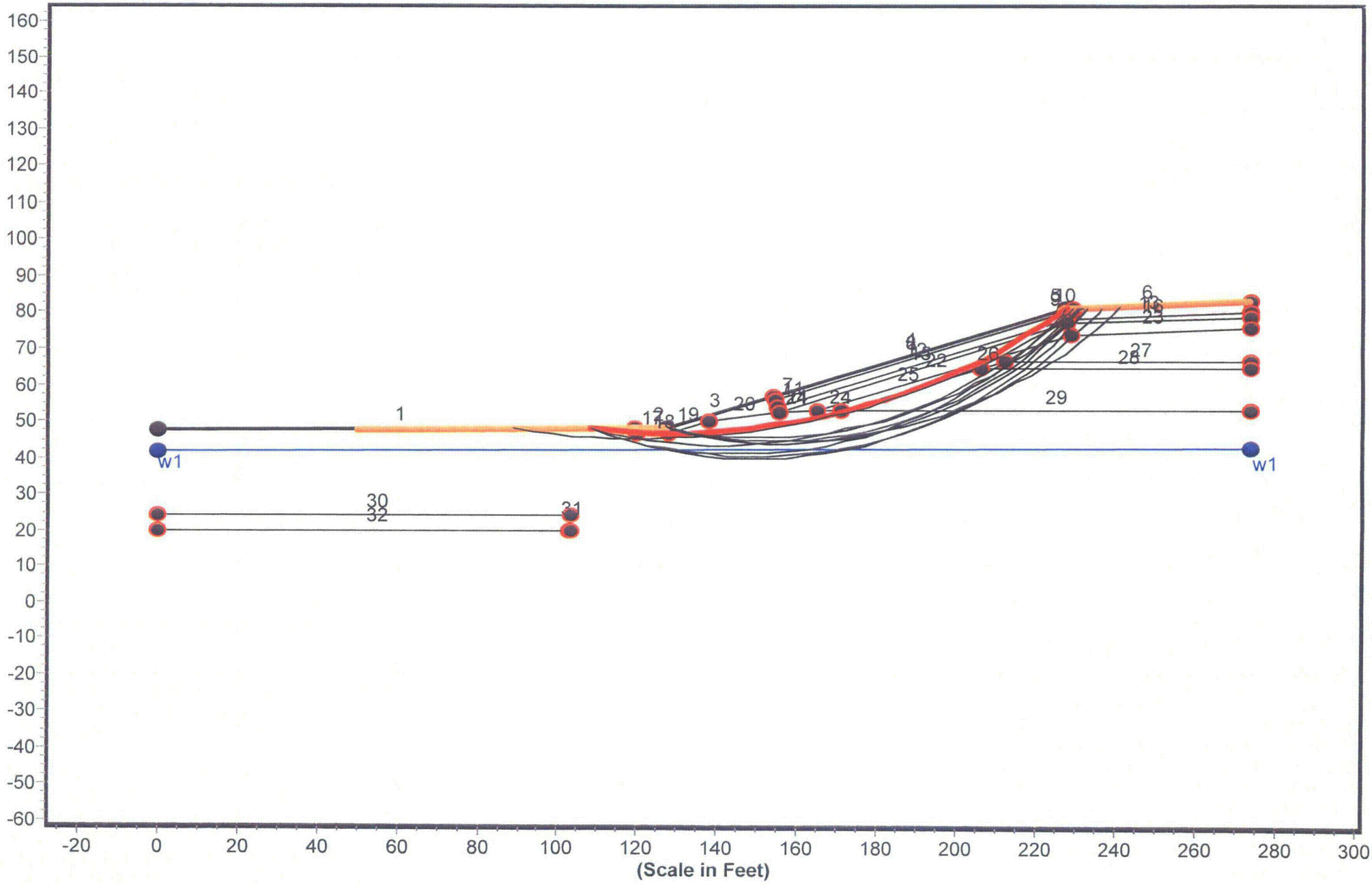

Geometry and Boundary Conditions
Problem: SMC Newfield Decommissioning - Section A-A' - FS Min = 2.262

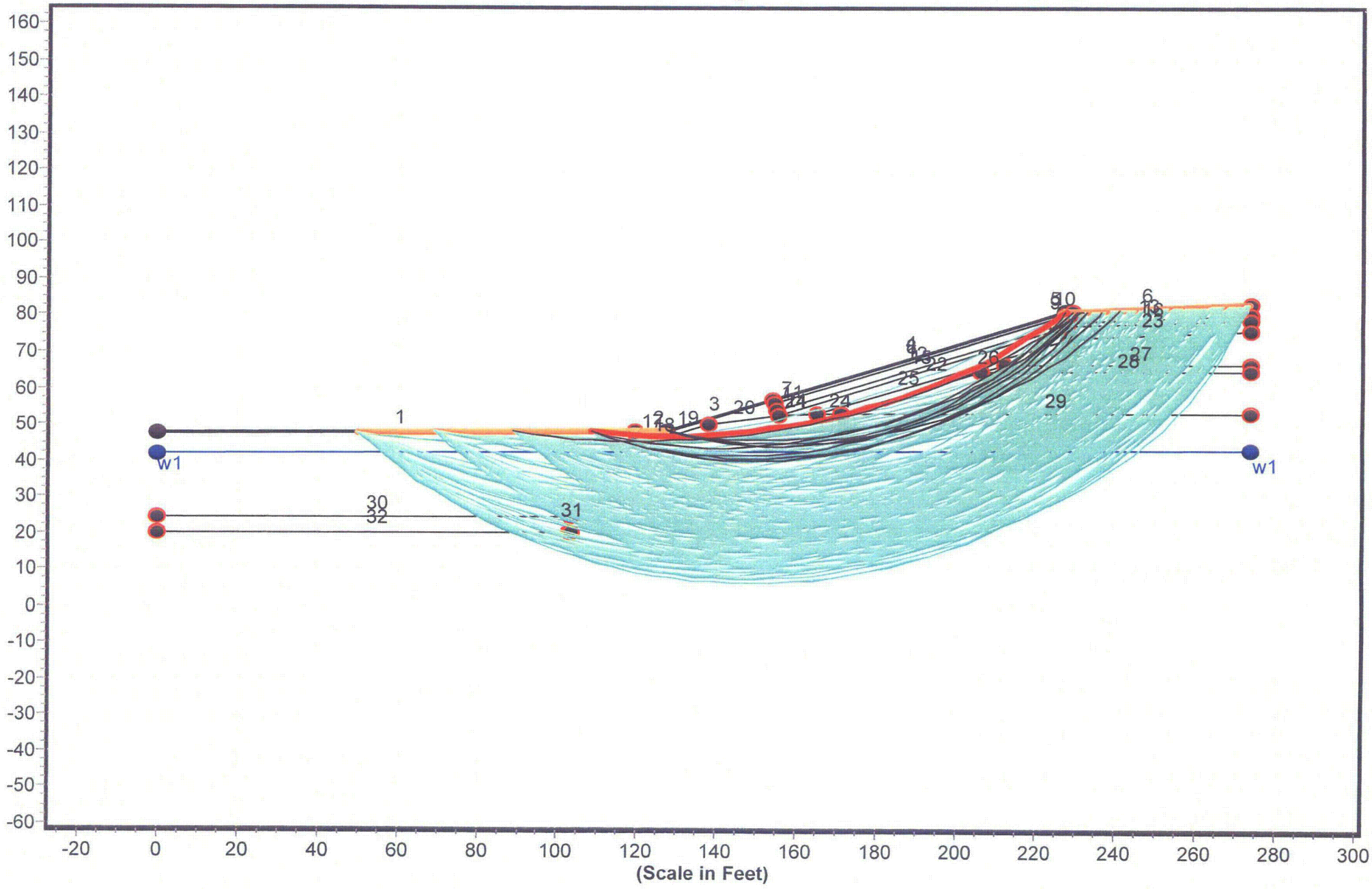

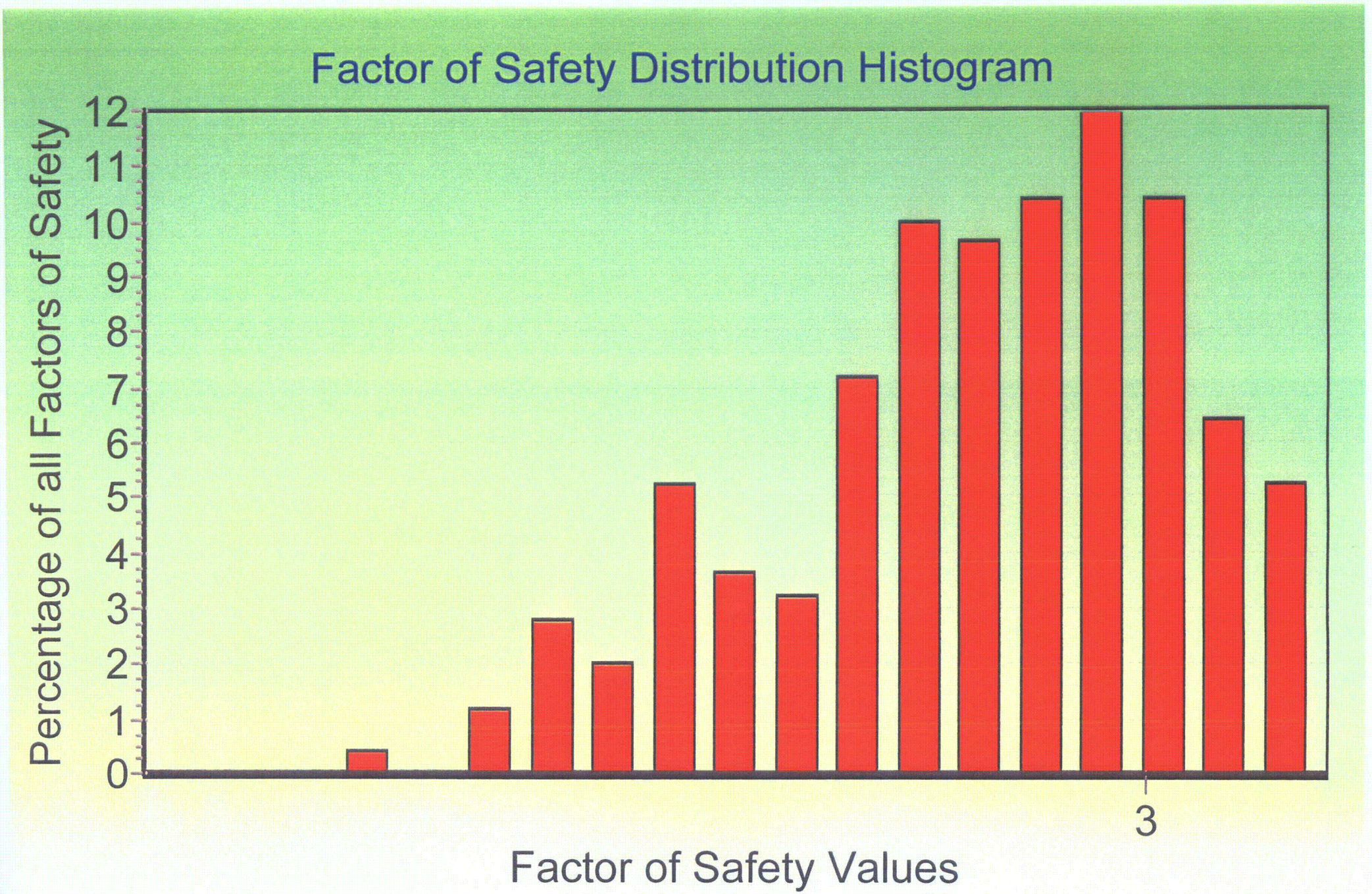
Factor of Safety Distribution Histogram
Percentage of all Factors of Safety
0
1
2
3
4
5
6
7
8
9
10
11
12
3
Factor of Safety Values

Spencer #3 Results.txt
** PCSTABL6 **

by
Purdue University

1

--Slope Stability Analysis--
Simplified Janbu, Simplified Bishop
or Spencer's Method of Slices

Run Date:
Time of Run:
Run By:
Input Data Filename: run.in
Output Filename: result.out
Unit: ENGLISH
Plotted Output Filename: result.plt

PROBLEM DESCRIPTION SMC Newfield Decommissioning - Section A -A'

BOUNDARY COORDINATES

6 Top Boundaries
32 Total Boundaries

Boundary No.	X-Left (ft)	Y-Left (ft)	X-Right (ft)	Y-Right (ft)	Soil Type Below Bnd
1	0.00	47.40	119.50	48.00	7
2	119.50	48.00	127.50	48.00	1
3	127.50	48.00	153.90	56.80	1
4	153.90	56.80	226.90	81.10	1
5	226.90	81.10	228.90	81.20	1
6	228.90	81.20	273.60	83.00	2
7	153.90	56.80	154.20	55.80	1
8	154.20	55.80	227.10	80.10	2
9	227.10	80.10	228.80	80.20	2
10	228.80	80.20	228.90	81.20	2
11	154.20	55.80	154.80	53.90	1
12	154.80	53.90	227.40	78.10	1
13	227.40	78.10	273.60	80.00	1
14	154.80	53.90	155.20	52.60	1
15	155.20	52.60	227.60	77.10	3
16	227.60	77.10	273.60	79.00	3
17	119.50	48.00	119.60	46.40	7
18	119.60	46.40	127.80	46.40	7
19	127.80	46.40	137.90	49.80	7
20	137.90	49.80	155.20	52.60	7
21	155.20	52.60	164.60	53.00	7
22	164.60	53.00	228.20	74.10	4
23	228.20	74.10	273.60	76.00	4
24	164.60	53.00	171.00	53.00	7
25	171.00	53.00	205.80	64.60	6
26	205.80	64.60	211.80	66.60	5

27	211.80	66.60	273.60	66.60	5
28	205.80	64.60	273.60	64.60	6
29	171.00	53.00	273.60	53.00	7
30	0.00	24.00	103.10	24.00	8
31	103.00	20.00	103.10	24.00	7
32	0.00	20.00	103.10	20.00	7

1

ISOTROPIC SOIL PARAMETERS

8 Type(s) of Soil

Soil Type No.	Total Unit Wt. (pcf)	Saturated Unit Wt. (pcf)	Cohesion Intercept (psf)	Friction Angle (deg)	Pore Pressure Param.	Pressure Constant (psf)	Piez. Surface No.
1	135.0	140.0	0.0	40.0	0.00	0.0	0
2	135.0	140.0	0.0	35.0	0.00	0.0	0
3	125.0	130.0	250.0	15.0	0.00	0.0	0
4	125.0	135.0	0.0	32.0	0.00	0.0	0
5	135.0	140.0	0.0	38.0	0.00	0.0	0
6	135.0	140.0	0.0	40.0	0.00	0.0	0
7	115.0	130.0	0.0	33.0	0.00	0.0	1
8	130.0	140.0	300.0	20.0	0.00	0.0	1

1

1 PIEZOMETRIC SURFACE(S) HAVE BEEN SPECIFIED

Unit Weight of Water = 62.40

Piezometric Surface No. 1 Specified by 2 Coordinate Points

Point No.	X-Water (ft)	Y-Water (ft)
1	0.00	41.70
2	273.60	42.50

1

A Critical Failure Surface Searching Method, Using A Random Technique For Generating Circular Surfaces, Has Been Specified.

250 Trial Surfaces Have Been Generated.

50 Surfaces Initiate From Each Of 5 Points Equally Spaced Along The Ground Surface Between X = 50.00 ft.
and X = 127.50 ft.

Each Surface Terminates Between X = 226.00 ft.
and X = 273.00 ft.

Unless Further Limitations Were Imposed, The Minimum Elevation At Which A Surface Extends Is Y = 0.00 ft.

5.00 ft. Line Segments Define Each Trial Failure Surface.

Restrictions Have Been Imposed Upon The Angle Of Initiation. The Angle Has Been Restricted Between The Angles Of -45.0 And -5.0 deg.

1

Following Are Displayed The Ten Most Critical Of The Trial Failure Surfaces Examined. They Are Ordered - Most Critical First.

* * Safety Factors Are Calculated By Spencer's Method * *

Number of convergent trials 250
Number of non convergent trials 0

Failure Surface Specified By 27 Coordinate Points

Point No.	X-Surf (ft)	Y-Surf (ft)
1	108.13	47.94
2	113.10	47.42
3	118.08	47.05
4	123.08	46.84
5	128.08	46.78
6	133.08	46.87
7	138.07	47.12
8	143.06	47.52
9	148.03	48.07
10	152.98	48.78
11	157.90	49.64
12	162.80	50.65
13	167.66	51.81
14	172.49	53.11
15	177.27	54.57
16	182.01	56.18
17	186.69	57.92
18	191.32	59.82
19	195.89	61.85
20	200.39	64.02
21	204.82	66.33
22	209.18	68.78
23	213.47	71.36
24	217.67	74.07
25	221.79	76.91
26	225.81	79.87
27	227.41	81.13

*** Factor of Safety = 2.262 ***

Individual data on the 44 slices

Slice No.	Width (ft)	Weight (lbs)	Water Force Top (lbs)	Water Force Bot (lbs)	Force Norm (lbs)	Force Tan (lbs)	Earthquake Force Hor (lbs)	Earthquake Force Ver (lbs)	Surcharge Load (lbs)
1	5.0	156.4	0.0	0.0	0.0	0.0	0.0	0.0	0.0
2	5.0	426.4	0.0	0.0	0.0	0.0	0.0	0.0	0.0
3	1.4	158.6	0.0	0.0	0.0	0.0	0.0	0.0	0.0
4	0.1	8.0	0.0	0.0	0.0	0.0	0.0	0.0	0.0
5	3.5	516.0	0.0	0.0	0.0	0.0	0.0	0.0	0.0
6	4.4	709.7	0.0	0.0	0.0	0.0	0.0	0.0	0.0
7	0.6	103.0	0.0	0.0	0.0	0.0	0.0	0.0	0.0
8	0.9	186.6	0.0	0.0	0.0	0.0	0.0	0.0	0.0
9	4.1	1246.6	0.0	0.0	0.0	0.0	0.0	0.0	0.0
10	4.8	2198.7	0.0	0.0	0.0	0.0	0.0	0.0	0.0
11	0.2	92.8	0.0	0.0	0.0	0.0	0.0	0.0	0.0
12	5.0	3099.4	0.0	0.0	0.0	0.0	0.0	0.0	0.0
13	5.0	3850.4	0.0	0.0	0.0	0.0	0.0	0.0	0.0
14	4.9	4501.9	0.0	0.0	0.0	0.0	0.0	0.0	0.0
15	0.9	908.0	0.0	0.0	0.0	0.0	0.0	0.0	0.0
16	0.3	298.7	0.0	0.0	0.0	0.0	0.0	0.0	0.0
17	0.6	603.2	0.0	0.0	0.0	0.0	0.0	0.0	0.0
18	0.4	406.5	0.0	0.0	0.0	0.0	0.0	0.0	0.0
19	2.7	2833.7	0.0	0.0	0.0	0.0	0.0	0.0	0.0
20	4.9	5485.0	0.0	0.0	0.0	0.0	0.0	0.0	0.0
21	1.8	2117.0	0.0	0.0	0.0	0.0	0.0	0.0	0.0
22	3.1	3702.0	0.0	0.0	0.0	0.0	0.0	0.0	0.0
23	3.3	4165.7	0.0	0.0	0.0	0.0	0.0	0.0	0.0
24	1.1	1355.5	0.0	0.0	0.0	0.0	0.0	0.0	0.0
25	0.4	541.2	0.0	0.0	0.0	0.0	0.0	0.0	0.0
26	4.8	6180.9	0.0	0.0	0.0	0.0	0.0	0.0	0.0
27	4.7	6153.3	0.0	0.0	0.0	0.0	0.0	0.0	0.0
28	4.7	6016.5	0.0	0.0	0.0	0.0	0.0	0.0	0.0
29	4.1	5067.2	0.0	0.0	0.0	0.0	0.0	0.0	0.0
30	0.6	707.4	0.0	0.0	0.0	0.0	0.0	0.0	0.0
31	4.6	5444.9	0.0	0.0	0.0	0.0	0.0	0.0	0.0
32	4.5	5032.3	0.0	0.0	0.0	0.0	0.0	0.0	0.0
33	4.4	4535.7	0.0	0.0	0.0	0.0	0.0	0.0	0.0
34	0.0	41.8	0.0	0.0	0.0	0.0	0.0	0.0	0.0
35	4.3	3919.2	0.0	0.0	0.0	0.0	0.0	0.0	0.0
36	4.3	3314.5	0.0	0.0	0.0	0.0	0.0	0.0	0.0
37	3.1	1999.4	0.0	0.0	0.0	0.0	0.0	0.0	0.0
38	1.1	601.9	0.0	0.0	0.0	0.0	0.0	0.0	0.0
39	2.2	1061.0	0.0	0.0	0.0	0.0	0.0	0.0	0.0
40	1.9	729.8	0.0	0.0	0.0	0.0	0.0	0.0	0.0
41	3.5	846.3	0.0	0.0	0.0	0.0	0.0	0.0	0.0
42	0.5	65.4	0.0	0.0	0.0	0.0	0.0	0.0	0.0
43	1.1	91.0	0.0	0.0	0.0	0.0	0.0	0.0	0.0
44	0.5	12.9	0.0	0.0	0.0	0.0	0.0	0.0	0.0

Failure Surface Specified By 24 Coordinate Points

Point No.	X-Surf (ft)	Y-Surf (ft)
1	127.50	48.00
2	132.41	47.04

3	137.35	46.31
4	142.33	45.81
5	147.32	45.55
6	152.32	45.53
7	157.32	45.73
8	162.30	46.17
9	167.25	46.85
10	172.17	47.76
11	177.04	48.90
12	181.85	50.26
13	186.59	51.85
14	191.25	53.66
15	195.82	55.69
16	200.29	57.92
17	204.65	60.37
18	208.89	63.02
19	213.00	65.87
20	216.98	68.90
21	220.80	72.12
22	224.48	75.51
23	227.98	79.08
24	229.92	81.24

*** Factor of Safety = 2.355 ***

1

Failure Surface Specified By 28 Coordinate Points

Point No.	X-Surf (ft)	Y-Surf (ft)
1	108.13	47.94
2	112.97	46.70
3	117.86	45.66
4	122.79	44.81
5	127.75	44.18
6	132.73	43.74
7	137.72	43.51
8	142.72	43.49
9	147.72	43.67
10	152.70	44.05
11	157.67	44.65
12	162.61	45.44
13	167.50	46.44
14	172.36	47.63
15	177.16	49.03
16	181.90	50.62
17	186.57	52.40
18	191.17	54.38
19	195.67	56.54
20	200.09	58.88
21	204.41	61.41
22	208.62	64.10
23	212.71	66.97
24	216.68	70.01
25	220.53	73.21
26	224.24	76.56
27	227.81	80.06

28	228.88	81.20

*** Factor of Safety = 2.376 ***

Failure Surface Specified By 24 Coordinate Points

Point No.	X-Surf (ft)	Y-Surf (ft)
1	127.50	48.00
2	132.36	46.81
3	137.27	45.87
4	142.22	45.17
5	147.20	44.73
6	152.20	44.54
7	157.20	44.60
8	162.19	44.91
9	167.15	45.47
10	172.09	46.29
11	176.97	47.35
12	181.80	48.65
13	186.55	50.20
14	191.23	51.98
15	195.80	54.00
16	200.27	56.25
17	204.62	58.72
18	208.83	61.40
19	212.91	64.29
20	216.84	67.39
21	220.60	70.68
22	224.20	74.15
23	227.61	77.80
24	230.54	81.27

*** Factor of Safety = 2.380 ***

1

Failure Surface Specified By 25 Coordinate Points

Point No.	X-Surf (ft)	Y-Surf (ft)
1	127.50	48.00
2	132.32	46.66
3	137.20	45.57
4	142.13	44.74
5	147.09	44.17
6	152.09	43.87
7	157.09	43.83
8	162.08	44.05
9	167.06	44.54
10	172.00	45.29
11	176.90	46.30

12	181.73	47.57
13	186.50	49.10
14	191.17	50.87
15	195.75	52.88
16	200.21	55.14
17	204.54	57.63
18	208.74	60.34
19	212.79	63.28
20	216.68	66.42
21	220.40	69.76
22	223.94	73.30
23	227.28	77.02
24	230.42	80.90
25	230.69	81.27

*** Factor of Safety = 2.401 ***

Failure Surface Specified By 28 Coordinate Points

Point No.	X-Surf (ft)	Y-Surf (ft)
1	108.13	47.94
2	112.83	46.26
3	117.62	44.81
4	122.47	43.59
5	127.37	42.61
6	132.31	41.86
7	137.29	41.36
8	142.28	41.09
9	147.28	41.07
10	152.28	41.28
11	157.26	41.74
12	162.21	42.44
13	167.12	43.37
14	171.98	44.54
15	176.78	45.95
16	181.50	47.58
17	186.14	49.44
18	190.69	51.53
19	195.13	53.83
20	199.45	56.34
21	203.65	59.05
22	207.71	61.97
23	211.63	65.08
24	215.39	68.37
25	218.99	71.85
26	222.41	75.49
27	225.66	79.29
28	227.07	81.11

*** Factor of Safety = 2.423 ***

Failure Surface Specified By 29 Coordinate Points

Point No.	X-Surf (ft)	Y-Surf (ft)
1	108.13	47.94
2	112.78	46.12
3	117.52	44.52
4	122.32	43.14
5	127.19	42.00
6	132.11	41.09
7	137.06	40.41
8	142.04	39.98
9	147.04	39.78
10	152.04	39.82
11	157.03	40.09
12	162.00	40.61
13	166.95	41.36
14	171.85	42.35
15	176.70	43.57
16	181.48	45.01
17	186.20	46.69
18	190.82	48.59
19	195.35	50.70
20	199.77	53.03
21	204.08	55.57
22	208.26	58.31
23	212.31	61.25
24	216.21	64.38
25	219.96	67.69
26	223.55	71.17
27	226.96	74.82
28	230.20	78.63
29	232.28	81.34

*** Factor of Safety = 2.428 ***

Failure Surface Specified By 32 Coordinate Points

Point No.	X-Surf (ft)	Y-Surf (ft)
1	88.75	47.85
2	93.69	47.07
3	98.65	46.43
4	103.62	45.92
5	108.61	45.54
6	113.60	45.29
7	118.60	45.18
8	123.60	45.20
9	128.60	45.35
10	133.59	45.64
11	138.57	46.05
12	143.54	46.60
13	148.50	47.28
14	153.43	48.10
15	158.34	49.04

16	163.22	50.12
17	168.08	51.32
18	172.90	52.65
19	177.68	54.11
20	182.42	55.70
21	187.12	57.41
22	191.77	59.24
23	196.37	61.20
24	200.92	63.28
25	205.41	65.48
26	209.84	67.80
27	214.20	70.23
28	218.50	72.78
29	222.73	75.45
30	226.89	78.22
31	230.98	81.11
32	231.23	81.29

*** Factor of Safety = 2.428 ***

1

Failure Surface Specified By 30 Coordinate Points

Point No.	X-Surf (ft)	Y-Surf (ft)
1	108.13	47.94
2	112.82	46.23
3	117.59	44.73
4	122.42	43.44
5	127.31	42.37
6	132.23	41.52
7	137.19	40.88
8	142.18	40.47
9	147.17	40.28
10	152.17	40.31
11	157.17	40.57
12	162.14	41.04
13	167.10	41.74
14	172.01	42.66
15	176.88	43.79
16	181.69	45.14
17	186.44	46.70
18	191.12	48.47
19	195.71	50.45
20	200.21	52.63
21	204.61	55.01
22	208.90	57.58
23	213.07	60.34
24	217.11	63.28
25	221.02	66.40
26	224.78	69.69
27	228.40	73.15
28	231.86	76.76
29	235.15	80.52
30	235.92	81.48

*** Factor of Safety = 2.435 ***

Failure Surface Specified By 26 Coordinate Points

Point No.	X-Surf (ft)	Y-Surf (ft)
1	127.50	48.00
2	132.37	46.86
3	137.28	45.93
4	142.23	45.22
5	147.21	44.73
6	152.20	44.46
7	157.20	44.40
8	162.20	44.56
9	167.18	44.94
10	172.15	45.54
11	177.08	46.35
12	181.97	47.38
13	186.82	48.62
14	191.60	50.08
15	196.32	51.74
16	200.96	53.60
17	205.51	55.67
18	209.97	57.93
19	214.32	60.39
20	218.57	63.03
21	222.69	65.86
22	226.69	68.86
23	230.55	72.04
24	234.27	75.38
25	237.84	78.88
26	240.44	81.66

*** Factor of Safety = 2.451 ***

1

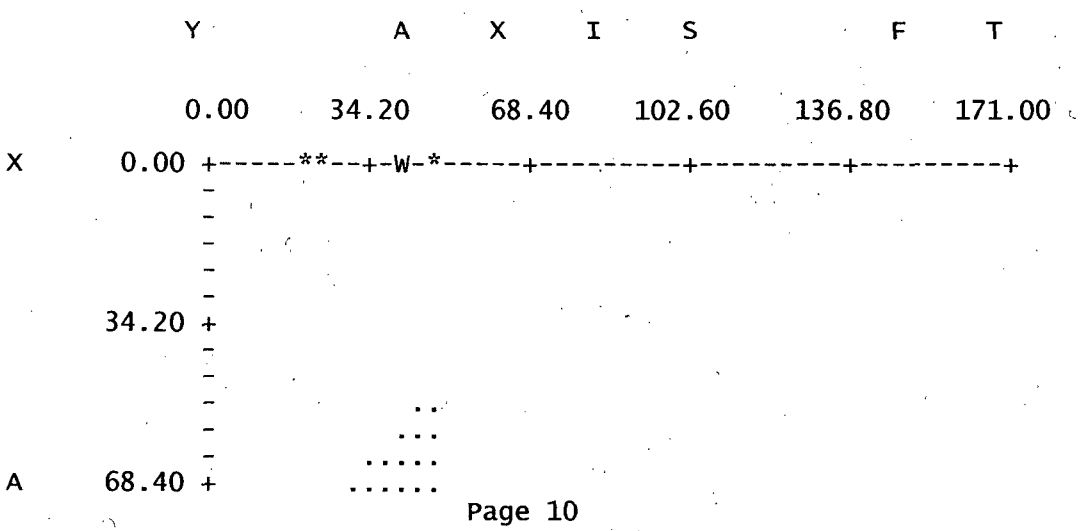

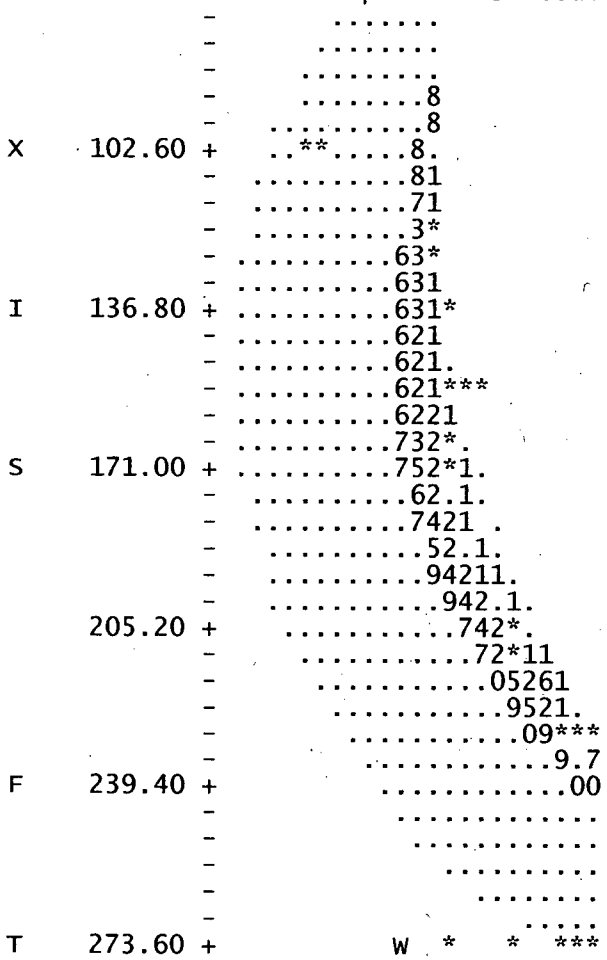
X
102.60
I
136.80
S
171.00
205.20
F
239.40
T
273.60

JANBU #4 STATIC CIRCULAR

EXTREME HIGH WATER

Geometry and Boundary Conditions

Problem: SMC Newfield Decommissioning - Section A-A' - FS Min = 2.006

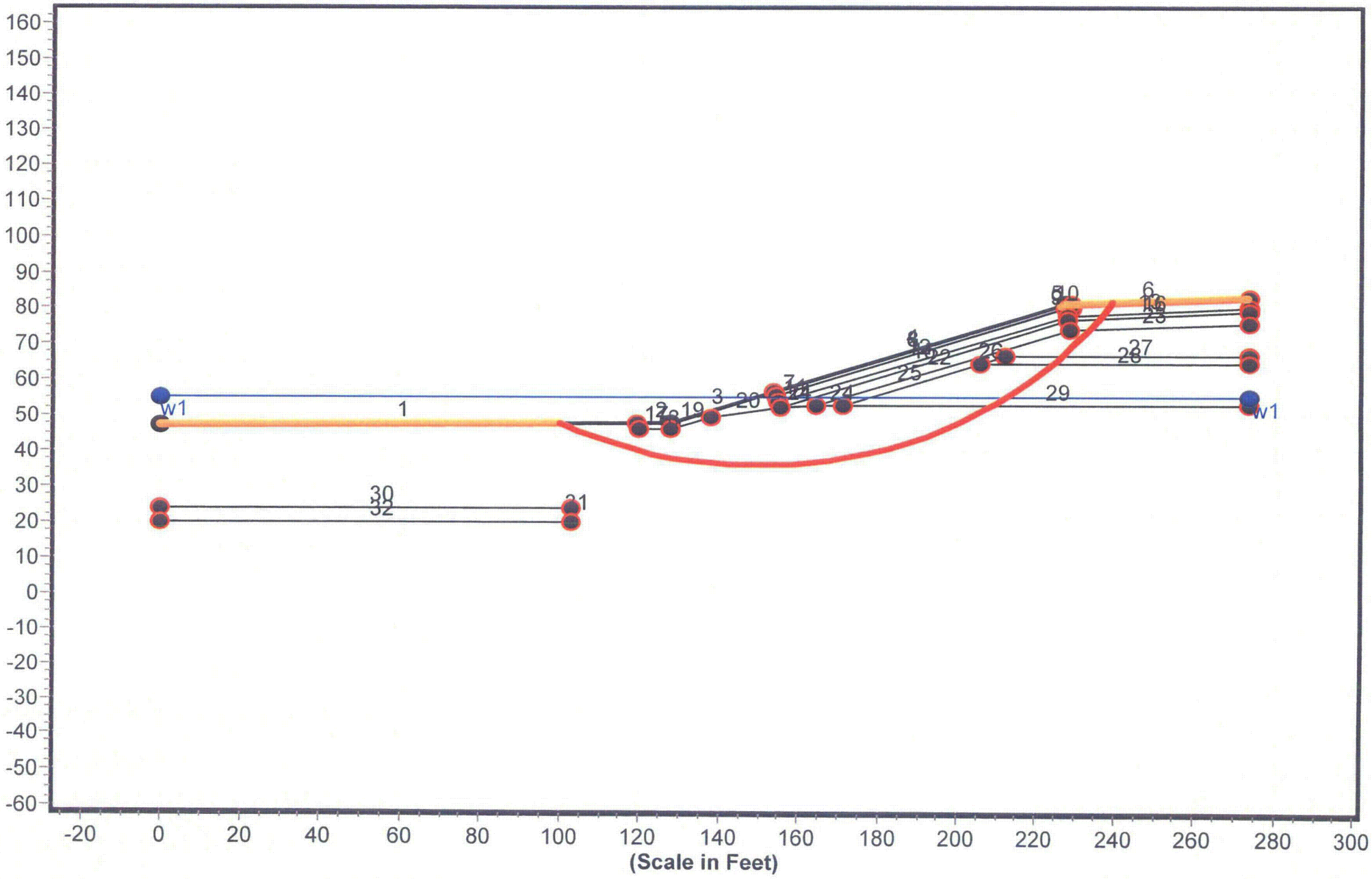

Geometry and Boundary Conditions
Problem: SMC Newfield Decommissioning - Section A-A' - FS Min = 2.006

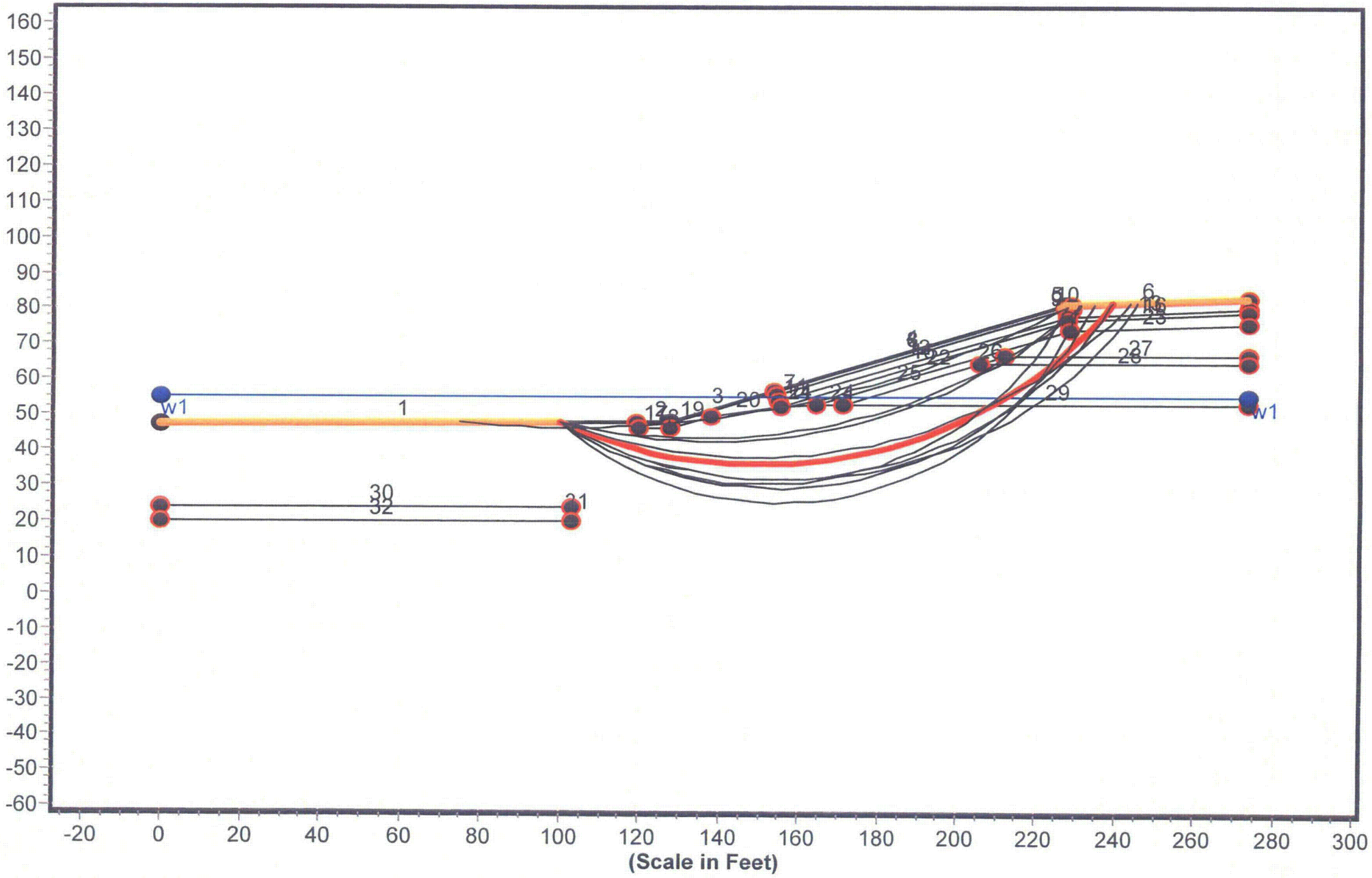

Geometry and Boundary Conditions
Problem: SMC Newfield Decommissioning - Section A-A' - FS Min = 2.006

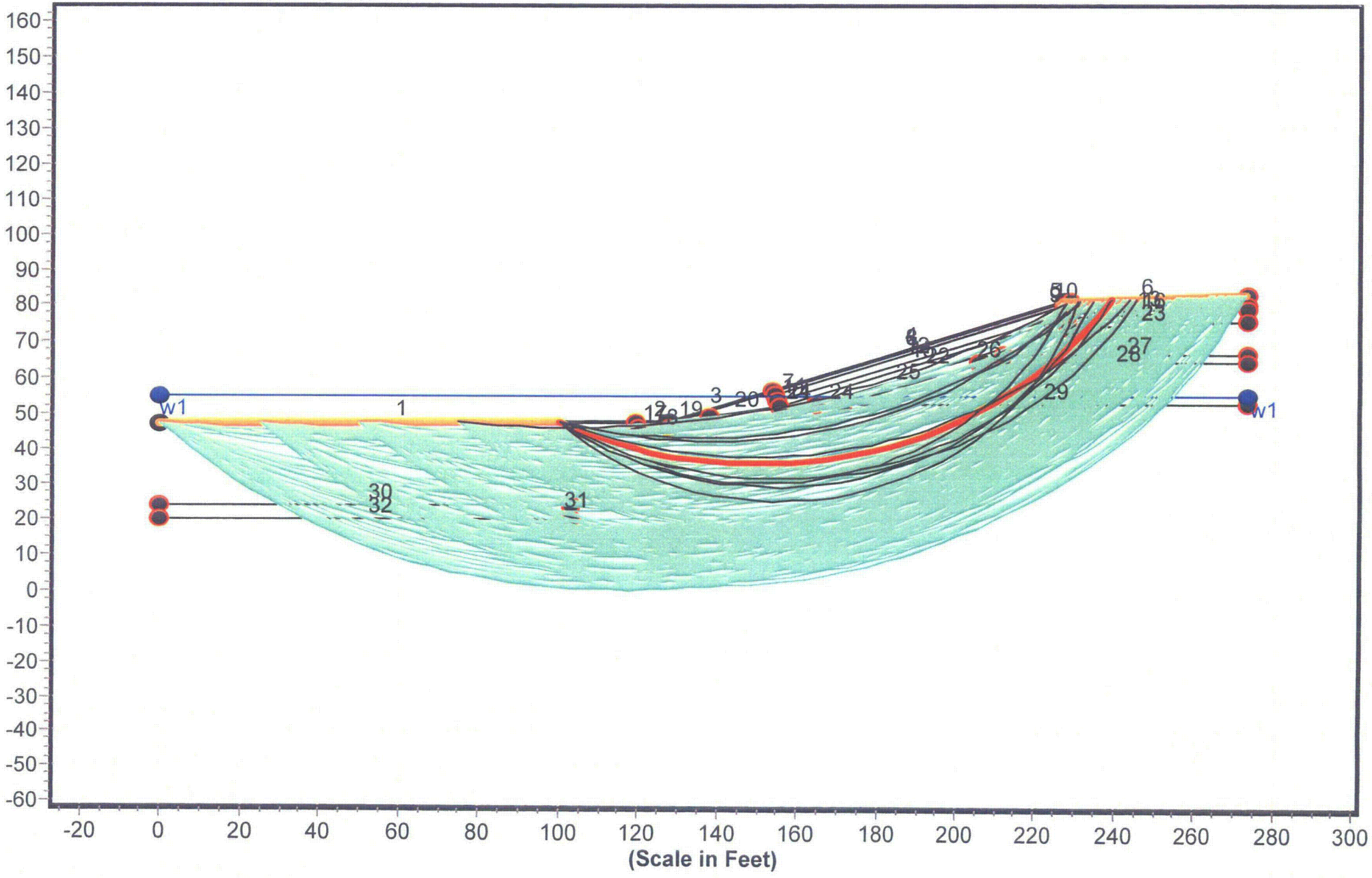

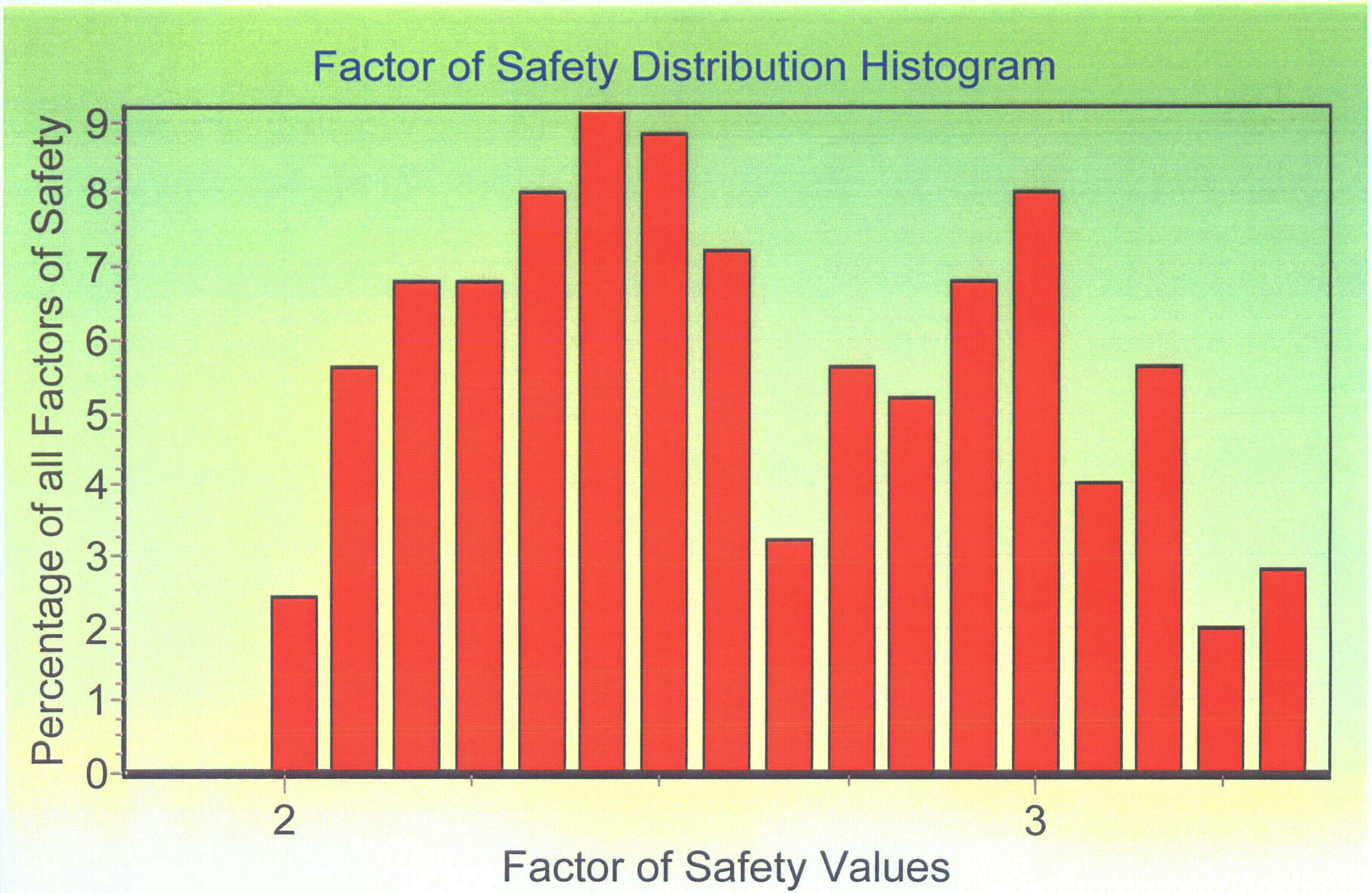
Factor of Safety Distribution Histogram
Percentage of all Factors of Safety
0
1
2
3
4
5
6
7
8
9
2
3
Factor of Safety Values

** PCSTABL6 **

by
Purdue University

1

--Slope Stability Analysis--
Simplified Janbu, Simplified Bishop
or Spencer's Method of Slices

Run Date:
Time of Run:
Run By:
Input Data Filename: run.in
Output Filename: result.out
Unit: ENGLISH
Plotted Output Filename: result.plt

PROBLEM DESCRIPTION SMC Newfield Decommissioning - Section A -A'

BOUNDARY COORDINATES

6 Top Boundaries
32 Total Boundaries

Boundary No.	X-Left (ft)	Y-Left (ft)	X-Right (ft)	Y-Right (ft)	Soil Type Below Bnd
1	0.00	47.40	119.50	48.00	7
2	119.50	48.00	127.50	48.00	1
3	127.50	48.00	153.90	56.80	1
4	153.90	56.80	226.90	81.10	1
5	226.90	81.10	228.90	81.20	1
6	228.90	81.20	273.60	83.00	2
7	153.90	56.80	154.20	55.80	1
8	154.20	55.80	227.10	80.10	2
9	227.10	80.10	228.80	80.20	2
10	228.80	80.20	228.90	81.20	2
11	154.20	55.80	154.80	53.90	1
12	154.80	53.90	227.40	78.10	1
13	227.40	78.10	273.60	80.00	1
14	154.80	53.90	155.20	52.60	1
15	155.20	52.60	227.60	77.10	3
16	227.60	77.10	273.60	79.00	3
17	119.50	48.00	119.60	46.40	7
18	119.60	46.40	127.80	46.40	7
19	127.80	46.40	137.90	49.80	7
20	137.90	49.80	155.20	52.60	7
21	155.20	52.60	164.60	53.00	7
22	164.60	53.00	228.20	74.10	4
23	228.20	74.10	273.60	76.00	4
24	164.60	53.00	171.00	53.00	7
25	171.00	53.00	205.80	64.60	6
26	205.80	64.60	211.80	66.60	5

27	211.80	66.60	273.60	66.60	5
28	205.80	64.60	273.60	64.60	6
29	171.00	53.00	273.60	53.00	7
30	0.00	24.00	103.10	24.00	8
31	103.00	20.00	103.10	24.00	7
32	0.00	20.00	103.10	20.00	7

1

ISOTROPIC SOIL PARAMETERS

8 Type(s) of Soil

Soil Type No.	Total Unit Wt. (pcf)	Saturated Unit Wt. (pcf)	Cohesion Intercept (psf)	Friction Angle (deg)	Pore Pressure Param.	Pressure Constant (psf)	Piez. Surface No.
1	135.0	140.0	0.0	40.0	0.00	0.0	1
2	135.0	140.0	0.0	35.0	0.00	0.0	1
3	125.0	130.0	250.0	15.0	0.00	0.0	1
4	125.0	135.0	0.0	32.0	0.00	0.0	1
5	135.0	140.0	0.0	38.0	0.00	0.0	1
6	135.0	140.0	0.0	40.0	0.00	0.0	1
7	115.0	130.0	0.0	33.0	0.00	0.0	1
8	130.0	140.0	300.0	20.0	0.00	0.0	1

1

1 PIEZOMETRIC SURFACE(S) HAVE BEEN SPECIFIED

Unit Weight of Water = 62.40

Piezometric Surface No. 1 Specified by 2 Coordinate Points

Point No.	X-Water (ft)	Y-Water (ft)
1	0.00	55.00
2	273.60	55.00

1

A Critical Failure Surface Searching Method, Using A Random Technique For Generating Circular Surfaces, Has Been Specified.

250 Trial Surfaces Have Been Generated.

50 Surfaces Initiate From Each Of 5 Points Equally Spaced Along The Ground Surface Between X = 0.00 ft.
and X = 100.00 ft.

Each Surface Terminates Between X = 226.00 ft.
and X = 273.00 ft.

Unless Further Limitations Were Imposed, The Minimum Elevation At Which A Surface Extends Is Y = 0.00 ft.

5.00 ft. Line Segments Define Each Trial Failure Surface.

Restrictions Have Been Imposed Upon The Angle Of Initiation. The Angle Has Been Restricted Between The Angles Of -45.0 And -5.0 deg.

1

Following Are Displayed The Ten Most Critical Of The Trial Failure Surfaces Examined. They Are Ordered - Most Critical First.

* * Safety Factors Are Calculated By The Modified Janbu Method * *

Failure Surface Specified By 33 Coordinate Points

Point No.	X-Surf (ft)	Y-Surf (ft)
1	100.00	47.90
2	104.50	45.72
3	109.10	43.75
4	113.78	41.99
5	118.53	40.45
6	123.35	39.13
7	128.23	38.02
8	133.15	37.14
9	138.11	36.49
10	143.09	36.06
11	148.09	35.86
12	153.09	35.89
13	158.08	36.15
14	163.06	36.63
15	168.01	37.34
16	172.92	38.28
17	177.78	39.44
18	182.59	40.82
19	187.33	42.41
20	191.99	44.23
21	196.56	46.25
22	201.03	48.48
23	205.40	50.91
24	209.66	53.54
25	213.79	56.36
26	217.78	59.36
27	221.64	62.54
28	225.34	65.90
29	228.89	69.42
30	232.28	73.10
31	235.49	76.93
32	238.53	80.91
33	239.01	81.61

*** 2.006 ***

Individual data on the 63 slices

Slice No.	Width (ft)	Weight (lbs)	Water Force Top (lbs)	Water Force Bot (lbs)	Force Norm (lbs)	Force Tan (lbs)	Earthquake Force Hor (lbs)	Earthquake Force Ver (lbs)	Surcharge Load (lbs)
1	4.5	643.8	1990.2	2554.3	0.0	0.0	0.0	0.0	0.0
2	4.6	1910.1	2025.6	3201.5	0.0	0.0	0.0	0.0	0.0
3	4.7	3094.2	2056.3	3783.3	0.0	0.0	0.0	0.0	0.0
4	4.8	4179.5	2082.4	4298.4	0.0	0.0	0.0	0.0	0.0
5	1.0	965.5	422.6	918.9	0.0	0.0	0.0	0.0	0.0
6	0.1	102.6	43.7	96.0	0.0	0.0	0.0	0.0	0.0
7	3.8	4138.9	1639.8	3731.0	0.0	0.0	0.0	0.0	0.0
8	4.1	5101.5	1810.9	4334.7	0.0	0.0	0.0	0.0	0.0
9	0.3	390.9	137.1	323.3	0.0	0.0	0.0	0.0	0.0
10	0.4	573.0	193.5	466.6	0.0	0.0	0.0	0.0	0.0
11	4.9	7429.1	1921.8	5434.0	0.0	0.0	0.0	0.0	0.0
12	4.7	8623.7	1350.3	5428.9	0.0	0.0	0.0	0.0	0.0
13	0.2	412.8	48.3	244.4	0.0	0.0	0.0	0.0	0.0
14	5.0	10527.2	862.8	5842.0	0.0	0.0	0.0	0.0	0.0
15	5.0	11883.9	318.8	5939.8	0.0	0.0	0.0	0.0	0.0
16	5.0	13057.1	0.0	5966.5	0.0	0.0	0.0	0.0	0.0
17	0.8	2220.5	0.0	969.0	0.0	0.0	0.0	0.0	0.0
18	0.3	826.0	0.0	357.3	0.0	0.0	0.0	0.0	0.0
19	0.3	698.2	0.0	300.6	0.0	0.0	0.0	0.0	0.0
20	0.3	963.8	0.0	413.0	0.0	0.0	0.0	0.0	0.0
21	0.4	1115.3	0.0	475.1	0.0	0.0	0.0	0.0	0.0
22	2.9	8198.4	0.0	3407.0	0.0	0.0	0.0	0.0	0.0
23	0.0	55.2	0.0	22.5	0.0	0.0	0.0	0.0	0.0
24	4.2	12397.0	0.0	4901.0	0.0	0.0	0.0	0.0	0.0
25	0.8	2317.6	0.0	883.0	0.0	0.0	0.0	0.0	0.0
26	1.5	4716.4	0.0	1775.5	0.0	0.0	0.0	0.0	0.0
27	3.4	10618.4	0.0	3844.7	0.0	0.0	0.0	0.0	0.0
28	2.6	8345.0	0.0	2899.2	0.0	0.0	0.0	0.0	0.0
29	0.4	1192.8	0.0	404.1	0.0	0.0	0.0	0.0	0.0
30	1.9	6198.2	0.0	2060.0	0.0	0.0	0.0	0.0	0.0
31	4.1	13362.4	0.0	4251.0	0.0	0.0	0.0	0.0	0.0
32	0.8	2584.4	0.0	785.5	0.0	0.0	0.0	0.0	0.0
33	4.8	15993.1	0.0	4640.5	0.0	0.0	0.0	0.0	0.0
34	4.7	15865.0	0.0	4176.1	0.0	0.0	0.0	0.0	0.0
35	4.7	15554.7	0.0	3644.2	0.0	0.0	0.0	0.0	0.0
36	4.6	15070.3	0.0	3046.0	0.0	0.0	0.0	0.0	0.0
37	4.5	14422.4	0.0	2382.7	0.0	0.0	0.0	0.0	0.0
38	4.4	13623.4	0.0	1655.7	0.0	0.0	0.0	0.0	0.0
39	0.4	1209.9	0.0	115.4	0.0	0.0	0.0	0.0	0.0
40	3.0	8938.2	0.0	640.7	0.0	0.0	0.0	0.0	0.0
41	0.9	2537.4	0.0	110.4	0.0	0.0	0.0	0.0	0.0
42	2.1	6103.0	0.0	118.5	0.0	0.0	0.0	0.0	0.0
43	2.0	5448.6	0.0	0.0	0.0	0.0	0.0	0.0	0.0
44	4.0	10283.2	0.0	0.0	0.0	0.0	0.0	0.0	0.0
45	3.9	8938.2	0.0	0.0	0.0	0.0	0.0	0.0	0.0
46	2.3	4747.2	0.0	0.0	0.0	0.0	0.0	0.0	0.0
47	1.4	2791.0	0.0	0.0	0.0	0.0	0.0	0.0	0.0
48	0.7	1303.8	0.0	0.0	0.0	0.0	0.0	0.0	0.0
49	0.9	1520.1	0.0	0.0	0.0	0.0	0.0	0.0	0.0

50	0.2	347.4	0.0	0.0	0.0	0.0	0.0	0.0	0.0
51	0.3	512.1	0.0	0.0	0.0	0.0	0.0	0.0	0.0
52	0.2	335.4	0.0	0.0	0.0	0.0	0.0	0.0	0.0
53	0.6	977.6	0.0	0.0	0.0	0.0	0.0	0.0	0.0
54	0.6	935.3	0.0	0.0	0.0	0.0	0.0	0.0	0.0
55	0.1	141.1	0.0	0.0	0.0	0.0	0.0	0.0	0.0
56	0.0	10.6	0.0	0.0	0.0	0.0	0.0	0.0	0.0
57	3.4	4358.7	0.0	0.0	0.0	0.0	0.0	0.0	0.0
58	1.0	1010.6	0.0	0.0	0.0	0.0	0.0	0.0	0.0
59	2.2	1682.2	0.0	0.0	0.0	0.0	0.0	0.0	0.0
60	0.4	223.1	0.0	0.0	0.0	0.0	0.0	0.0	0.0
61	0.8	378.9	0.0	0.0	0.0	0.0	0.0	0.0	0.0
62	1.9	464.3	0.0	0.0	0.0	0.0	0.0	0.0	0.0
63	0.5	22.2	0.0	0.0	0.0	0.0	0.0	0.0	0.0

Failure Surface Specified By 32 Coordinate Points

Point No.	X-Surf (ft)	Y-Surf (ft)
1	100.00	47.90
2	104.03	44.94
3	108.23	42.23
4	112.59	39.77
5	117.08	37.59
6	121.70	35.68
7	126.43	34.05
8	131.25	32.71
9	136.14	31.67
10	141.08	30.92
11	146.06	30.47
12	151.06	30.32
13	156.06	30.48
14	161.04	30.93
15	165.98	31.69
16	170.87	32.75
17	175.68	34.09
18	180.41	35.73
19	185.02	37.65
20	189.52	39.84
21	193.87	42.30
22	198.06	45.02
23	202.09	47.99
24	205.93	51.19
25	209.56	54.63
26	212.98	58.27
27	216.18	62.12
28	219.14	66.15
29	221.85	70.35
30	224.30	74.71
31	226.48	79.21
32	227.27	81.12

*** 2.007 ***

1

Failure Surface Specified By 34 Coordinate Points

Point No.	X-Surf (ft)	Y-Surf (ft)
1	100.00	47.90
2	104.22	45.23
3	108.58	42.77
4	113.06	40.55
5	117.65	38.56
6	122.33	36.81
7	127.10	35.30
8	131.94	34.04
9	136.83	33.04
10	141.78	32.29
11	146.75	31.79
12	151.75	31.55
13	156.75	31.57
14	161.74	31.85
15	166.71	32.39
16	171.65	33.18
17	176.54	34.23
18	181.36	35.53
19	186.12	37.08
20	190.79	38.87
21	195.36	40.89
22	199.82	43.16
23	204.15	45.65
24	208.36	48.36
25	212.41	51.28
26	216.31	54.41
27	220.04	57.74
28	223.60	61.25
29	226.97	64.94
30	230.14	68.81
31	233.11	72.83
32	235.87	77.00
33	238.41	81.31
34	238.56	81.59

*** 2.011 ***

Failure Surface Specified By 33 Coordinate Points

Point No.	X-Surf (ft)	Y-Surf (ft)
1	100.00	47.90
2	104.02	44.93
3	108.20	42.19
4	112.54	39.69
5	117.00	37.45
6	121.59	35.46
7	126.29	33.74
8	131.07	32.29
9	135.93	31.12
10	140.85	30.22
11	145.81	29.61
12	150.80	29.28

13	155.80	29.24
14	160.80	29.48
15	165.77	30.00
16	170.70	30.81
17	175.58	31.90
18	180.39	33.27
19	185.12	34.91
20	189.74	36.81
21	194.25	38.98
22	198.62	41.40
23	202.85	44.06
24	206.92	46.96
25	210.82	50.09
26	214.54	53.44
27	218.06	56.99
28	221.36	60.74
29	224.45	64.67
30	227.31	68.78
31	229.94	73.03
32	232.31	77.43
33	234.17	81.41

*** 2.013 ***

1

Failure Surface Specified By 30 Coordinate Points

Point No.	X-Surf (ft)	Y-Surf (ft)
1	100.00	47.90
2	104.82	46.56
3	109.68	45.40
4	114.58	44.42
5	119.52	43.63
6	124.49	43.04
7	129.47	42.63
8	134.46	42.41
9	139.46	42.38
10	144.46	42.54
11	149.45	42.89
12	154.42	43.43
13	159.37	44.16
14	164.28	45.07
15	169.16	46.18
16	173.99	47.46
17	178.77	48.93
18	183.49	50.59
19	188.14	52.42
20	192.72	54.42
21	197.22	56.60
22	201.64	58.95
23	205.96	61.46
24	210.18	64.14
25	214.30	66.97
26	218.31	69.96
27	222.20	73.10
28	225.97	76.39

29	229.61	79.81
30	231.06	81.29

*** 2.031 ***

Failure Surface Specified By 33 Coordinate Points

Point No.	X-Surf (ft)	Y-Surf (ft)
1	75.00	47.78
2	79.97	47.25
3	84.96	46.84
4	89.95	46.52
5	94.94	46.31
6	99.94	46.20
7	104.94	46.20
8	109.94	46.30
9	114.93	46.50
10	119.93	46.81
11	124.91	47.22
12	129.88	47.73
13	134.84	48.35
14	139.79	49.07
15	144.72	49.89
16	149.64	50.81
17	154.53	51.84
18	159.40	52.97
19	164.25	54.19
20	169.07	55.52
21	173.86	56.95
22	178.62	58.48
23	183.35	60.10
24	188.04	61.83
25	192.70	63.65
26	197.32	65.56
27	201.90	67.57
28	206.43	69.68
29	210.92	71.88
30	215.37	74.17
31	219.76	76.56
32	224.10	79.03
33	227.62	81.14

*** 2.049 ***

1

Failure Surface Specified By 30 Coordinate Points

Point No.	X-Surf (ft)	Y-Surf (ft)
1	100.00	47.90

2	104.86	46.71
3	109.75	45.70
4	114.68	44.86
5	119.64	44.20
6	124.62	43.72
7	129.61	43.42
8	134.61	43.30
9	139.61	43.36
10	144.60	43.60
11	149.58	44.02
12	154.55	44.61
13	159.49	45.39
14	164.39	46.34
15	169.27	47.47
16	174.09	48.77
17	178.87	50.25
18	183.59	51.89
19	188.25	53.71
20	192.84	55.69
21	197.36	57.84
22	201.79	60.14
23	206.14	62.61
24	210.40	65.23
25	214.56	68.00
26	218.62	70.92
27	222.57	73.98
28	226.41	77.19
29	230.13	80.53
30	230.92	81.28

*** 2.053 ***

Failure Surface Specified By 35 Coordinate Points

Point No.	X-Surf (ft)	Y-Surf (ft)
1	100.00	47.90
2	104.28	45.31
3	108.67	42.92
4	113.17	40.75
5	117.78	38.80
6	122.47	37.07
7	127.24	35.57
8	132.07	34.29
9	136.96	33.26
10	141.90	32.46
11	146.87	31.89
12	151.86	31.57
13	156.86	31.48
14	161.85	31.64
15	166.84	32.04
16	171.80	32.67
17	176.72	33.54
18	181.60	34.65
19	186.41	35.99
20	191.16	37.56
21	195.83	39.36

22	200.40	41.38
23	204.87	43.61
24	209.23	46.06
25	213.47	48.72
26	217.57	51.57
27	221.54	54.62
28	225.35	57.86
29	229.00	61.27
30	232.48	64.86
31	235.79	68.61
32	238.91	72.51
33	241.85	76.56
34	244.58	80.75
35	245.23	81.86

*** 2.055 ***

1

Failure Surface Specified By 33 Coordinate Points

Point No.	X-Surf (ft)	Y-Surf (ft)
1	100.00	47.90
2	104.64	46.03
3	109.34	44.35
4	114.12	42.85
5	118.94	41.55
6	123.82	40.45
7	128.74	39.54
8	133.69	38.83
9	138.66	38.32
10	143.65	38.02
11	148.65	37.91
12	153.65	38.00
13	158.64	38.30
14	163.62	38.79
15	168.57	39.49
16	173.49	40.38
17	178.37	41.48
18	183.20	42.76
19	187.97	44.24
20	192.69	45.91
21	197.33	47.77
22	201.89	49.82
23	206.37	52.05
24	210.75	54.45
25	215.03	57.03
26	219.21	59.78
27	223.27	62.70
28	227.21	65.77
29	231.03	69.01
30	234.71	72.39
31	238.25	75.92
32	241.65	79.59
33	243.53	81.79

*** 2.056 ***

Failure Surface Specified By 34 Coordinate Points

Point No.	X-Surf (ft)	Y-Surf (ft)
1	100.00	47.90
2	103.65	44.49
3	107.51	41.31
4	111.57	38.39
5	115.80	35.73
6	120.20	33.35
7	124.74	31.25
8	129.40	29.45
9	134.17	27.95
10	139.03	26.76
11	143.95	25.88
12	148.92	25.32
13	153.92	25.08
14	158.91	25.15
15	163.90	25.55
16	168.85	26.26
17	173.74	27.29
18	178.56	28.63
19	183.28	30.28
20	187.89	32.22
21	192.36	34.46
22	196.68	36.97
23	200.83	39.76
24	204.80	42.80
25	208.56	46.10
26	212.10	49.63
27	215.41	53.37
28	218.48	57.32
29	221.28	61.46
30	223.82	65.77
31	226.07	70.23
32	228.04	74.83
33	229.70	79.55
34	230.19	81.25

*** 2.074 ***

1

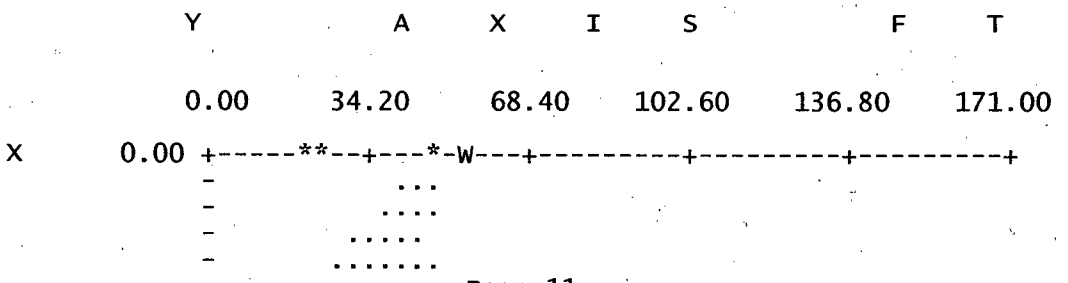

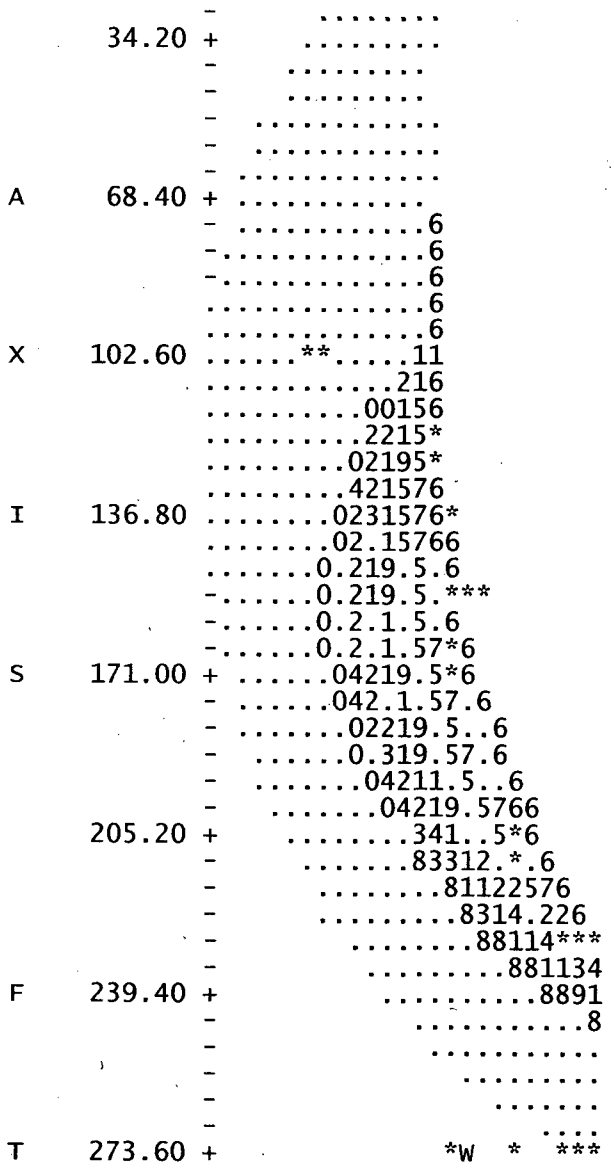
A
I
S
F
T
34.20
68.40
102.60
136.80
171.00
205.20
239.40
273.60

BISHOP #4 STATIC CIRCULAR

EXTREME HIGH WATER

Geometry and Boundary Conditions

Problem: SMC Newfield Decommissioning - Section A-A' - FS Min = 2.076

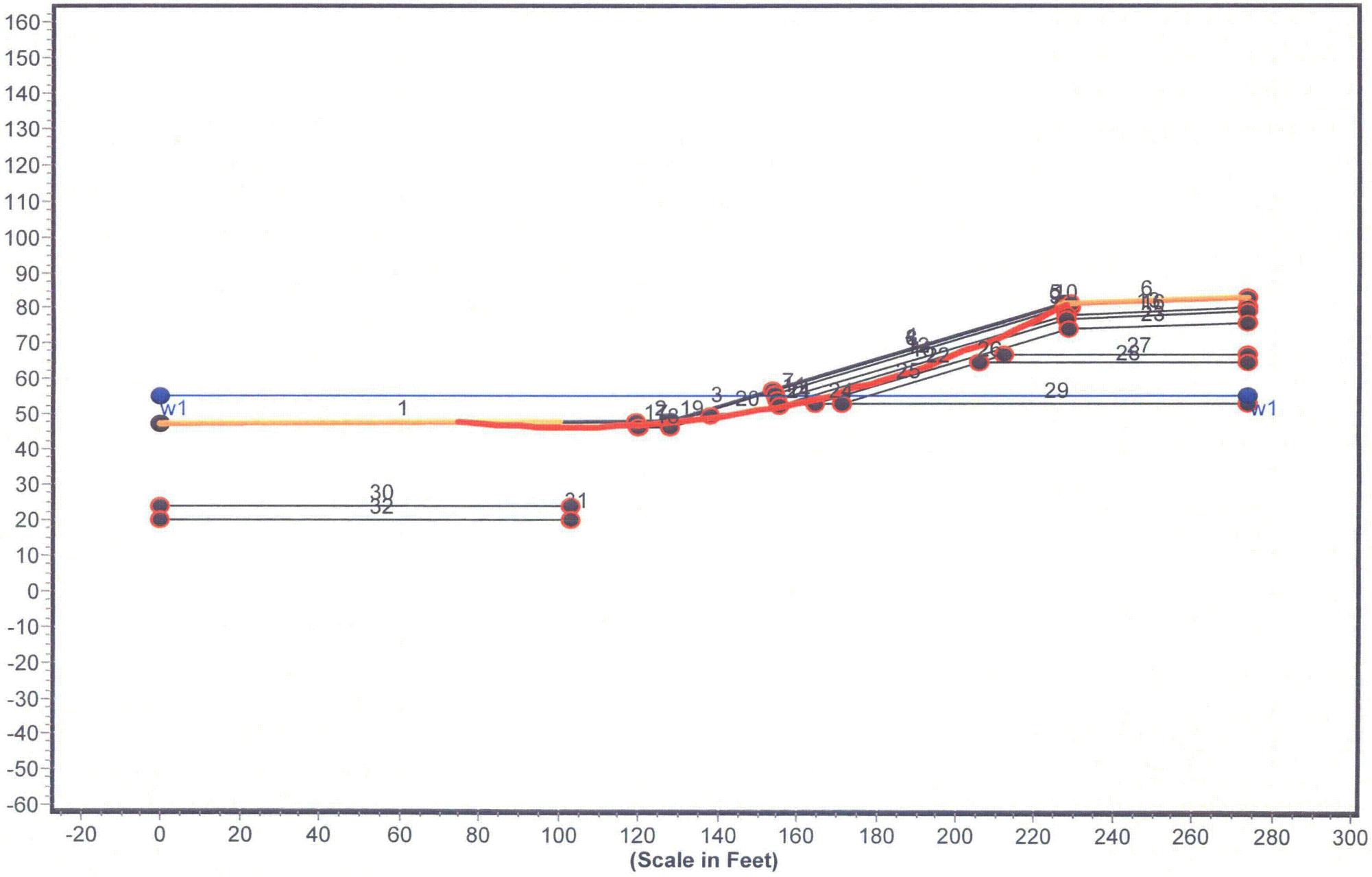

Geometry and Boundary Conditions

Problem: SMC Newfield Decommissioning - Section A-A' - FS Min = 2.076

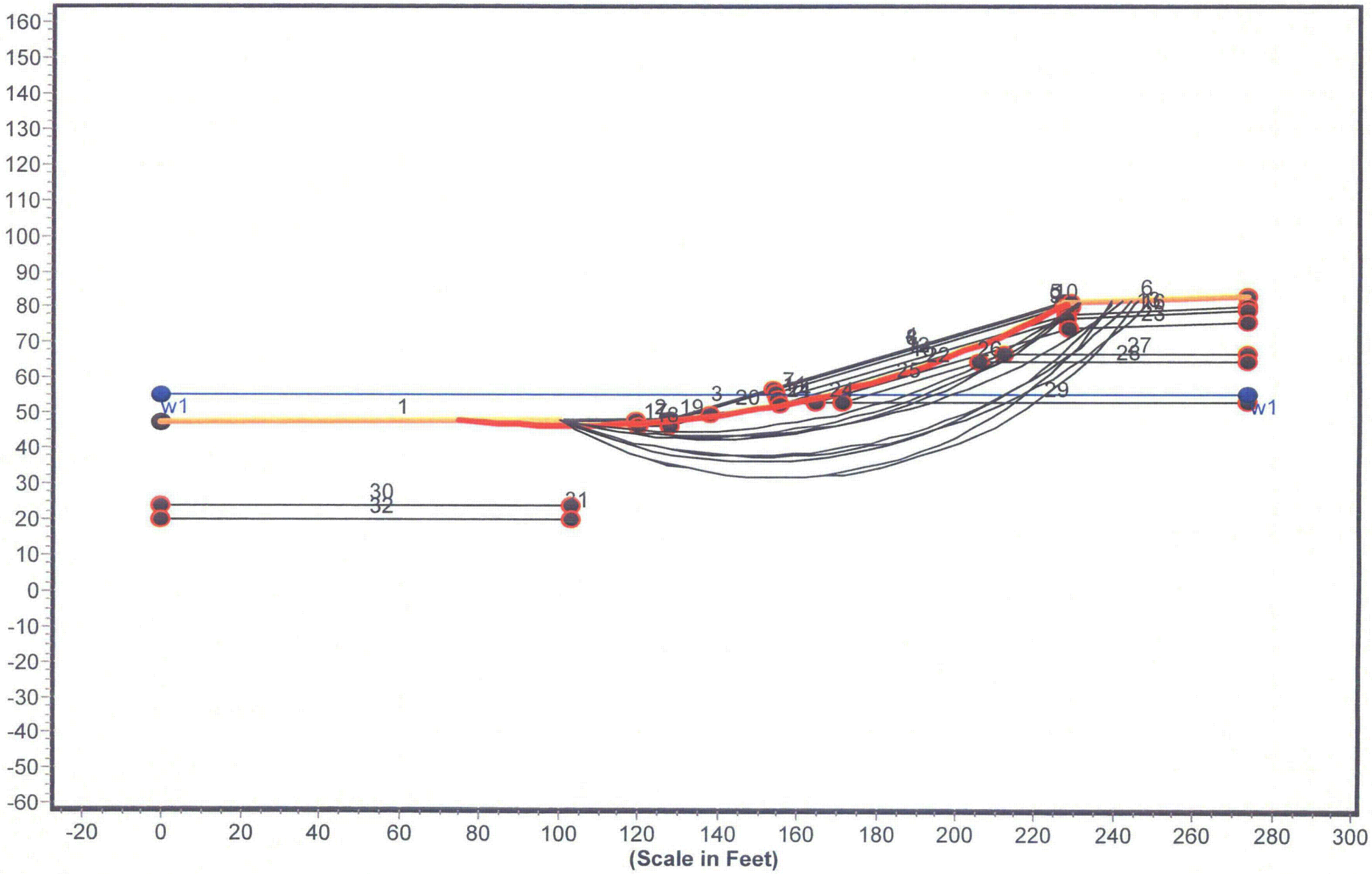

Geometry and Boundary Conditions

Problem: SMC Newfield Decommissioning - Section A-A' - FS Min = 2.076

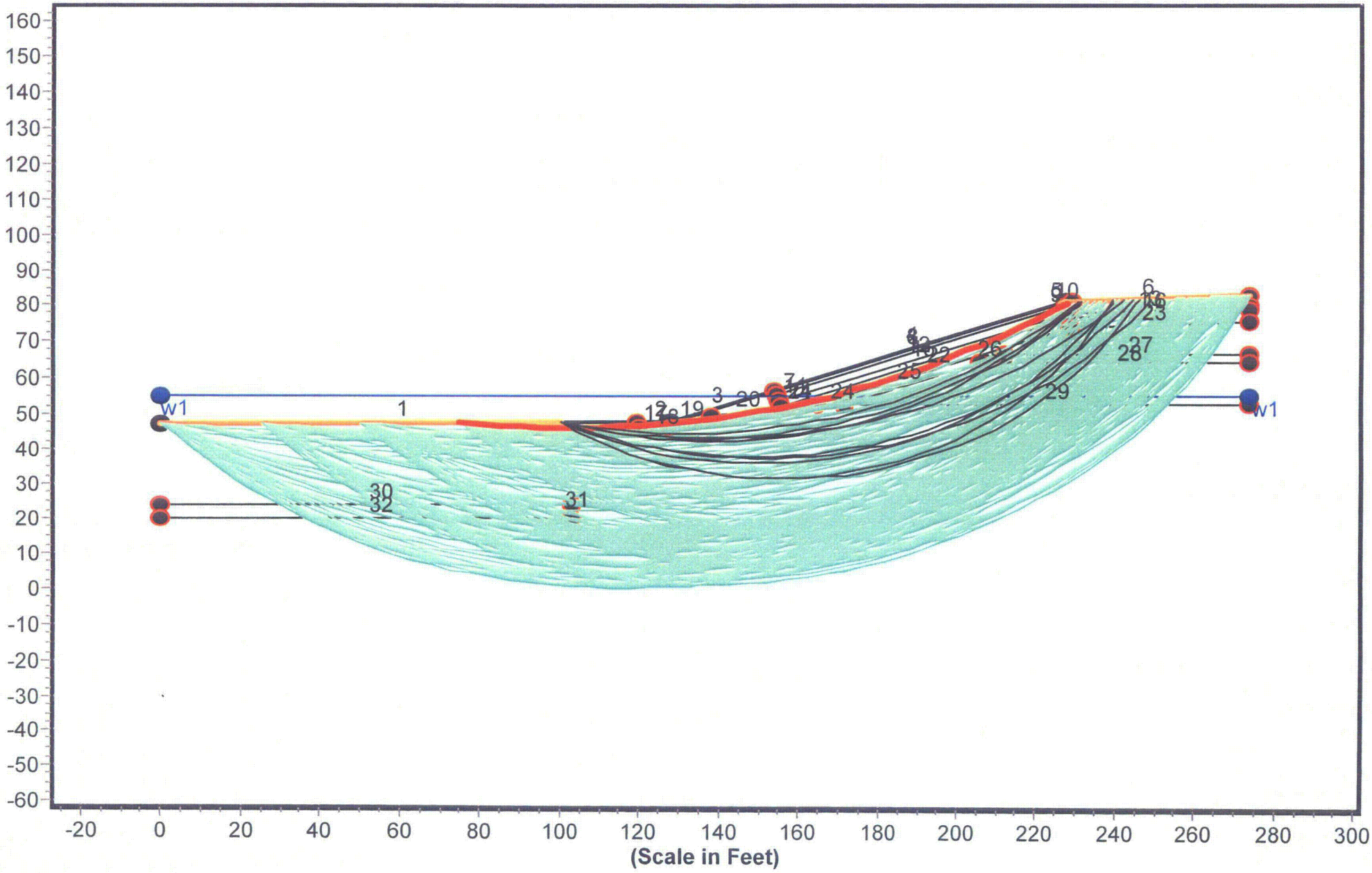

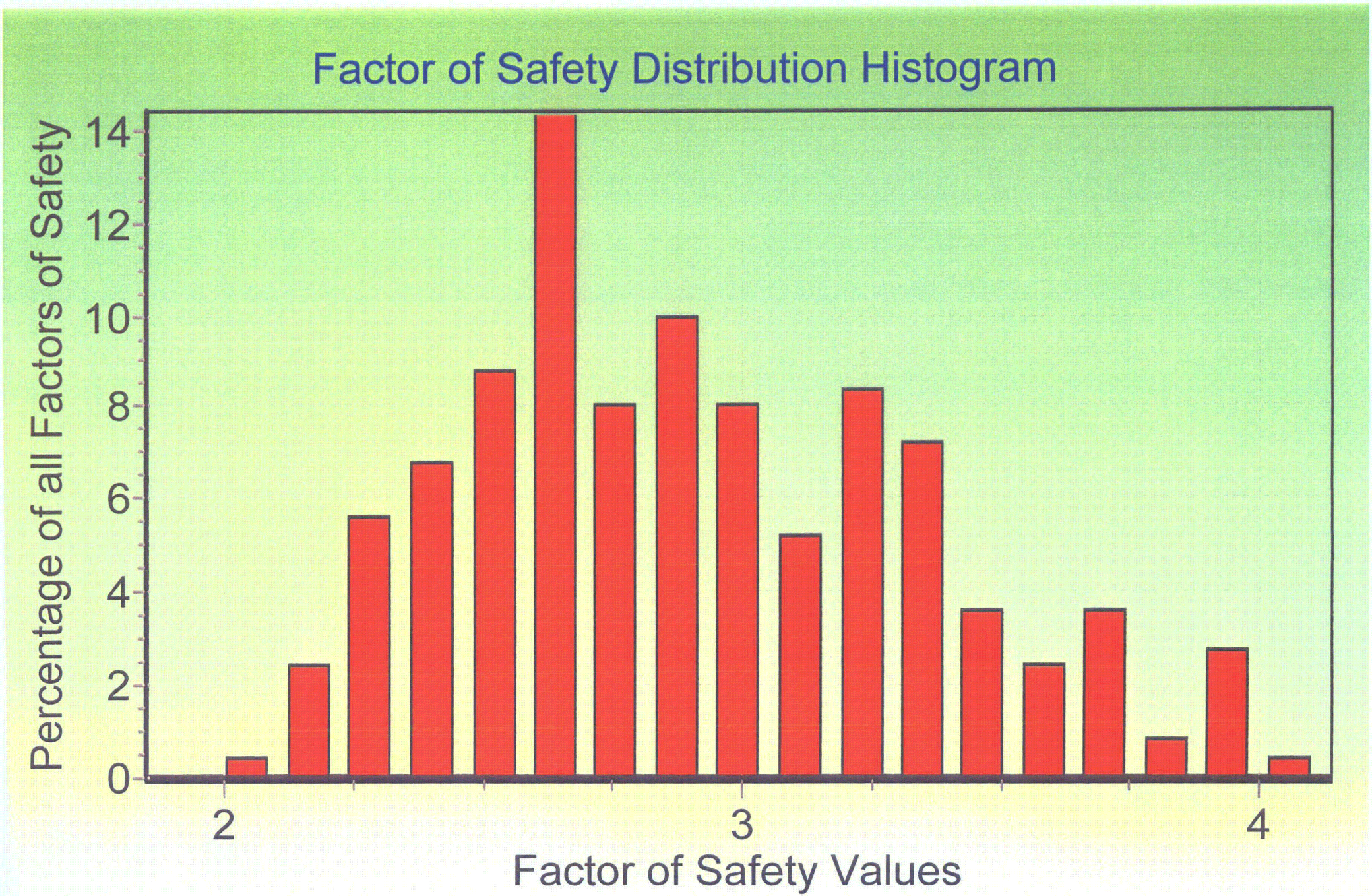
Factor of Safety Distribution Histogram
Percentage of all Factors of Safety
0
2
4
6
8
10
12
14
2
3
4
Factor of Safety Values

Bishop #4 High Water Results.txt
** PCSTABL6 **

by
Purdue University

1

--Slope Stability Analysis--
Simplified Janbu, Simplified Bishop
or Spencer's Method of Slices

Run Date:
Time of Run:
Run By:
Input Data Filename: run.in
Output Filename: result.out
Unit: ENGLISH
Plotted Output Filename: result.plt

PROBLEM DESCRIPTION SMC Newfield Decommissioning - Section A -A'

BOUNDARY COORDINATES

6 Top Boundaries
32 Total Boundaries

Boundary No.	X-Left (ft)	Y-Left (ft)	X-Right (ft)	Y-Right (ft)	Soil Type Below Bnd
1	0.00	47.40	119.50	48.00	7
2	119.50	48.00	127.50	48.00	1
3	127.50	48.00	153.90	56.80	1
4	153.90	56.80	226.90	81.10	1
5	226.90	81.10	228.90	81.20	1
6	228.90	81.20	273.60	83.00	2
7	153.90	56.80	154.20	55.80	1
8	154.20	55.80	227.10	80.10	2
9	227.10	80.10	228.80	80.20	2
10	228.80	80.20	228.90	81.20	2
11	154.20	55.80	154.80	53.90	1
12	154.80	53.90	227.40	78.10	1
13	227.40	78.10	273.60	80.00	1
14	154.80	53.90	155.20	52.60	1
15	155.20	52.60	227.60	77.10	3
16	227.60	77.10	273.60	79.00	3
17	119.50	48.00	119.60	46.40	7
18	119.60	46.40	127.80	46.40	7
19	127.80	46.40	137.90	49.80	7
20	137.90	49.80	155.20	52.60	7
21	155.20	52.60	164.60	53.00	7
22	164.60	53.00	228.20	74.10	4
23	228.20	74.10	273.60	76.00	4
24	164.60	53.00	171.00	53.00	7
25	171.00	53.00	205.80	64.60	6
26	205.80	64.60	211.80	66.60	5

27	211.80	66.60	273.60	66.60	5
28	205.80	64.60	273.60	64.60	6
29	171.00	53.00	273.60	53.00	7
30	0.00	24.00	103.10	24.00	8
31	103.00	20.00	103.10	24.00	7
32	0.00	20.00	103.10	20.00	7

1

ISOTROPIC SOIL PARAMETERS

8 Type(s) of Soil

Soil Type No.	Total Unit Wt. (pcf)	Saturated Unit Wt. (pcf)	Cohesion Intercept (psf)	Friction Angle (deg)	Pore Pressure Param.	Pressure Constant (psf)	Piez. Surface No.
1	135.0	140.0	0.0	40.0	0.00	0.0	1
2	135.0	140.0	0.0	35.0	0.00	0.0	1
3	125.0	130.0	250.0	15.0	0.00	0.0	1
4	125.0	135.0	0.0	32.0	0.00	0.0	1
5	135.0	140.0	0.0	38.0	0.00	0.0	1
6	135.0	140.0	0.0	40.0	0.00	0.0	1
7	115.0	130.0	0.0	33.0	0.00	0.0	1
8	130.0	140.0	300.0	20.0	0.00	0.0	1

1

1 PIEZOMETRIC SURFACE(S) HAVE BEEN SPECIFIED

Unit Weight of Water = 62.40

Piezometric Surface No. 1 Specified by 2 Coordinate Points

Point No.	X-Water (ft)	Y-Water (ft)
1	0.00	55.00
2	273.60	55.00

1

A Critical Failure Surface Searching Method, Using A Random Technique For Generating Circular Surfaces, Has Been Specified.

250 Trial Surfaces Have Been Generated.

50 Surfaces Initiate From Each Of 5 Points Equally Spaced Along The Ground Surface Between X = 0.00 ft.
and X = 100.00 ft.

Each Surface Terminates Between X = 226.00 ft.
and X = 273.60 ft.

Unless Further Limitations Were Imposed, The Minimum Elevation At Which A Surface Extends Is Y = 0.00 ft.

5.00 ft. Line Segments Define Each Trial Failure Surface.

Restrictions Have Been Imposed Upon The Angle Of Initiation. The Angle Has Been Restricted Between The Angles Of -45.0 And -5.0 deg.

1

Following Are Displayed The Ten Most Critical Of The Trial Failure Surfaces Examined. They Are Ordered - Most Critical First.

* * Safety Factors Are Calculated By The Modified Bishop Method * *

Failure Surface Specified By 33 Coordinate Points

Point No.	X-Surf (ft)	Y-Surf (ft)
1	75.00	47.78
2	79.97	47.25
3	84.96	46.84
4	89.95	46.52
5	94.94	46.31
6	99.94	46.20
7	104.94	46.20
8	109.94	46.30
9	114.93	46.50
10	119.93	46.81
11	124.91	47.22
12	129.88	47.73
13	134.84	48.35
14	139.79	49.07
15	144.72	49.89
16	149.64	50.81
17	154.53	51.84
18	159.40	52.96
19	164.25	54.19
20	169.07	55.52
21	173.86	56.95
22	178.62	58.48
23	183.35	60.10
24	188.05	61.82
25	192.70	63.64
26	197.32	65.56
27	201.90	67.57
28	206.43	69.68
29	210.92	71.88
30	215.37	74.17
31	219.76	76.55
32	224.11	79.03
33	227.63	81.14

Circle Center At X = 102.6 ; Y = 287.2 and Radius, 241.0

*** 2.076 ***

Individual data on the 50 slices

Slice No.	Width (ft)	Weight (lbs)	Water Force Top (lbs)	Water Force Bot (lbs)	Force Norm (lbs)	Force Tan (lbs)	Earthquake Force Hor (lbs)	Earthquake Force Ver (lbs)	Surcharge Load (lbs)
1	5.0	176.8	2237.6	2335.1	0.0	0.0	0.0	0.0	0.0
2	5.0	497.9	2234.2	2481.9	0.0	0.0	0.0	0.0	0.0
3	5.0	752.9	2229.8	2596.3	0.0	0.0	0.0	0.0	0.0
4	5.0	941.1	2224.4	2678.5	0.0	0.0	0.0	0.0	0.0
5	5.0	1061.8	2218.1	2728.4	0.0	0.0	0.0	0.0	0.0
6	5.0	1114.9	2210.8	2745.9	0.0	0.0	0.0	0.0	0.0
7	5.0	1100.0	2202.5	2731.0	0.0	0.0	0.0	0.0	0.0
8	5.0	1017.3	2193.3	2683.8	0.0	0.0	0.0	0.0	0.0
9	4.6	800.3	1997.3	2385.9	0.0	0.0	0.0	0.0	0.0
10	0.1	12.5	33.2	39.0	0.0	0.0	0.0	0.0	0.0
11	0.3	58.9	152.7	179.3	0.0	0.0	0.0	0.0	0.0
12	5.0	689.6	2176.6	2492.4	0.0	0.0	0.0	0.0	0.0
13	2.6	235.6	1131.9	1243.5	0.0	0.0	0.0	0.0	0.0
14	2.4	263.4	1034.6	1104.8	0.0	0.0	0.0	0.0	0.0
15	3.0	569.8	1113.2	1320.1	0.0	0.0	0.0	0.0	0.0
16	2.0	525.3	642.3	851.9	0.0	0.0	0.0	0.0	0.0
17	3.1	1000.0	812.6	1239.2	0.0	0.0	0.0	0.0	0.0
18	1.9	736.5	400.5	724.4	0.0	0.0	0.0	0.0	0.0
19	4.9	2326.1	675.0	1723.2	0.0	0.0	0.0	0.0	0.0
20	4.9	2849.7	142.1	1450.8	0.0	0.0	0.0	0.0	0.0
21	4.3	2825.9	0.0	1016.7	0.0	0.0	0.0	0.0	0.0
22	0.3	210.0	0.0	62.4	0.0	0.0	0.0	0.0	0.0
23	0.3	177.9	0.0	51.6	0.0	0.0	0.0	0.0	0.0
24	0.1	55.8	0.0	16.0	0.0	0.0	0.0	0.0	0.0
25	0.3	190.4	0.0	53.8	0.0	0.0	0.0	0.0	0.0
26	0.4	285.5	0.0	78.2	0.0	0.0	0.0	0.0	0.0
27	2.9	2125.9	0.0	496.4	0.0	0.0	0.0	0.0	0.0
28	0.3	239.8	0.0	47.0	0.0	0.0	0.0	0.0	0.0
29	1.0	746.8	0.0	135.4	0.0	0.0	0.0	0.0	0.0
30	2.9	2245.4	0.0	310.5	0.0	0.0	0.0	0.0	0.0
31	2.0	1562.2	0.0	133.0	0.0	0.0	0.0	0.0	0.0
32	2.9	2388.6	0.0	76.6	0.0	0.0	0.0	0.0	0.0
33	1.9	1568.0	0.0	0.0	0.0	0.0	0.0	0.0	0.0
34	4.8	4058.9	0.0	0.0	0.0	0.0	0.0	0.0	0.0
35	4.8	4098.7	0.0	0.0	0.0	0.0	0.0	0.0	0.0
36	4.7	4071.3	0.0	0.0	0.0	0.0	0.0	0.0	0.0
37	4.7	3978.0	0.0	0.0	0.0	0.0	0.0	0.0	0.0
38	4.7	3820.4	0.0	0.0	0.0	0.0	0.0	0.0	0.0
39	4.6	3600.1	0.0	0.0	0.0	0.0	0.0	0.0	0.0
40	4.6	3319.2	0.0	0.0	0.0	0.0	0.0	0.0	0.0
41	4.5	2979.7	0.0	0.0	0.0	0.0	0.0	0.0	0.0
42	1.7	1032.1	0.0	0.0	0.0	0.0	0.0	0.0	0.0
43	2.8	1546.0	0.0	0.0	0.0	0.0	0.0	0.0	0.0
44	4.0	1910.3	0.0	0.0	0.0	0.0	0.0	0.0	0.0
45	0.4	187.7	0.0	0.0	0.0	0.0	0.0	0.0	0.0
46	4.4	1560.6	0.0	0.0	0.0	0.0	0.0	0.0	0.0
47	4.3	970.9	0.0	0.0	0.0	0.0	0.0	0.0	0.0

48	0.3	41.3	0.0	0.0	0.0	0.0	0.0	0.0	0.0
49	2.5	249.7	0.0	0.0	0.0	0.0	0.0	0.0	0.0
50	0.7	19.9	0.0	0.0	0.0	0.0	0.0	0.0	0.0

Failure Surface Specified By 30 Coordinate Points

Point No.	X-Surf (ft)	Y-Surf (ft)
1	100.00	47.90
2	104.82	46.56
3	109.68	45.40
4	114.58	44.42
5	119.52	43.63
6	124.49	43.04
7	129.47	42.62
8	134.46	42.40
9	139.46	42.37
10	144.46	42.53
11	149.45	42.88
12	154.42	43.42
13	159.37	44.15
14	164.28	45.07
15	169.16	46.17
16	173.99	47.46
17	178.77	48.92
18	183.49	50.57
19	188.14	52.40
20	192.72	54.41
21	197.23	56.58
22	201.64	58.93
23	205.96	61.44
24	210.19	64.12
25	214.31	66.95
26	218.32	69.94
27	222.21	73.08
28	225.98	76.36
29	229.62	79.79
30	231.10	81.29

Circle Center At X = 137.8 ; Y = 173.7 and Radius, 131.4

*** 2.126 ***

1

Failure Surface Specified By 30 Coordinate Points

Point No.	X-Surf (ft)	Y-Surf (ft)
1	100.00	47.90
2	104.86	46.71
3	109.75	45.70
4	114.68	44.86
5	119.64	44.20
6	124.62	43.72
7	129.61	43.42

8	134.61	43.30
9	139.60	43.36
10	144.60	43.60
11	149.58	44.01
12	154.55	44.61
13	159.49	45.38
14	164.39	46.33
15	169.27	47.46
16	174.09	48.76
17	178.87	50.24
18	183.59	51.88
19	188.25	53.70
20	192.84	55.68
21	197.36	57.82
22	201.80	60.13
23	206.15	62.59
24	210.41	65.21
25	214.57	67.98
26	218.63	70.90
27	222.58	73.96
28	226.42	77.16
29	230.15	80.50
30	230.96	81.28

Circle Center At X = 135.5 ; Y = 182.3 and Radius, 139.0

*** 2.136 ***

Failure Surface Specified By 29 Coordinate Points

Point No.	X-Surf (ft)	Y-Surf (ft)
1	100.00	47.90
2	104.91	46.94
3	109.84	46.14
4	114.80	45.51
5	119.78	45.04
6	124.77	44.73
7	129.77	44.59
8	134.77	44.61
9	139.77	44.80
10	144.75	45.16
11	149.73	45.68
12	154.68	46.36
13	159.61	47.20
14	164.50	48.21
15	169.37	49.38
16	174.19	50.71
17	178.96	52.19
18	183.68	53.84
19	188.35	55.64
20	192.95	57.59
21	197.49	59.69
22	201.95	61.94
23	206.34	64.34
24	210.65	66.88
25	214.87	69.56

26	219.00	72.38
27	223.03	75.33
28	226.96	78.42
29	230.35	81.26

Circle Center At X = 131.5 ; Y = 196.0 and Radius, 151.4

*** 2.149 ***

1

Failure Surface Specified By 33 Coordinate Points

Point No.	X-Surf (ft)	Y-Surf (ft)
1	100.00	47.90
2	104.50	45.72
3	109.10	43.75
4	113.78	41.99
5	118.53	40.45
6	123.35	39.12
7	128.23	38.02
8	133.15	37.14
9	138.11	36.48
10	143.09	36.05
11	148.09	35.85
12	153.09	35.88
13	158.08	36.13
14	163.06	36.61
15	168.01	37.32
16	172.92	38.25
17	177.78	39.41
18	182.59	40.78
19	187.33	42.38
20	191.99	44.18
21	196.57	46.20
22	201.04	48.43
23	205.41	50.85
24	209.67	53.48
25	213.80	56.29
26	217.80	59.29
27	221.66	62.47
28	225.37	65.82
29	228.93	69.34
30	232.32	73.01
31	235.54	76.84
32	238.58	80.81
33	239.14	81.61

Circle Center At X = 150.0 ; Y = 145.5 and Radius, 109.7

*** 2.180 ***

Failure Surface Specified By 33 Coordinate Points

Point No.	X-Surf (ft)	Y-Surf (ft)
1	100.00	47.90
2	104.64	46.03
3	109.34	44.35
4	114.12	42.85
5	118.94	41.55
6	123.82	40.45
7	128.74	39.54
8	133.69	38.83
9	138.66	38.32
10	143.65	38.01
11	148.65	37.90
12	153.65	37.99
13	158.64	38.28
14	163.62	38.77
15	168.57	39.46
16	173.49	40.35
17	178.37	41.44
18	183.20	42.72
19	187.98	44.20
20	192.69	45.86
21	197.34	47.72
22	201.90	49.76
23	206.38	51.98
24	210.77	54.38
25	215.05	56.95
26	219.23	59.69
27	223.30	62.60
28	227.25	65.67
29	231.07	68.90
30	234.75	72.28
31	238.30	75.80
32	241.71	79.46
33	243.70	81.80

Circle Center At X = 148.9 ; Y = 162.3 and Radius, 124.4

*** 2.192 ***

1

Failure Surface Specified By 32 Coordinate Points

Point No.	X-Surf (ft)	Y-Surf (ft)
1	100.00	47.90
2	104.87	46.76
3	109.77	45.78
4	114.70	44.95
5	119.66	44.28
6	124.63	43.76
7	129.62	43.41
8	134.61	43.21
9	139.61	43.17

10	144.61	43.30
11	149.60	43.57
12	154.58	44.01
13	159.55	44.61
14	164.49	45.36
15	169.41	46.27
16	174.29	47.34
17	179.14	48.56
18	183.95	49.93
19	188.71	51.46
20	193.42	53.14
21	198.08	54.96
22	202.67	56.93
23	207.20	59.05
24	211.66	61.31
25	216.05	63.71
26	220.35	66.25
27	224.58	68.92
28	228.72	71.73
29	232.76	74.67
30	236.71	77.73
31	240.57	80.92
32	241.46	81.71

Circle Center At X = 138.3 ; Y = 200.5 and Radius, 157.3

*** 2.203 ***

Failure Surface Specified By 34 Coordinate Points

Point No.	X-Surf (ft)	Y-Surf (ft)
1	100.00	47.90
2	104.63	46.01
3	109.33	44.30
4	114.09	42.77
5	118.90	41.42
6	123.77	40.27
7	128.67	39.31
8	133.61	38.53
9	138.58	37.95
10	143.56	37.56
11	148.56	37.37
12	153.56	37.37
13	158.56	37.57
14	163.54	37.96
15	168.51	38.54
16	173.45	39.32
17	178.35	40.28
18	183.22	41.44
19	188.03	42.78
20	192.79	44.31
21	197.49	46.03
22	202.12	47.93
23	206.67	50.00
24	211.13	52.25
25	215.51	54.67

26	219.78	57.26
27	223.96	60.01
28	228.02	62.93
29	231.97	66.00
30	235.79	69.22
31	239.49	72.59
32	243.05	76.09
33	246.47	79.74
34	248.43	81.99

Circle Center At X = 151.0 ; Y = 165.9 and Radius, 128.6

*** 2.234 ***

1

Failure Surface Specified By 34 Coordinate Points

Point No.	X-Surf (ft)	Y-Surf (ft)
1	100.00	47.90
2	104.22	45.23
3	108.58	42.77
4	113.06	40.55
5	117.65	38.56
6	122.33	36.81
7	127.10	35.30
8	131.93	34.04
9	136.83	33.03
10	141.78	32.28
11	146.75	31.78
12	151.74	31.54
13	156.74	31.56
14	161.74	31.83
15	166.71	32.37
16	171.65	33.16
17	176.54	34.20
18	181.37	35.49
19	186.12	37.04
20	190.79	38.82
21	195.36	40.84
22	199.83	43.10
23	204.16	45.59
24	208.37	48.29
25	212.43	51.21
26	216.33	54.33
27	220.07	57.66
28	223.63	61.17
29	227.01	64.86
30	230.18	68.71
31	233.16	72.73
32	235.93	76.90
33	238.47	81.20
34	238.68	81.59

Circle Center At X = 153.9 ; Y = 128.3 and Radius, 96.8

*** 2.256 ***

Failure Surface Specified By 35 Coordinate Points

Point No.	X-Surf (ft)	Y-Surf (ft)
1	100.00	47.90
2	104.28	45.31
3	108.67	42.92
4	113.17	40.75
5	117.77	38.80
6	122.47	37.07
7	127.23	35.56
8	132.07	34.29
9	136.96	33.25
10	141.89	32.44
11	146.86	31.88
12	151.85	31.55
13	156.85	31.46
14	161.85	31.61
15	166.83	32.00
16	171.79	32.63
17	176.72	33.50
18	181.59	34.60
19	186.41	35.93
20	191.16	37.50
21	195.83	39.29
22	200.41	41.30
23	204.88	43.53
24	209.25	45.97
25	213.49	48.62
26	217.60	51.46
27	221.57	54.50
28	225.39	57.73
29	229.05	61.14
30	232.54	64.72
31	235.85	68.46
32	238.98	72.36
33	241.93	76.40
34	244.67	80.58
35	245.43	81.87

Circle Center At X = 156.2 ; Y = 135.7 and Radius, 104.2

*** 2.281 ***

1

Y A X I S F T

0.00 34.20 68.40 102.60 136.80 171.00

X 0.00 +-----**--+---*-W---+---------+---------+---------+

...

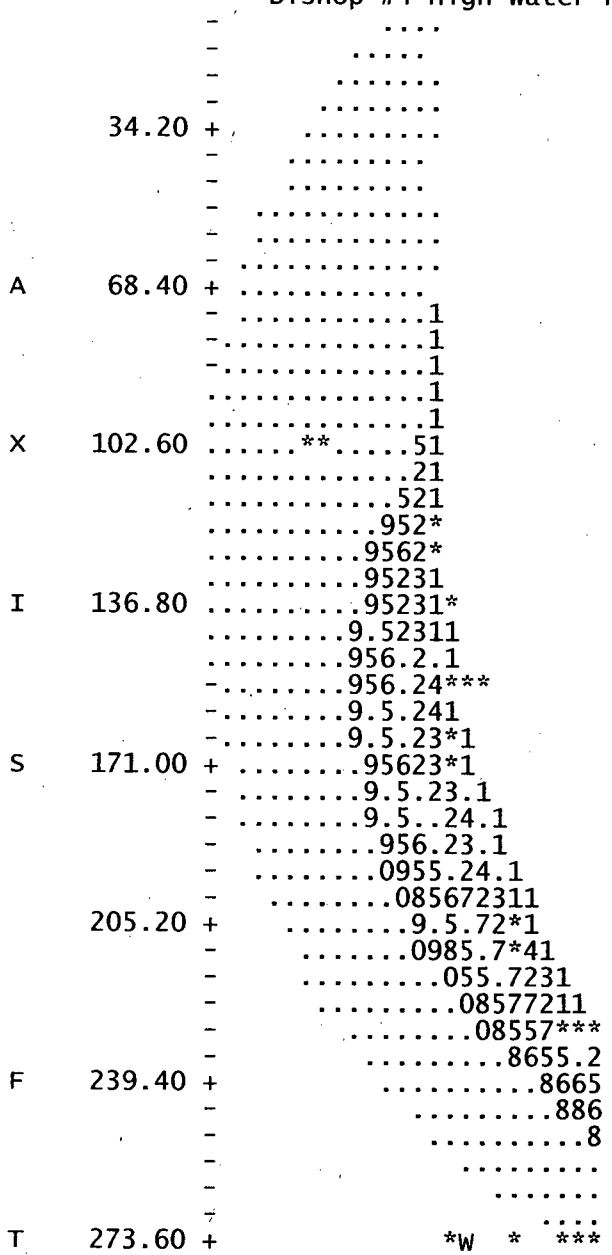
34.20
68.40
A
102.60
X
136.80
I
171.00
S
205.20
239.40
F
273.60
T

SPENCER #4 STATIC SLICES

EXTREME HIGH WATER

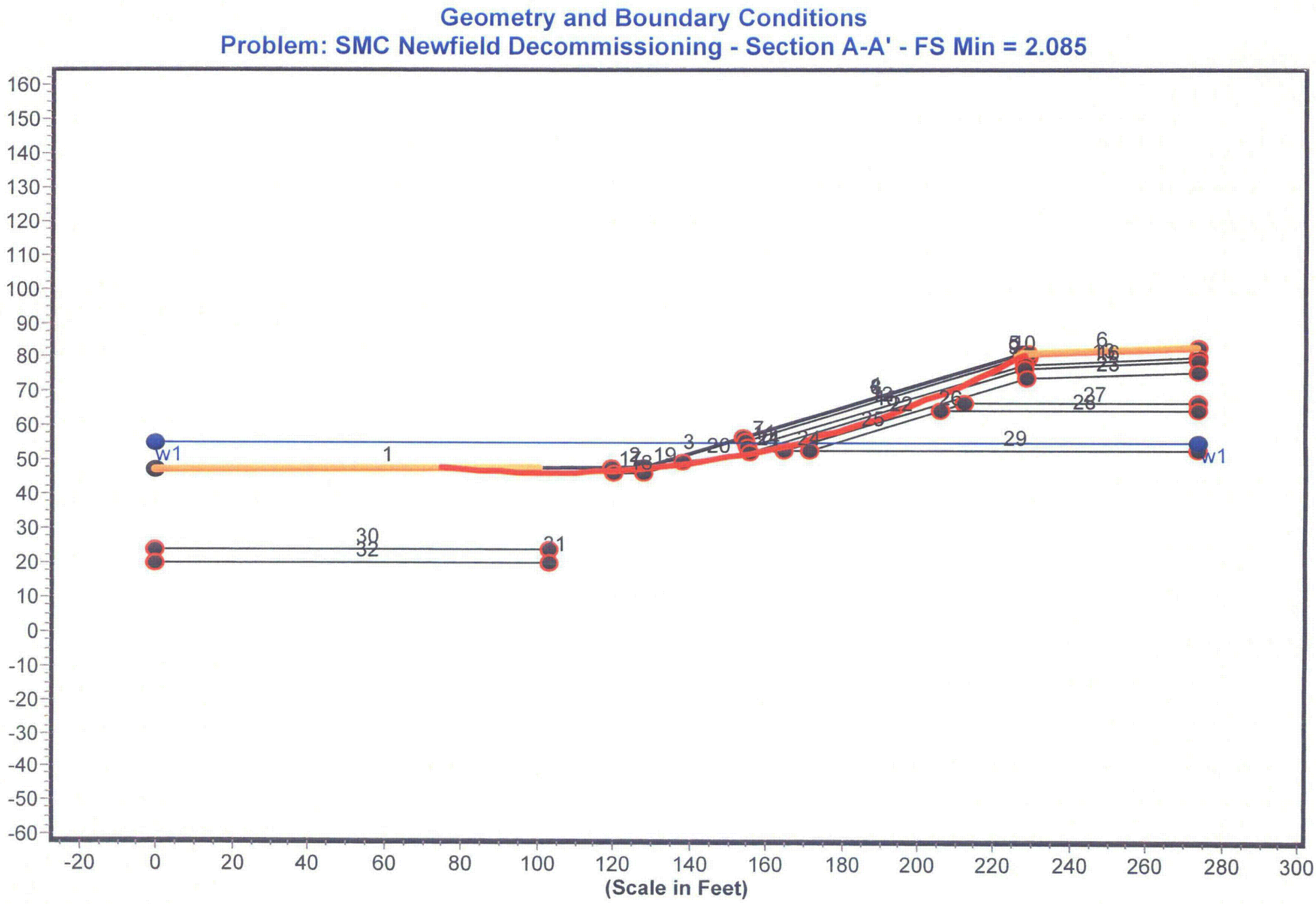
Geometry and Boundary Conditions
Problem: SMC Newfield Decommissioning - Section A-A' - FS Min = 2.085
160
150
140
130
120
110
100
90
80
70
60
50
40
30
20
10
0
-10
-20
-30
-40
-50
-60
-20
0
20
40
60
80
100
120
140
160
180
200
220
240
260
280
300
(Scale in Feet)
w1
w1
1
3
19
20
26
27
28
29
30
32
21

Geometry and Boundary Conditions

Problem: SMC Newfield Decommissioning - Section A-A' - FS Min = 2.085

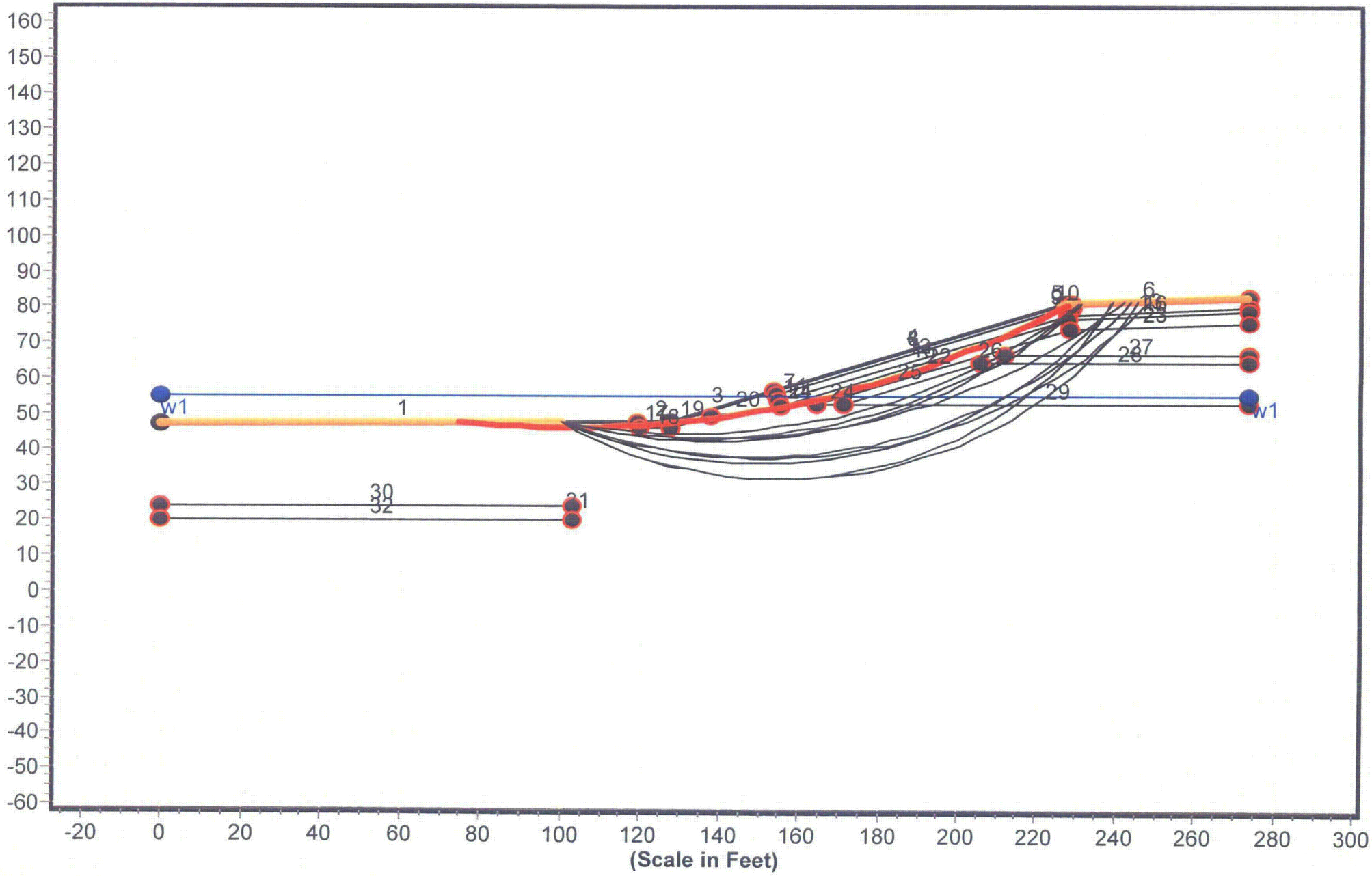

Geometry and Boundary Conditions
Problem: SMC Newfield Decommissioning - Section A-A' - FS Min = 2.085

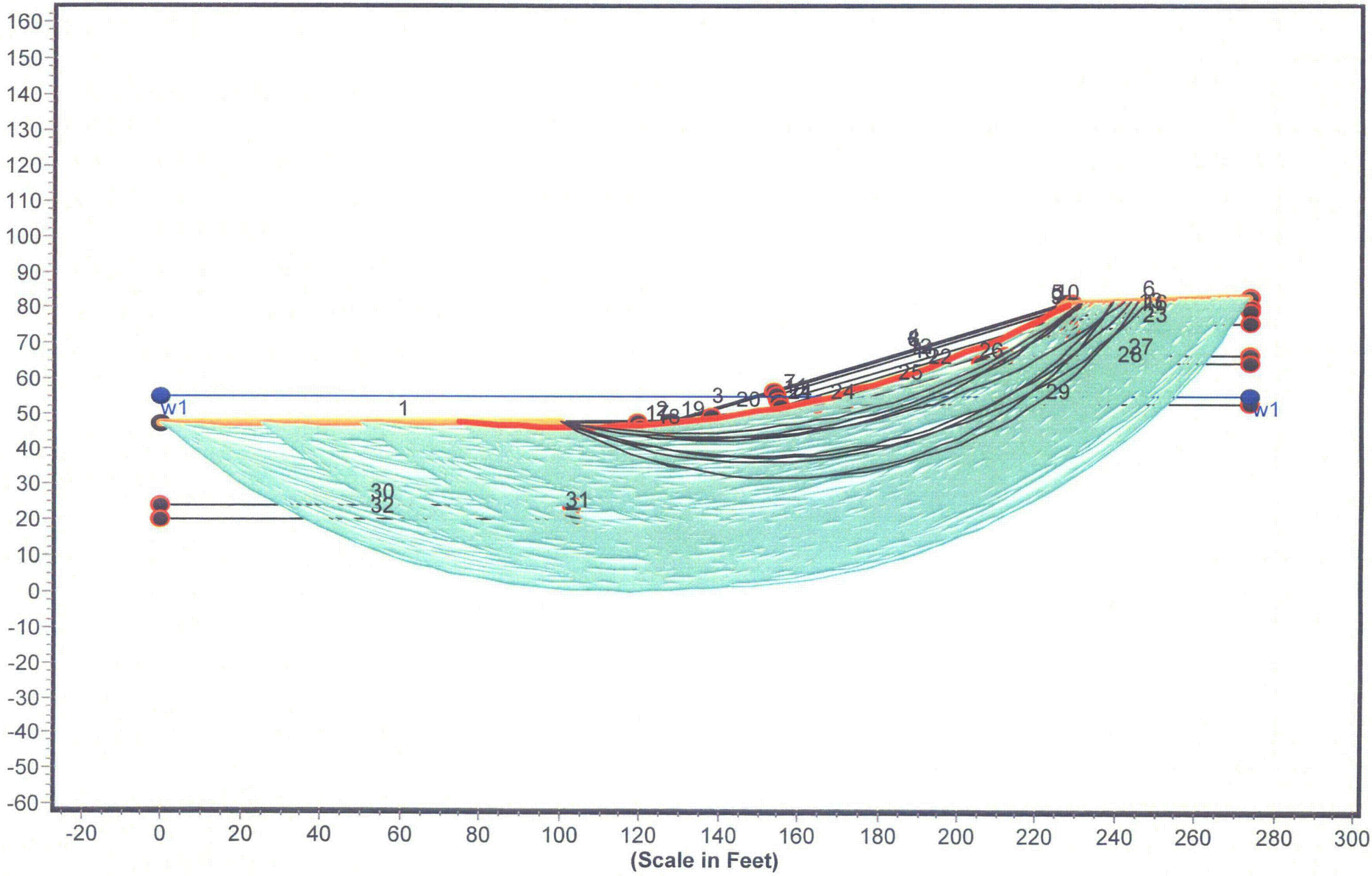

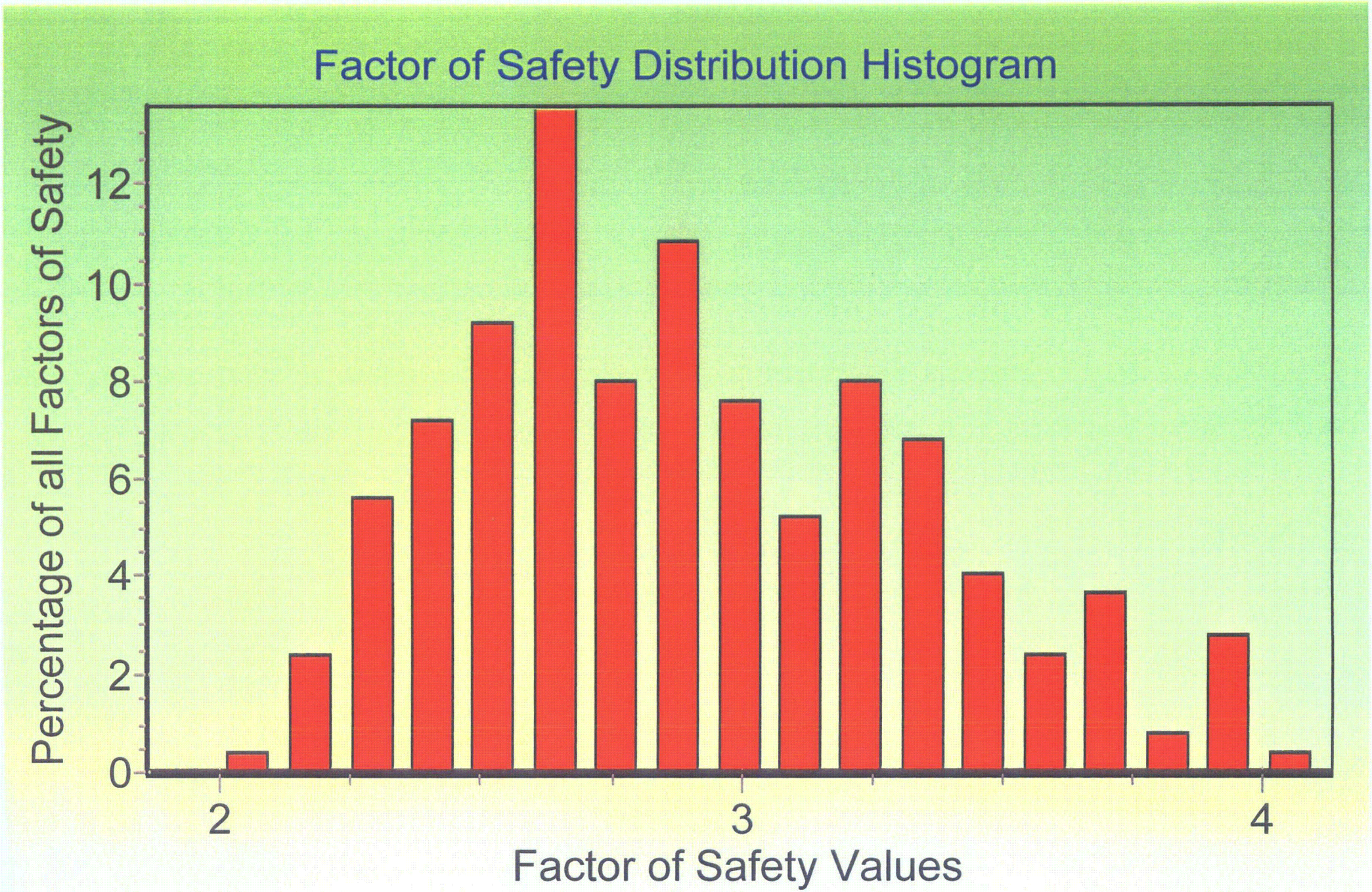
Factor of Safety Distribution Histogram
Percentage of all Factors of Safety
0
2
4
6
8
10
12
2
3
4
Factor of Safety Values

Spencer #4 High Water Results.txt
** PCSTABL6 **

by
Purdue University

1

--Slope Stability Analysis--
Simplified Janbu, Simplified Bishop
or Spencer's Method of Slices

Run Date:
Time of Run:
Run By:
Input Data Filename: run.in
Output Filename: result.out
Unit: ENGLISH
Plotted Output Filename: result.plt

PROBLEM DESCRIPTION SMC Newfield Decommissioning - Section A -A'

BOUNDARY COORDINATES

6 Top Boundaries
32 Total Boundaries

Boundary No.	X-Left (ft)	Y-Left (ft)	X-Right (ft)	Y-Right (ft)	Soil Type Below Bnd
1	0.00	47.40	119.50	48.00	7
2	119.50	48.00	127.50	48.00	1
3	127.50	48.00	153.90	56.80	1
4	153.90	56.80	226.90	81.10	1
5	226.90	81.10	228.90	81.20	1
6	228.90	81.20	273.60	83.00	2
7	153.90	56.80	154.20	55.80	1
8	154.20	55.80	227.10	80.10	2
9	227.10	80.10	228.80	80.20	2
10	228.80	80.20	228.90	81.20	2
11	154.20	55.80	154.80	53.90	1
12	154.80	53.90	227.40	78.10	1
13	227.40	78.10	273.60	80.00	1
14	154.80	53.90	155.20	52.60	1
15	155.20	52.60	227.60	77.10	3
16	227.60	77.10	273.60	79.00	3
17	119.50	48.00	119.60	46.40	7
18	119.60	46.40	127.80	46.40	7
19	127.80	46.40	137.90	49.80	7
20	137.90	49.80	155.20	52.60	7
21	155.20	52.60	164.60	53.00	7
22	164.60	53.00	228.20	74.10	4
23	228.20	74.10	273.60	76.00	4
24	164.60	53.00	171.00	53.00	7
25	171.00	53.00	205.80	64.60	6
26	205.80	64.60	211.80	66.60	5

27	211.80	66.60	273.60	66.60	5
28	205.80	64.60	273.60	64.60	6
29	171.00	53.00	273.60	53.00	7
30	0.00	24.00	103.10	24.00	8
31	103.00	20.00	103.10	24.00	7
32	0.00	20.00	103.10	20.00	7

1

ISOTROPIC SOIL PARAMETERS

8 Type(s) of Soil

Soil Type No.	Total Unit Wt. (pcf)	Saturated Unit Wt. (pcf)	Cohesion Intercept (psf)	Friction Angle (deg)	Pore Pressure Param.	Pressure Constant (psf)	Piez. Surface No.
1	135.0	140.0	0.0	40.0	0.00	0.0	1
2	135.0	140.0	0.0	35.0	0.00	0.0	1
3	125.0	130.0	250.0	15.0	0.00	0.0	1
4	125.0	135.0	0.0	32.0	0.00	0.0	1
5	135.0	140.0	0.0	38.0	0.00	0.0	1
6	135.0	140.0	0.0	40.0	0.00	0.0	1
7	115.0	130.0	0.0	33.0	0.00	0.0	1
8	130.0	140.0	300.0	20.0	0.00	0.0	1

1

1 PIEZOMETRIC SURFACE(S) HAVE BEEN SPECIFIED

Unit Weight of Water = 62.40

Piezometric Surface No. 1 Specified by 2 Coordinate Points

Point No.	X-Water (ft)	Y-Water (ft)
1	0.00	55.00
2	273.60	55.00

1

A Critical Failure Surface Searching Method, Using A Random Technique For Generating Circular Surfaces, Has Been Specified.

250 Trial Surfaces Have Been Generated.

50 Surfaces Initiate From Each Of 5 Points Equally Spaced Along The Ground Surface Between X = 0.00 ft.
and X = 100.00 ft.

Each Surface Terminates Between X = 226.00 ft.
and X = 273.00 ft.

Unless Further Limitations Were Imposed, The Minimum Elevation At Which A Surface Extends Is Y = 0.00 ft.

5.00 ft. Line Segments Define Each Trial Failure Surface.

Restrictions Have Been Imposed Upon The Angle Of Initiation. The Angle Has Been Restricted Between The Angles Of -45.0 And -5.0 deg.

1

Following Are Displayed The Ten Most Critical Of The Trial Failure Surfaces Examined. They Are Ordered - Most Critical First.

* * Safety Factors Are Calculated By Spencer's Method * *

Number of convergent trials 250
Number of non convergent trials 0

Failure Surface Specified By 33 Coordinate Points

Point No.	X-Surf (ft)	Y-Surf (ft)
1	75.00	47.78
2	79.97	47.25
3	84.96	46.84
4	89.95	46.52
5	94.94	46.31
6	99.94	46.20
7	104.94	46.20
8	109.94	46.30
9	114.93	46.50
10	119.93	46.81
11	124.91	47.22
12	129.88	47.73
13	134.84	48.35
14	139.79	49.07
15	144.72	49.89
16	149.64	50.81
17	154.53	51.84
18	159.40	52.97
19	164.25	54.19
20	169.07	55.52
21	173.86	56.95
22	178.62	58.48
23	183.35	60.10
24	188.04	61.83
25	192.70	63.65
26	197.32	65.56
27	201.90	67.57
28	206.43	69.68
29	210.92	71.88
30	215.37	74.17
31	219.76	76.56

32	224.10	79.03
33	227.62	81.14

*** Factor of Safety = 2.085 ***

Individual data on the 50 slices

Slice No.	Width (ft)	Weight (lbs)	Water Force Top (lbs)	Water Force Bot (lbs)	Force Norm (lbs)	Force Tan (lbs)	Earthquake Force Hor (lbs)	Earthquake Force Ver (lbs)	Surcharge Load (lbs)
1	5.0	176.8	2237.6	2335.1	0.0	0.0	0.0	0.0	0.0
2	5.0	497.9	2234.2	2481.9	0.0	0.0	0.0	0.0	0.0
3	5.0	752.9	2229.8	2596.3	0.0	0.0	0.0	0.0	0.0
4	5.0	941.1	2224.4	2678.5	0.0	0.0	0.0	0.0	0.0
5	5.0	1061.8	2218.1	2728.3	0.0	0.0	0.0	0.0	0.0
6	5.0	1114.8	2210.8	2745.8	0.0	0.0	0.0	0.0	0.0
7	5.0	1099.9	2202.5	2730.9	0.0	0.0	0.0	0.0	0.0
8	5.0	1017.2	2193.3	2683.7	0.0	0.0	0.0	0.0	0.0
9	4.6	800.1	1997.3	2385.8	0.0	0.0	0.0	0.0	0.0
10	0.1	12.5	33.2	39.0	0.0	0.0	0.0	0.0	0.0
11	0.3	58.9	152.7	179.3	0.0	0.0	0.0	0.0	0.0
12	5.0	689.3	2176.6	2492.3	0.0	0.0	0.0	0.0	0.0
13	2.6	235.5	1131.9	1243.4	0.0	0.0	0.0	0.0	0.0
14	2.4	263.2	1034.6	1104.7	0.0	0.0	0.0	0.0	0.0
15	3.0	570.3	1114.3	1321.4	0.0	0.0	0.0	0.0	0.0
16	2.0	524.4	641.2	850.4	0.0	0.0	0.0	0.0	0.0
17	3.1	999.7	812.6	1239.1	0.0	0.0	0.0	0.0	0.0
18	1.9	736.2	400.5	724.2	0.0	0.0	0.0	0.0	0.0
19	4.9	2325.5	675.0	1722.9	0.0	0.0	0.0	0.0	0.0
20	4.9	2849.0	142.1	1450.5	0.0	0.0	0.0	0.0	0.0
21	4.3	2825.3	0.0	1016.4	0.0	0.0	0.0	0.0	0.0
22	0.3	209.9	0.0	62.4	0.0	0.0	0.0	0.0	0.0
23	0.3	177.9	0.0	51.6	0.0	0.0	0.0	0.0	0.0
24	0.1	55.7	0.0	15.9	0.0	0.0	0.0	0.0	0.0
25	0.3	190.5	0.0	53.8	0.0	0.0	0.0	0.0	0.0
26	0.4	285.4	0.0	78.2	0.0	0.0	0.0	0.0	0.0
27	2.9	2125.4	0.0	496.1	0.0	0.0	0.0	0.0	0.0
28	0.3	233.9	0.0	45.8	0.0	0.0	0.0	0.0	0.0
29	1.0	752.3	0.0	136.4	0.0	0.0	0.0	0.0	0.0
30	2.9	2244.9	0.0	310.2	0.0	0.0	0.0	0.0	0.0
31	2.0	1561.6	0.0	132.8	0.0	0.0	0.0	0.0	0.0
32	2.9	2382.7	0.0	76.3	0.0	0.0	0.0	0.0	0.0
33	1.9	1572.8	0.0	0.0	0.0	0.0	0.0	0.0	0.0
34	4.8	4057.6	0.0	0.0	0.0	0.0	0.0	0.0	0.0
35	4.8	4097.3	0.0	0.0	0.0	0.0	0.0	0.0	0.0
36	4.7	4069.8	0.0	0.0	0.0	0.0	0.0	0.0	0.0
37	4.7	3976.3	0.0	0.0	0.0	0.0	0.0	0.0	0.0
38	4.7	3818.6	0.0	0.0	0.0	0.0	0.0	0.0	0.0
39	4.6	3598.2	0.0	0.0	0.0	0.0	0.0	0.0	0.0
40	4.6	3317.1	0.0	0.0	0.0	0.0	0.0	0.0	0.0
41	4.5	2977.4	0.0	0.0	0.0	0.0	0.0	0.0	0.0
42	1.7	1015.4	0.0	0.0	0.0	0.0	0.0	0.0	0.0
43	2.8	1560.2	0.0	0.0	0.0	0.0	0.0	0.0	0.0
44	4.0	1897.2	0.0	0.0	0.0	0.0	0.0	0.0	0.0
45	0.5	198.1	0.0	0.0	0.0	0.0	0.0	0.0	0.0
46	4.4	1557.7	0.0	0.0	0.0	0.0	0.0	0.0	0.0
47	4.3	967.9	0.0	0.0	0.0	0.0	0.0	0.0	0.0

48	0.3	38.3	0.0	0.0	0.0	0.0	0.0	0.0	0.0
49	2.5	250.8	0.0	0.0	0.0	0.0	0.0	0.0	0.0
50	0.7	19.3	0.0	0.0	0.0	0.0	0.0	0.0	0.0

Failure Surface Specified By 30 Coordinate Points

Point No.	X-Surf (ft)	Y-Surf (ft)
1	100.00	47.90
2	104.82	46.56
3	109.68	45.40
4	114.58	44.42
5	119.52	43.63
6	124.49	43.04
7	129.47	42.63
8	134.46	42.41
9	139.46	42.38
10	144.46	42.54
11	149.45	42.89
12	154.42	43.43
13	159.37	44.16
14	164.28	45.07
15	169.16	46.18
16	173.99	47.46
17	178.77	48.93
18	183.49	50.59
19	188.14	52.42
20	192.72	54.42
21	197.22	56.60
22	201.64	58.95
23	205.96	61.46
24	210.18	64.14
25	214.30	66.97
26	218.31	69.96
27	222.20	73.10
28	225.97	76.39
29	229.61	79.81
30	231.06	81.29

*** Factor of Safety = 2.127 ***

1

Failure Surface Specified By 30 Coordinate Points

Point No.	X-Surf (ft)	Y-Surf (ft)
1	100.00	47.90
2	104.86	46.71
3	109.75	45.70
4	114.68	44.86
5	119.64	44.20
6	124.62	43.72
7	129.61	43.42
8	134.61	43.30
9	139.61	43.36

10	144.60	43.60
11	149.58	44.02
12	154.55	44.61
13	159.49	45.39
14	164.39	46.34
15	169.27	47.47
16	174.09	48.77
17	178.87	50.25
18	183.59	51.89
19	188.25	53.71
20	192.84	55.69
21	197.36	57.84
22	201.79	60.14
23	206.14	62.61
24	210.40	65.23
25	214.56	68.00
26	218.62	70.92
27	222.57	73.98
28	226.41	77.19
29	230.13	80.53
30	230.92	81.28

*** Factor of Safety = 2.138 ***

Failure Surface Specified By 29 Coordinate Points

Point No.	X-Surf (ft)	Y-Surf (ft)
1	100.00	47.90
2	104.91	46.94
3	109.84	46.14
4	114.80	45.51
5	119.78	45.04
6	124.77	44.73
7	129.77	44.59
8	134.77	44.62
9	139.77	44.80
10	144.75	45.16
11	149.73	45.68
12	154.68	46.36
13	159.61	47.21
14	164.50	48.21
15	169.37	49.38
16	174.19	50.71
17	178.96	52.20
18	183.68	53.85
19	188.35	55.65
20	192.95	57.60
21	197.48	59.70
22	201.95	61.95
23	206.34	64.35
24	210.64	66.89
25	214.86	69.58
26	218.99	72.40
27	223.02	75.35
28	226.96	78.44
29	230.31	81.26

*** Factor of Safety = 2.152 ***

1

Failure Surface Specified By 33 Coordinate Points

Point No.	X-Surf (ft)	Y-Surf (ft)
1	100.00	47.90
2	104.50	45.72
3	109.10	43.75
4	113.78	41.99
5	118.53	40.45
6	123.35	39.13
7	128.23	38.02
8	133.15	37.14
9	138.11	36.49
10	143.09	36.06
11	148.09	35.86
12	153.09	35.89
13	158.08	36.15
14	163.06	36.63
15	168.01	37.34
16	172.92	38.28
17	177.78	39.44
18	182.59	40.82
19	187.33	42.41
20	191.99	44.23
21	196.56	46.25
22	201.03	48.48
23	205.40	50.91
24	209.66	53.54
25	213.79	56.36
26	217.78	59.36
27	221.64	62.54
28	225.34	65.90
29	228.89	69.42
30	232.28	73.10
31	235.49	76.93
32	238.53	80.91
33	239.01	81.61

*** Factor of Safety = 2.181 ***

Failure Surface Specified By 33 Coordinate Points

Point No.	X-Surf (ft)	Y-Surf (ft)
1	100.00	47.90
2	104.64	46.03
3	109.34	44.35

4	114.12	42.85
5	118.94	41.55
6	123.82	40.45
7	128.74	39.54
8	133.69	38.83
9	138.66	38.32
10	143.65	38.02
11	148.65	37.91
12	153.65	38.00
13	158.64	38.30
14	163.62	38.79
15	168.57	39.49
16	173.49	40.38
17	178.37	41.48
18	183.20	42.76
19	187.97	44.24
20	192.69	45.91
21	197.33	47.77
22	201.89	49.82
23	206.37	52.05
24	210.75	54.45
25	215.03	57.03
26	219.21	59.78
27	223.27	62.70
28	227.21	65.77
29	231.03	69.01
30	234.71	72.39
31	238.25	75.92
32	241.65	79.59
33	243.53	81.79

*** Factor of Safety = 2.191 ***

1

Failure Surface Specified By 32 Coordinate Points

Point No.	X-Surf (ft)	Y-Surf (ft)
1	100.00	47.90
2	104.87	46.76
3	109.77	45.78
4	114.70	44.95
5	119.66	44.28
6	124.63	43.77
7	129.62	43.41
8	134.61	43.22
9	139.61	43.18
10	144.61	43.30
11	149.60	43.59
12	154.59	44.03
13	159.55	44.62
14	164.49	45.38
15	169.41	46.29
16	174.29	47.36
17	179.14	48.59
18	183.95	49.96
19	188.71	51.49

20	193.42	53.17
21	198.07	55.00
22	202.66	56.98
23	207.19	59.10
24	211.65	61.37
25	216.03	63.77
26	220.34	66.31
27	224.56	68.99
28	228.69	71.81
29	232.73	74.75
30	236.68	77.82
31	240.53	81.01
32	241.31	81.70

*** Factor of Safety = 2.202 ***

Failure Surface Specified By 34 Coordinate Points

Point No.	X-Surf (ft)	Y-Surf (ft)
1	100.00	47.90
2	104.63	46.01
3	109.33	44.30
4	114.09	42.77
5	118.90	41.43
6	123.77	40.27
7	128.67	39.31
8	133.62	38.54
9	138.58	37.96
10	143.57	37.58
11	148.56	37.39
12	153.56	37.39
13	158.56	37.59
14	163.54	37.99
15	168.51	38.57
16	173.45	39.36
17	178.35	40.33
18	183.22	41.49
19	188.03	42.84
20	192.79	44.38
21	197.48	46.10
22	202.10	48.00
23	206.65	50.09
24	211.11	52.34
25	215.48	54.77
26	219.76	57.37
27	223.92	60.13
28	227.98	63.05
29	231.92	66.13
30	235.74	69.36
31	239.43	72.73
32	242.98	76.25
33	246.40	79.90
34	248.19	81.98

*** Factor of Safety = 2.232 ***

1

Failure Surface Specified By 34 Coordinate Points

Point No.	X-Surf (ft)	Y-Surf (ft)
1	100.00	47.90
2	104.22	45.23
3	108.58	42.77
4	113.06	40.55
5	117.65	38.56
6	122.33	36.81
7	127.10	35.30
8	131.94	34.04
9	136.83	33.04
10	141.78	32.29
11	146.75	31.79
12	151.75	31.55
13	156.75	31.57
14	161.74	31.85
15	166.71	32.39
16	171.65	33.18
17	176.54	34.23
18	181.36	35.53
19	186.12	37.08
20	190.79	38.87
21	195.36	40.89
22	199.82	43.16
23	204.15	45.65
24	208.36	48.36
25	212.41	51.28
26	216.31	54.41
27	220.04	57.74
28	223.60	61.25
29	226.97	64.94
30	230.14	68.81
31	233.11	72.83
32	235.87	77.00
33	238.41	81.31
34	238.56	81.59

*** Factor of Safety = 2.260 ***

Failure Surface Specified By 35 Coordinate Points

Point No.	X-Surf (ft)	Y-Surf (ft)
1	100.00	47.90
2	104.28	45.31
3	108.67	42.92
4	113.17	40.75
5	117.78	38.80

6	122.47	37.07
7	127.24	35.57
8	132.07	34.29
9	136.96	33.26
10	141.90	32.46
11	146.87	31.89
12	151.86	31.57
13	156.86	31.48
14	161.85	31.64
15	166.84	32.04
16	171.80	32.67
17	176.72	33.54
18	181.60	34.65
19	186.41	35.99
20	191.16	37.56
21	195.83	39.36
22	200.40	41.38
23	204.87	43.61
24	209.23	46.06
25	213.47	48.72
26	217.57	51.57
27	221.54	54.62
28	225.35	57.86
29	229.00	61.27
30	232.48	64.86
31	235.79	68.61
32	238.91	72.51
33	241.85	76.56
34	244.58	80.75
35	245.23	81.86

*** Factor of Safety = 2.283 ***

1

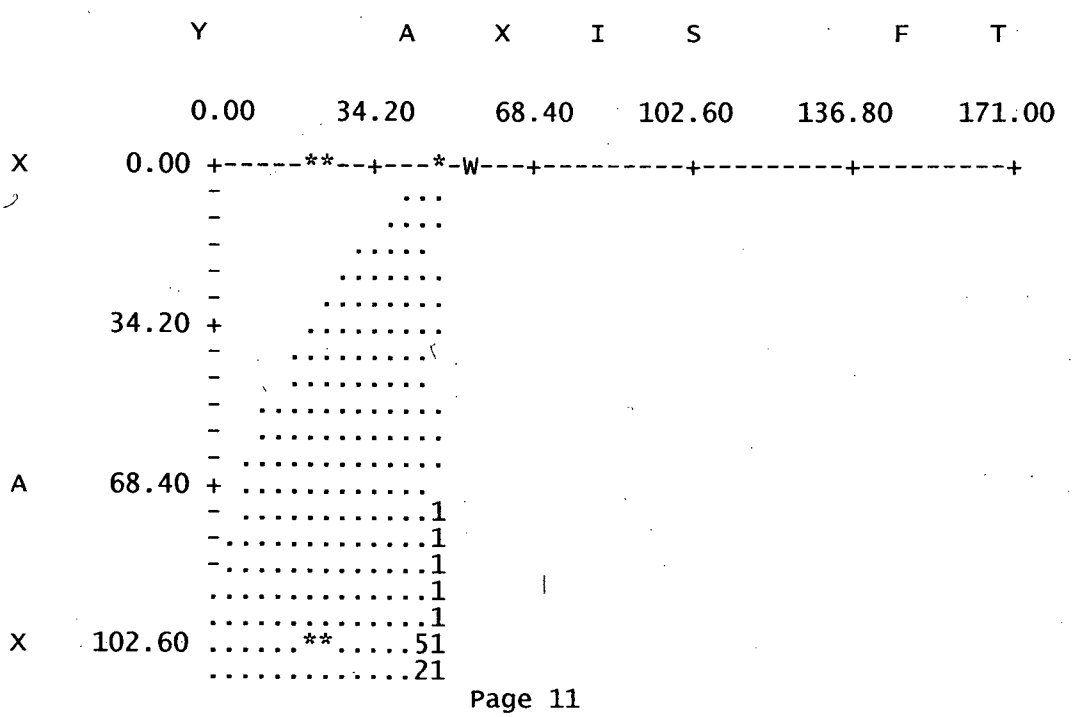

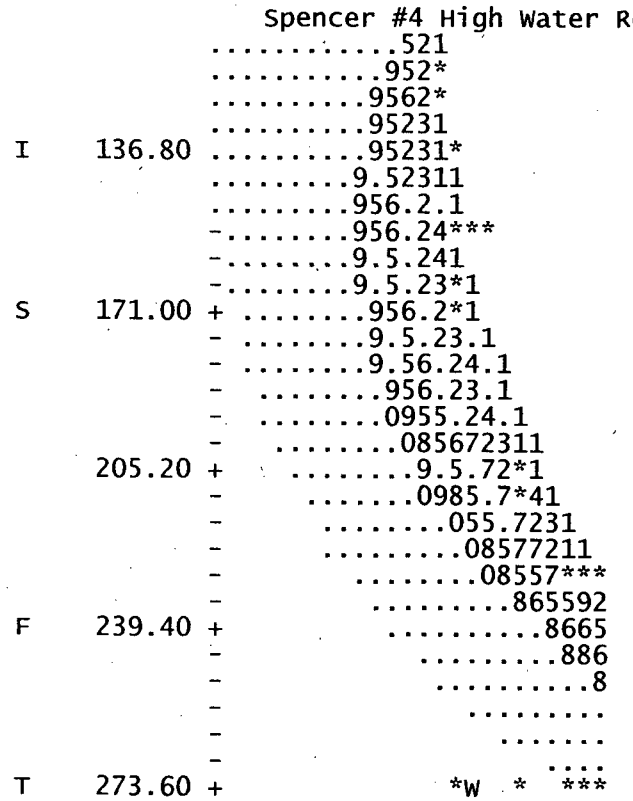
I
136.80
S
171.00
205.20
F
239.40
T
273.60

JANBU #4 STATIC SLIDING BLOCK

Geometry and Boundary Conditions
Problem: SMC Newfield Decommissioning - Section A-A' - FS Min = 2.187

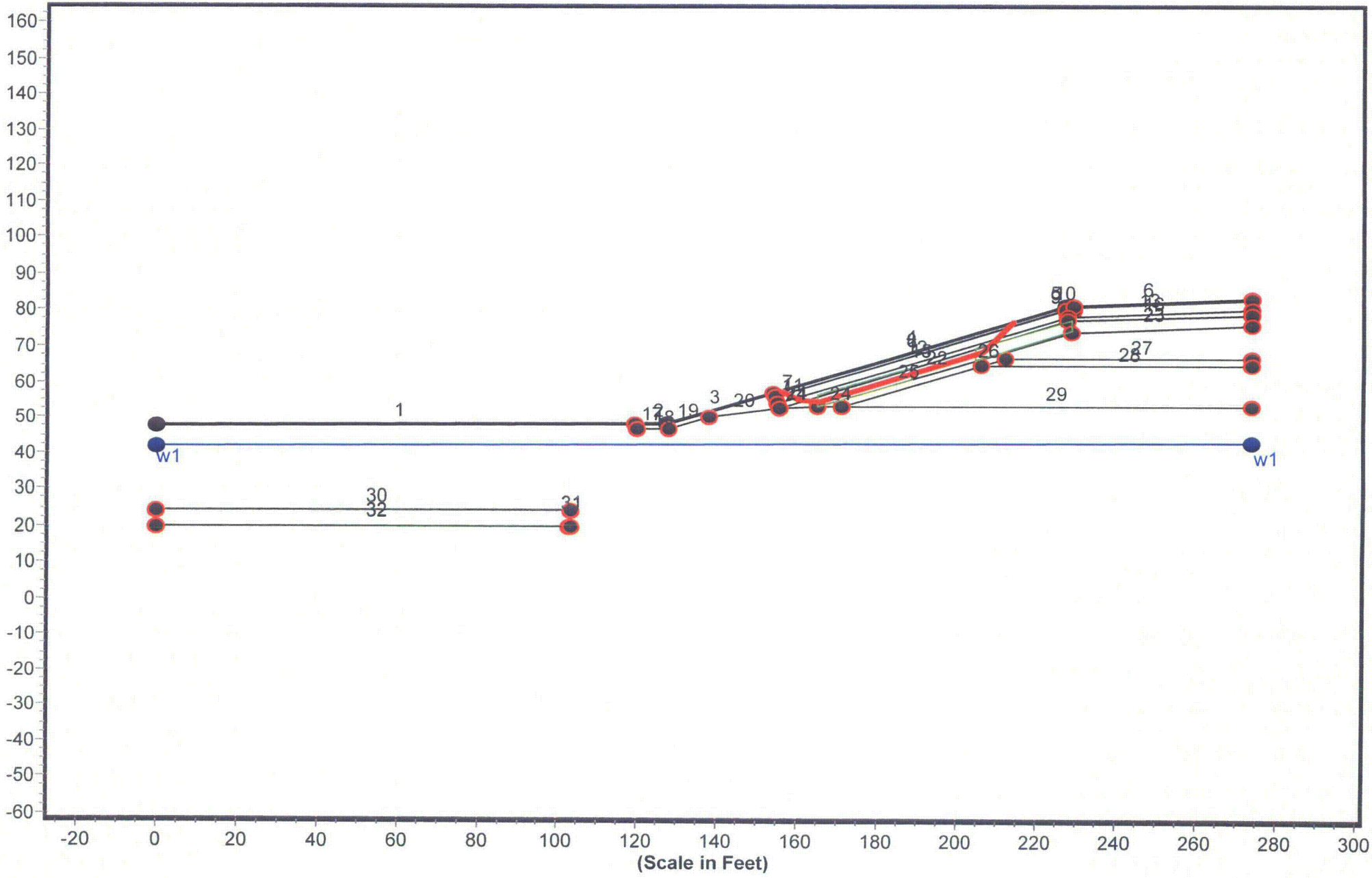

Geometry and Boundary Conditions
Problem: SMC Newfield Decommissioning - Section A-A' - FS Min = 2.187

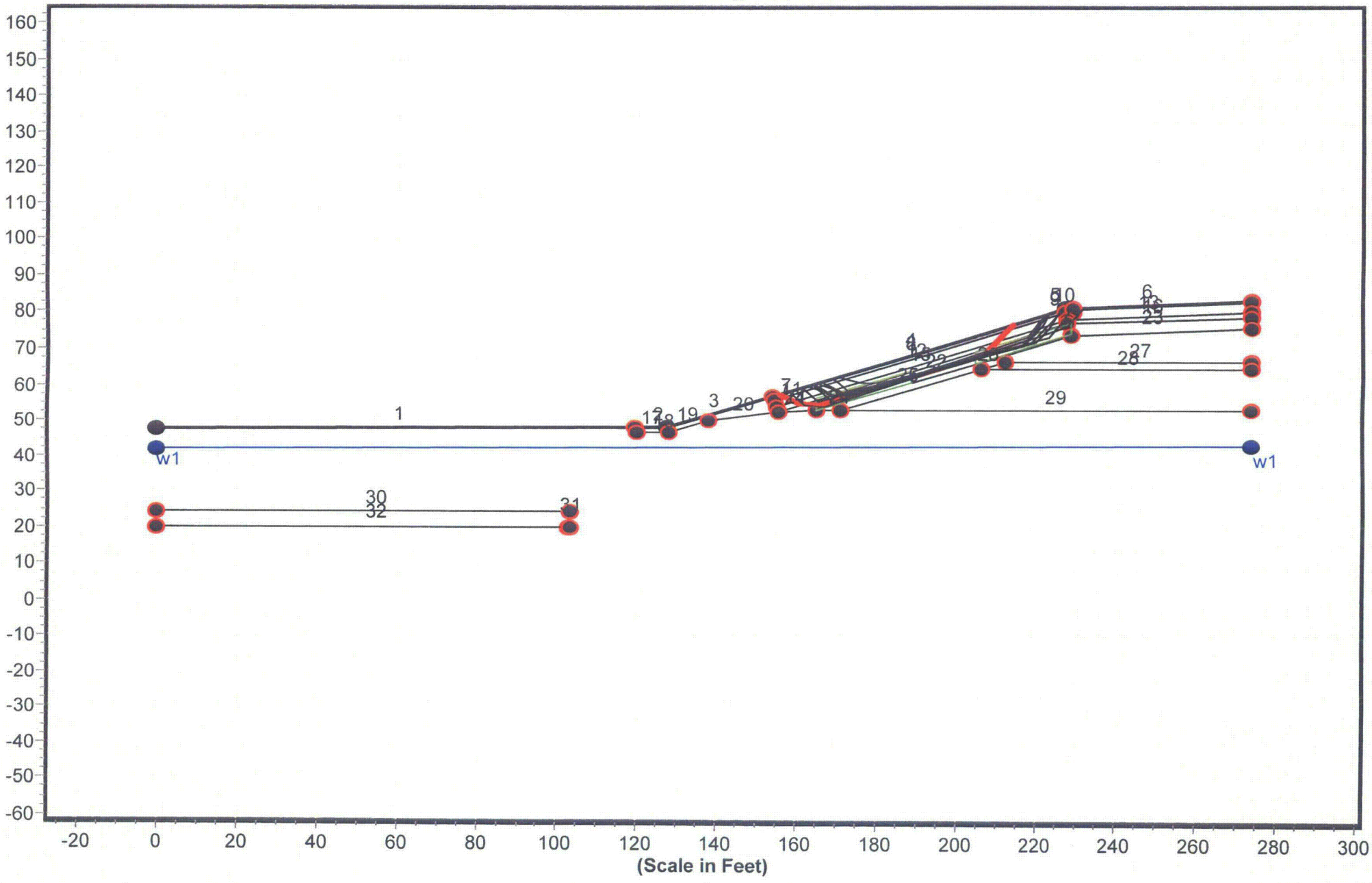

Geometry and Boundary Conditions
Problem: SMC Newfield Decommissioning - Section A-A' - FS Min = 2.187

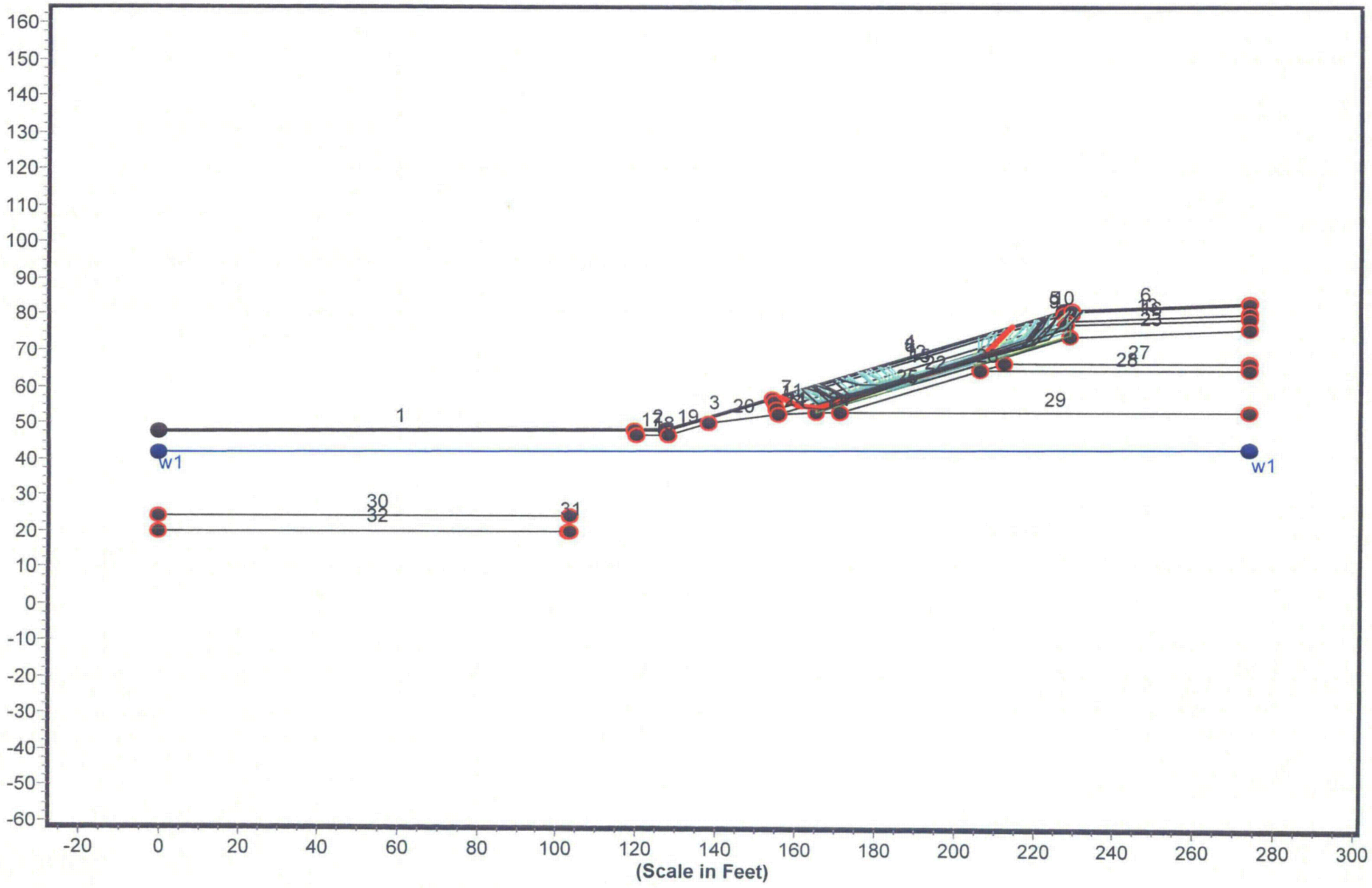

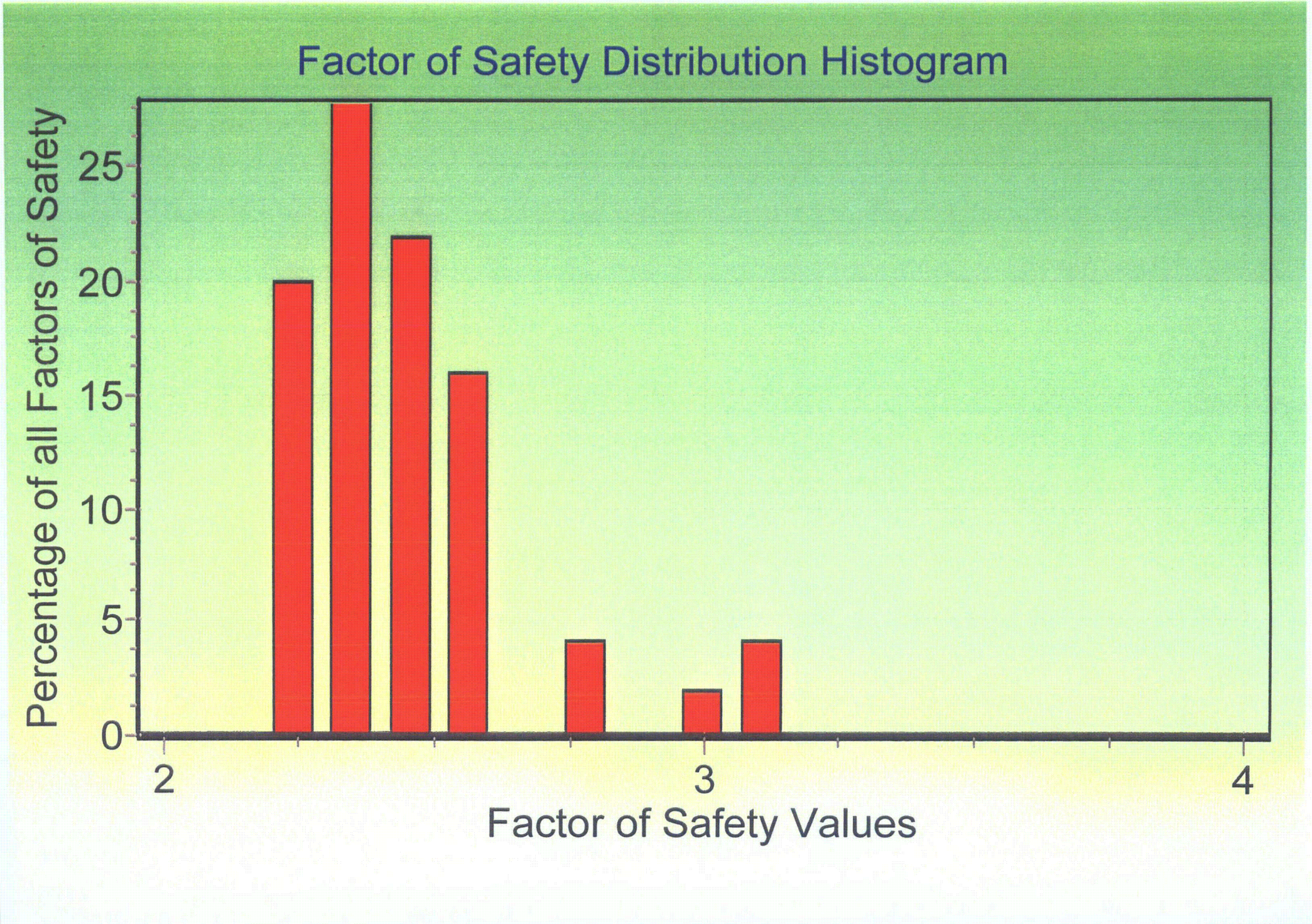
Factor of Safety Distribution Histogram
Percentage of all Factors of Safety
0
5
10
15
20
25
2
3
4
Factor of Safety Values

Janbu Sliding Block #1.txt
** PCSTABL6 **

by
Purdue University

1

--Slope Stability Analysis--
Simplified Janbu, Simplified Bishop
or Spencer's Method of Slices

Run Date:
Time of Run:
Run By:
Input Data Filename: run.in
Output Filename: result.out
Unit: ENGLISH
Plotted Output Filename: result.plt

PROBLEM DESCRIPTION SMC Newfield Decommissioning - Section A -A'

BOUNDARY COORDINATES

6 Top Boundaries
32 Total Boundaries

Boundary No.	X-Left (ft)	Y-Left (ft)	X-Right (ft)	Y-Right (ft)	Soil Type Below Bnd
1	0.00	47.40	119.50	48.00	7
2	119.50	48.00	127.50	48.00	1
3	127.50	48.00	153.90	56.80	1
4	153.90	56.80	226.90	81.10	1
5	226.90	81.10	228.90	81.20	1
6	228.90	81.20	273.60	83.00	2
7	153.90	56.80	154.20	55.80	1
8	154.20	55.80	227.10	80.10	2
9	227.10	80.10	228.80	80.20	2
10	228.80	80.20	228.90	81.20	2
11	154.20	55.80	154.80	53.90	1
12	154.80	53.90	227.40	78.10	1
13	227.40	78.10	273.60	80.00	1
14	154.80	53.90	155.20	52.60	1
15	155.20	52.60	227.60	77.10	3
16	227.60	77.10	273.60	79.00	3
17	119.50	48.00	119.60	46.40	7
18	119.60	46.40	127.80	46.40	7
19	127.80	46.40	137.90	49.80	7
20	137.90	49.80	155.20	52.60	7
21	155.20	52.60	164.60	53.00	7
22	164.60	53.00	228.20	74.10	4
23	228.20	74.10	273.60	76.00	4
24	164.60	53.00	171.00	53.00	7
25	171.00	53.00	205.80	64.60	6
26	205.80	64.60	211.80	66.60	5

27	211.80	66.60	273.60	66.60	5
28	205.80	64.60	273.60	64.60	6
29	171.00	53.00	273.60	53.00	7
30	0.00	24.00	103.10	24.00	8
31	103.00	20.00	103.10	24.00	7
32	0.00	20.00	103.10	20.00	7

1

ISOTROPIC SOIL PARAMETERS

8 Type(s) of Soil

Soil Type No.	Total Unit Wt. (pcf)	Saturated Unit Wt. (pcf)	Cohesion Intercept (psf)	Friction Angle (deg)	Pore Pressure Param.	Pressure Constant (psf)	Piez. Surface No.
1	135.0	140.0	0.0	40.0	0.00	0.0	0
2	135.0	140.0	0.0	35.0	0.00	0.0	0
3	125.0	130.0	250.0	15.0	0.00	0.0	0
4	125.0	135.0	0.0	32.0	0.00	0.0	0
5	135.0	140.0	0.0	38.0	0.00	0.0	0
6	135.0	140.0	0.0	40.0	0.00	0.0	0
7	115.0	130.0	0.0	33.0	0.00	0.0	1
8	130.0	140.0	300.0	20.0	0.00	0.0	1

1

1 PIEZOMETRIC SURFACE(S) HAVE BEEN SPECIFIED

Unit Weight of Water = 62.40

Piezometric Surface No. 1 Specified by 2 Coordinate Points

Point No.	X-Water (ft)	Y-Water (ft)
1	0.00	41.70
2	273.60	42.50

Janbus Empirical Coef is being used for the case of c & phi both > 0

1

A Critical Failure Surface Searching Method, Using A Random Technique For Generating Sliding Block Surfaces, Has Been Specified.

50 Trial Surfaces Have Been Generated.

2 Boxes Specified For Generation Of Central Block Base

Length Of Line Segments For Active And Passive Portions Of Sliding Block Is 5.0

Box No.	X-Left (ft)	Y-Left (ft)	X-Right (ft)	Y-Right (ft)	Height (ft)
1	164.70	54.58	188.42	62.47	3.16
2	204.48	67.89	228.20	75.78	3.16

1

Following Are Displayed The Ten Most Critical Of The Trial Failure Surfaces Examined. They Are Ordered - Most Critical First.

* * Safety Factors Are Calculated By The Modified Janbu Method * *

Failure Surface Specified By 8 Coordinate Points

Point No.	X-Surf (ft)	Y-Surf (ft)
1	155.51	57.33
2	155.69	57.19
3	160.24	55.09
4	165.20	54.52
5	206.19	68.70
6	209.50	72.44
7	213.00	76.02
8	213.59	76.67

*** 2.187 ***

Individual data on the 13 slices

Slice No.	Width (ft)	Weight (lbs)	Water Force Top (lbs)	Water Force Bot (lbs)	Force Norm (lbs)	Force Tan (lbs)	Earthquake Force Hor (lbs)	Earthquake Force Ver (lbs)	Surcharge Load (lbs)
1	0.2	2.7	0.0	0.0	0.0	0.0	0.0	0.0	0.0
2	1.1	98.8	0.0	0.0	0.0	0.0	0.0	0.0	0.0
3	2.6	766.7	0.0	0.0	0.0	0.0	0.0	0.0	0.0
4	0.8	369.2	0.0	0.0	0.0	0.0	0.0	0.0	0.0
5	1.7	985.4	0.0	0.0	0.0	0.0	0.0	0.0	0.0
6	3.2	2297.2	0.0	0.0	0.0	0.0	0.0	0.0	0.0
7	41.0	31419.8	0.0	0.0	0.0	0.0	0.0	0.0	0.0
8	1.5	961.5	0.0	0.0	0.0	0.0	0.0	0.0	0.0
9	1.5	744.2	0.0	0.0	0.0	0.0	0.0	0.0	0.0
10	0.4	158.5	0.0	0.0	0.0	0.0	0.0	0.0	0.0
11	2.6	689.4	0.0	0.0	0.0	0.0	0.0	0.0	0.0
12	0.9	92.7	0.0	0.0	0.0	0.0	0.0	0.0	0.0
13	0.6	17.9	0.0	0.0	0.0	0.0	0.0	0.0	0.0

Failure Surface Specified By 7 Coordinate Points

Point No.	X-Surf (ft)	Y-Surf (ft)
1	157.93	58.14
2	158.28	57.89
3	161.85	54.39
4	166.84	54.12
5	227.30	76.12
6	230.16	80.22
7	231.12	81.29

*** 2.188 ***

1

Failure Surface Specified By 6 Coordinate Points

Point No.	X-Surf (ft)	Y-Surf (ft)
1	164.63	60.37
2	168.22	59.43
3	172.34	56.61
4	216.84	71.33
5	219.30	75.68
6	222.01	79.47

*** 2.207 ***

Failure Surface Specified By 7 Coordinate Points

Point No.	X-Surf (ft)	Y-Surf (ft)
1	166.25	60.91
2	167.75	60.04
3	172.13	57.63
4	219.19	72.30
5	222.66	75.90
6	225.44	80.05
7	225.52	80.64

*** 2.215 ***

1

Failure Surface Specified By 7 Coordinate Points

Point No.	X-Surf (ft)	Y-Surf (ft)

1	170.55	62.34
2	171.00	62.25
3	175.81	60.86
4	180.81	60.74
5	222.95	73.47
6	225.97	77.45
7	228.39	81.17

*** 2.222 ***

Failure Surface Specified By 7 Coordinate Points

Point No.	X-Surf (ft)	Y-Surf (ft)
1	163.78	60.09
2	165.00	59.66
3	169.10	56.80
4	215.82	70.74
5	218.88	74.70
6	221.92	78.67
7	223.07	79.83

*** 2.233 ***

1

Failure Surface Specified By 7 Coordinate Points

Point No.	X-Surf (ft)	Y-Surf (ft)
1	169.03	61.84
2	169.79	61.15
3	173.36	57.65
4	218.19	71.68
5	221.69	75.26
6	224.78	79.19
7	226.34	80.91

*** 2.262 ***

Failure Surface Specified By 7 Coordinate Points

Point No.	X-Surf (ft)	Y-Surf (ft)
1	160.91	59.13

2	161.75	58.87
3	165.36	55.42
4	215.90	70.97
5	219.39	74.54
6	221.22	79.20
7	221.22	79.21

*** 2.276 ***

1

Failure Surface Specified By 6 Coordinate Points

Point No.	X-Surf (ft)	Y-Surf (ft)
1	162.60	59.70
2	165.35	58.73
3	169.11	55.44
4	217.87	73.01
5	221.40	76.56
6	222.95	79.78

*** 2.282 ***

Failure Surface Specified By 6 Coordinate Points

Point No.	X-Surf (ft)	Y-Surf (ft)
1	164.51	60.33
2	168.51	57.50
3	173.51	57.22
4	217.63	73.44
5	220.46	77.56
6	222.51	79.64

*** 2.282 ***

1

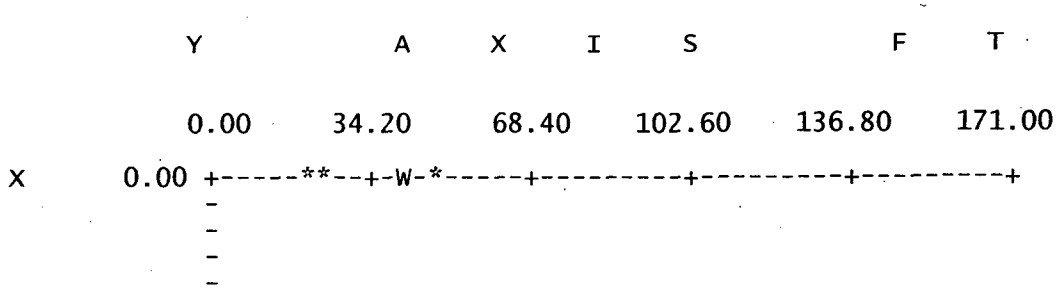

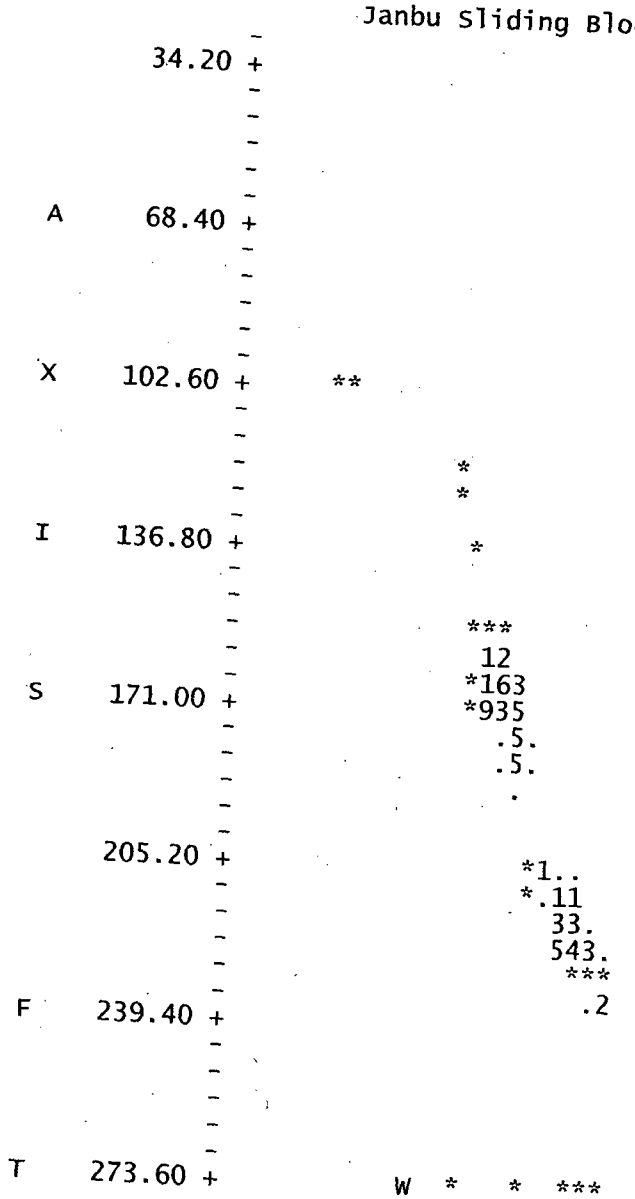
34.20
A 68.40
X 102.60
I 136.80
S 171.00
205.20
F 239.40
T 273.60
W

JANBU #4 STATIC SLIDING BLOCK

EXTREME HIGH WATER

Geometry and Boundary Conditions
Problem: SMC Newfield Decommissioning - Section A-A' - FS Min = 2.183

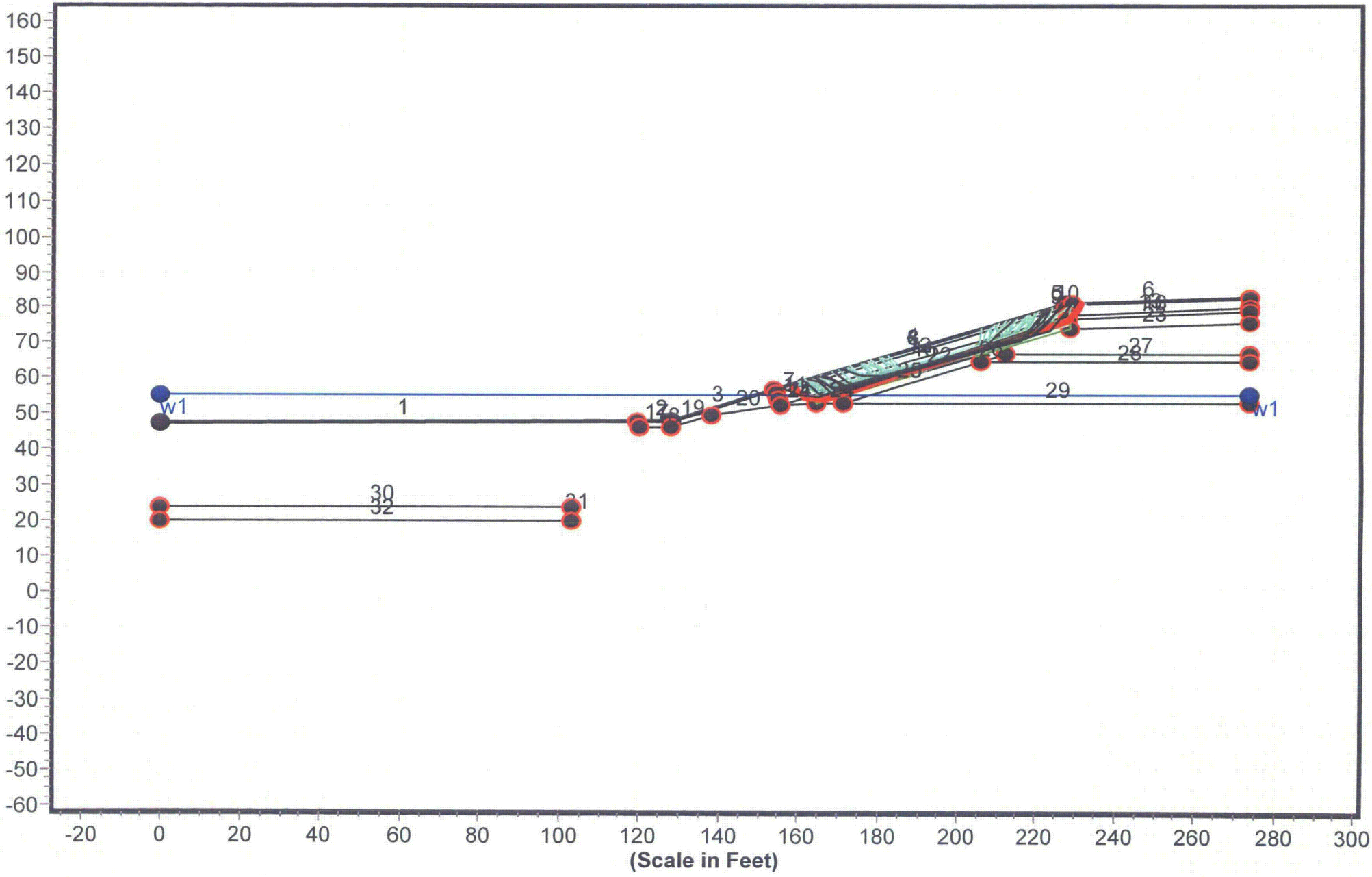

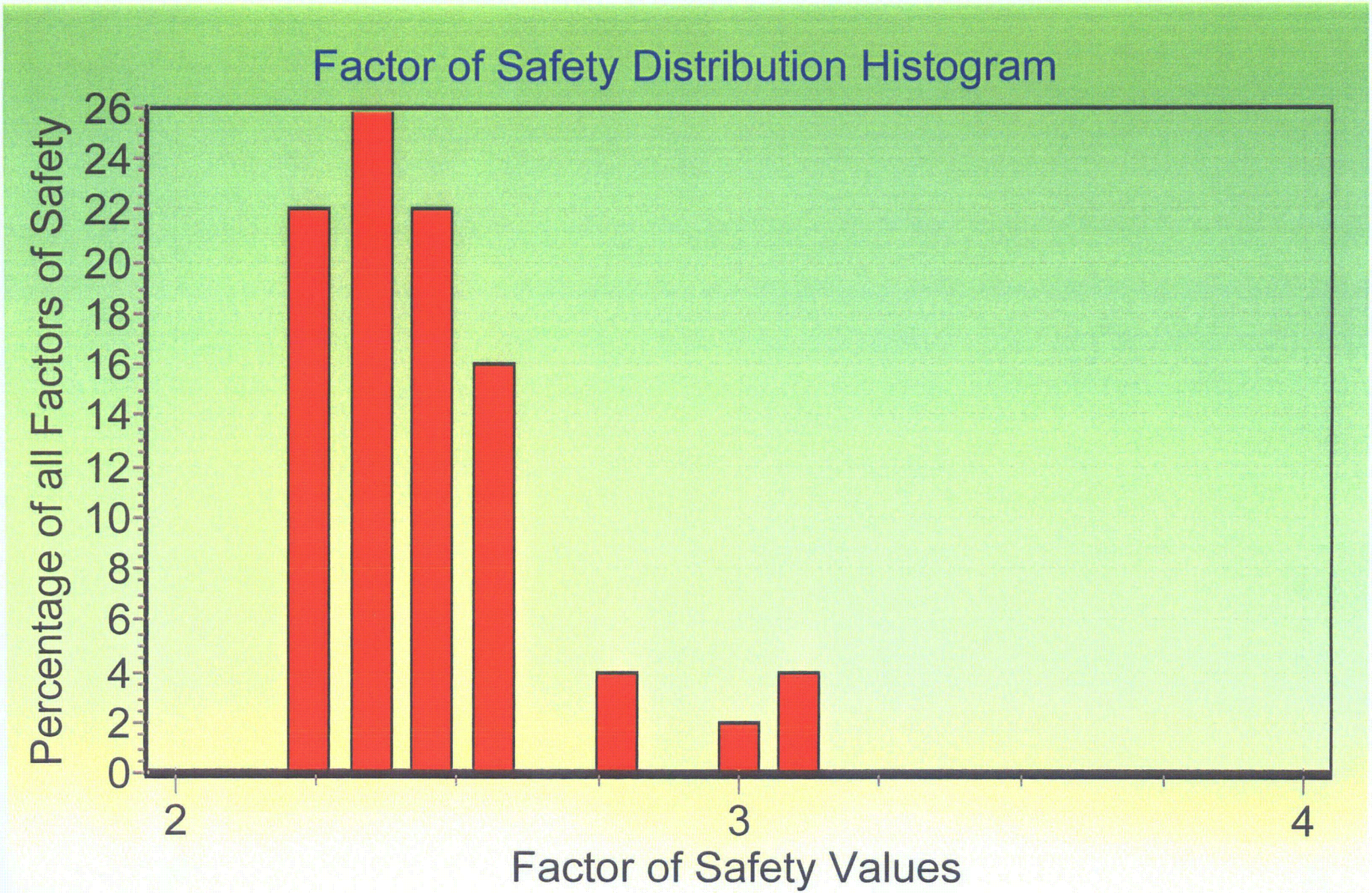
Factor of Safety Distribution Histogram
Percentage of all Factors of Safety
26
24
22
20
18
16
14
12
10
8
6
4
2
0
2
3
4
Factor of Safety Values

Geometry and Boundary Conditions

Problem: SMC Newfield Decommissioning - Section A-A' - FS Min = 2.183

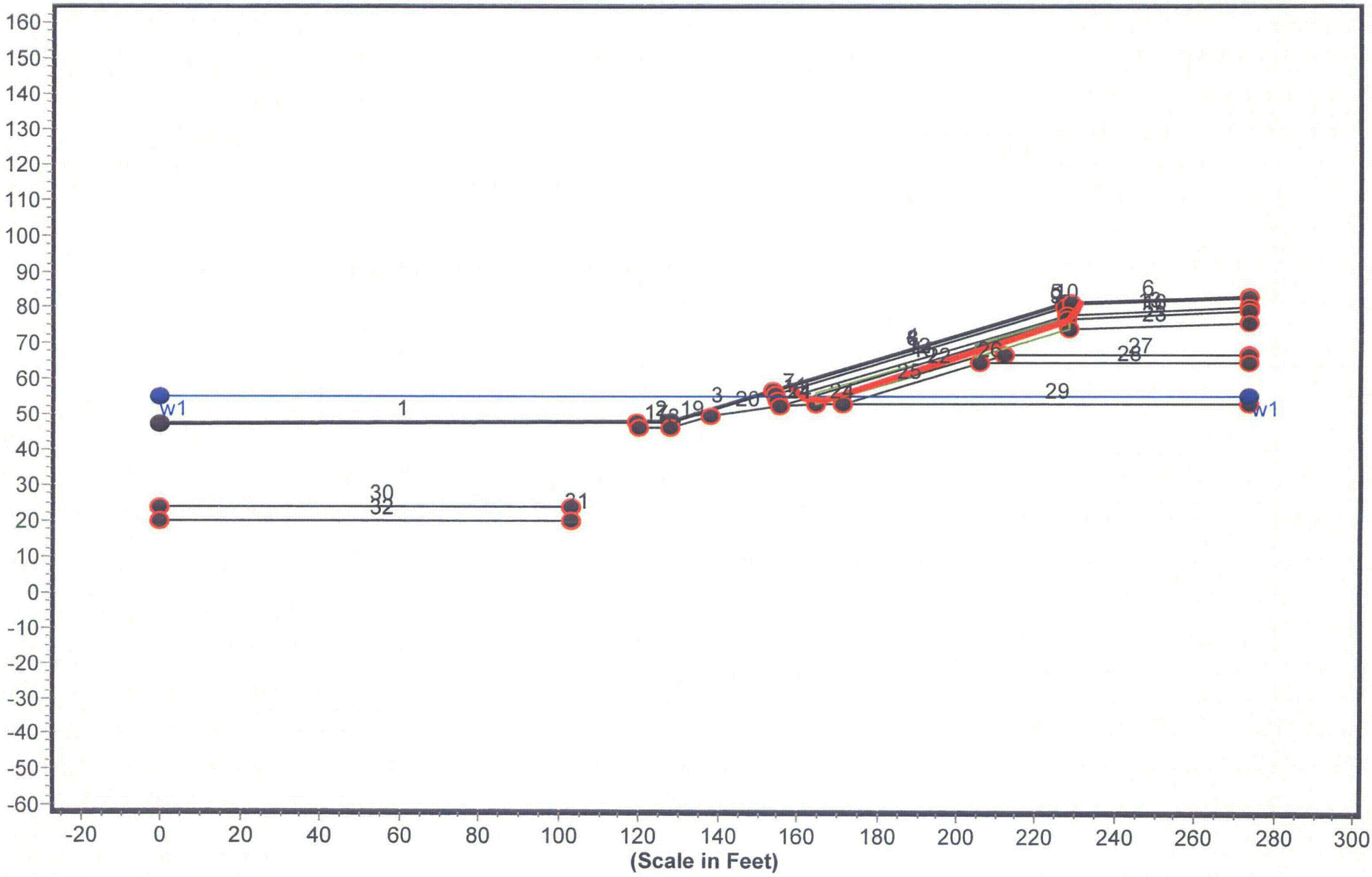

Geometry and Boundary Conditions

Problem: SMC Newfield Decommissioning - Section A-A' - FS Min = 2.183

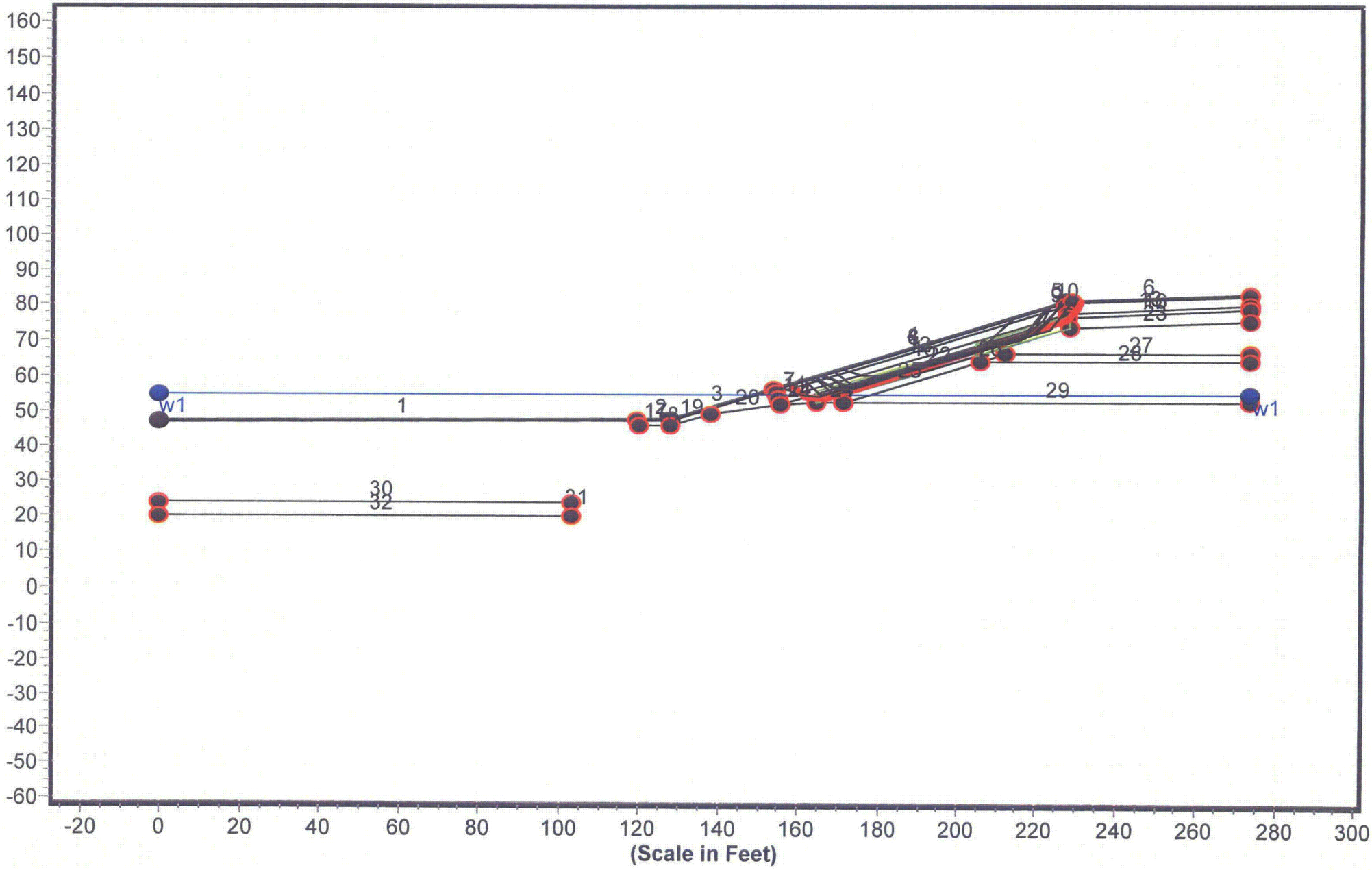

Janbu Block #2 High Water Results.txt
** PCSTABL6 **

by
Purdue University

1

--Slope Stability Analysis--
Simplified Janbu, Simplified Bishop
or Spencer's Method of Slices

Run Date:
Time of Run:
Run By:
Input Data Filename: run.in
Output Filename: result.out
Unit: ENGLISH
Plotted Output Filename: result.plt

PROBLEM DESCRIPTION SMC Newfield Decommissioning - Section A -A'

BOUNDARY COORDINATES

6 Top Boundaries
32 Total Boundaries

Boundary No.	X-Left (ft)	Y-Left (ft)	X-Right (ft)	Y-Right (ft)	Soil Type Below Bnd
1	0.00	47.40	119.50	48.00	7
2	119.50	48.00	127.50	48.00	1
3	127.50	48.00	153.90	56.80	1
4	153.90	56.80	226.90	81.10	1
5	226.90	81.10	228.90	81.20	1
6	228.90	81.20	273.60	83.00	2
7	153.90	56.80	154.20	55.80	1
8	154.20	55.80	227.10	80.10	2
9	227.10	80.10	228.80	80.20	2
10	228.80	80.20	228.90	81.20	2
11	154.20	55.80	154.80	53.90	1
12	154.80	53.90	227.40	78.10	1
13	227.40	78.10	273.60	80.00	1
14	154.80	53.90	155.20	52.60	1
15	155.20	52.60	227.60	77.10	3
16	227.60	77.10	273.60	79.00	3
17	119.50	48.00	119.60	46.40	7
18	119.60	46.40	127.80	46.40	7
19	127.80	46.40	137.90	49.80	7
20	137.90	49.80	155.20	52.60	7
21	155.20	52.60	164.60	53.00	7
22	164.60	53.00	228.20	74.10	4
23	228.20	74.10	273.60	76.00	4
24	164.60	53.00	171.00	53.00	7
25	171.00	53.00	205.80	64.60	6
26	205.80	64.60	211.80	66.60	5

27	211.80	66.60	273.60	66.60	5
28	205.80	64.60	273.60	64.60	6
29	171.00	53.00	273.60	53.00	7
30	0.00	24.00	103.10	24.00	8
31	103.00	20.00	103.10	24.00	7
32	0.00	20.00	103.10	20.00	7

1

ISOTROPIC SOIL PARAMETERS

8 Type(s) of Soil

Soil Type No.	Total Unit Wt. (pcf)	Saturated Unit Wt. (pcf)	Cohesion Intercept (psf)	Friction Angle (deg)	Pore Pressure Param.	Pressure Constant (psf)	Piez. Surface No.
1	135.0	140.0	0.0	40.0	0.00	0.0	1
2	135.0	140.0	0.0	35.0	0.00	0.0	1
3	125.0	130.0	250.0	15.0	0.00	0.0	1
4	125.0	135.0	0.0	32.0	0.00	0.0	1
5	135.0	140.0	0.0	38.0	0.00	0.0	1
6	135.0	140.0	0.0	40.0	0.00	0.0	1
7	115.0	130.0	0.0	33.0	0.00	0.0	1
8	130.0	140.0	300.0	20.0	0.00	0.0	1

1

1 PIEZOMETRIC SURFACE(S) HAVE BEEN SPECIFIED

Unit Weight of Water = 62.40

Piezometric Surface No. 1 Specified by 2 Coordinate Points

Point No.	X-Water (ft)	Y-Water (ft)
1	0.00	55.00
2	273.60	55.00

Janbus Empirical Coef is being used for the case of c & phi both > 0

1

A Critical Failure Surface Searching Method, Using A Random Technique For Generating Sliding Block Surfaces, Has Been Specified.

50 Trial Surfaces Have Been Generated.

2 Boxes Specified For Generation Of Central Block Base

Length Of Line Segments For Active And Passive Portions Of Sliding Block Is 5.0

Box No.	X-Left (ft)	Y-Left (ft)	X-Right (ft)	Y-Right (ft)	Height (ft)
1	164.70	54.58	188.42	62.47	3.16
2	204.48	67.89	228.20	75.78	3.16

1

Following Are Displayed The Ten Most Critical Of The Trial Failure Surfaces Examined. They Are Ordered - Most Critical First.

* * Safety Factors Are Calculated By The Modified Janbu Method * *

Failure Surface Specified By 7 Coordinate Points

Point No.	X-Surf (ft)	Y-Surf (ft)
1	157.93	58.14
2	158.28	57.89
3	161.85	54.39
4	166.84	54.12
5	227.30	76.12
6	230.16	80.22
7	231.12	81.29

*** 2.183 ***

Individual data on the 20 slices

Slice No.	Width (ft)	Weight (lbs)	Water Force Top (lbs)	Water Force Bot (lbs)	Force Norm (lbs)	Force Tan (lbs)	Earthquake Force Hor (lbs)	Earthquake Force Ver (lbs)	Surcharge Load (lbs)
1	0.3	8.5	0.0	0.0	0.0	0.0	0.0	0.0	0.0
2	0.6	55.1	0.0	0.0	0.0	0.0	0.0	0.0	0.0
3	1.6	464.0	0.0	0.0	0.0	0.0	0.0	0.0	0.0
4	0.8	399.0	0.0	0.0	0.0	0.0	0.0	0.0	0.0
5	0.3	163.2	0.0	3.2	0.0	0.0	0.0	0.0	0.0
6	0.3	226.4	0.0	13.3	0.0	0.0	0.0	0.0	0.0
7	0.4	306.1	0.0	17.1	0.0	0.0	0.0	0.0	0.0
8	4.5	3699.1	0.0	215.2	0.0	0.0	0.0	0.0	0.0
9	2.4	2221.3	0.0	70.9	0.0	0.0	0.0	0.0	0.0
10	57.6	45919.5	0.0	0.0	0.0	0.0	0.0	0.0	0.0
11	0.2	135.9	0.0	0.0	0.0	0.0	0.0	0.0	0.0
12	0.2	137.2	0.0	0.0	0.0	0.0	0.0	0.0	0.0
13	0.1	62.8	0.0	0.0	0.0	0.0	0.0	0.0	0.0
14	0.2	126.4	0.0	0.0	0.0	0.0	0.0	0.0	0.0
15	0.4	232.3	0.0	0.0	0.0	0.0	0.0	0.0	0.0
16	0.7	345.4	0.0	0.0	0.0	0.0	0.0	0.0	0.0
17	0.1	30.7	0.0	0.0	0.0	0.0	0.0	0.0	0.0
18	0.1	38.6	0.0	0.0	0.0	0.0	0.0	0.0	0.0

19	1.3	325.9	0.0	0.0	0.0	0.0	0.0	0.0	0.0
20	1.0	66.7	0.0	0.0	0.0	0.0	0.0	0.0	0.0

Failure Surface Specified By 8 Coordinate Points

Point No.	X-Surf (ft)	Y-Surf (ft)
1	155.51	57.33
2	155.69	57.19
3	160.24	55.09
4	165.20	54.52
5	206.19	68.70
6	209.50	72.44
7	213.00	76.02
8	213.59	76.67

*** 2.185 ***

1

Failure Surface Specified By 6 Coordinate Points

Point No.	X-Surf (ft)	Y-Surf (ft)
1	164.63	60.37
2	168.22	59.43
3	172.34	56.61
4	216.84	71.33
5	219.30	75.68
6	222.01	79.47

*** 2.207 ***

Failure Surface Specified By 7 Coordinate Points

Point No.	X-Surf (ft)	Y-Surf (ft)
1	166.25	60.91
2	167.75	60.04
3	172.13	57.63
4	219.19	72.30
5	222.66	75.90
6	225.44	80.05
7	225.52	80.64

*** 2.215 ***

Failure Surface Specified By 7 Coordinate Points

Point No.	X-Surf (ft)	Y-Surf (ft)
1	170.55	62.34
2	171.00	62.25
3	175.81	60.86
4	180.81	60.74
5	222.95	73.47
6	225.97	77.45
7	228.39	81.17

*** 2.222 ***

Failure Surface Specified By 7 Coordinate Points

Point No.	X-Surf (ft)	Y-Surf (ft)
1	163.78	60.09
2	165.00	59.66
3	169.10	56.80
4	215.82	70.74
5	218.88	74.70
6	221.92	78.67
7	223.07	79.83

*** 2.233 ***

Failure Surface Specified By 7 Coordinate Points

Point No.	X-Surf (ft)	Y-Surf (ft)
1	169.03	61.84
2	169.79	61.15
3	173.36	57.65
4	218.19	71.68
5	221.69	75.26
6	224.78	79.19
7	226.34	80.91

*** 2.262 ***

Failure Surface Specified By 7 Coordinate Points

Point No.	X-Surf (ft)	Y-Surf (ft)
1	160.91	59.13
2	161.75	58.87
3	165.36	55.42
4	215.90	70.97
5	219.39	74.54
6	221.22	79.20
7	221.22	79.21

*** 2.276 ***

1

Failure Surface Specified By 6 Coordinate Points

Point No.	X-Surf (ft)	Y-Surf (ft)
1	162.60	59.70
2	165.35	58.73
3	169.11	55.44
4	217.87	73.01
5	221.40	76.56
6	222.95	79.78

*** 2.282 ***

Failure Surface Specified By 6 Coordinate Points

Point No.	X-Surf (ft)	Y-Surf (ft)
1	164.51	60.33
2	168.51	57.50
3	173.51	57.22
4	217.63	73.44
5	220.46	77.56
6	222.51	79.64

*** 2.282 ***

1

Y A X I S F T

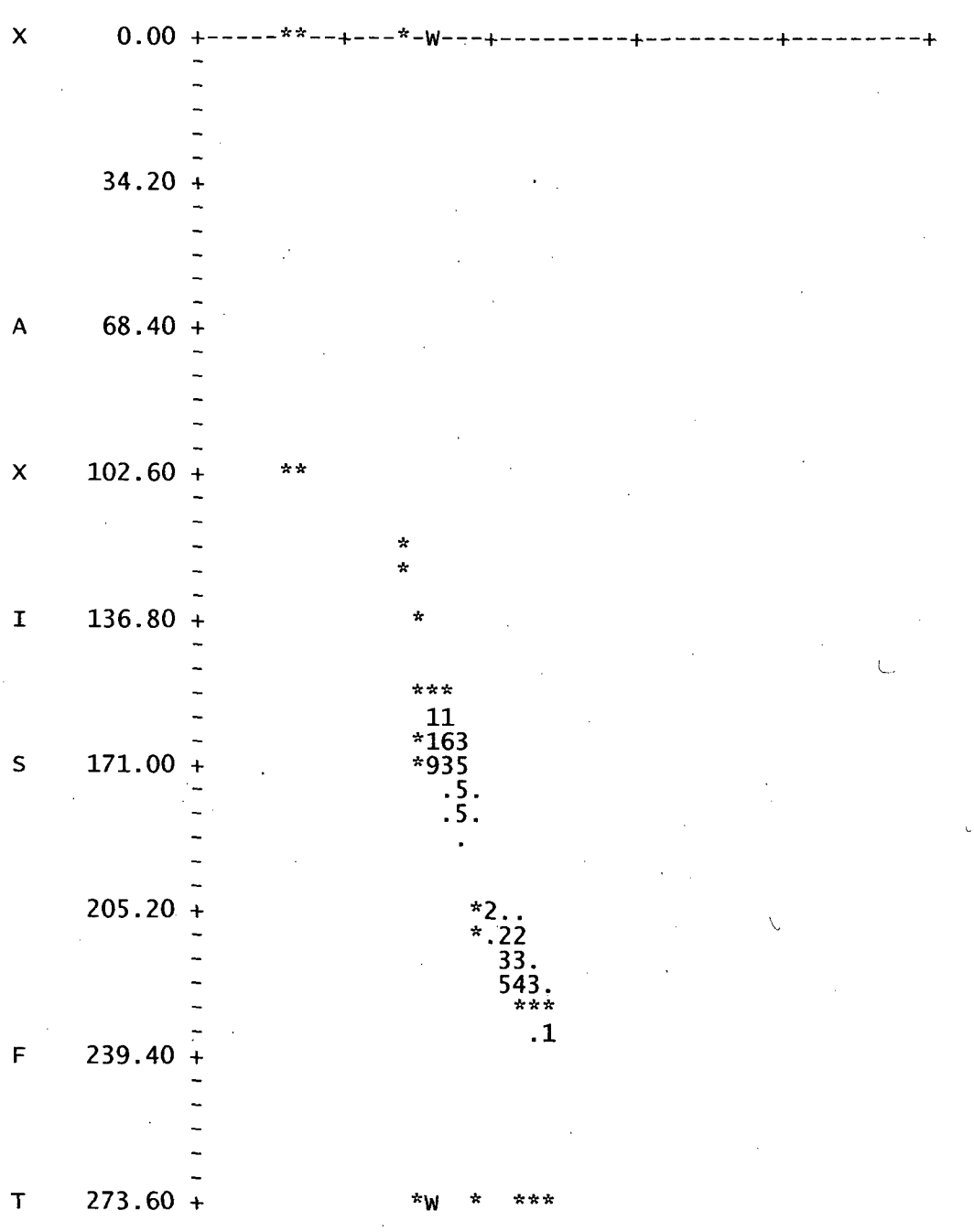
0.00
34.20
68.40
102.60
136.80
171.00
X 0.00
34.20
A 68.40
X 102.60
I 136.80
S 171.00
205.20
F 239.40
T 273.60

KOERNER & SOONG STATIC SLIDING BLOCK

landfilldesign.com

Slope Stability:Seismic Force - Design Calculator

Problem Statement

This slope stability calculator utilizes a pseudo-static analysis to determine the factor of safety (FS) of a geosynthetic lined slope. This calculator assumes that no seepage forces are present. The unit gradient calculator can be used to calculate the required transmissivity of the drainage geocomposite to assure adequate drainage.

Subtitle "D" of the U.S. EPA regulations requires a seismic analysis if the site has experienced a 0.1 g horizontal acceleration, or more, in the past 250 years. For the continental USA, this does not only include the western states, but major sections of the midwest and northeast as well. The map below shows the seismic coefficients for various zones in the USA.

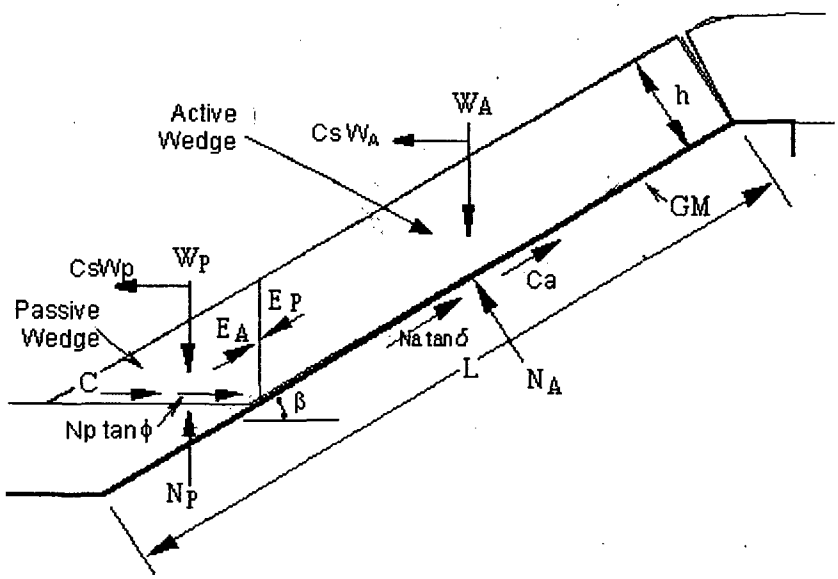

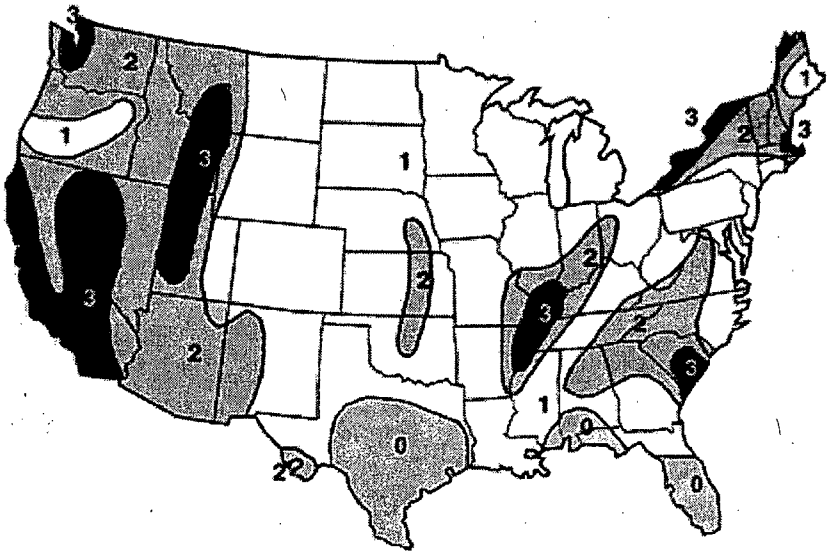

Legend

Zone 0: No damage

Zone 1: Minor damage; corresponds to intensities V and VI on the modified Mercalli intensity scale

Zone 2: Moderate damage; corresponds to intensity VII on the modified Mercalli intensity scale

Zone 3: Major damage; corresponds to intensity VIII and higher on the modified Mercalli intensity scale

Seismic coefficients corresponding to each zone

Zone	Remark	Modified Mercalli Scale	Average Seismic Coefficient (Cs)
0	No damage	-	0
1	Minor damage	V and VI	0.03 to 0.07
2	Moderate damage	VII	0.13
3	Major damage	VIII and higher	0.27

Input Values

Design Inputs

Slope characteristics

Thickness of cover soil (h)	2.13	m
Slope angle (ß)	18.4	degrees
Lenght of slope measured along geomembrane (L)	22.5	m

Soil characteristics

Unit weight of the cover soil (g)	19.6	kN/m^3
Friction angle of the cover soil (F)	15	degrees
Cohesion of the cover soil (c)	11.97	kN/m^2
Interface friction(d)		degrees

	30	
Interface adhesion (Ca)	0	kN/m^2

Seismic characteristic

Seismic coefficient (Cs)	.08468	g

Seismic Stability Calculation

Solution

Factor of Safety with seismic activity (FS) 1.772

Factor of Safety no seismic activity (FS) 2.386

Additional Assistance

If you would like to have Advanced Geotech Systems provide material specifications that meet your performance criteria, please fill in the following fields and click the submit button. All information is kept strictly confidential.

Name *

Company

Email Address *

Phone

Project Reference

Comments

*required fields

Submit Design Results

References

R. M. Koerner, and T-Y. Soong, 1998. "Analysis and Design of Veneer Cover Soils". Proceedings of 6th International Conference on Geosynthetics, Vol. 1, pp. 1-23, Atlanta, Georgia, USA.